Combination of platinums and phytochemicals aimed to overcome drug resistance in cancer

Yahya Farahat Solayman Solayman

A thesis submitted in fulfillment of the requirements for the

degree of Doctor of Philosophy

Concord Clinical School

Faculty of Medicine and Health

The University of Sydney, Australia

2020

Declaration

I, the author of the thesis, declare that none of the material in this thesis has been previously submitted by me or any other candidate for any degree to this or any other university.

Yahya Farahat Solayman Solayman

Acknowledgement

I would like to express my deepest gratitude to my former supervisor, Associate Professor Dr Fazlul Huq, for giving me the opportunity to join his group and for his continuous support, guidance and encouragement throughout this work. I would like to express my sincere gratitude and heartfelt appreciation to my current supervisor, Associate Professor Dr Philip Beale, for his excellent guidance, valuable suggestions and truly appreciated support during all the stages of my work, and for his sincere efforts to ensure the completion of this research project. It would have never been possible to complete this work without these people.

I would like to thank my auxiliary supervisor, Dr Moni, for his kind support and valuable suggestions during the project, especially with the bio-informatics part.

Also, a special thanks goes to our Laboratory Research Officer, Dr Jun Qing Yu, for all her help, invaluable expertise and her companionship in the laboratory throughout the project.

Furthermore, I feel truly privileged that I had the experience of being among this group of distinguished researchers in the laboratory: Dr Nur Alam, Dr Mohammad Al-Moyad, Dr Fahad Nasser Al Onazi, Dr Laila Arzuman, Dr Md Sheikh Anwar, Dr Hana Bali and Dr Safia Al Thurwi. I would like to thank all of them for their generous help.

I would also like to thank the academic and office staff members of the Discipline of Biomedical Science and the Discipline of Pathology, including Associate Professor Kay Double, Dr Peter Knight, Dr Damian Holsinger, Dr Diana Oakes, Felicia Lim, Helen Ananin, Ann Korabelnikoff and Goutham Jayachandan. Also, I would like to thank Dr Mark Halaki from the Discipline

of Exercise and Sport Science and everyone else I met along the way, for their kind help and support throughout my candidature.

Thanks also goes to Giselle Alegria for her help with editing my thesis and putting the finishing touches to the project.

I would like also to acknowledge and thank my whole family for their heartfelt support, patience, faith, kindness and love throughout my journey, in particular, my dearest mother **Soheir Hussien**, my father, Dr **Farahat Solayman**, my siblings, **Nesreen**, **Tamir**, **Hatim**, **Mohammad** and **Zakaria**, my niece, **Selene,** and my nephews, **Yahya** and **Ammar**. Finally, I would like to thank my life-long friends, **Imad** and **Sultan,** for their valued friendship and let them know that they have been and always will be in my thoughts.

DEDICATION

With a heart filled with love, happiness and gratitude,
the thesis is dedicated to a great poet of this era

Jujube (Dr Fazlul Huq)

Who is my former Research Supervisor, Associate Professor and pioneer of Cancer Research Group, Discipline of Pathology, The University of Sydney

Abstract

Combined chemotherapy has drawn much attention for overcoming drug resistance and improving outcomes during the treatment of advanced stages of cancer. In the present study, cisplatin, oxaliplatin, LH5, gemcitabine, camptothecin and cucurbitacin B have been combined in a binary mode using three different sequences; i.e. bolus, 0/4 h and 4/0 h, in the ovarian and colorectal cancer models. Among the tested combinations of drugs, the combination of cisplatin with camptothecin and gemcitabine at all concentrations and for all sequences of addition, proved to be beneficial in overcoming cisplatin resistance in the $A2780^{cisR}$ ovarian cell line. In contrast, cisplatin, in combination with camptothecin; LH5, in combination with camptothecin; and gemcitabine, in combination with oxaliplatin, demonstrated a dose- and sequence-dependent enhancement in cell kill in the colorectal cancer models (HT-29 and/or Lim-1215 cell lines). The proteomic study revealed 20 proteins that showed significant changes in expression following different drug treatments in ovarian cancer models; e.g., cofilin 1, actin cytoplasmic 1, tropomyosin alpha-4 chain, tubulin beta chain, vimentin, peroxiredoxin-1, pyruvate kinase, peptidyl-prolyl cis-trans isomerase A, ATPase mitochondrial inhibitor, ATP synthase subunit beta, 60kDa heat shock protein, stress-70 protein, nucleophosmin, HSP 90-beta heat shock protein, GTP-binding nuclear protein Ran, elongation factor 1-alpha, histone H4, heterogeneous nuclear ribonucleoproteins C1/C2, annexin A1 and calmodulin-1. Among these proteins, peptidyl-prolyl cis-trans isomerase A, pyruvate kinase, nucleophosmin, elongation factor -1 alpha, histone H4 and calmodulin-1, have been identified as being anti-apoptotic proteins, whereas the ATPase mitochondrial inhibitor protein has been identified as being an apoptotic protein. Finally, bioinformatics analysis revealed that ovarian cancer patients with altered expressions of ACTB, HST1H4F, HNRNPC,

HSP90AB1 and PKM genes, had lower survival rates, in comparison with the control group.

Table of Content

List of Figures

List of Tables

List of Abbreviations

5-FU	5-fluorouracil
2D-PAGE	two-dimensional polyacrylamide gel electrophoresis
AAS	Atomic absorption spectroscopy
ACTB	Actin, cytoplasmic 1
ACTB gene	Gene encoding Actin, cytoplasmic 1 protein
BRAF	serine/threonine-protein kinase B-Raf
BSA	Bovine serum albumin
CA	Cancer antigen
Camp	Camptothecin
CI	Combination indices
Cis	Cisplatin
CMS	Consensus molecular subtype
COF1	Cofilin-1
CTRs	Copper efflux transporters
Cuc	Cucurbitacin B
DACH	Diaminocyclohexane
dCK	deoxycytidine kinase
dCyd	Deoxy-cytidine
dFdC	2′,2′-difluorodeoxycytidine
Dm	Median effect dose
DMF	Dimethylformamide
DMSO	Dimethyl sulfoxide
DNA	Deoxyribonucleic acid

DTT	Dithiothreitol
EB	Emulsifying buffer
ED_{50}	median effective dose in 50% of the cell kill
ED_{75}	median effective dose in 75% of the cell kill
ED_{90}	median effective dose in 90% of the cell kill
EDTA	Ethylenediaminetetraacetic acid
eEF1A	Eukaryotic elongation factor 1 alpha
fa	Affected fraction by the dose
FAP	Familial adenomatous polyposis
Gem	Gemcitabine
GSH	Glutathione
HNPCC	Hereditary nonpolyposis colorectal cancer
HNRNPC	Heterogeneous Nuclear Ribonucleoprotein C (C1/C2)
HNRNPC gene	Gene encoding Heterogeneous Nuclear Ribonucleoprotein C protein
hnRNPs	The heterogeneous nuclear ribonucleoproteins
HSP 90	Heat shock protein 90
HSP90AB1 gene	Gene encoding Heat Shock Protein HSP 90-Beta
HSP60	Heat shock protein 60
HST1H4F gene	Gene encoding Histone H4 protein
IC_{50}	Concentration required to kill half of the cells
IEF	Iso-electric focusing
IF1	ATPase inhibitor mitochondrial protein natural inhibitor protein
INK4	Inhibitor of Cyclin-Dependent Kinase 4

IPG	Immobilized pH gradient
m	Exponent defining shape of the dose effect curve
MALDI	Matrix Assisted Laser Desorption Ionisation
MAPK	Mitogen-activated protein kinase
Milli-Q water	Ultrapure water
miRNAs	microRNAs
MMR	Mismatch repair
MRI	Magnetic resonance imaging
MRPs	Multidrug resistance proteins
MS	Mass spectrometry
MTT	Methylthiazolyldiphenyl-tetrazolium bromide
NCI	National cancer institute
NER	Nucleotide excision repair
NF-κB	Nuclear factor kappa B
nM	Nanomolar
OCTs	Organic cation transporters
OD	Optical density
Oxa	Oxaliplatin
PARP	Poly (ADP-ribose) polymerase
PBS	Phosphate-buffered saline
PI	Isoelectric points
PKM gene	Gene encoding pyruvate kinase protein
PPIA	Peptidyl-prolyl cis-trans isomerase A
PTEN	Phosphatase and tensin homolog
r	Reliability coefficient

ROS	Reactive oxygen species
RPMI	Roswell Park Memorial Institute
STRING	Search Tool for the Retrieval of Interacting Genes/Proteins
SDS	Sodium dodecyl sulfate
TAE	Tris-acetate-EDTA
TGCA	The Cancer Genome Atlas

1 Introduction

1.1 Cancer

Cancer is the term used to describe the uncontrolled proliferation of cells in the body. The word ‘cancer’ came from the Latin word for crab. The disease is characterised by six special features, namely continual growth signalling, resistance to tumour suppression, ability to escape programmed cell death, an unbounded ability to replicate, constant blood vessel formation and the ability to invade normal tissues or metastasise (Hanahan and Weinberg 2011). The world’s oldest record of cancer goes back to ancient Egypt in 1500 BC, where the lack of effective treatment is mentioned.

1.2 Global incidence of cancer

Currently, cancer is considered to be one of the most frightful diseases in the world and is ranked as the second most leading cause of death. As applied to cancer, The International Agency for Cancer Research, WHO, compiled a list of incidence and mortality estimates for 2018. It was estimated that among 18.1 million new cases, more than a third would die worldwide. Men were found to have higher rate of incidence than women by nearly 20%. The mortality rates for all combined cancers was also higher in men than women by almost 50%, although the percentage varied significantly from one country to another. The most commonly diagnosed cancers were lung (2.09 million), breast (2.08 million), prostate (1.27 million), colon (1.09 million), stomach (1.03 million) and liver (0.841 million). In the case of mortality, the most common causes were lung cancer (1.76 million deaths), followed by stomach cancer (0.782 million deaths), liver cancer (0.781 million deaths), breast cancer (0.626 million deaths), colon

cancer (0.551 million deaths) and then prostate cancer (0.358 million) (Bray, Ferlay et al. 2018).

1.3 Aetiology of cancer

Genetic mutations in cells, due to exposure to carcinogenic agents, are responsible for carcinogenesis (cancer formation). Three classes of carcinogenic agents have been identified up until now; i.e., chemicals, radiation and oncogenic viruses. Chemical carcinogens can act as either direct carcinogens (without any metabolic conversion) or indirect carcinogens (requiring metabolic conversion before acting, ultimately, as a carcinogen). Examples of direct-acting chemical carcinogens are alkylating agents (e.g., dimethyl sulfate, diepoxybutane, β-propiolactone) and acylating agents (e.g., dimethylcarbamyl chloride, 1-acetyl-imidazole). A few examples of indirectly acting chemical carcinogens are benz(α)anthracene, benzo(α)pyrene, aflatoxin B_1, benzidine, griseofulvin, safrole, betel nuts and heavy metals. These chemical carcinogens possess reactive electrophiles that directly damage DNA and lead to genetic mutation and, ultimately, cancer (Garner 1998). UV rays of sunlight, X-rays, nuclear fission and radionuclides are all established carcinogens. These ionising radiations cause breakage in chromosomes, point mutations and eventually start carcinogenesis (Burtt, Thompson et al. 2016). Two types of oncogenic viruses have been implicated in human cancer: RNA and DNA viruses. Among RNA viruses, Human-T-cell leukaemia virus type 1 (HTLV-1) is the most prominent. Whereas, human papillomavirus (HPV), epstein-barr virus (EPV), hepatitis B virus (HBV) and hepatitis C virus (HCV) are noticeable carcinogens among DNA viruses (Kgatle, Spearman et al. 2017). Moreover, *helicobacter pylori* infection has been identified with gastric cancers (Plummer, Franceschi et al. 2015).

1.4 Different forms of cancer

Broadly, tumours can be classified as being benign or malignant, and distinguished from each other on the basis of their magnitude of differentiation, local invasiveness and distant spread (Kumar, Abbas et al. 2014). Benign tumour cells look similar to that of the tissue of origin, grow slowly and remain localised to the site of origin. On the contrary, malignant tumour cells are poorly differentiated or completely undifferentiated, grow swiftly, are locally invasive and metastasise to distant sites.

The general public classifies various cancers, based on their sites of origin, but oncologists frequently categorise them, based on their histology. According to the primary sites of origin, cancers may be named as lung cancer when a tumour is evidenced in the lung; prostate cancer when a cancer appears in the prostate; and colorectal cancer when a cancer is evidenced in the colorectal region. Along these lines, cancer can be labelled as ovarian cancer, hepatic cancer, brain cancer, testicular cancer, uterine cancer, etc., depending on its location.

According to histological classification, cancers may be classified as carcinoma, sarcoma, myeloma, leukaemia, lymphoma and mixed types (Miller, L Young Jr et al. 1995).

Carcinoma: Malignant neoplasms of epithelial cells are called carcinoma and account for 80% to 90% of all cancer cases. They can be further divided into two types: adenocarcinoma and squamous cell carcinoma.

Sarcoma: Cancers of connective tissue (bone, cartilage, etc.) are called sarcoma.

Leukaemia (liquid cancers): Boundless proliferation of blood–forming tissue (bone marrow) leads to leukaemia.

Lymphoma (solid cancers): Cancers of the lymphatic system are known as lymphomas and may affect lymph nodes in the stomach, brain, intestines, etc. Lymphomas can be

classified into – Hodgkin's lymphoma (Reed-Sternberg cells present) and non-Hodgkin's lymphomas.

Myeloma: These cancers originate in plasma cells of bone marrow responsible for producing various antibodies in response to infections.

Mixed type: These contain two or more types of cancerous cell components, such as mixed mesodermal tumour, carcinosarcoma, teratocarcinoma and adenosquamous carcinoma.

1.5 Cancer genes

Cancer is a disease that is caused by mutations that alter the function of a finite subset of 20,000 human genes that are called cancer genes. These genes are constantly affected by genetic aberrations, due to acquired mutations (exposure of chemicals, radiations and viruses) or inherited mutations (inherited in the germ line). If such mutations lead to carcinogenesis, each cell in an individual tumour shares the mutations that were present in the parent cell at the time of transformation. Cancer genes can be grouped into four functional classes, namely: oncogenes, tumour suppressor genes, apoptosis regulating genes and genes that regulate interactions between the tumour and host cells (Kumar, Abbas et al. 2014).

1.5.1 Oncogenes

These are the genes that induce transformed phenotypes, when expressed in cells, by promoting increased cell growth. These are considered dominant genes because a mutation involving a single allele oncogene mutates due to the overexpression of proto-oncogenes. A few examples include: myc gene, ras protein, Src family and cyclin dependent kinase (Croce 2008).

1.5.2 Tumour suppressor genes

The genes that prevent a cell from becoming cancerous are referred to as tumour suppressor genes or anti-oncogenes. When tumour suppressor genes are inactivated, the result is the removal of negative regulators of cell proliferation and the promotion of the growth of abnormal cancer cells (Marshall 1991). A few examples of tumour suppressor genes include: p53, the INK4 and PTEN.

1.5.3 Apoptosis regulating genes

Apoptosis is also called programmed cell death, which is inevitable to maintain the balance of homeostasis, and occurs commonly in multicellular organisms. Disorders in apoptosis, due to mutations in regulating genes, can induce cancer. Most common apoptosis regulating genes are: bcl-2, bcl-xl, bax and fas (Kiraz, Adan et al. 2016).

1.5.4 Genes that regulate interaction between tumour cells and host cells

These genes are primarily responsible for the recognition of tumour cells by the host immune system. Based on mutation frequency and pattern, the most remarkable genes that belong to this group are: β2-microglobulin, HLA-A, HLA-B, and TAP1, as well as the CD1D gene (Corthay 2014).

1.6 MicroRNAs (miRNAs) and cancer

MicroRNAs (miRNAs) are highly conserved, short, non-coding RNAs of 20–24 nucleotides that act in almost all biological pathways in multicellular living entities. In mammals, this regulation is predominantly carried out by repression of translation. miRNAs play significant roles in many processes, such as cell proliferation, cell cycle regulation, apoptosis, differentiation, migration and metabolism (Lynam-Lennon,

Maher et al. 2009). Recently, both the initiation and progression of tumour has been linked to miRNAs dysregulation. This indicates ability of miRNAs to act as oncogenes, which, in turn, may provide an insight into cancer development and resistance.

1.7 Ovarian cancer

Among all gynaecologic cancers, ovarian cancer has the highest rate of mortality in Western countries (Van Driel, Koole et al. 2018). Ovarian cancer is often detected at a late stage, with a significantly lower rate of survival (being less than 29%) (Reid, Permuth et al. 2017). Ovarian cancer is not a single disease and can be grouped into three major categories, on the basis of anatomical sites from where the cancer originates, such as: surface epithelial-stromal cancer, sex cord-stromal cancer, and germ cell cancer. Among the different subtypes of ovarian cancer, more than 90% have an epithelial origin, 5%–6% relate to sex cord-stromal cancer, while germ cell tumours account for 2%–3%.

1.7.1 Risk factors of ovarian cancer

1.7.1.1 Family history

One of the key risk factors for ovarian cancer is linked to family history of the disease with first-degree relatives of probands having a three to seven fold higher risk, especially if multiple relatives are affected by the disease. Mutations of BRCA1 and BRCA2 genes are mainly responsible for majority of hereditary cases of ovarian cancer representing 10%-15% of all cases of ovarian cancer. Colorectal cancer syndrome, related to non-polyposis, accounts for 2-20 % of cases with a lifetime risk. Mutations

in DNA repair genes, such as *BRIP1*, *RAD51C*, and *RAD51D* account for 5.8%, 5.2% and 12% lifetime risks, respectively (Bahcall 2013).

1.7.1.2 Hormonal risk factors

The greater the number of ovulatory cycles, the more heightened the cellular division rate becomes as part of the repair process of the epithelial surface after each cycle, and thus there is an increase in spontaneous mutations and, ultimately, cases of ovarian cancer (Casagrande, Pike et al. 1979). Moreover, the higher release of luteinising hormones and follicle-stimulating hormones cause an increased risk of ovarian cancer (Riman, Nilsson et al. 2004).

1.7.1.3 Parity and infertility

Parous women have a 30%-60% lower risk of ovarian cancer than nulliparous women, with the risk being lowered by about 15% for each additional full-term pregnancy (Adami, Lambe et al. 1994; La Vecchia 2001). Infertility also appears to be a risk factor for ovarian cancer in most studies, with a few exceptions (Reid, Permuth et al. 2017).

1.7.1.4 Benign gynaecological conditions and obesity

Among several conditions examined as being risk factors for ovarian cancer, are endometriosis and pelvic inflammatory disease (PID). Both were found to be positively associated with ovarian cancer. Obesity has also been considered to be a risk factor of ovarian cancer (Olsen, Nagle et al. 2013).

1.7.2 Clinical presentation of ovarian cancer

Ovarian cancer is not so often diagnosed at an early stage because few specific symptoms are present when the disease is still restricted to the ovaries. Only 15% of ovarian malignancies are limited to the ovary, 17% are regionally localised and 62% spread to distant organs and body parts. Due to its insidious nature, it has been termed 'the silent killer'. When a tumour invades the pelvis and the neighbouring upper abdomen, the observed symptoms are abdominal discomfort, bloating, dyspepsia and early satiety. With further progression of the disease, patients can experience weight loss and increased abdominal pain, and can develop obstruction in ureters.

1.7.3 Diagnosis and staging of ovarian cancer

Palpation of adnexal mass detected in pelvic examination is the most frequently used method for diagnosis of the disease. However, ultrasound screening is a very useful non-invasive diagnostic tool. Blood testing can also be used by physicians to screen for tumour markers of ovarian cancer. The cancer antigen (CA) 125 test can detect a protein often found on the surface of ovarian cancer cells. Approximately 20% of suspicious adnexal masses surgically removed from women will turn out to be ovarian malignancies. Among the factors influencing the recommendation for surgery, are age, menopause status, family history, tumour mass features, unilaterality versus bilaterality and characteristics detected in ultrasound.

The staging system for ovarian cancer, proposed by the International Society for Gynaecology and Obstetrics (FIGO), is shown in Figure 1.1.

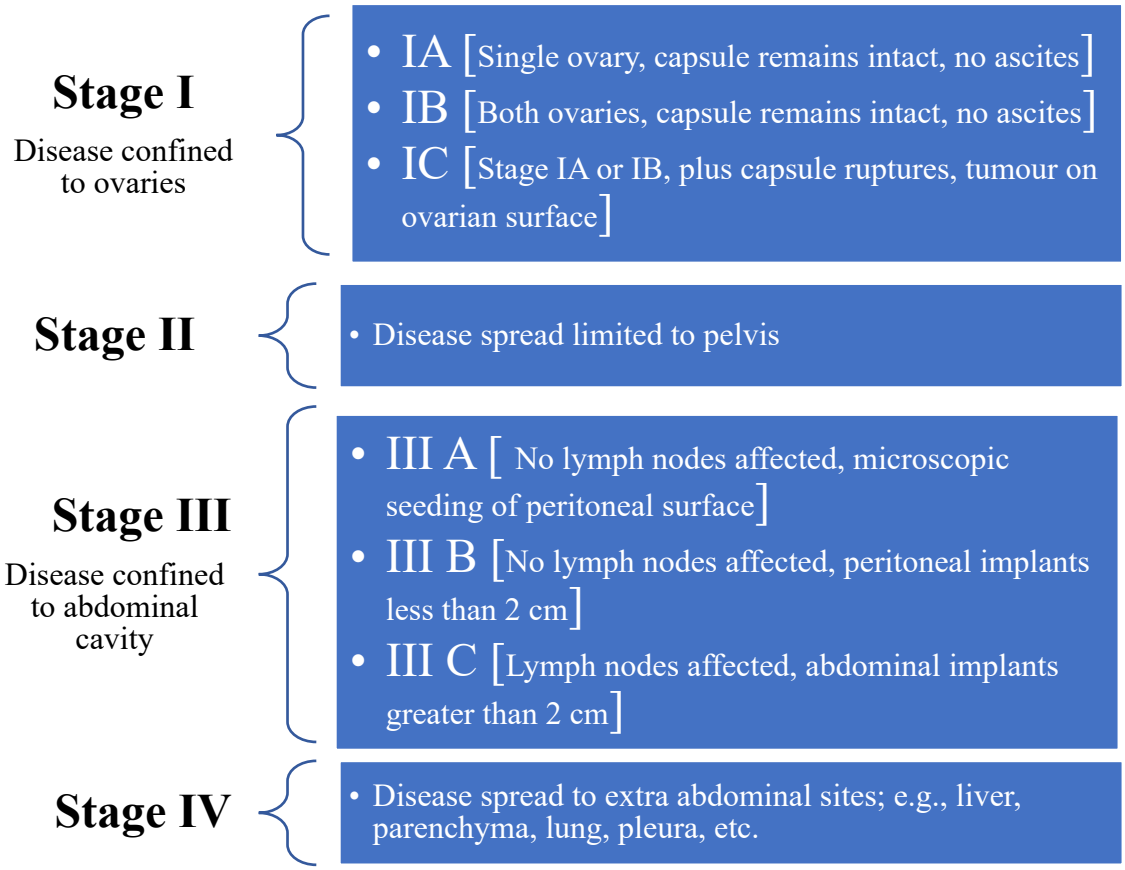

Figure 1.1: Staging of ovarian cancer [adapted from (Prat and Oncology 2014)]

1.7.4 Treatment of ovarian cancer

1.7.4.1 Surgery

Surgical operations to remove ovarian cancer include the removal of a single affected ovary and its fallopian tube, in the early stage of cancer; removal of the two ovaries and their fallopian tubes; removal of ovaries, fallopian tubes, uterus, adjacent lymph nodes and a fold of fatty abdominal tissue.

1.7.4.2 Chemotherapy

Chemotherapy is a drug treatment that is used to kill cancer cells in advanced stages. The drugs can be administered intravenously or orally. Occasionally, the drugs are injected directly into the intraperitoneal cavity (intraperitoneal chemotherapy). Combined chemotherapy, by applying two or more drugs simultaneously, is now the more preferred method used by oncologists, over monotherapy. Commonly used drugs are cisplatin, carboplatin, paclitaxel and docetaxel.

1.7.4.3 Targeted therapy

Targeted therapy employs drugs that are designed to target specific genes and/or proteins or tissue environments present within the cancer cells. Targeted therapy medications are usually used during recurrence of the disease. Examples include: angiogenesis inhibitor (bevacizumab), PARP (poly ADP ribose polymerase) inhibitor (olaparib, rucaparib and niraparib).

1.7.4.4 Supportive (palliative) care

Palliative care is an expert medical care that is centred around supporting patients in alleviating pain and the symptoms of ongoing treatment. Palliative care specialists work with patients, their carers and other healthcare professionals to provide an extra layer of support that complements patients' ongoing care. The primary focus of palliative care is to advance the quality of life for cancer patients and their family members.

1.7.5 Platinum drug resistance in ovarian cancer

There has been significant improvement in survival rate of ovarian cancer patients over the past decade, but a five-year survival rate of patients is still below 50%. Retrospective studies have revealed that, while the majority of patients had a favourable response to platinum-based chemotherapy to begin with, relapse occurred in most patients and the disease became resistant to platinum drugs. Moreover, in a few instances, patients showed intrinsic resistance to platinum drugs. As cisplatin has been investigated in the present study, in combination with other drugs, the mechanism of cisplatin resistance is discussed in this section. Cisplatin resistance mechanisms can be divided into three categories: pre-target, on-target and post-target. Pre-target resistance mechanisms include any alterations prior to the binding of cisplatin to DNA; on-target resistance mechanisms include the alterations that are directly related to DNA-cisplatin adducts; and post-target resistance mechanisms include the alterations downstream to cisplatin-mediated DNA damage (Galluzzi, Senovilla et al. 2012).

1.7.5.1 Pre-target resistance mechanisms

Before the binding of cisplatin with cellular DNA, cancer cells can escape death by decreasing the cellular accumulation of cisplatin, increasing the efflux of cisplatin or by increasing the deactivation of cisplatin. Uptake of cisplatin into the cells is mediated by passive diffusion or facilitated transport. The mutation of copper transporters; e.g., SLC31A1, has been implicated as a cisplatin resistance mechanism (Safaei and Howell 2005). Several ATP-binding cassette transporters, including MDR1, have been demonstrated to be associated with a resistance mechanism through the efflux of cisplatin (Singh, Fazal et al. 2019). The increased deactivation of cisplatin is often linked with the increased expression of thiol-containing proteins; e.g., glutathione

(GSH) and metallothionein, which are responsible for the detoxification of cisplatin through conjugation (Masters, Thomas et al. 1996).

1.7.5.2 On-target resistance mechanisms

Formed DNA adducts can malfunction in resistant cancer cells and subsequently retard apoptosis, due to a variety of mechanisms. The resistant cells may have developed capacity to repair adducts with DNA at a higher rate or be able to tolerate unrepaired damage. Most of cisplatin-DNA lesions are repaired by NER meaning nucleotide excision repair system. Cisplatin resistance occurs as a result of interference in the NER system via the enhanced expression of the high-mobility group box protein 1 (HMGB1) and the high-mobility group box protein 4 (HMGB4) (Shu, Xiong et al. 2016). Moreover, many studies have implicated faulty mismatch repair (MMR), microsatellite instability and BRAF (serine/threonine-protein kinase B-Raf) mutations, with reversion and treatment failure occurring in cancer patients. Decreased expression of MMR genes, including MLH1, MLH2, or MSH6, have been reported to cause cisplatin resistance (Singh, Fazal et al. 2019).

1.7.5.3 Post-target resistance mechanisms

Post-target resistance to the platinum drug, cisplatin, can occur as a result of changes in the pathways associated with signal transduction and the mediation of apoptosis in response to damage to the DNA. Mutations in p53 and the overexpression of MDM2, cell cycle regulators, CCND1 and IGF1R, have been found to be linked with resistance to cisplatin in various cancers. Moreover, somatic mutations within PI3KCA, AKT and FGFR3 have also detected cisplatin resistance.

1.7.5.4 Epigenetics in the resistance mechanism

It is now an established fact that an increase in DNA methylation may be linked to cisplatin resistance. Methylation of a number of specific gene promoters, including RASSF1A, HIC1, MGMT and CALCA, have been linked with both intrinsic and acquired cisplatin resistance (Koul, McKiernan et al. 2004; Wermann, Stoop et al. 2010). It has been proposed that epigenetic silencing can act on both on-target and post-target mechanisms.

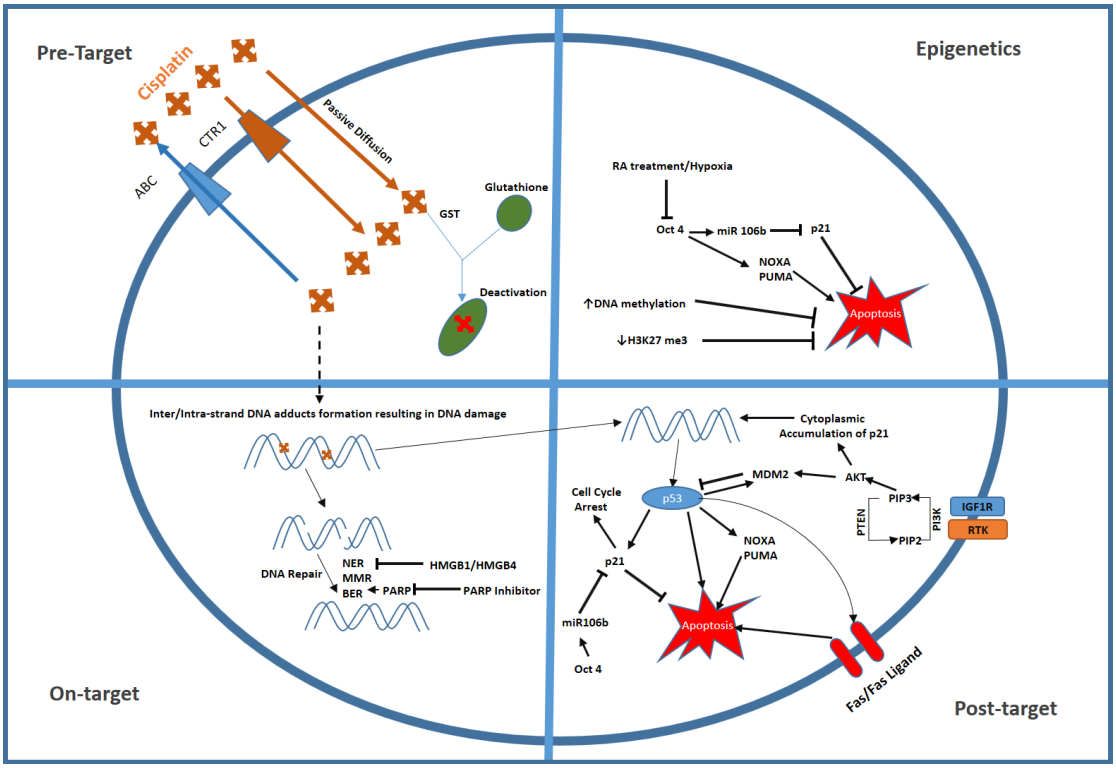

Figure 1.2: Mechanism of cisplatin resistance [adapted from Singh, Fazal et al. 2019]

1.8 Colorectal cancer

Colorectal cancer is the third most frequently diagnosed cancer and ranks fourth as the leading cause of cancer-related death. It is thought that its incidence will increase by 60%, amounting to over 2.2 million new cases and more than one million deaths by 2030. Colorectal cancer serves as a strong marker of cancer transition in countries experiencing fast economical and societal development (Arnold, Sierra et al. 2017). Colorectal cancer can be classified into four consensus molecular subtypes, with distinguishing features: consensus molecular subtype 1 (CMS1), consensus molecular subtype 2 (CMS2), consensus molecular subtype 3 (CMS3) and consensus molecular subtype 4 (CMS4). CMS1 shares 14% of the total diagnosed colorectal cancer samples and is characterised by hypermutated cells that have microsatellite, unstable and strong immune activation. This is why CMS1 is also referred to as the microsatellite instability immune subtype. In contrast, CMS2 (canonical subtype) represents 37% of the total diagnosed colorectal cancer samples that are distinguished by epithelial cells having noticeable WNT and MYC signalling activation. CMS3 (metabolic subtype) represents 13% of the total diagnosed colorectal cancer samples that are manifested by epithelial cells having metabolic dysregulation. CMS4 (mesenchymal subtype) represents 23% of the total diagnosed colorectal cancer samples that are featured by noticeable activation of the transforming growth factor–β, stromal invasion and angiogenesis (Guinney, Dienstmann et al. 2015).

Seventy percent of colorectal cancers occur due to somatic mutations, and family history has been associated with 10-30% of colorectal cancers, whereas genetic diseases represent about 5-7% (Burt 2000). Familial colorectal cancer has been found to develop, due to a germline minor variant and/or single-nucleotide mutation in the oncogenes or tumour suppressor genes, while inactivating mutations in oncogenes or tumour

suppressor genes lead to hereditary colorectal cancer (Jasperson, Tuohy et al. 2010). Hereditary non-polyposis colorectal cancer (HNPCC) and adenomatous polyposis syndrome are the prominent hereditary colorectal cancer syndromes.

1.8.1 Risk factors of colorectal cancer

Several risk factors have been identified that are associated with the incidence of colorectal cancer. The risk factors (few are non-modifiable) that an individual cannot control include: bowel disease, family history and old age (Haggar and Boushey 2009). Modifiable factors associated with increased colorectal cancer risk include: the consumption of alcohol, tobacco and red meat, and being overweight. An increased level of physical activity, post-menopausal hormonal therapy, non-steroidal anti-inflammatory drugs and the consumption of vegetables/fruits have been reported to be linked to a decreased incidence of colorectal cancer (Johnson, Wei et al. 2013).

1.8.2 Clinical presentation of colorectal cancer

More than 25% of colorectal cancer patients demonstrate initial symptoms including: abdominal pain, anaemia, a change in bowel habit, anorexia and weight loss (Rosen, Buell et al. 2000; De Rosa, Pace et al. 2015). Other minor symptoms include: haematochezia, malaise, nausea, vomiting, an abdominal mass, tenesmus and an occult lesion. Approximately 20-25% of colon cancer patients and 18% of those with rectal cancer demonstrate metastasis at the time of the first diagnosis of the disease.

1.8.3 Diagnosis and staging of colorectal cancer

The gold standard for the diagnosis of colorectal cancer is colonoscopy, up to the caecum, combined with biopsy. In many cases, incomplete colonoscopy results from

inadequate bowel preparation and poor patient tolerance, as well as an obstruction or other technical problems. When additional computed tomography-colonography (CT or CTC) is used, it sheds further light on the diagnosis of colorectal lesions. The staging system for colorectal cancer that has been adopted by the National Cancer Institute (NCI) is provided in Figure 1.3.

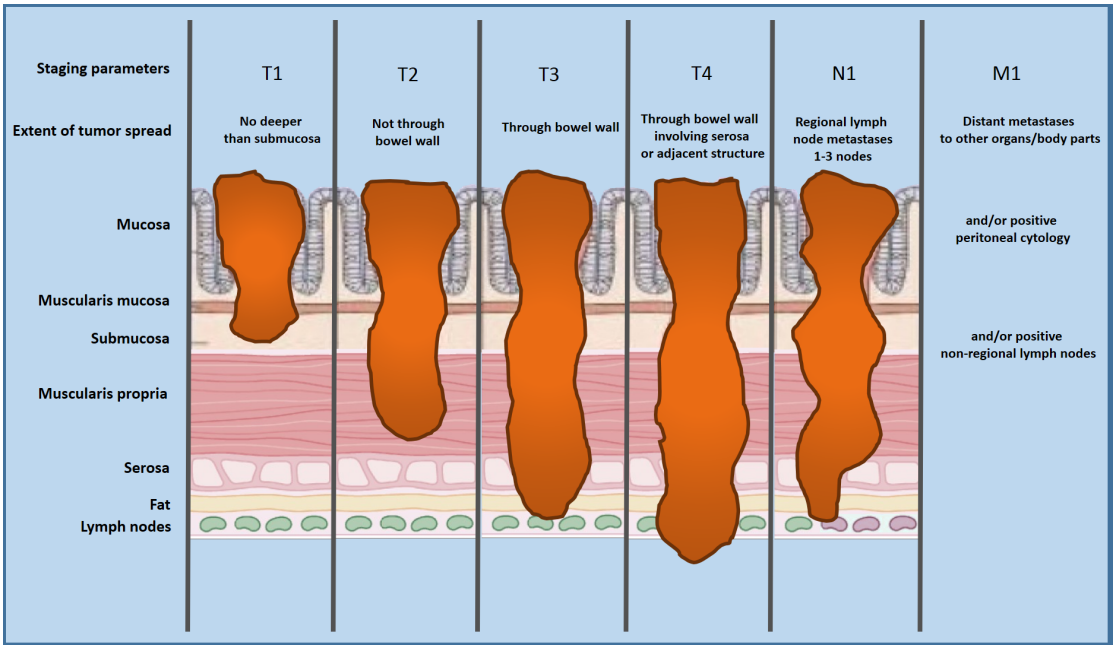

Figure 1.3: Staging system of colorectal cancer [adapted from (O'Connell, Maggard et al. 2004)]

1.8.4 Treatment of colorectal cancer

For the treatment of an early stage colorectal cancer, local excision is preferred, through a traditional transanal procedure or by a video-assisted technique; i.e., transanal endoscopic microsurgery (TEM) and transanal minimally invasive surgery (TAMIS) (Sgourakis, Lanitis et al. 2011; Guerrieri, Gesuita et al. 2014). In cases of early stage colon cancer, complete mesocolic excision (CME) is conducted, whereas total mesorectal excision (TME) is the appropriate procedure for early stage rectal cancer (Siani and Pulica 2014; Søndenaa, Quirke et al. 2014). On the basis of the patient's condition and choice, surgery can be performed laparoscopically or as an open surgery. Neoadjuvant chemoradiotherapy can also allow for radical surgery with TME to be carried out in locally, advanced colorectal cancer. Combinations of 5-fluorouracil (5-FU), using different chemotherapeutics, such as irinotecan and oxaliplatin, and targeted therapeutics, have been widely used by oncologists during the past decade (De Rosa, Pace et al. 2015).

1.9 Combined chemotherapy in cancer

Combination chemotherapy can be defined as the simultaneous use of more than one chemotherapeutic drug to treat advanced stages of cancer. In earlier days, cancer was routinely treated with a single drug, but a recent strategy is to use a combination of two or more drugs in unison (Carrick, Parker et al. 2009). As chemotherapeutic drugs kill cancer cells using different mechanisms, applying a combined chemotherapy increases the likelihood of the complete eradication of all cancer cells.

The idea of a combination chemotherapy against cancer first appeared in the 1960s, when scientists noticed that, in treating tuberculosis, a combination of antibiotics would reduce the risk of resistance. They also suggested that the combination of drugs would

work better in combatting cancer; for example, against fatal; i.e., acute lymphocytic leukaemia and Hodgkin's lymphoma, which became, essentially, remediable (Lister, Cullen et al. 1978). In the 1970s, combination chemotherapy was found to be more effective than monotherapy against lung cancer. Moreover, sequential chemotherapy (administering combined chemotherapeutic drugs one at a time and in sequence) provided better outcomes than using combined drugs at the same time. In the last decade, chemotherapeutic drug have been combined with immunotherapy, which has made immunotherapy drugs more effective (Lazzari, Karachaliou et al. 2018).

1.9.1 Basis of selecting drug combinations

The majority of currently used combination regimens have been developed empirically, but patterns of cross-resistance, toxicity, and mechanisms of action are taken into consideration during designing such regimens. Moreover, a mathematical model has been developed to describe the potency of drug combinations. The most typical drug combinations studied thus far that have been used by oncologists clinically are showing only additive-to-minimal synergistic outcomes (Yardley 2013). A few examples of such drug combinations are given in Table 1.1.

Table 1.1: Examples of drug combinations used in an oncology clinic

Drugs in combination	**Type of cancer**
Cisplatin + Vinorelbine	Non-small-cell lung cancer
(Doxorubicin + Cyclophosphamide) followed by Taxol	Lung cancer
Doxorubicin + Bleomycin + Vinblastine + Dacarbazine	Hodgkin lymphoma
Folinic acid + 5-fluorouracil + Oxaliplatin (FOLFOX)	Colorectal cancer
Folinic acid + 5-fluorouracil + Irinotecan (FOLFIRI)	Colorectal cancer
Folinic acid + 5-fluorouracil + Irinotecan + Oxaliplatin (FOLFIRINOX)	Pancreatic and colorectal cancer
Carboplatin + Paclitaxel	Ovarian cancer
Carboplatin + Docetaxel	Ovarian cancer
Paclitaxel + Bevacizumab	Ovarian cancer

The traditional approach has been to add a drug to an already approved regimen. Since the objective of combination therapy is to achieve desirable synergism, the exploration continues for the perfect drug partnership that will provide maximum tumour responses, while counteracting tumour progression.

1.9.2 Drugs chosen for combination in the present study

In the present study, the three platinum drugs are: cisplatin, oxaliplatin and LH5; gemcitabine, camptothecin, cucurbitacin B. They were selected for their binary sequenced combination. A brief description of the selected chemotherapeutic drugs is given in the following section.

1.9.2.1 Cisplatin (Cis)

Cisplatin, also known as *cis*-diamminedichloroplatinum (II), is a platinum complex with a square planar geometry in *cis* configuration. It was first synthesized in 1844 by Peyrone and its chemical structure was first described in 1893 by Alfred Werner. The cytotoxic property of cisplatin was first discovered serendipitously in the 1960s and, by the end of the 1970s, it had become the key component in systemic treatment of different tumours. Now it is difficult to find any cancer hospital in the world where cisplatin is not being used. Cisplatin is clinically proven to be the drug of choice against different types of cancers, such as testicular, lung, ovarian and leukaemia. As cisplatin is associated with drug resistance and has various side effects, combinations of cisplatin with other chemotherapeutics have been used to treat many human cancers (Dasari and Tchounwou 2014).

Cisplatin is an alkylating antineoplastic agent that becomes activated upon entry into a cell. When chloride ligands of cisplatin get replaced by water molecules in the cytoplasm, the hydrolysed product acts as a potent electrophile and reacts with the sulfhydryl groups present in proteins and peptides and nitrogen donor centres in DNA and RNA. Cisplatin prefers to bind to the N7 sites on the purine bases of guanine and adenine.

This binding can cause DNA distortion and damage to cancer cells, followed by cell cycle arrest and, finally, apoptosis. The formation of 1,2-intrastrand cross-links between purine bases and cisplatin are found to be the most significant changes in DNA. About 90% of all cisplatin-DNA adducts are 1,2-intrastrand d (GpG) adducts, while 10% are 1,2-intrastrand d (ApG) adducts. Other adducts, such as 1,3-intrastrand d (GpXpG) adducts, interstrand cross-links and non-functional adducts have also been reported to contribute to cisplatin's toxicity (Dasari and Tchounwou 2014). Molecular mechanisms for cisplatin action have been attributed to changes in calcium signalling, oxidative stress, caspases mediated apoptosis, interactions with protein kinase C (PKC), interactions with mitogen-activated protein kinase (MAPK) and p53 mediated apoptosis. Figure 1.4 shows the structure of cisplatin, whereas Figure 1.5 depicts the molecular mechanisms of cisplatin in cancer.

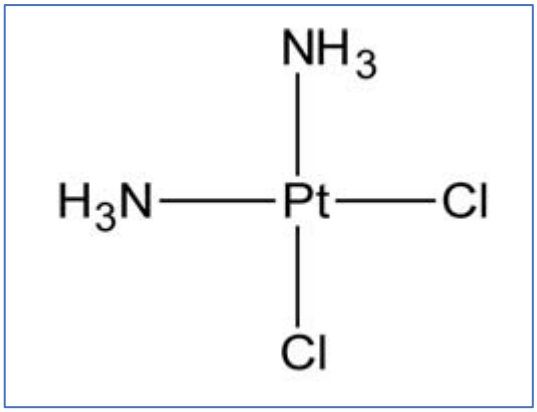

Figure 1.4: Chemical structure of cisplatin

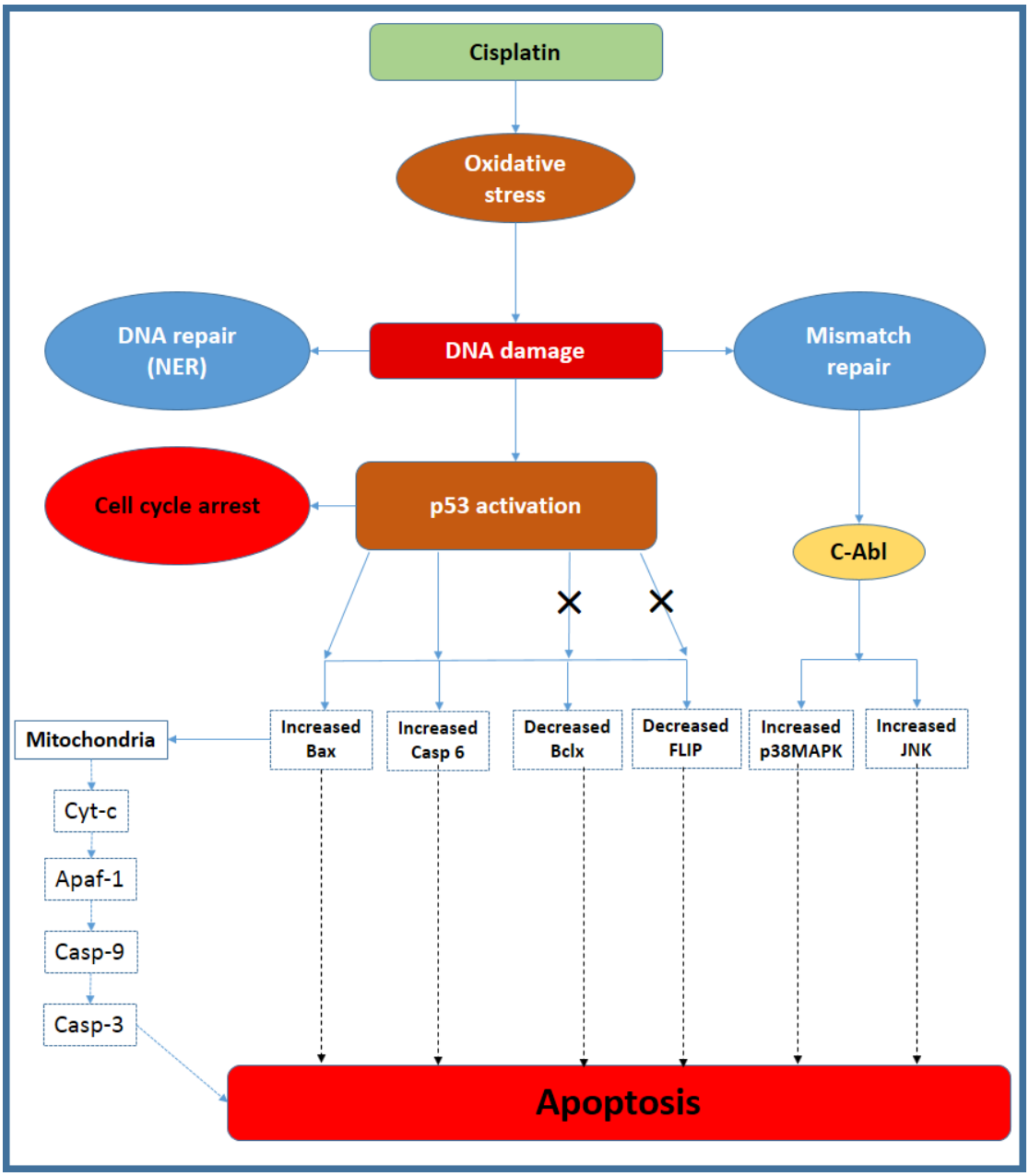

Figure 1.5: Molecular mechanism of cisplatin action [adapted from (Dasari and Tchounwou 2014)]

The major drawback of cisplatin use is its non-selectivity towards rapidly growing normal cells. High doses of cisplatin commonly cause nephrotoxicity, hepatotoxicity,

cardiotoxicity, neurotoxicity and ototoxicity. In a few instances, myelosuppression and gastrotoxicity have also been reported in the prolonged use of cisplatin.

1.9.2.2 Oxaliplatin (Oxa)

Oxaliplatin is the newer platinum derivative used in clinics throughout the world as a standard chemotherapy. It was discovered by Yoshinori Kidani in 1976 at the University of Nagoya City. Oxaliplatin differs from other platinum drugs in having a bulky diaminocyclohexane (DACH) moiety and an oxalate 'leaving group'. After entry into the cells, oxaliplatin undergoes extensive non-enzymatic transformation into intermediate (monoaquoDACH(1,2-diaminocyclohexane)platinum $[Pt(H_2O)Cl(DACH)]^+$ and diaquoDACHplatinum $[Pt(H_2O)_2(DACH)]^{2+}$), which can covalently bind with molecules like glutathione (GSH) or macromolecules containing methionine (Met) and cysteine (Cys). It is assumed that the presence of DACH moiety leads to the enhancement of antitumour activity via the differences in the patterns of molecular distortions, relative to the other approved platinum anticancer drugs; i.e., cisplatin and carboplatin. Oxaliplatin exerts its antitumour activity mainly by forming intrastrand platinum-DNA adducts, together with a relatively smaller proportion of interstrand cross-links. This inhibits tumoural DNA synthesis and repair, resulting in eventual cell apoptosis (Faivre, Chan et al. 2003). Several transport proteins, such as copper efflux transporters (CTRs), organic cation transporters (OCTs) 1, 2 and 3 (SLC22A1, SLC22A2 and SLC22A3), P-type ATPases, ATP7A and ATP7B, act in influx or efflux of oxaliplatin and may also play an important role in tumour response to oxaliplatin (Panczyk 2014). The antitumour activity of oxaliplatin is often found to be greater than that of cisplatin and/or carboplatin against various types of cell lines,

such as colon, ovarian, breast, neuroblastoma, endometrial, leukaemia, melanoma, non-small-cell lung, and gastric cancers.

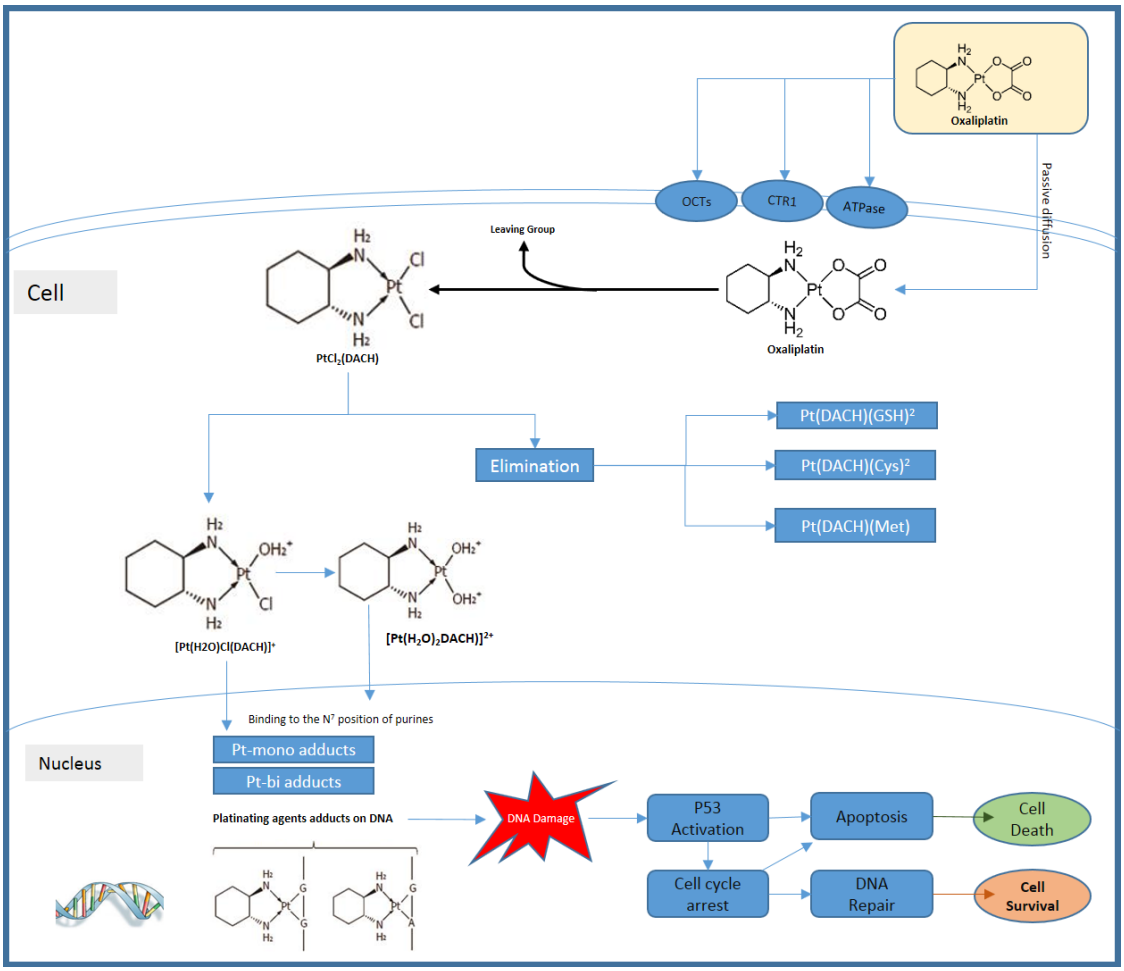

Figure 1.6: Mechanism of action of oxaliplatin [Adapted from Panczyk 2014]

Oxaliplatin is used in the FOFIRI, FOFOX and FOLFIRINOX combination regimen for the treatment of colorectal and pancreatic cancers. The major adverse effects of oxaliplatin use include: myelotoxicity, peripheral neuropathy, nausea, vomiting diarrhoea, nose bleeding, fatigue, headache and mouth sores (Alcindor and Beauger 2011).

1.9.2.3 LH5

LH5 [tris(quinoline) monochloroplatinum chloride] is a monofunctional planaramine platinum compound, synthesised by Laila Arzuman in 2016. LH5 has shown greater antitumour activity, compared to cisplatin, against A2780^{cisR} (cisplatin resistant) and A2780^{ZD0473R} (picoplatin resistant) ovarian cancer cell lines. The drug has shown strong synergy in combination with capsaicin and curcumin against A2780, A2780^{cisR} and A2780^{ZD0473R} ovarian cancer cell lines at different sequences of administration. In addition to the covalent interactions of LH5 with DNA as a monofunctional adduct, the antitumour action of LH5 has also been attributed to the presence of the bulky quinoline ligand, which can stack in between DNA base pairs and form hydrogen bonds (Arzuman, Beale et al. 2016).

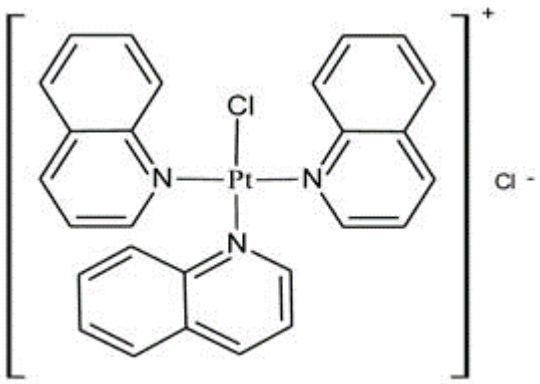

Figure 1.7: Chemical structure of LH5

1.9.2.4 Gemcitabine (Gem)

Gemcitabine (2′,2′-difluorodeoxycytidine or dFdC), is a deoxy-cytidine (dCyd) analog with two fluorine atoms substituted at the 2′-position of the ribose ring. It was first synthesised as an antiviral agent in the 1980s by Eli Lilly from the USA. However, further studies proved that gemcitabine works better as an anticancer drug. Since

another drug, dCyd analog 1-β-D-arabinofuranosylcytosine (ara-C), shares some structural and functional similarity with gemcitabine and is known to be active against leukaemia, gemcitabine was initially investigated for anticancer activity in blood cancers. Unexpectedly, unlike ara-C, gemcitabine had profound activity in solid tumours and in certain lymphomas. Currently, gemcitabine is considered as the drug of choice for the treatment of pancreatic, bladder, breast, ovarian and non-small-cell lung cancers, and has off-label indications for the treatment of other types of cancer (Bergman and Peters 2006).

Due to the hydrophilic nature of gemcitabine, it requires carrier proteins to enter into the cells. Seven different types of transporters have been identified, to date, that can be sodium dependent (concentrative nucleoside transporter [CNT]) or sodium independent (equilibrative nucleoside transporter [ENT]). Multidrug resistance proteins (MRPs) are responsible for pumping multiple agents out of a cell by active transport. Among all identified MRPs, gemcitabine is only the substrate for MRP4 and MRP5. After it has entered into the cell, gemcitabine is phosphorylated to produce gemcitabine monophosphate. Subsequently, this is converted by other pyrimidine kinases leading to the activation of diphosphate and triphosphate derivatives (dFdCTP). dFdCTP is thought to exert its cytotoxic affect by means of a number of distinct mechanisms (Binenbaum, Na'ara et al. 2015). Figure 1.9 demonstrates the molecular mechanism for gemcitabine-induced apoptotic cell death. The common side effects of gemcitabine use are flu-like symptoms, gastrointestinal tract disturbances, fever, fatigue, loss of appetite, skin rashes and changes to blood counts.

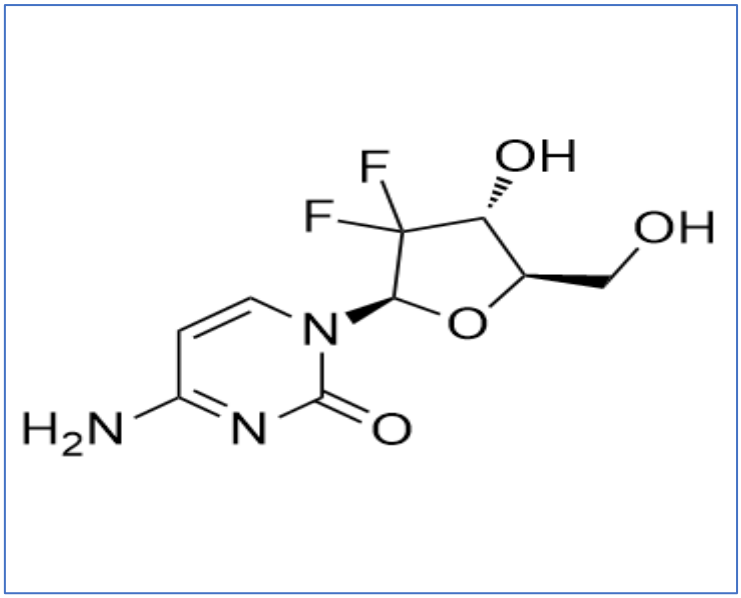

Figure 1.8: Chemical structure of gemcitabine.

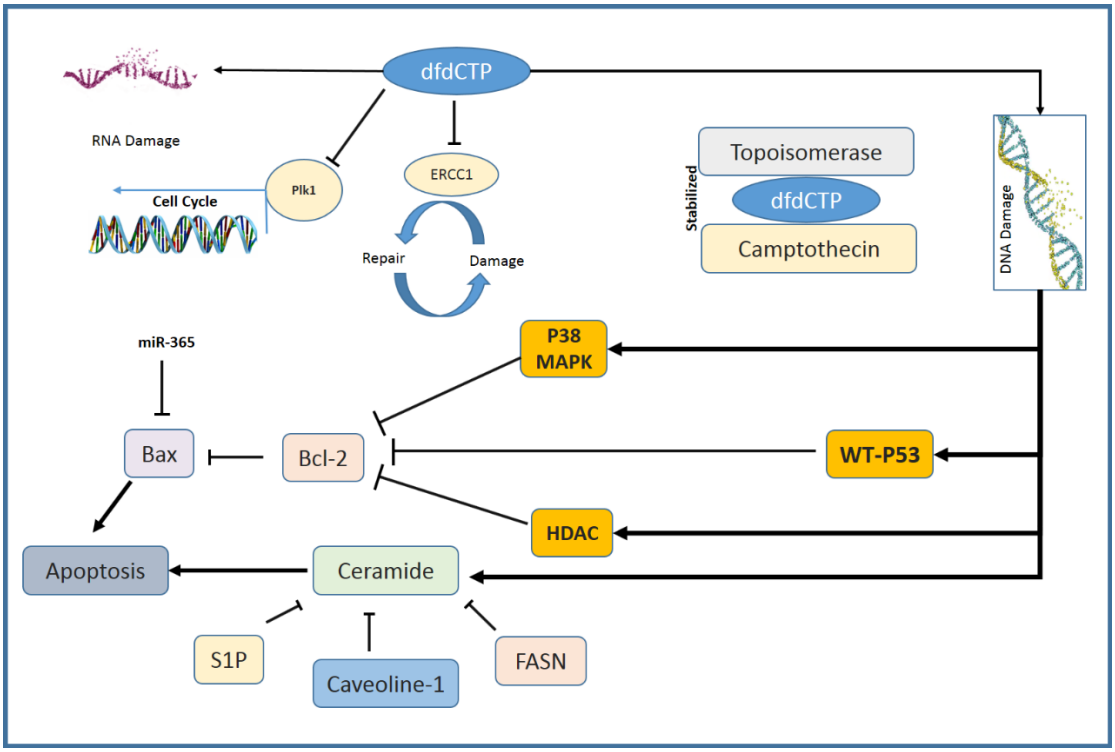

Figure 1.9: Molecular mechanism for gemcitabine-induced apoptosis [adapted from (Binenbaum, Na'ara et al. 2015)]

1.9.2.5 Camptothecin (Camp)

Camptothecin, a pentacyclic alkaloid, was first isolated in 1958 by Mansukh C. Wani and Monroe E. Wall from extracts of the Chinese native tree, *Camptotheca acuminate*. The promising results of camptothecin as an antitumour in preclinical animal models led to its evaluation in the clinic, but this was limited by its water insolubility. The sodium salt of camptothecin was found to be water soluble, but produced significant adverse effects, such as hemorrhagic cystitis and myelotoxicity, that led to the suspension of clinical trials. Later on, in the 1980s, more water soluble anologues of camptothecin; e.g., topotecan and irinotecan, were synthesised and received FDA approval for clinical use against colon and ovarian cancers (Liu, Li et al. 2015).

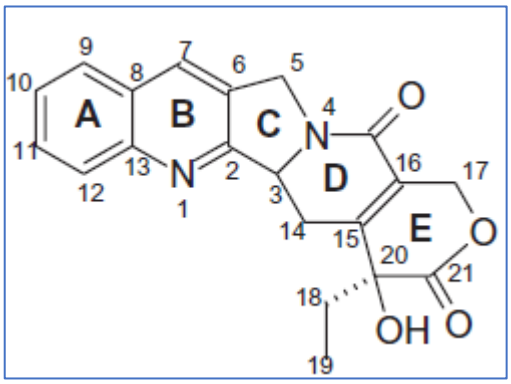

Figure 1.10: Structure of camptothecin

Camptothecin shows its antitumour activity by binding to the topoisomerase I-DNA complex. Camptothecin induces single DNA strand breaks and stabilises cleavable complex formed between topoisomerase I and DNA. When a DNA replication fork comes into contact with the complex, reversible single-strand breaks are changed into double-strand breaks that are not reversible and, thus, initiate programmed cell death via caspase activation. Inhibition of such activation will shift the cell from apoptotic state to transient G1 cell cycle arrest, followed by necrosis (Sriram, Yogeeswari et al. 2005).

Other than antitumour action, camptothecin has also shown antiviral, antiparasitic, pesticidal, antifungal and antipsoriasis activity. The adverse effects of camptothecin use include neurotoxicity and myelosuppression.

1.9.2.6 Cucurbitacin B (Cuc)

Cucurbitacins are tetracyclic triterpenoids derived from plants in the Cucurbitaceae family, as well as several other families of plants. Cucurbitacins came into focus in the 1960s, due to their promising anticancer activity in multiple cancers. In the 1990s, studies on cucurbitacin started to reappear after the NCI60 cell line screen, as a standard tool, had allowed for the systematic study of cucurbitacins (Lee, Iwanski et al. 2010).

At present, 12 main categories of cucurbitacins have been identified, based on their side-chain differences. There are 17 key cucurbitacins from cucurbitacin A to cucurbitacin T, and hundreds of derivatives from the key molecules have been synthesised. Among those, cucurbitacin B, curcurbitacin D, cucurbitacin E, cucurbitacin I, and their derivatives, have demonstrated profound anticancer activity.

The molecular mechanisms for the antitumour activity of cucurbitacin B have been attributed mainly to the JAK-STAT pathway, the Akt-PKB pathway, and the MAPK pathway of cancer cells (Lee, Iwanski et al. 2010). Inhibition of the JAK-STAT pathway was found to affect various downstream targets associated with pro-growth signalling (e.g., c-myc, cyclins, survivin) and apoptosis (e.g., p53, Bcl-xL, Bcl2). Despite the excellent anticancer activity of cucurbitacin B, its clinical use has some limitations; e.g., a low therapeutic index and dose-related adverse effects.

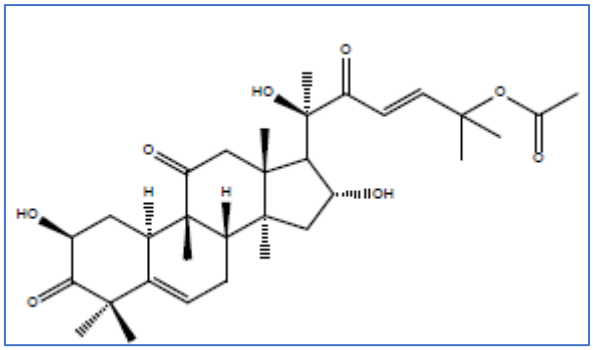

Figure 1.11: Chemical structure of cucurbitacin B

1.10 Bioinformatics in cancer

Cancer bioinformatics is now considered to be an important tool in the investigation of cancer in clinical medicine systems. It is anticipated that it will play a key role in the recognition and validation of biomarkers, explicit to clinical phenotypes linked with early diagnoses (Lu, Lu et al. 2015). Moreover, it can be employed as a measure in monitoring the progress of the disease and response to therapy. Recent targeting of protein-protein interactions associated with cancer, has become an emerging area of research interest. This is because the tumour-enhancing function of many abnormally expressed proteins in cancerous cells, are openly linked with the capacity to interact with a protein- binding partner. In 2012, Barry Honig and his colleagues first reported a milestone algorithm and created a database, named PrePPI (Predicting Protein-Protein Interactions) (Zhang, Petrey et al. 2012). The invention of PrePPI dramatically increased the number of available interactions (40,000 to 200,000) in the human interactome, when compared with experimentally generated resources. With enrichments made to their algorithm and the integration of other new types of data into its analysis, the PrePPI database now comprises approximately 1,350,000 predictions of protein-protein interactions, encompassing around 85% of the entire human proteome.

Recently, investigation of potential biomarkers for the progression and prognosis of various cancers using integrated bioinformatics has become a new arena of research. Differentially expressed genes for a particular cancer type can be filtered from available databases using software. Functional analysis can also be conducted by employing suitable software. Genes and pathways discovered from the integrated bioinformatics may pave the way for new treatments of cancer (Liu, Meng et al. 2019; Shen, Yu et al. 2019).

1.11 Aim of the present study

Currently, chemotherapy is being considered as the major treatment option for metastasised cancer. Around 70% of cancer patients receive chemotherapy during their treatment, but the problems of dose-related side effects and resistance to chemotherapy are the main challenges of the day for oncologists. A solution to the problems can be the use of drug combinations. Currently, many anticancer agents are given in combination, not only to increase efficacy, but also to overcome resistance to cancer cells. In addition, some drug combinations have been found to exhibit strong synergy towards therapeutic effects, with lower doses and reduced side effects.

The present study aims to explore combined drug effects from binary sequenced combinations of cisplatin with LH5, cisplatin with camptothecin, LH5 with camptothecin, LH5 with oxaliplatin, gemcitabine with LH5, gemcitabine with cisplatin, gemcitabine with oxaliplatin, cucurbitacin B with cisplatin and cucurbitacin B with LH5, against ovarian and colorectal cancer models. Mechanisms behind combined drug actions have also been subject of investigation based on DNA damage, cellular accumulation of platinum, Pt–DNA binding studies and proteomics. A bioinformatics study has been carried out with the identified proteins using publicly available datasets.

The specific objectives of the current project, as in other studies done in the host laboratory, are:

- the determination of the anticancer activity of the selected compounds (cisplatin, oxaliplatin, LH5, gemcitabine, camptothecin and cucurbitacin B), alone, against the ovarian and colorectal cancer models
- the determination of combined drug effects from selected binary sequenced combinations against the ovarian and colorectal cancer models
- the investigation of the nature of interaction with DNA of the selected compounds alone and in combinations
- the investigations of cellular platinum accumulation and the level of Pt-DNA binding alone and in combinations
- the investigation of changes in expression of main proteins associated with combined drug actions
- the identification of chemotherapy resistance pathways and successive exploration of key pathway proteins using The Cancer Genome Atlas (TCGA) data.

2 MATERIALS & METHODS

Preamble:

The present study constitutes continuation of effort in searching suitable binary combinations of anticancer drugs and tumour active phytochemicals against ovarian and colorectal cancer models. The research was conducted using established methodology in the host laboratory (Cancer Research Group, Discipline of Pathology, The University of Sydney) under the supervision of Associate Professor Fazlul Huq. Prior to combination study, IC_{50} values were determined for each of the selected drug (cisplatin, oxaliplatin, LH5, camptothecin, gemcitabine and cucurbitacine B) against human ovarian (A2780 and $A2780^{cisR}$) and colorectal (HT-29, Lim-1215 and Lim-2405) cancer cell lines. Combined drug actions for the binary combinations of the selected drugs were determined as a factor of added concentrations and sequence of administration. Mechanism underlying the combined drug action was investigated through DNA damage, platinum–DNA binding, cellular accumulation of platinum and proteomic study. Since similar research has been carried out in the host laboratory for more than twenty years, the methods used in the present study are essentially the same as those of previous studies. Only brief description of the used protocols will be mentioned in this chapter, detail of the experimental methods has been added in appendices.

2.1 Materials and instruments

The key reagents and equipment used in the present study as well as the suppliers' information are presented in Table 2.1.

Table 2.1: Important chemicals and equipment used in the present study

Reagents/Equipment	Used study method	Supplier
Oxaliplatin, Camptothecin, Gemcitabine and Cucurbitacine B	Cytotoxicity as a single drug and in binary combination, mechanistic studies	Sigma-Aldrich, USA
Cisplatin, LH5	Cytotoxicity as a single drug and in binary combination, mechanistic studies	Synthesized in the host laboratory
10% heat-inactivated fetal bovine serum (FBS)	Cell culture	Bovogen, Australia.
Roswell Park Memorial Institute (RPMI) 1640 medium, 200 mM L-glutamine and 5.6% (w/v) sodium bicarbonate	Cell Culture	Thermo Trace Pty Ltd, Australia.
Trypsin, Hepes, Dulbecco's phosphate buffered saline powder (DPBS), Dimethyl sulfoxide (DMSO) and Thiazolyl Blue Tetrazolium Blue / Methylthiazolyldiphenyl-tetrazolium bromide (MTT)	Cell culture during single drug cytotoxicity and combined drug activity	Sigma Aldrich Pty Ltd, Australia
96 well flat bottom plates with lids	Cell culture, DNA extraction	Edward Keller
25 cm^2 tissue culture flasks	Cell culture	Crown Scientific, NSW, Australia
DISMIC-25cs and DISMIC-45cs filter (cellulose acetate, 0.22 µm /0.45 µm hydrophilic, pressure limitation: 0.51MPa)	Sterilization by filtration	ADVANTEC
iMark™ Bio-Rad Microplate Reader Version 1.04.02E	Single drug cytotoxicity and combined drug activity	BIO-RAD, Australia
CO_2 Incubator, 5% CO_2 in air at 37ºC	Cell culture	SANYO, Japan
TC 10 BIO-RAD automated cell counter	Cell culture	BIO-RAD, Australia
EZ-10 spin column genomic DNA minipreps KIT and RNase	DNA binding, DNA damage	Astral Scientific Pty Ltd., Australia
Kodak Gel Logic 100 imaging system	DNA damage	Eastman Kodak Company, USA
SpectraMax-M3 multi-mode microplate reader, Molecular Devices	DNA binding, DNA damage	Biostrategy, v3.0.22

Atomic absorption spectroscopy (AAS) with GTA-120 graphite furnace tube atomizer	DNA binding	Varian SpectrAA 240
Triton-X, Disodium salt of ethylene diamine tetra acetic acid, Boric acid, Acetic acid, Tris base, Tris-HCL, Ethidium bromide	DNA damage	Sigma Aldrich Pty Ltd, NSW, Australia.
Agarose	DNA damage	BIO-RAD, USA
1,4-Dithiothreitol (DTT), Urea, Glycerol, Sodium dodecyl sulfate (SDS) and CHAPS (3[(3-Cholamidopropyl) dimethylammonio]-1-propanesulfonate hydrate	Proteomic	MP Biomedicals, LLC., USA
Protease inhibitor cocktail tablets (Complete, Mini, EDTA-free)	Proteomic	Roche Diagnostics, Germany
Protean® plus overlay agarose, Bovine serum albumin (BSA), (1.44 mg/ml)10x tris/glycine buffer, 0.2% Carrier ampholytes, Bio-Rad protein assay standard II kit (500-0007), Iodoacetamide, Mineral oil, Gels for 1st dimensional electrophoresis [ReadyStrip IPG strip of 11cm long, 3.3 mm wide, 3-10 NL (nonlinear) pH gradient and 0.5 mm thick gel], Sodium azide, Thiourea, Dye reagent concentrate (500-0006), BioSafe Coomassie G-250 Stain, Bromophenol Blue, Criterion TGX Precast gel, Wicks, ChemiDoc XRS system (Serial: 720BR1508), Phosphate buffered saline (PBS), Power Pac Universal, PROTEAN i12 IEF Cell, DeStreak reagent and Criterion Dodeca cell (Serial: 561BR 01908)	Proteomic	Bio-Rad, USA
Melanie (Version 7.0)	Proteomic	Swiss Institute of Bioinformatics, Switzerland

2.2 Preparation of the standard (stock) solution of drugs

Table 2.2 below provides details of stock solutions used in the determination of cytotoxicity, combination study and mechanistic studies.

Table 2.2: Concentrations of the stock solutions used in the study

Compound	Molecular weight	Concentration (g/5mL)	Solvent
Cis	300.00	1 mM (0.0015)	1 mL DMF+ 4 mL mQ water
Oxa	397.29	1 mM (0.0019)	1 mL DMF+ 4 mL mQ water
LH5	653.46	0.5 mM (0.00163)	2.5 mL mQ water +2.5 mL DMSO
Gem	263.198	1 mM (0.00132)	mQ water
Camp	348.35	1 mM (0.00143)	DMSO

2.3 Human cancer cell lines

The five human tumour cells used in the present study were A2780 and A2780^{cisR} (which were from ovarian cancer in origin) and HT-29, Lim-1215 and Lim-2405 (which were were from colorectal cancer in origin). Human parent ovarian cancer cell line A2780 was obtained as a gift from Dr. Philip Beale (Clinical Director, Oncology department, Concord Repatriation General Hospital, Australia). Cisplatin resistant A2780^{cisR} cancer cell line was produced by continual exposure to cisplatin in parent A2780 cell line. HT-29 human colorectal cell line was obtained as a gift from Dr. Mu Yao (Department of Endocrinology, The University of Sydney). Other two human colorectal cell lines: Lim-1215 and Lim-2405 were bought from Cell Bank, Australia.

2.4 Routine cell culture and antitumour activity of single drug

2.4.1 Regenerating cancer cells from cryovials

Previously stored cell line kept in cryovial was removed from the liquid nitrogen tank and defrosted within 50 seconds using preheated water bath at 37°C. When about 80% of ice in the cryovial melted, the contents were placed in a centrifuge tube containing 9 mL of pre-warmed 10% RPMI media inside the laminar airflow cabinet. The tube was then centrifuged for 5 minutes at 2000 rpm. The medium was discarded, and 2 mL of fresh medium was added. After resuspending the cell pellet in the fresh medium using pipette, the cell suspension was transferred into a cell culture flask bearing 8 mL of 10% RPMI media and then incubated for the cells to grow in 5% CO_2 incubator.

2.4.2 Monolayer subculturing technique

In subculturimg, monolayer subculturing technique was used throughout the study. In short, cells were allowed to reach 80-90% confluence in 25 cm^2 cell culture flask, checked under microscope. If there was no sign of contamination observed, the previous medium was removed, and the cells were washed with PBS. Trypsin was then added followed by incubation of the cell culture flask for 3 minutes. Trypsinization effect was confirmed under microscope by the presence of rounded up and detached cells from the substrate. Fresh media was added followed by transfer of cell suspension into a new corning flask with forceful pipetting. This was followed by incubation of new cell culture flask for 24 h in 5% CO_2 incubator. Cells were counted regularly, and the cell suspension was diluted as per the need of the desired experimental condition.

2.4.3 Preparation of media, PBS and trypsin solution

For the preparation of cell culture media, 200 mL of RPMI solution (5 X) was taken into a 500 mL container. 100 mL of FCS 10% in strength, 20 mL of hepes (1 M), 20 mL of 5.6% $NaHCO_3$, 10 mL of glutamine (200 mM) and 0.5 mL of saturated NaOH were mixed with the solution designated as RPMI. During preparation of PBS solution, 19.2 g of PBS powder was weighed and mixed with milli-Q water (1800 mL) in a 2 L volumetric flask. After gentle stirring for several minutes, pH was adjusted to 7.3 using 1 M HCl. The final volume of the PBS solution was 2 L adjusted by gradually adding milli-Q water and sterilized by filtration.

For the preparation of trypsin solution, 0.04 g of EDTA meaning ethylene diamine tetra-acetic acid was weighed and taken into a 200 mL volumetric flask. Measured amount of EDTA was mixed thoroughly in 2 mL of milli-Q water to dissolve. 20 mL of 2.5% trypsin was then added followed by adjustment of final volume to 200 mL by adding 178 mL of PBS. After tilting the volumetric flask for 2/3 minutes and the solution was then sterilized by filtration.

2.4.4 Cell counting and seeding

Depending on the cell line and experimental conditions, different concentrations of cells were used. The cell concentrations were determined through automated cell counter, counting slide and trypan blue. For quantification of cells, equal volume (10 µL) of cell suspension and trypan blue was taken and mixed. Then the dye-cell suspension was added on the both sides of counting slide. Cell counting was done and recorded by insertion of the slide into automated counter.

For seeding the cells, 100 µL of corresponding cell suspensions were added into each well of 96-well plates. The cell concentrations were varied from 2 X 10^5 cells/mL to 4 2 X 10^5 cells/mL of suspension. The plates were then incubated at 37°C for 24 h for seeding.

2.4.5 Long-term cryopreservation of cell lines

DMSO was used as a cryoprotective agent in the present study and the cell lines were preserved for long time in a nitrogen tank (below -130°C). The cells at late log phase were harvested at a concentration of 3 X 10^6 cells/mL. The cell suspensions were transferred into a centrifuge tube and spun for 3 min for 3000 rpm. The supernatant was discarded followed by resuspension of the pellet in 10% FCS. 5 mL of cell suspension was then mixed with 5 mL of 20% DMSO (2 mL DMSO + 8 mL of 10% FCS) to obtain the desired final concentration of 10% DMSO. The mixture was then transferred into prelabelled cryovials for future use.

2.4.6 MTT reduction assay

Solution of MTT was made by dissolving measured amount of powder in 500 mL of RPMI medium freed from serum to get the concentration of 1 mg/mL. Gentle rotation of the container was done for around 1 h to 3 h to mix each particle of MTT powder into the medium. During the entire period of mixing, the container was covered with aluminum foil to avoid from sunlight. The solution was then passed through the filters (0.45 µM) for sterilization and aliquoted into ten different 50 mL tubes, kept under refrigerated condition.

96-well plate was brought out from incubator and medium was removed by tilting the plate. MTT solution (50 µL) was then added to each well of 96-well plate and

reincubated for 4 h in 5% CO_2 incubator. After MTT solution was removed by tilting 96-well plate, to each well was added 150 µL of DMSO (Abdullah, Huq et al. 2003). The optical density (OD) was measured using microplate reader set at 595 nm. The percentage cell survival was calculated using the following equation:

$$\frac{\text{OD of compound or drug-treated cells}}{\text{OD of control}}$$

2.4.7 Determination of cell killing

The antitumour activity of the investigated compounds was expressed in terms of IC_{50} value meaning concentration required to kill half of the cancer cells. It was estimated from dose response curve obtained from the plot of percentage of alive cells against drug concentration. Each experiment was repeated at least five times to obtain statistically significant results.

2.5 Activity of drugs in binary combination

Combination study was carried out to find combined drug action (synergism, antagonism or additiveness) from the binary combination of selected drugs as a factor of sequence of administration and added concentrations. Three different sequences meaning: bolus or 0/0 (two drugs added at the same time); 0/4 (Drug1 added first followed by Drug2 four hours later) and 4/0 (Drug2 added first followed by Drug1 added four hours later) were used for combined drug administration. Drugs were

combined at the constant ratio of their activities meaning IC_{50} values and the combined cell effects were estimated from combination indices.

2.5.1 Drug additions

Studies on drug combinations were done by treating cancer cells under investigation with three different concentrations of compounds and for three different sequences of administration. Molar ratios of drugs in selected cell lines are shown in Table 2.4. The desired concentrations of cells were seeded in 96-well plate and incubated 24 h before addition of drugs. The plates were taken out from the incubator and 100 µL of respective drugs were added to each well for single drug additions. While for the wells planned for combined drug, it was made with 50 µL of Drug1 and 50 µL of Drug2. To each of the wells selected to serve as control, was added 100 µL of RPMI medium (Yunos, Beale et al. 2010). A working model applying to studies on drug combination is given in Figure 2.1. 72 h later of drug addition, percentage of alive cell was determined through MTT reduction assay.

Table 2.3: Summary of the molar concentration ratios between the drugs in the tested cell lines

Combination	Cell line	Molar Ratio
Cis+LH5	A2780, A2780^{cisR}, HT-29, Lim-1215	8.33, 1.18, 5.28, 3.80
Cis+Camp	A2780, A2780^{cisR}, HT-29, Lim-1215	0.018, 0.01, 0.01, 005
LH5+Camp	A2780, A2780^{cisR}, HT-29, Lim-1215, Lim-2405	0.0022, 0.0018, 0.0017, 0.0015, 0.0017
LH5+Oxa	A2780, A2780^{cisR}, HT-29, Lim-1215	0.098, 0.1049, 0.134, 0.071
Gem+LH5	A2780, A2780^{cisR}, HT-29, Lim-1215, Lim-2405	1609.8, 810.08, 581.66, 370.58, 0.002
Gem+Cis	A2780, A2780^{cisR}	193.02, 681.44
Oxa+Camp	Lim-2405	0.03
Gem+Oxa	Lim-1215, HT-29, Lim-2405	78.33, 26.47, 0.04
Cuc+Cis	A2780, A2780^{cisR}	81.96, 305.47
Cuc+LH5	A2780, A2780^{cisR}	683.19, 363.09

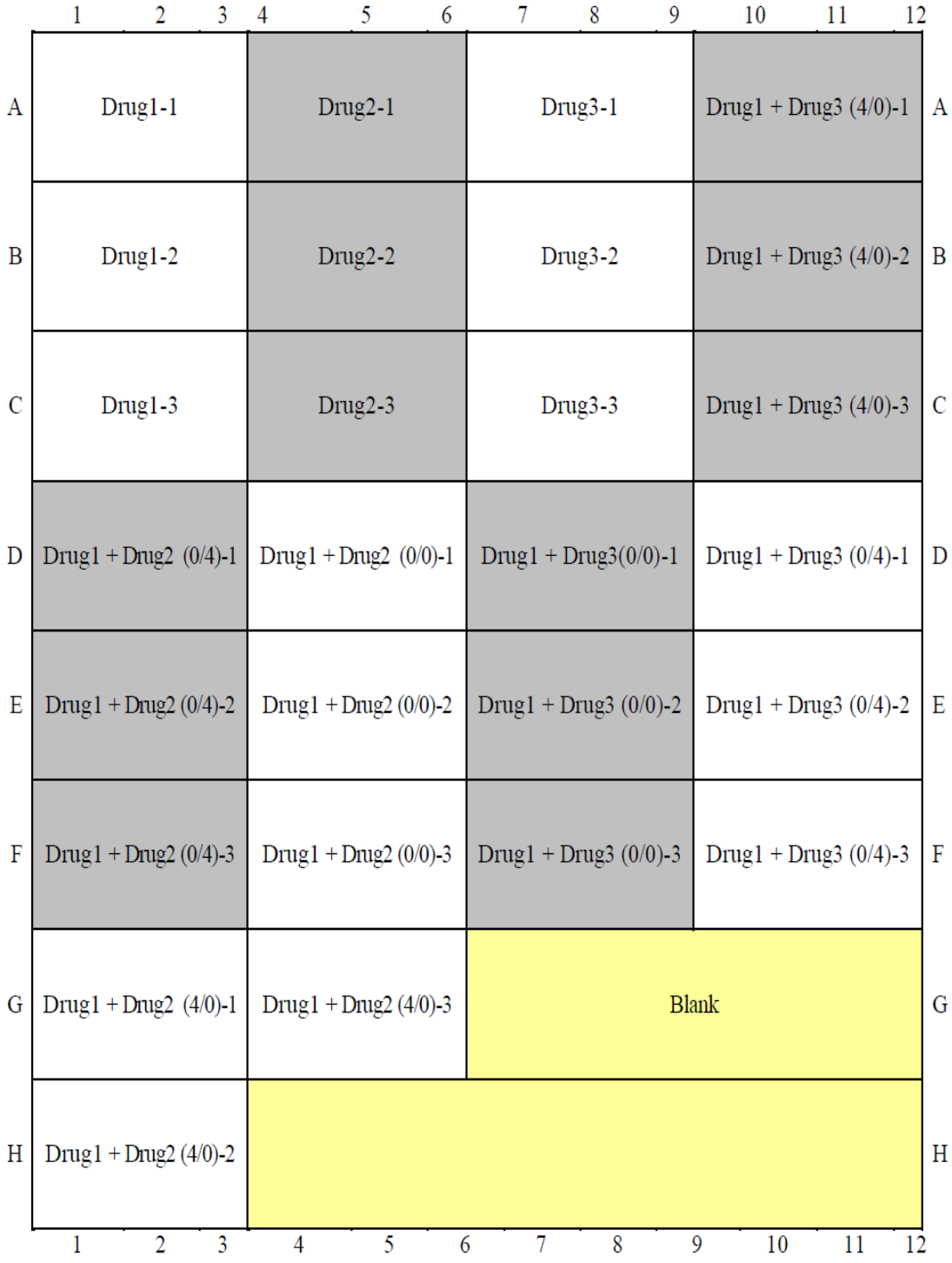

Figure 2.1: Combination study design for the addition of drugs in a 96 well plate, where 1 = 1/5 X IC_{50} concentration; 2 = IC_{50} concentration and 3 = 5 X IC_{50} concentration

2.5.2 Analysis of combined drug action

The combined drug effects were analysed both qualitatively and quantitatively using dose response curves and combination index values respectively. Dose response curves although visually attracting, provide only qualitative measure of combined drug action. In contrast, combination indices (CI) provide more accurate and precise measure of the combined drug action. CI value is defined as being sum of average concentration ratios of the drugs used in combination. CI value of less than 1 indicate synergistic effect, greater than 1 indicate antagonistic effect and close to 1 indicate additive effect. CI values were obtained from the software called Calcusyn which calculates the combined drug effects using the method of Chou-Talalay. The method was originally developed to study enzyme kinetics but has been modified and is widely used for determination of combined drug effects (Chou and Talalay 1984; Chou 2010; Chou 2018). CI values for binary combination can be obtained from the following formula

$$CI = \frac{D_1}{D_{1A}} + \frac{D_2}{D_{2A}}$$

Where, D_1 relates to concentration of first drug needed for A% cell kill while in combination; D_2 relates to second drug concentration needed for A% cell kill in combination; D_{1A} refers to concentration of first drug needed for A% cell kill when given alone; D_{2A} refers to concentration of second drug needed for A% cell kill when given alone. D_A can be calculated using the formula

$D_A = D_m [f_a/(1-f_a)]^{1/m}$

D_m is median effect dose; f_a is affected fraction and m is exponent of the dose response curve.

2.6 Cellular accumulation of platinum

2.6.1 Drug addition to cells followed by collection

Cellular accumulation study was conducted to gather mechanistic information relating towards the combined drug action. Few combinations were selected for ovarian cancer cell lines (Table 2.5) and few for colorectal cancer cell lines (Table 2.6), based on the results from combination study. During selection of combinations for the study, all types of combined outcome (synergistic, antagonistic and additive) from all studied cell lines was considered.

At the beginning of the study, stock solutions of compounds were freshly prepared. Final concentrations of compounds investigated in the present study are listed in Table 2.7.

Table 2.4: Final concentrations of drugs used in cellular accumulation study

Compound	Molecular weight	Concentration (g/5mL)
Cis	300.00	1 mM (0.0015)
Oxa	397.29	0.121 mM (0.00024)
LH5	653.46	1.17 mM (0.003)
Gemcitabine	263.198	0.0023 mM (0.0000031)
Camptothecin	348.35	0.00792 mM (0.00001)

Table 2.5: Combinations selected for cellular accumulation study against ovarian cancer models

Cell line	Combination	Combined effect
A2780	Cis + Camp (0/0)	Antagonistic
	Cis + Camp (0/4)	Additive
	Cis + Camp (4/0)	Antagonistic
	Cis + LH5 (0/0)	Antagonistic
	Cis + LH5 (0/4)	Antagonistic
	Cis + LH5 (4/0)	Synergistic
	LH5 + Camp (0/0)	Antagonistic
	LH5 + Camp (0/4)	Antagonistic
	LH5 + Camp (4/0)	Antagonistic
	LH5 + Oxa (4/0)	Antagonistic
	Gem + Cis (0/4)	Additive
	Cis + Camp (0/0)	Antagonistic
$A2780^{cisR}$	Cis + Camp (0/0)	Synergistic
	Cis + Camp (0/4)	Synergistic
	Cis + Camp (4/0)	Synergistic
	Cis + LH5 (0/0)	Antagonistic
	Cis + LH5 (0/4)	Antagonistic
	Cis + LH5 (4/0)	Antagonistic
	LH5 + Camp (0/0)	Additive
	LH5 + Camp (0/4)	Antagonistic
	LH5 + Camp (4/0)	Synergistic
	LH5 + Oxa (0/0)	Antagonistic
	LH5 + Oxa (0/4)	Antagonistic
	Gem + Cis (0/4)	Synergistic

Table 2.6: Combinations selected for cellular accumulation study against colorectal cancer models

Cell line	Combination	Combined effect
HT-29	Cis	Not Applicable
HT-29	LH5	Not Applicable
HT-29	Oxa	Not Applicable
HT-29	LH5 + Oxa (0/0)	Additive
HT-29	Cis + Camp (0/4)	Synergistic
HT-29	Cis + LH5 (0/0)	Antagonistic
Lim-1215	Cis	Not Applicable
Lim-1215	LH5	Not Applicable
Lim-1215	Oxa	Not Applicable
Lim-1215	LH5 + Camp (0/0)	Antagonistic
Lim-1215	LH5 + Camp (0/4)	Antagonistic
Lim-1215	LH5 + Camp (4/0)	Antagonistic
Lim-1215	LH5 + Oxa (0/0)	Antagonistic
Lim-1215	Cis + Camp (0/4)	Antagonistic
Lim-1215	Cis + LH5 (0/0)	Antagonistic
Lim-1215	Oxa + Gem (0/4)	Synergistic

Before addition of drugs, exponentially growing cells (50 x 10^4 cells/mL) in 4.75 mL medium were seeded into cell culture dishes and then incubated for 24 h. In case of single drug treatments, 125 µL of corresponding drug (Cis/Oxa/LH5) and 125 µL of each medium were added. For combined drug treatments, 125 µL of each selected drug was added to the cells. Following which culture dishes were again incubated for 24 h. The cells were collected as per the protocol given in Appendix I (Alam 2018).

2.6.2 Determination of accumulated platinum

0.5 mL of freshly prepared Triton-X was added to each prelabelled cell pellet. The cells were lysed using sonicator held on ice for 30 min which were then spun for 2 min at 14,000 rpm for 2 min. The supernatant was taken, and platinum contents were determined using Atomic absorption spectrophotometer. At first calibration curve was established by filling successively diluted platinum standard solution (made by adding 0.001 mL of concentrated 970 ppm standard platinum solution with 9.999 mL of 0. 1 M of HCl) using auto sampler (Almoyad 2018). Three different experiments were done for each sample.

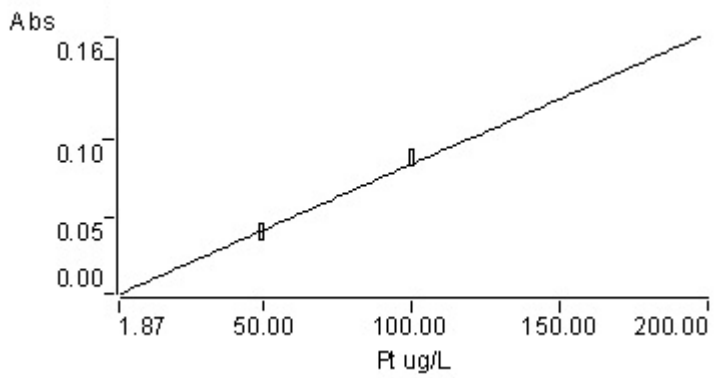

Figure 2.2: Calibration curve for determination of platinum

2.7 Binding of platinum with DNA

Similar to cellular accumulation of platinum study, platinum–DNA binding study was also conducted to identify any existed association between the combined drug effects and platinum–DNA binding. Methodology for addition of drugs and cell collection was exactly the same as described in the earlier section (2.6.1). EZ-10 spin column minipreps KIT was used to isolate pure genomic DNA. The detail method has been given in Appendix II. Pure genomic DNA concentration was estimated by using the relationship:

DNA concentration = Absorbance at 260 nm X 50 ng/µL.

200 µL of each pure genomic DNA sample was loaded into atomic absorption spectrophotometer and the extent of platinum-DNA binding was determined. Three different discrete experiments were accompanied for each sample.

2.8 DNA damage study

The study was conducted through agar-gel electrophoresis method to obtain the mechanistic insight concerning with the combined drug effects and DNA damage. Only ovarian cancer cell lines (A2780 and A2780^{cisR}) were used in the present DNA interactions study. Final concentrations of drugs used in DNA damage study are listed in Table 2.7. Chosen combinations for DNA damage study are presented in Table 2.8.

Table 2.7: Final concentrations of drugs used in DNA damage study

Compound	Molecular weight	Concentration (g/5mL)
Cis	300	1 mM (0.0015)
LH5	653.46	1.17 mM (0.003)
Camptothecin	348.35	0.00792 mM (0.00001)

Table 2.8: Selected combinations for DNA damage study

Combined drugs	Sequence of Addition
Blank (Control)	Not applicable
Cis	Not applicable
LH5	Not applicable
Cis +Camp	0/0
Cis +Camp	0/4
Cis +Camp	4/0
Cis +LH5	0/0
Cis +LH5	0/4
Cis +LH5	4/0

Drugs were added according to the same technique stated in section 2.6.

Methodology for addition of drugs and cell collection was exactly the same as described in the earlier section (2.6.1). Agar-gel electrophoresis technique has been portrayed in Figure-2.3.

Firstly 100 mL 50 X TAE buffer is prepared by dissolving 2M Tris base (24.22g), 2M glacial acetic acid (5.71 mL), 50 mM EDTA (1.861 g) in 94.3ml of mQ water

⇩

Then 1% agarose gel was prepared by measuring 2 g agarose gel power and mixing with 200 mL of ready prepare 1 X TAE buffer.

⇩

125uL of ethidium bromide was added into the gel and dissolved by using microwave.

⇩

Then the gel was gently poured into the tray with comb placed in position, left at room temperature for 45 min to solidify

⇩

250 µL of ethidium bromide was added in both side of electrophoresis chamber and the gel was immersed into the electrophoresis chamber filled with TAE buffer.

⇩

Few µL (calculated as equivalent to 0.2µg of DNA) of DNA sample was taken and added with few µL (calculated as to make the volume of 18 µL) of mQ water.

⇩

2 µL of chromatograph (0.25% bromophenol blue in 49% sucrose water prepared previously) dye was added to each sample and then added to respective well. Electrophoresis was conducted at 120 V for 2 hours. The gel was taken out and placed in the UV lamp to visualize the bands. Photograph of these bands were taken by Kodak Gel Logic 100 imaging system (GL 100).

Figure 2.3: Agar-gel electrophoresis for DNA damage study

2.9 Proteomic study

Lastly, proteomics was conducted to find out the proteins responsible for activity in terms of cell kill of drugs alone or in combination. Only ovarian cancer cells (A2780 and A2780^{cisR}) were used for this study and only for a few selected treatments (single or combined). A2780 cell line was treated with Oxa, Cis, LH5 each given alone, Cis+Camp (0/0), Cis+LH5 (0/0), Cis+LH5 (4/0), LH5+Oxa (0/0) and LH5+Camp (4/0). While for A2780^{cisR} cell line, the cells were treated with Oxa alone, Cis alone, LH5 alone, LH5+Camp (0/0), LH5+Camp (0/4), LH5+Camp (4/0), LH5+Oxa (0/0) and LH5+Oxa (4/0). The images of respective gels from A2780 and A2780^{cisR} ovarian cancer cells treated with drugs and were matched and compared with the untreated gels from the same cell lines. Later on, expression of different proteins was paralleled into treated and untreated groups. Figure 2.4 demonstrates important steps schematically, while the details of each step is given in Appendix II (Anwar 2018).

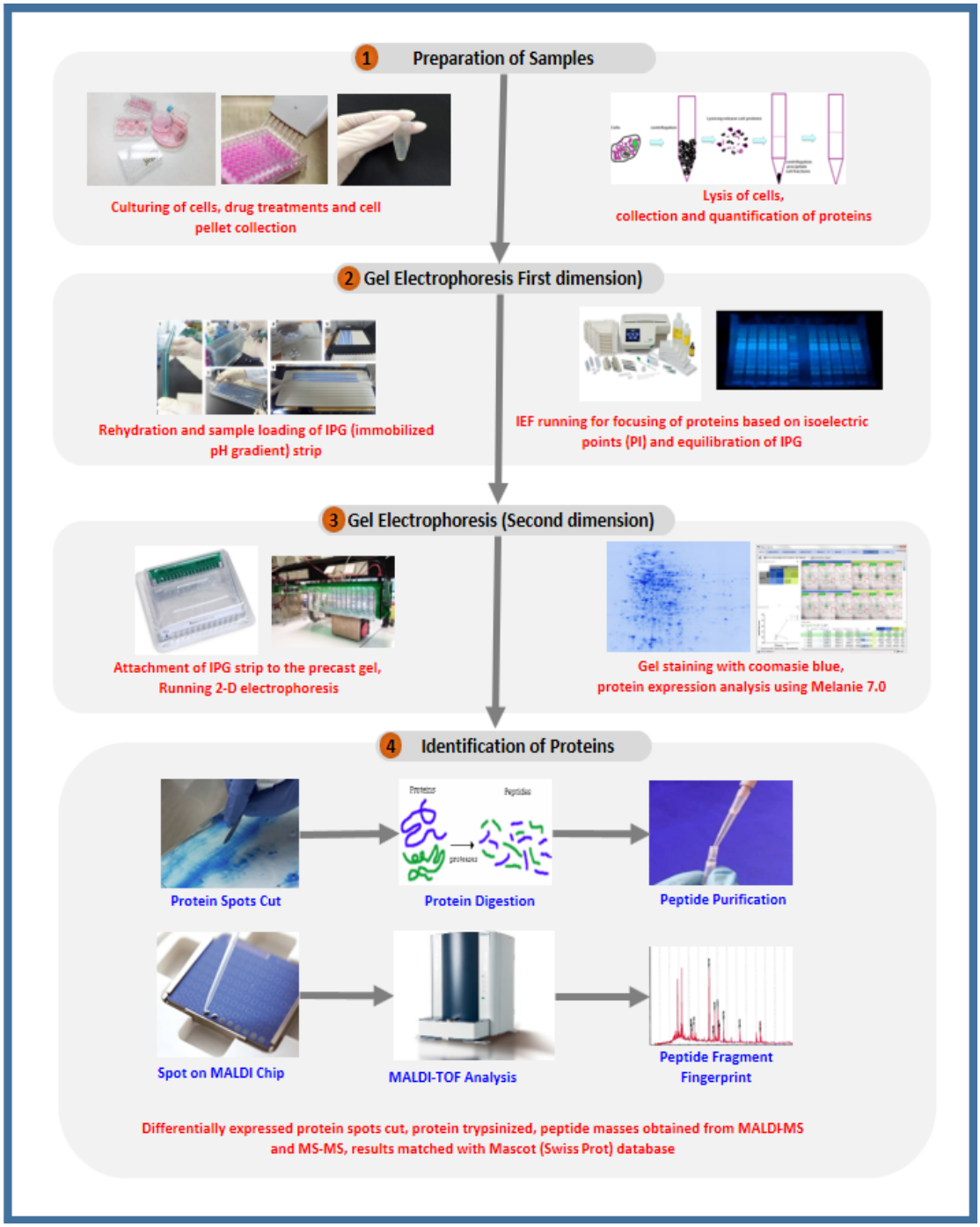

Figure 2.4: Key steps involved proteomic study

2.10 Bioinformatics

Clinical transcriptomic data derived from the patients of ovarian cancer have been used to identify the pathways connected with the resistance to chemotherapy and subsequent analysis of significant pathway proteins. To identify the proteins linked with the survival of patients having ovarian cancer, rich data set generated from The Cancer Genome Atlas (TCGA) project have been used. Cox Proportional Hazard models have been used to determine the contribution of clinical issues and expression of genes on the survival of ovarian cancer patients. Twenty genes of interest (confirmed as significant in the present study) have been selected to conduct the bioinformatics study. Histological grade of ovarian cancer as well as age during first identification were obtained from pathology recording. The stage of ovarian cancer was documented according to the classification system proposed by the American Joint Committee (Hossain, Islam, Quinn, Huq, & Moni, 2018). Patient survival data were derived from the total number of months of patient survival after the initial diagnosis of ovarian cancer. TCGA barcode was used to differentiate between normal and tumour samples. In RNAseq analyses, gene expression value was calculated by z-scores for each expression value following the same methodology described by Arzuman and Moni et. al (Arzuman et al., 2019). Pathways and functional correlation analyses of the identified 20 proteins from proteomics were also performed following the methodology described by Arzuman and Moni et. al (Arzuman et al., 2019). Enrichr software tool has been used to perform ontology enrichment analysis of the validated important genes. A web-based visualization software resource, STRING has been used to investigate the protein-protein interaction network.

3 RESULTS

Preamble:

In the present study, two platinum anticancer drugs (Cis, Oxa) and one designed platinum complex (LH5) were combined with other three non-platinum tumour active compounds (Gem, Camp and Cuc) in quest of suitable combinations to overcome drug resistance and better therapeutic outcome with reduced side effects. The study was conducted for two ovarian cancer cell lines (A2780 and A2780^{cisR}) and three colorectal cancer cell lines (HT-29, Lim-1215 and Lim-2405). This chapter details results of cytotoxicity of each selected compounds against the tumour models either alone or in selected binary combinations, cellular accumulation of platinum, Pt–DNA binding, DNA damage and proteomic study.

3.1 Antitumour activity of the compounds alone

Anticancer activity of the compounds against ovarian and colorectal cell lines was determined through MTT reduction assay. IC_{50} values were employed as measures of anticancer activity. To obtain the IC_{50} value of a drug, dose response curves were generated by plotting cell survival fractions against concentrations.

3.1.1 Dose response curves (Ovarian cancer cell lines)

Dose response curves of the investigated compounds (cisplatin, camptothechin, LH5, oxaliplatin, gemcitabine and cucurbitacine-B) obtained from A2780 and A2780^{cisR} cell lines are presented in Figure 3.1 and Figure 3.2.

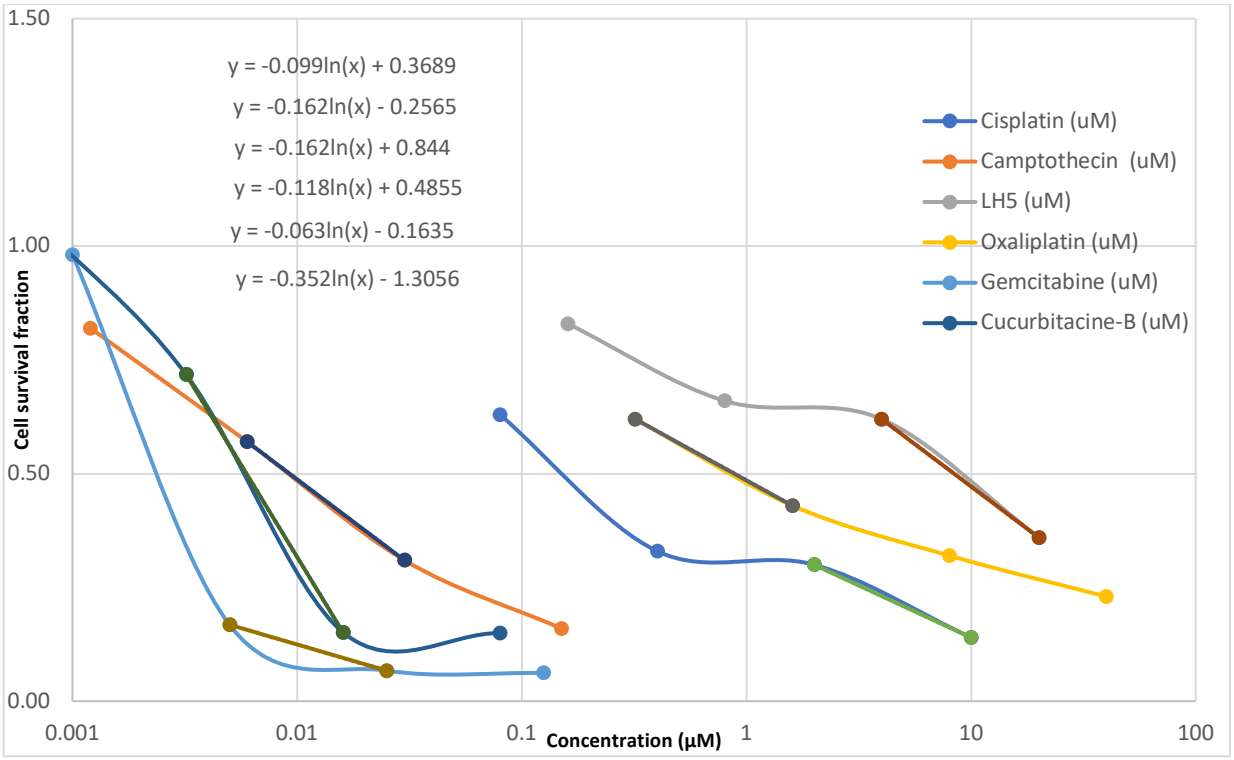

Figure 3.1: Activity versus concentration plots against A2780 cell line

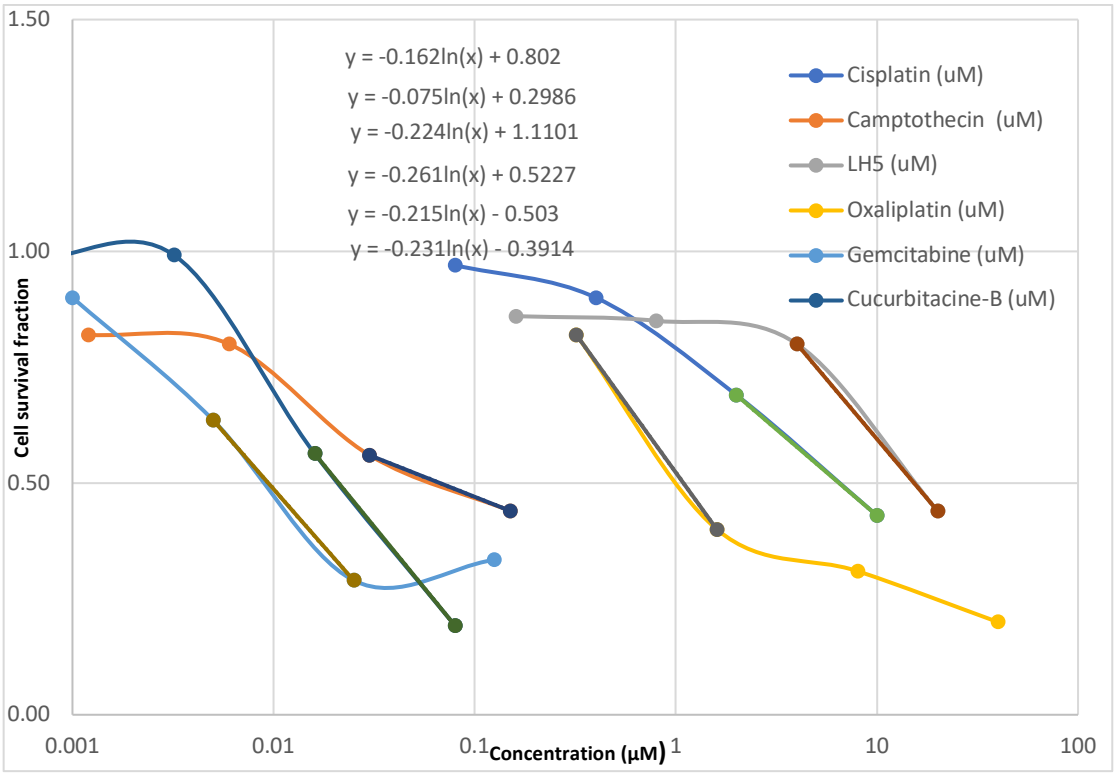

Figure 3.2: Activity versus concentration plots against A2780^{cisR} cell lines

It can be seen from Figure 3.1 that gemcitabine, cucurbitacine-B and camptothecine are more active than cisplatin, oxaliplatin and LH5 against A2780 human ovarian cancer cell line. Among the studied compounds, gemcitabine showed the highest activity whereas LH5 was the least active against A2780 cell line. Dose response curves obtained from $A2780^{cisR}$ cell lines (Figure 3.2) also demonstrated that gemcitabine, cucurbitacine-B and camptothecine were more active than cisplatin, oxaliplatin and LH5. As in parent A2780 cell line, gemcitabine was the most active compound and LH5 was the least active one among all the tested compounds against cisplatin resistant $A2780^{cisR}$ cell line.

3.1.2 Dose response curves (colorectal cancer cell lines)

Dose response curves of the investigated compounds (cisplatin, camptothechin, LH5, oxaliplatin, gemcitabine and cucurbitacine-B) obtained from HT-29, Lim-1215 and Lim-2405 cell lines are presented in Figure 3.3, Figure 3.4 and Figure 3.5 respectively.

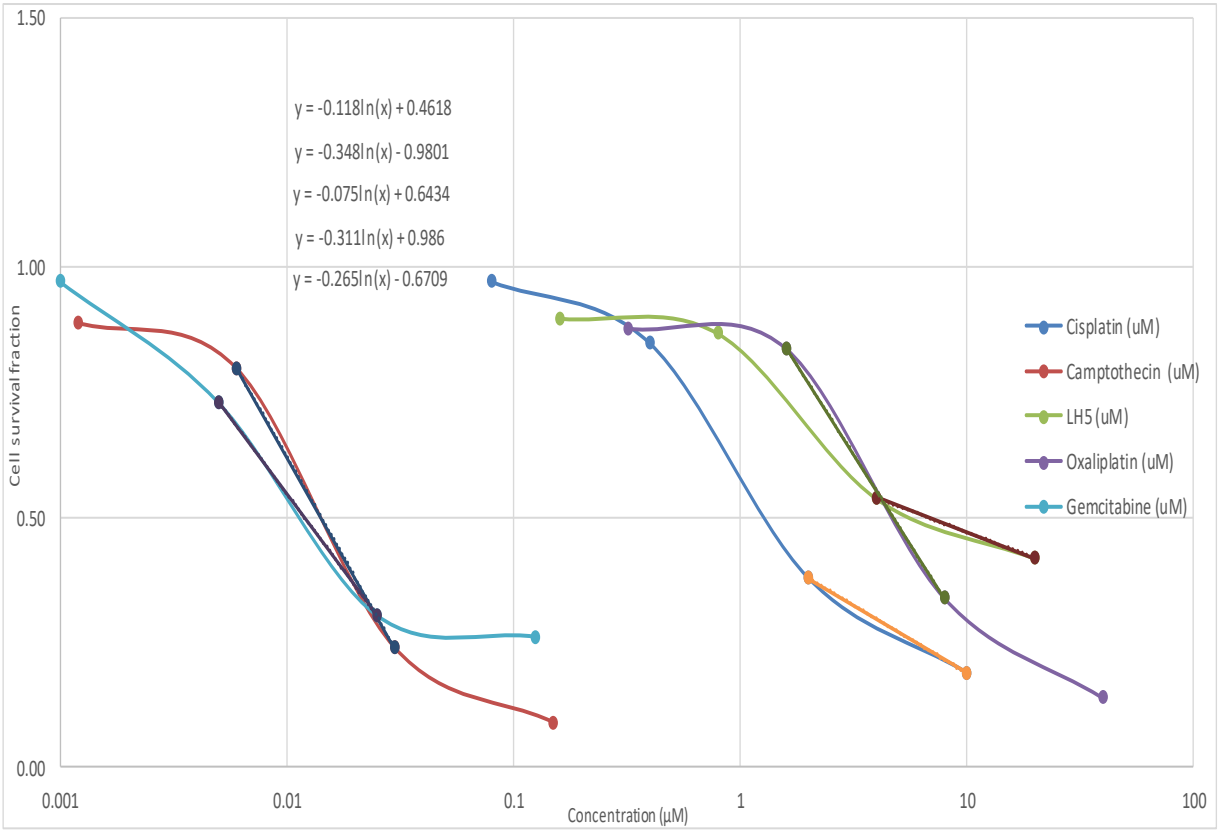

Figure 3.3: Activity versus concentration plots against HT-29 cell line

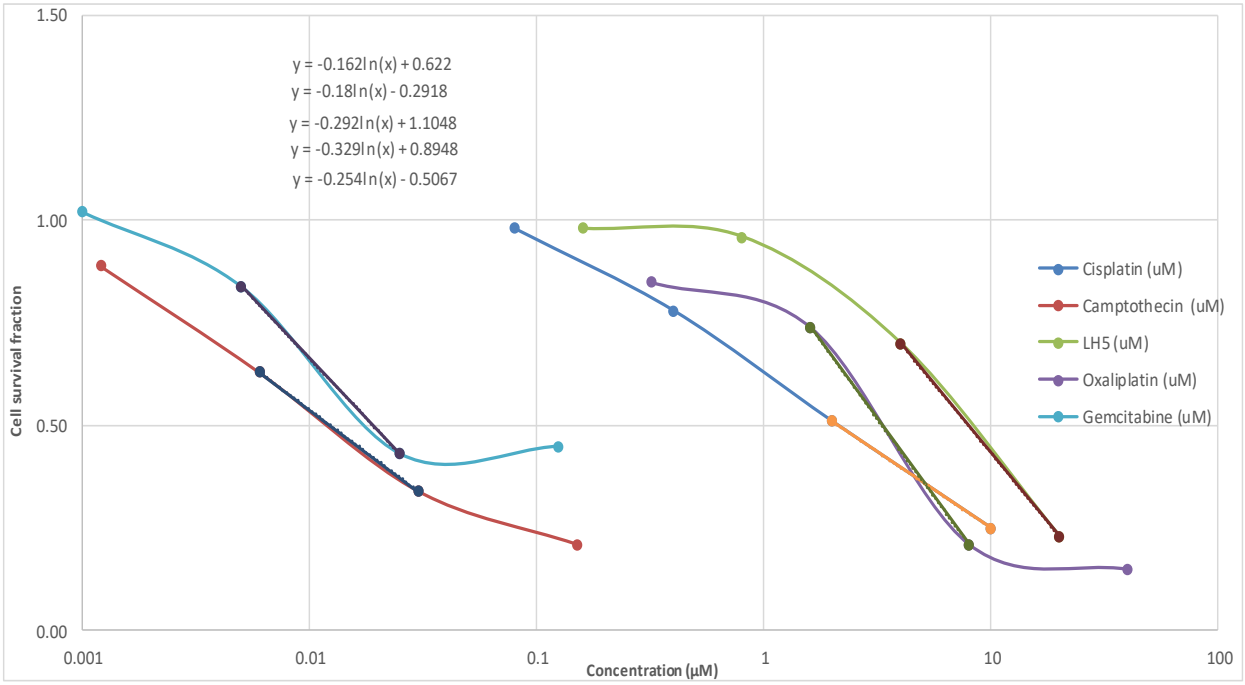

Figure 3.4: Activity versus concentration plots against Lim-1215 cell line

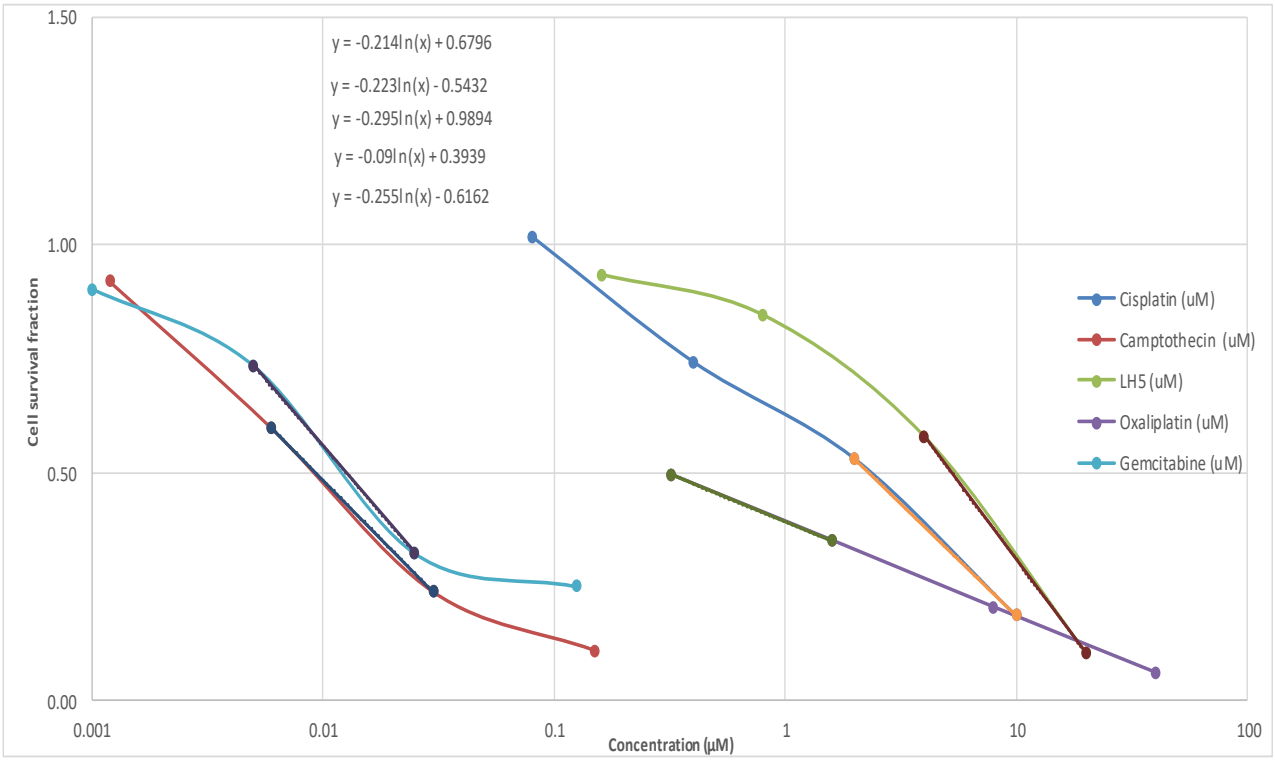

Figure 3.5: Activity versus concentration plots against Lim-2405 cell line

It is evident from Figure 3.3 that, gemcitabine showed the greatest activity among the tested compounds followed by camptothecine, cisplatin, oxaliplatin and LH5 against HT-29 cell line. However, against Lim-1215 (Figure 3.4) and Lim-2405 (Figure 3.5) cell lines, greatest activity was shown by camptothecine and lowest by LH5.

3.1.3 IC_{50} values (ovarian cancer cell lines)

IC_{50} values were obtained from dose response curves for the investigated compounds. Table 3.1 shows the IC_{50} values of compounds against ovarian cancer cell lines, whereas Figure 3.6 gives the graphical presentation of the same.

Table 3.1: IC_{50} values (μM) of the compounds against ovarian cancer cell lines

Compound	IC_{50} values	
	A2780 cell line	$A2780^{cisR}$ cell line
Cis	0.26 ± 0.02	6.45 ± 0.68
Camp	0.009 ± 0.0002	0.07 ± 0.0003
LH5	8.36 ± 1.18	15.24 ± 2.04
Oxa	0.88 ± 0.03	1.09 ± 0.13
Gem	0.00002 ± 0.00007	0.009 ± 0.0006
Cuc	0.006 ± 0.003	0.02 ± 0.003

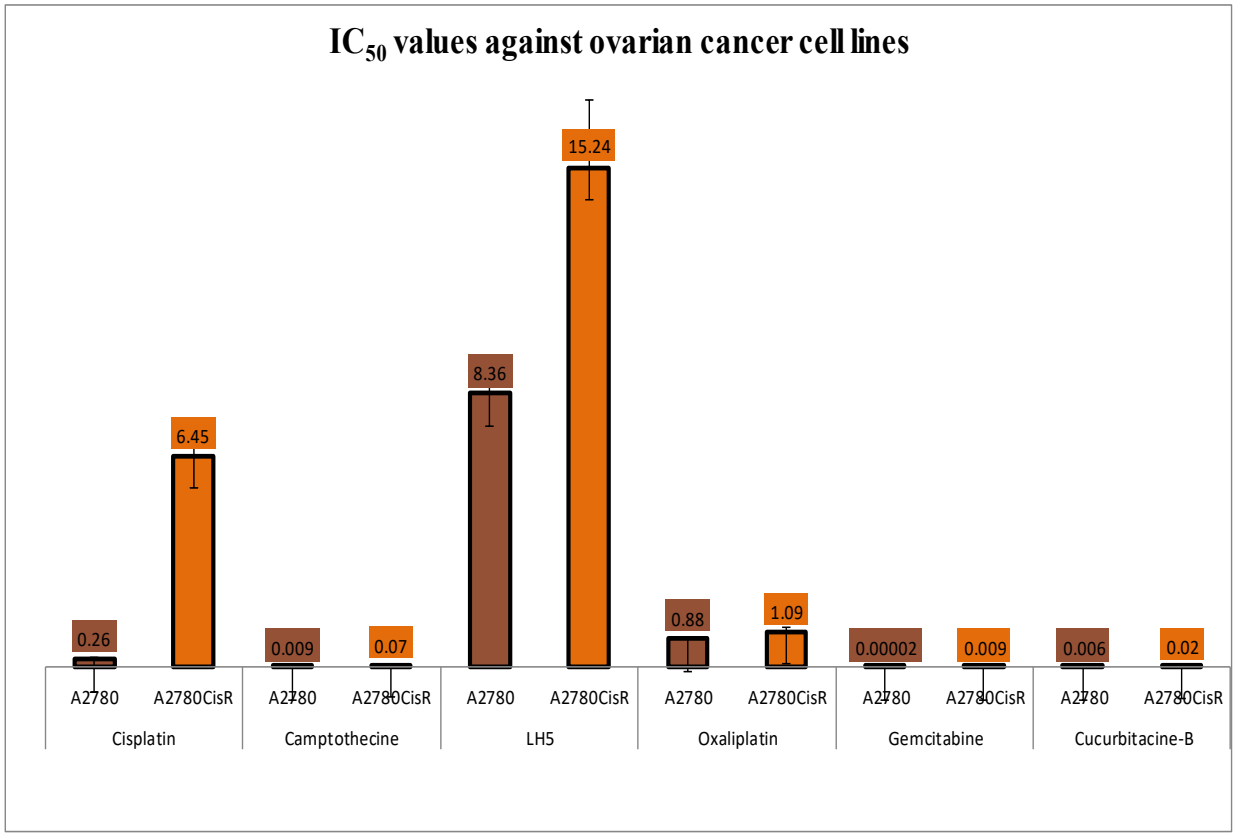

Figure 3.6: IC_{50} values against ovarian cancer models

It is clear from Table 3.1 and Figure 3.6 that, among the six compounds, gemcitabine showed the greatest anticancer activity seen in the lowest IC_{50} values against both the human ovarian cancer cell lines. Cucurbitacine-B is the second most active compound among the tested compounds in both parent and resistant A2780 and A2780^{cisR} cancer cell lines. The order of activity of all compounds against A2780 cell line was gemcitabine>cucrurbitacine-B>camptothecine>cisplatin>oxaliplatin>LH5. However, the order of activity against A2780^{cisR} cell line was gemcitabine>cucrurbitacin-B>camptothecin>oxaliplatin>cisplatin>LH5.

3.1.4 IC_{50} values (colorectal cancer cell lines)

Table 3.2 represents IC_{50} values of the compounds against selected colorectal cancer cell lines, whereas Figure 3.7 gives graphical presentation of the same. It can be seen that as in ovarian cancer models, gemcitabine was the most active against HT-29 colorectal cancer cell line. However, camptothecine was the most active against Lim-1215 and Lim-2405 cell lines. The order of activity of all compounds against HT-29 and Lim-1215 cell line was camptothecin>gemcitabine>cisplatin>oxaliplatin>LH5. However, the activity order of all investigated compounds against Lim-2405 cell line was camptothecin>gemcitabine>oxaliplatin>cisplatin>LH5.

Table 3.2: IC_{50} values (μM) of the compounds against colorectal cancer cell lines

Compound	IC_{50} values (μM)		
	HT-29 cell line	Lim-1215 cell line	Lim-2405 cell line
Cis	0.72 ± 0.08	2.12 ± 0.38	2.31 ± 0.47
Camp	0.0142 ± 0.0001	0.0123 ± 0.0003	0.0093 ± 0.0002
LH5	6.77 ± 0.98	7.93 ± 1.04	5.25 ± 0.96
Oxa	4.77 ± 0.83	3.32 ± 0.63	0.31 ± 0.50
Gem	0.012 ± 0.0009	0.018999 ± 0.0009	0.0126 ± 0.001

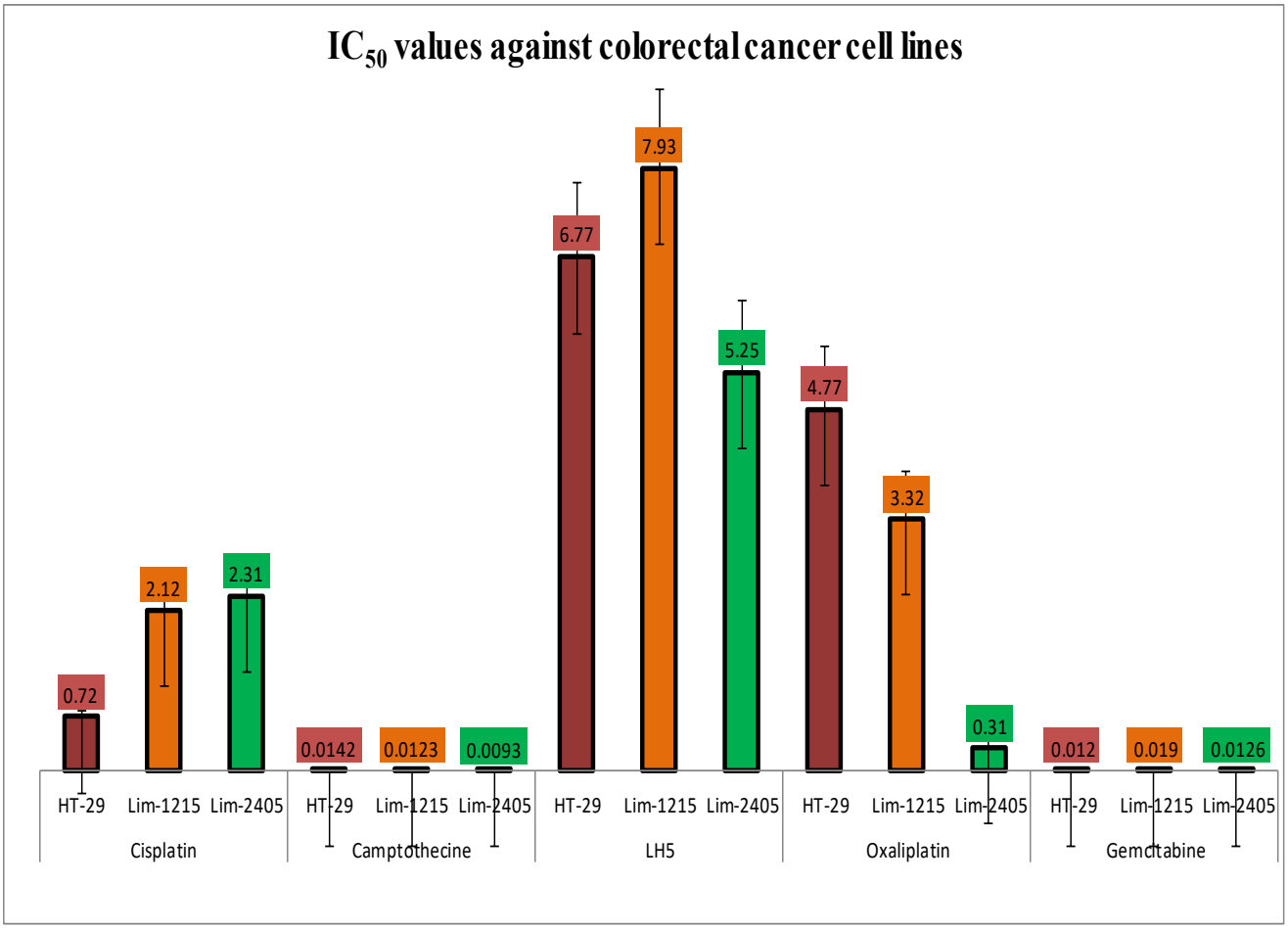

Figure 3.7: IC_{50} values against colorectal cancer models

3.2 Combination of drugs

3.2.1 Dose response curves

Dose response curves describe the qualitative measure of combined drug action which pictorially represents the effect. This section deals with the dose response curves obtained from various combinations of selected drugs in different cell lines.

3.2.1.1 Combination of Cis with LH5

Figures 3.8 to 3.11 show the dose response curves obtained for the combinations of Cis with LH5 against ovarian A2780 and A2780^{cisR} ovarian cancer cell lines, colorectal HT-29 and Lim-1215 cancer cell lines respectively at three sequences of administration (0/0, 0/4 and 4/0).

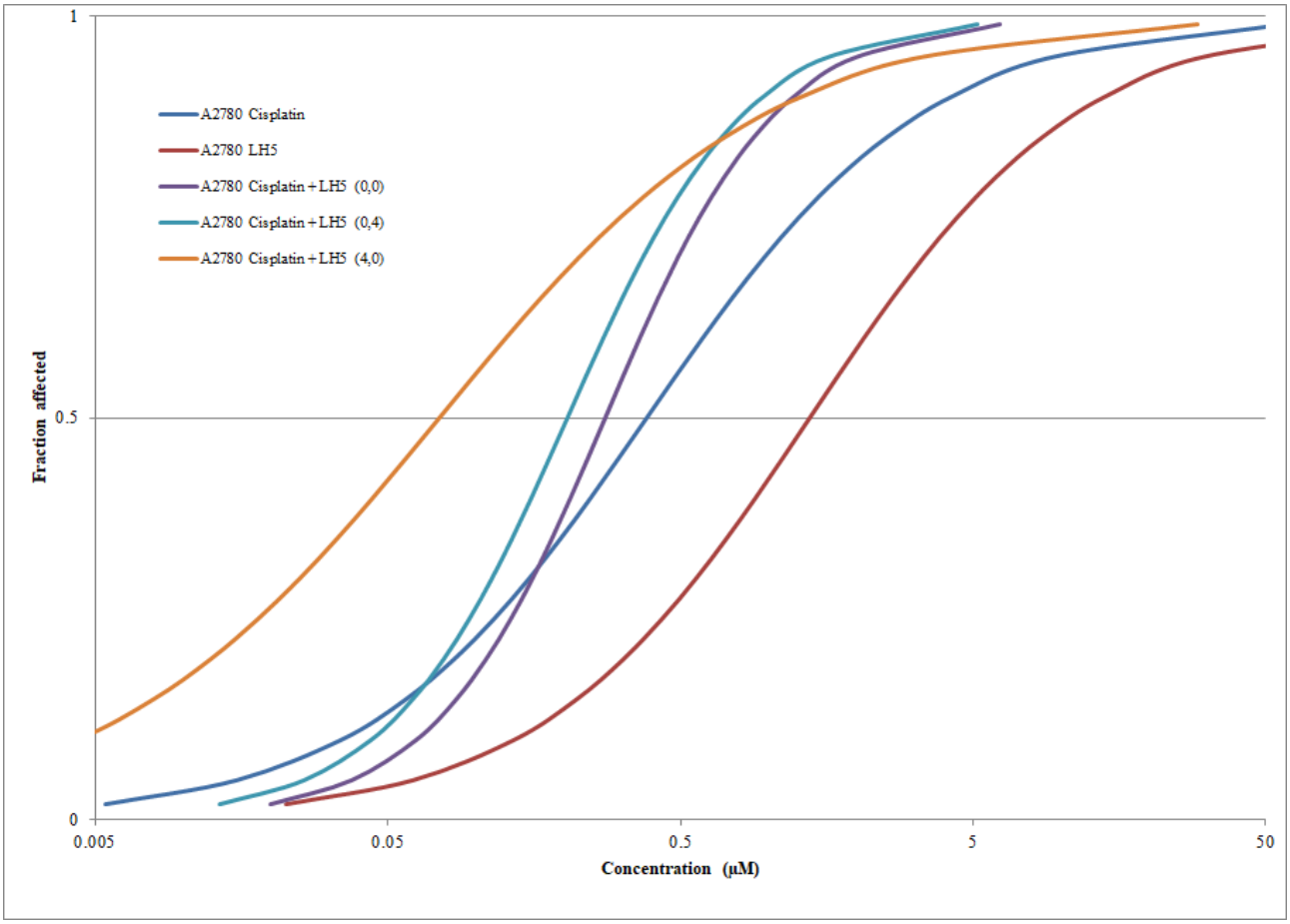

Figure 3.8: Activity versus concentration plots from combination of Cis with LH5 against A2780 cell line

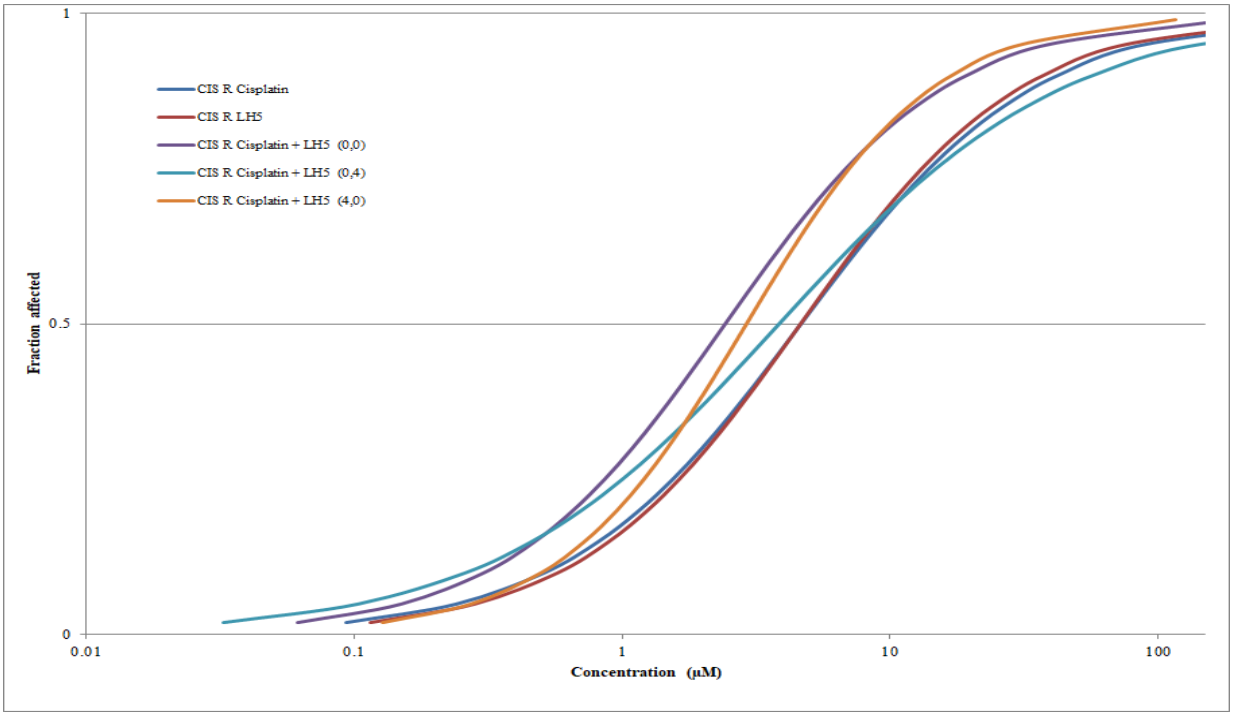

Figure 3.9: Activity versus concentration plots from combination of Cis with LH5 against A2780^{cisR} cell line

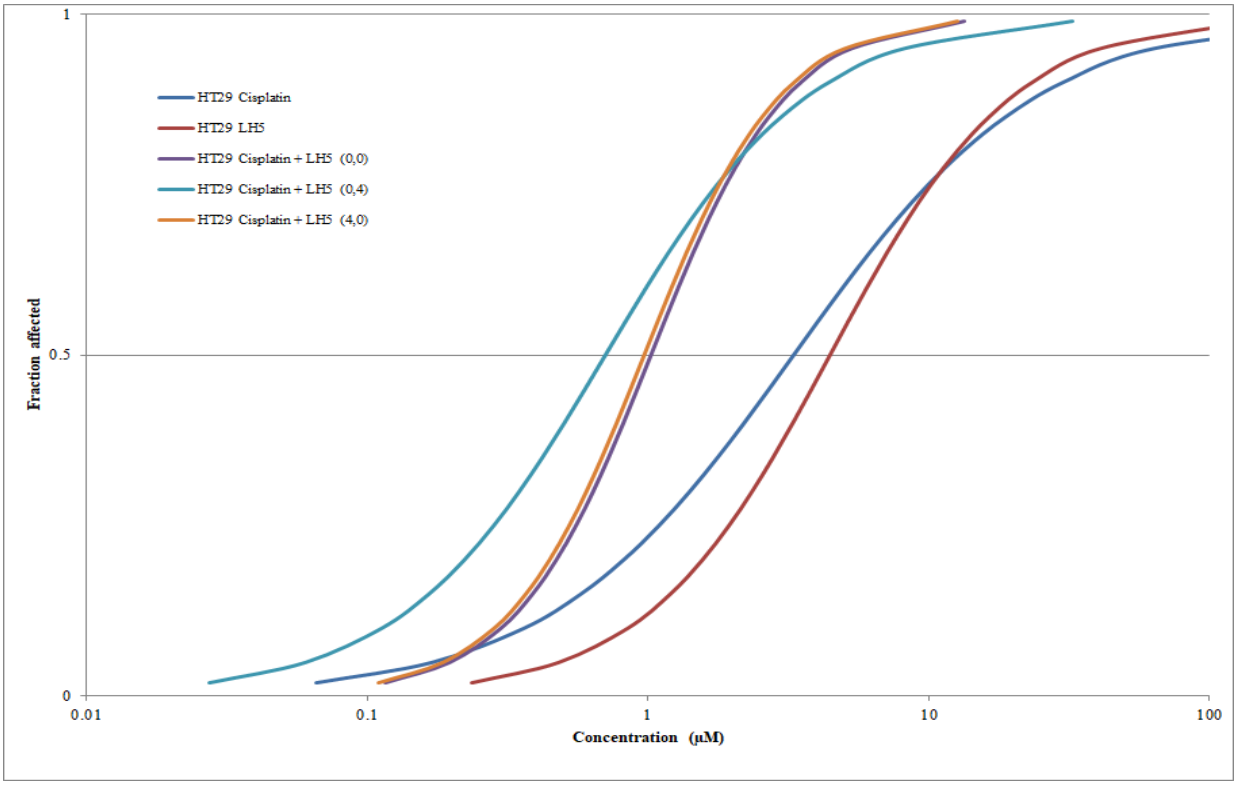

Figure 3.10: Activity versus concentration plots from combination of Cis with LH5 against HT-29 cell line

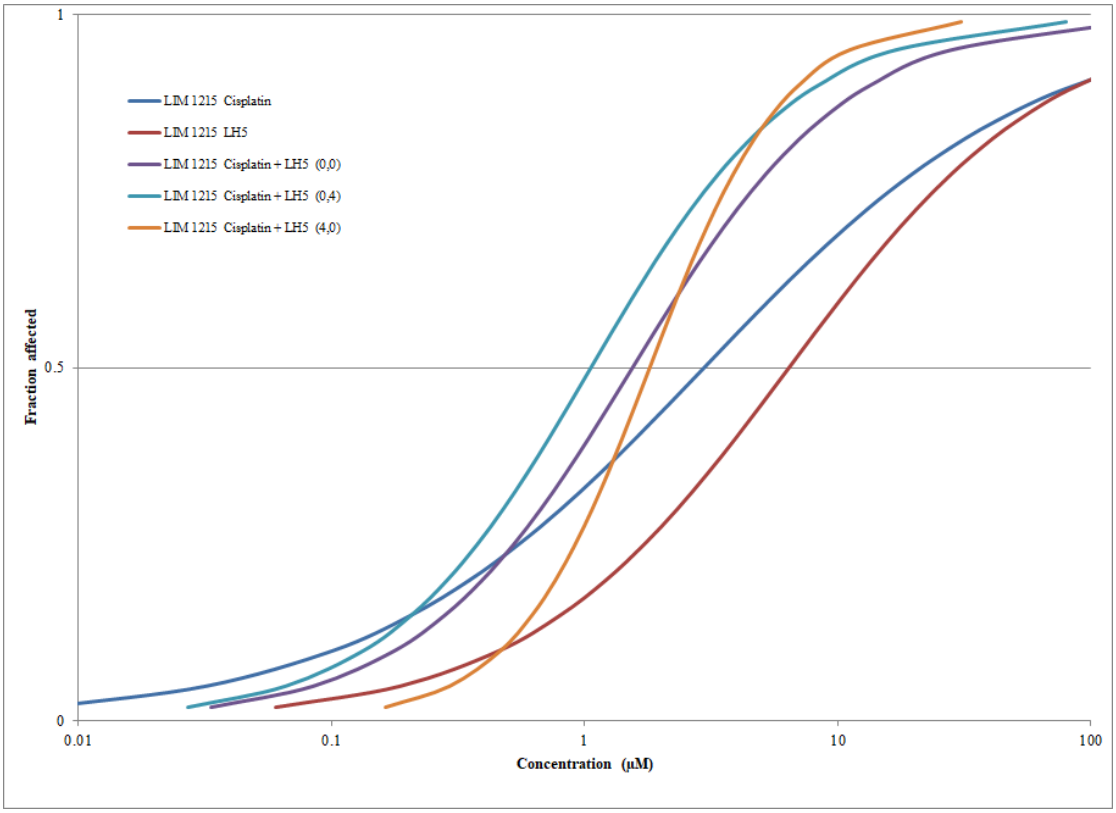

Figure 3.11: Activity versus concentration plots from combination of Cis with LH5 against Lim-1215 cell line

It can be seen from Figures 3.8 to 3.11 that, combination of Cis with LH5 at any sequence of administration produced greater cell kill than either Cis alone or LH5 alone against all investigated cancer cell lines. And in all cases LH5 produced the least cell kill. When Cis was combined with LH5, 4/0 sequence of administration caused greatest cell kill whereas bolus administration of the same was least effective against A2780 ovarian cell line (Figure 3.8). As in the parent cell line, combined administration of Cis with LH5 using 4/0 sequence of administration demonstrated greatest cell kill whereas bolus administration was least effective against A2780^{cisR} ovarian cell line (Figure 3.9). Likewise, in both ovarian cancer cell lines, combination of Cis with LH5 using 4/0 sequence of administration produced greatest cell kill whereas bolus administration was least effective against both colorectal cancer cell lines (Figure 3.10 and Figure 3.11).

3.2.1.2 Combination of Cis with Camp

Figures 3.12 to 3.15 show the dose response curves for the combinations of Cis with Camp as applied to parent A2780 ovarian cancer cell line, A2780^{cisR} ovarian cancer cell line, HT-29 colorectal cancer cell line, and Lim-1215 colorectal cancer cell line respectively at three sequences of administration (0/0, 0/4 and 4/0).

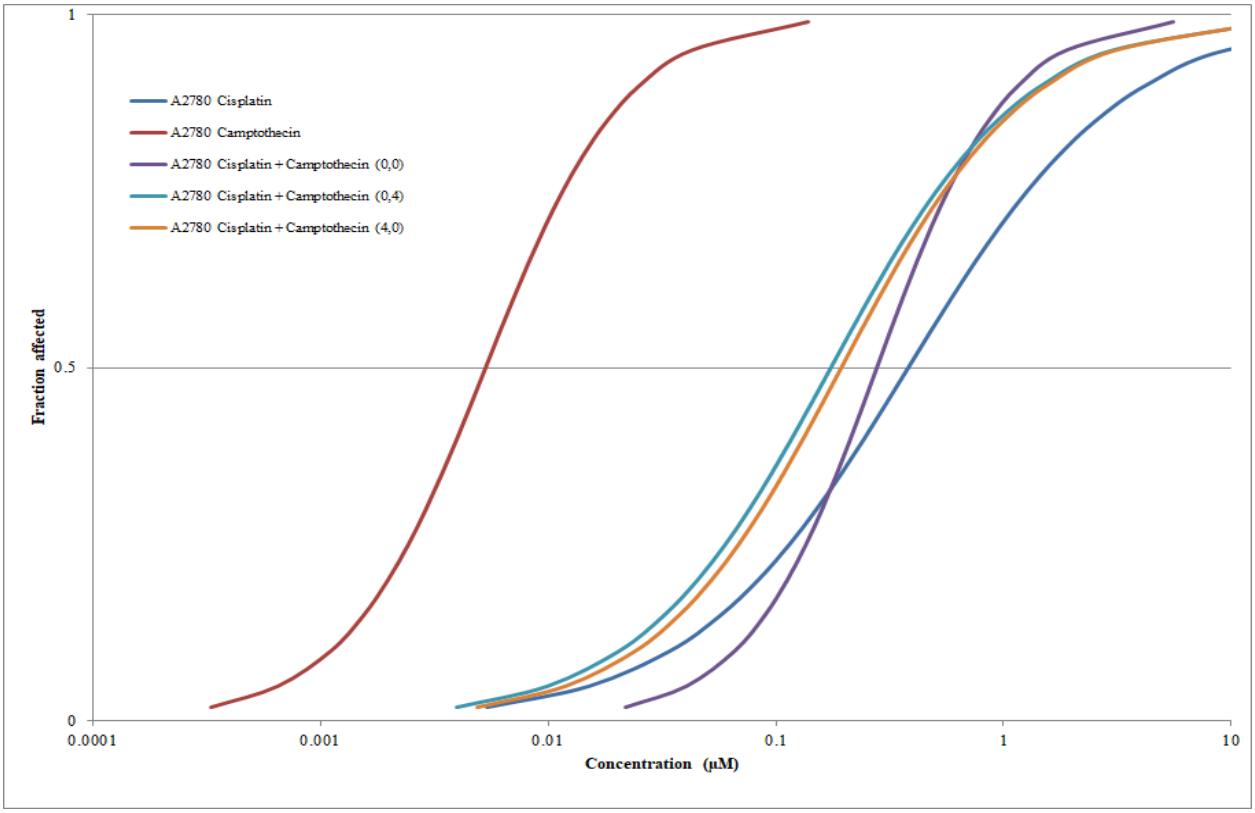

Figure 3.12: Activity versus concentration plots from combination of Cis with Camp against A2780 cell line

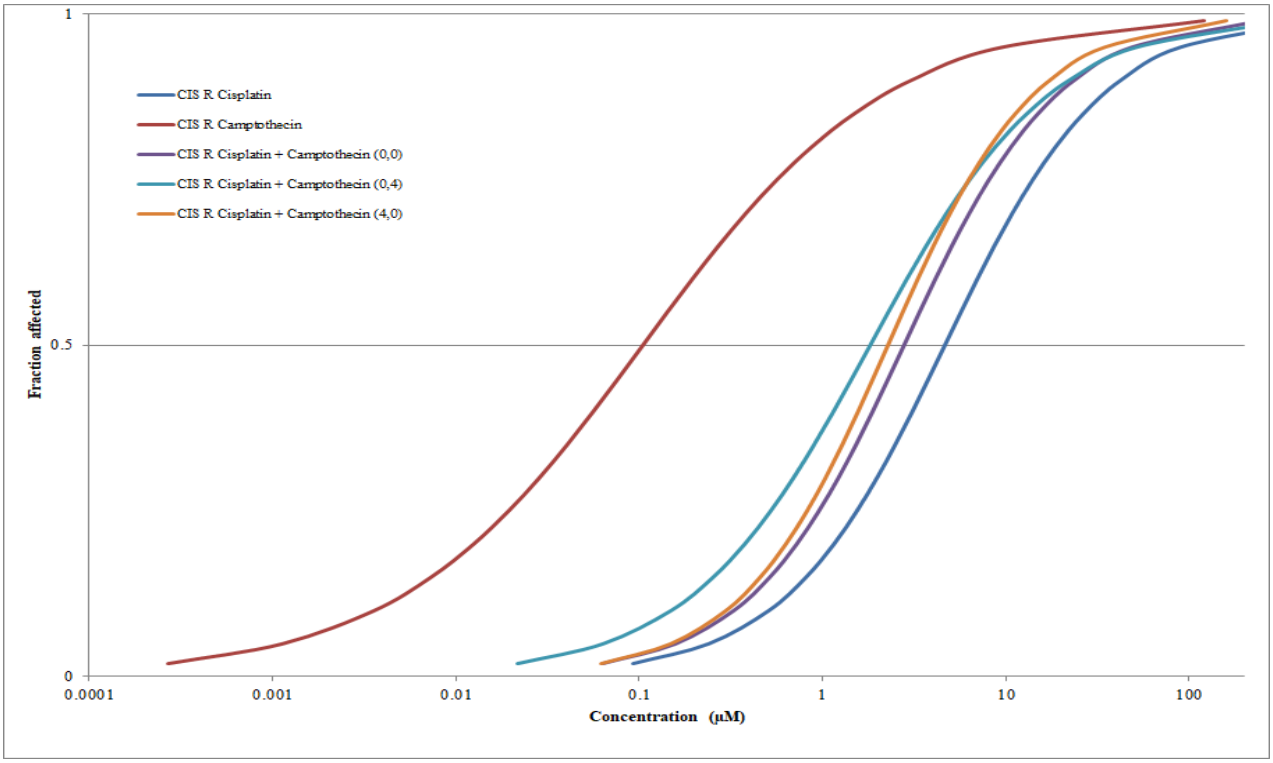

Figure 3.13: Activity versus concentration plots from combination of Cis with Camp against A2780^{cisR} cell line

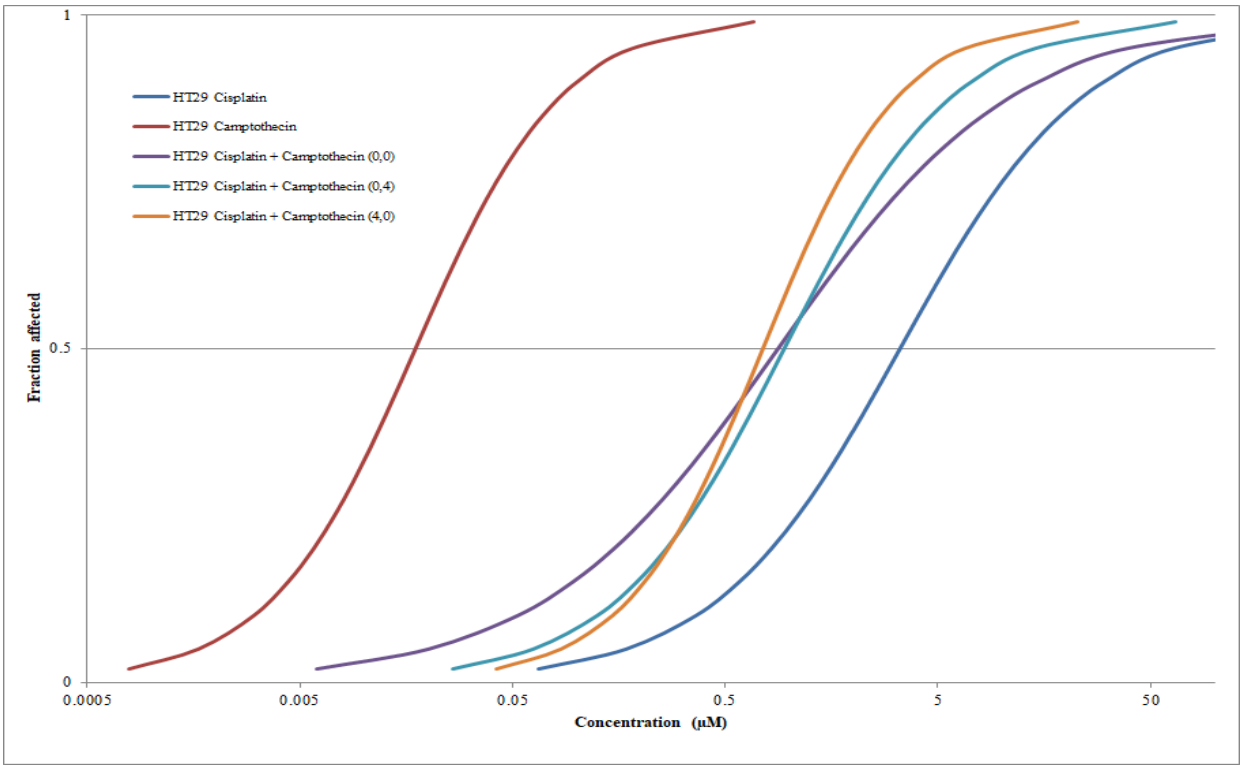

Figure 3.14: Activity versus concentration plots from combination of Cis with Camp against HT-29 cell line

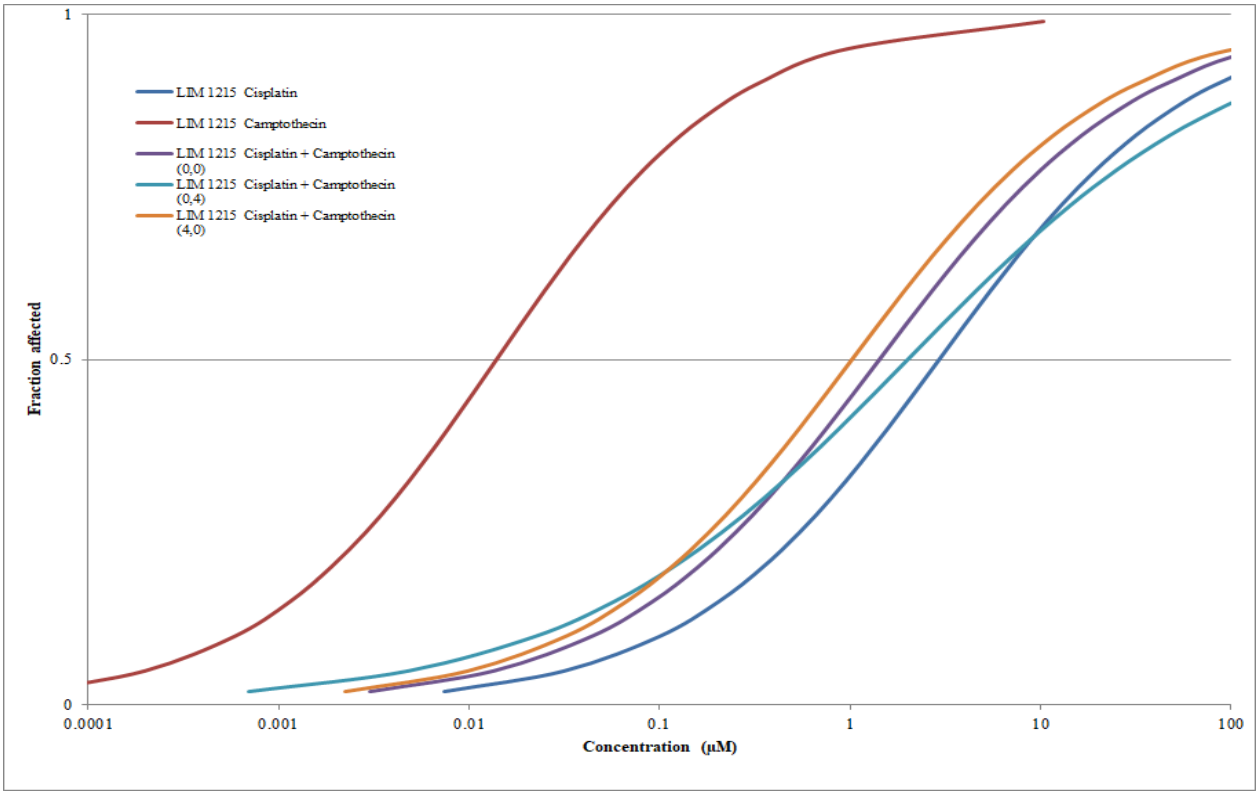

Figure 3.15: Activity versus concentration plots from combination of Cis with Camp against Lim-1215 cell line

It can be seen from Figures 3.12 to 3.15 that, among different sequences of administration, 0/4 administration of Cis with Camp caused greater cell kill than other sequences against both ovarian and colorectal cell lines. In all instances, bolus administration of Cis with Camp demonstrated least cell kill against all cell lines.

3.2.1.3 Combination of LH5 with Camp

Figures 3.16 to 3.19 show dose response curves for the combinations of LH5 with Camp against A2780 ovarian cancer cell line, A2780^{cisR} ovarian cancer cell line, HT-29 colorectal cancer cell line, Lim-1215 colorectal cancer cell line and Lim-2405 cell line respectively at different sequences of administration (0/0, 0/4 and 4/0).

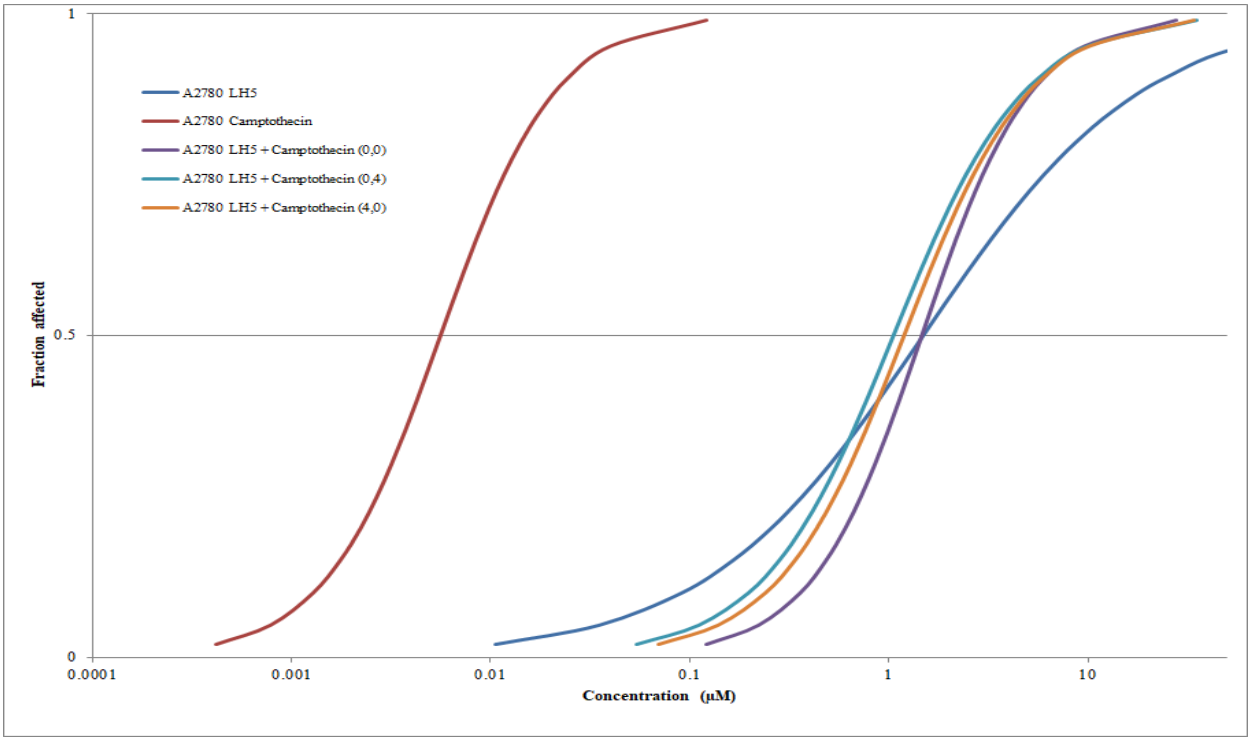

Figure 3.16: Activity versus concentration plots from combination of LH5 with Camp against A2780 cell line

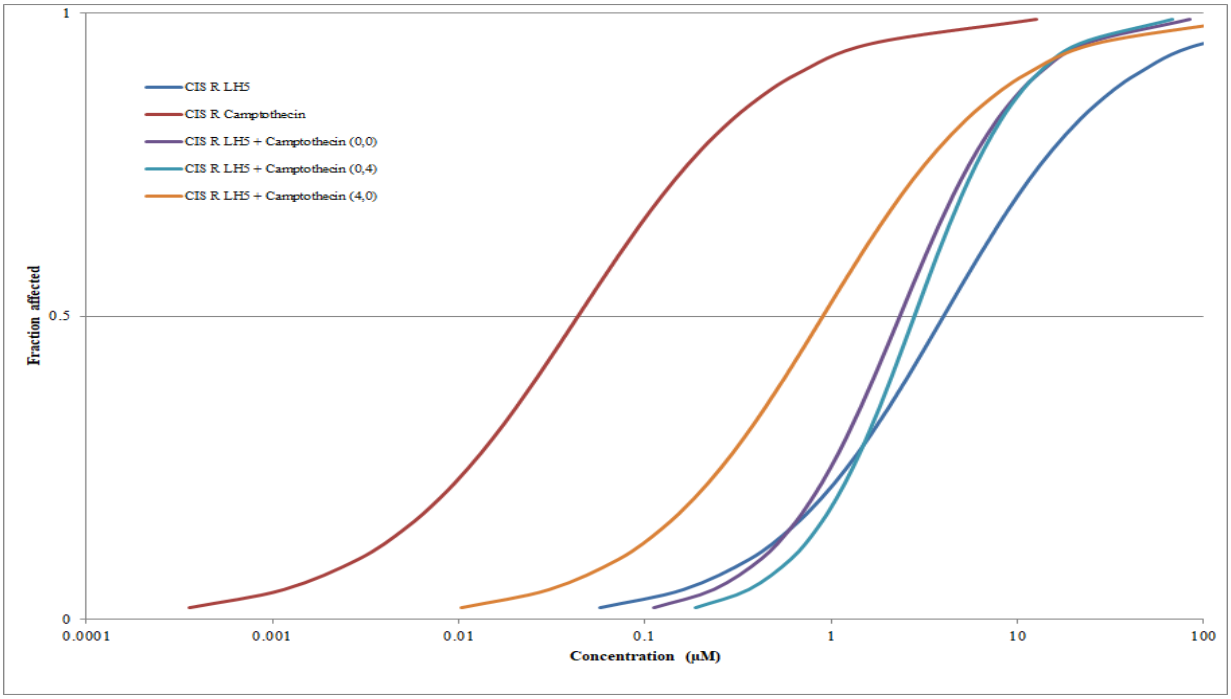

Figure 3.17: Activity versus concentration plots from combination of LH5 with Camp against A2780^{cisR} cell line

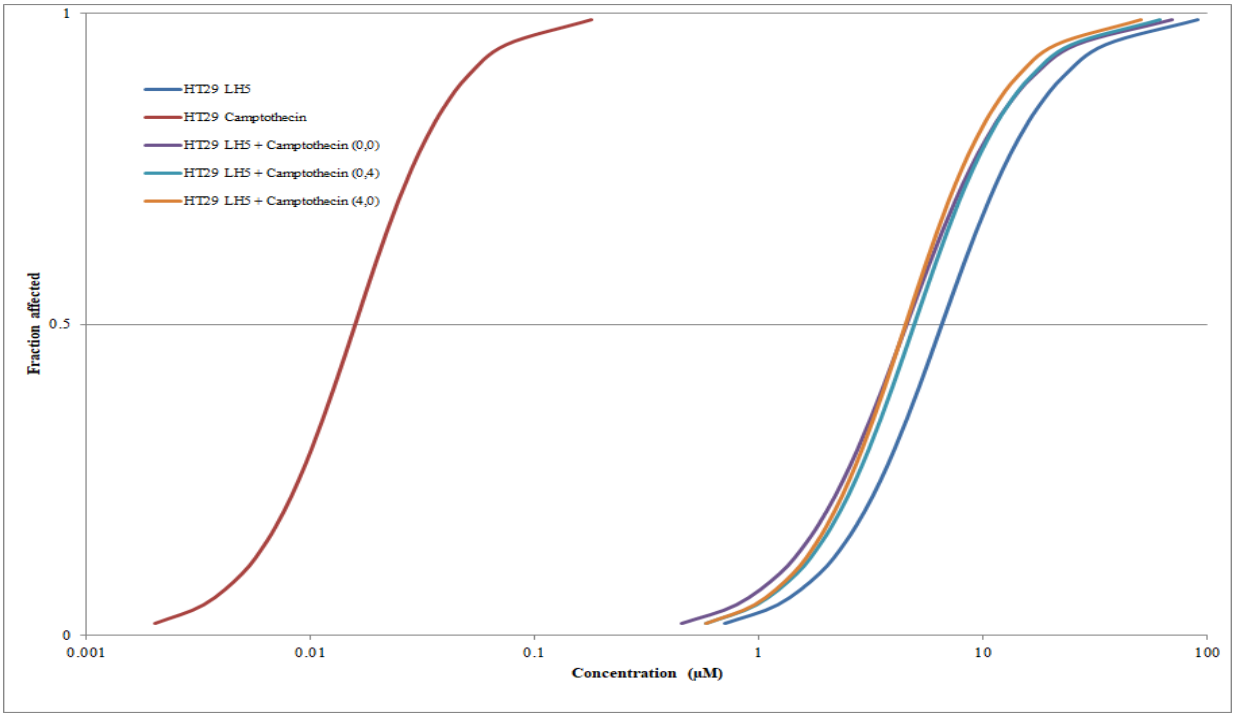

Figure 3.18: Activity versus concentration plots from combination of LH5 with Camp against HT-29 cell line

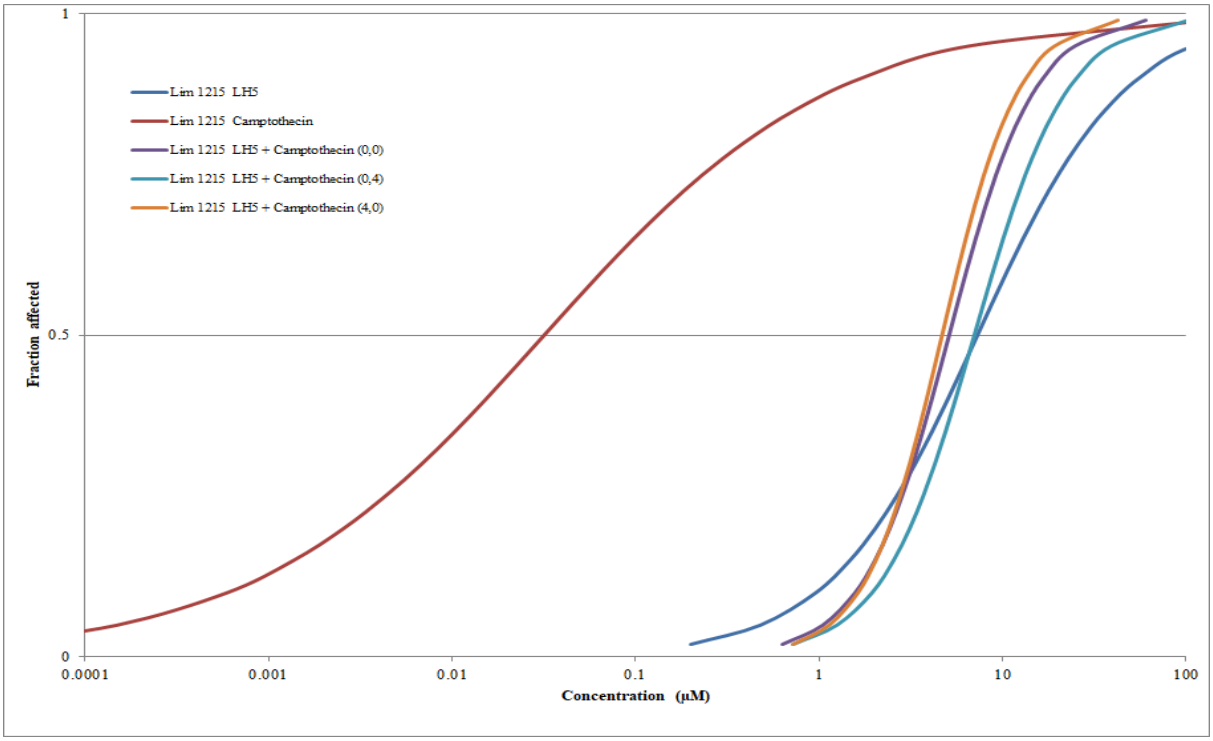

Figure 3.19: Activity versus concentration plots from combination of LH5 with Camp against Lim-1215 cell line

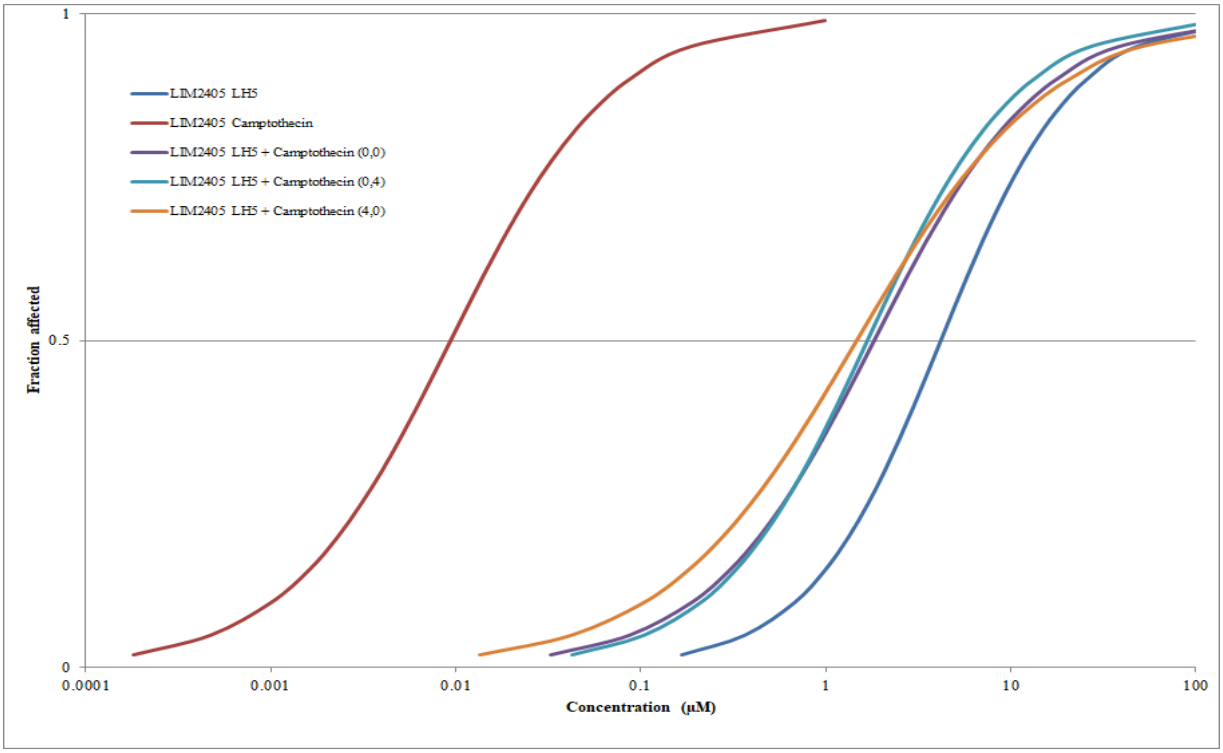

Figure 3.20: Activity versus concentration plots from combination of LH5 with Camp against Lim-2405 cell line

From the dose response curve (Figure 3.16), it can be said that 0/4 administration of LH5 with Camp against parent ovarian A2780 cell line produced greatest cell kill whereas bolus addition of LH5 with Camp was the least effective. However, in the resistant A2780^{cisR} ovarian cell line 4/0 administration of LH5 with Camp demonstrated greatest cell kill and 0/4 administration of the same was the least effective (Figure 3.17). In contrast, against all tested colorectal cancer cell lines 4/0 administration of LH5 with Camp showed greater cell kill and 0/4 did the least cell kill except for Lim-2405 cell line where bolus administration did the least cell kill (Figure 3.18 to Figure 3.20).

3.2.1.4 Combination of LH5 with Oxa

Figures 3.21 to 3.24 show the dose response curves for the combinations of LH5 with Oxa as applied to parent A2780 ovarian cancer cell line, A2780^{cisR} ovarian cancer cell line, HT-29 colorectal cancer cell line and Lim-1215 colorectal cancer cell line respectively using three sequences of administration (0/0, 0/4 and 4/0).

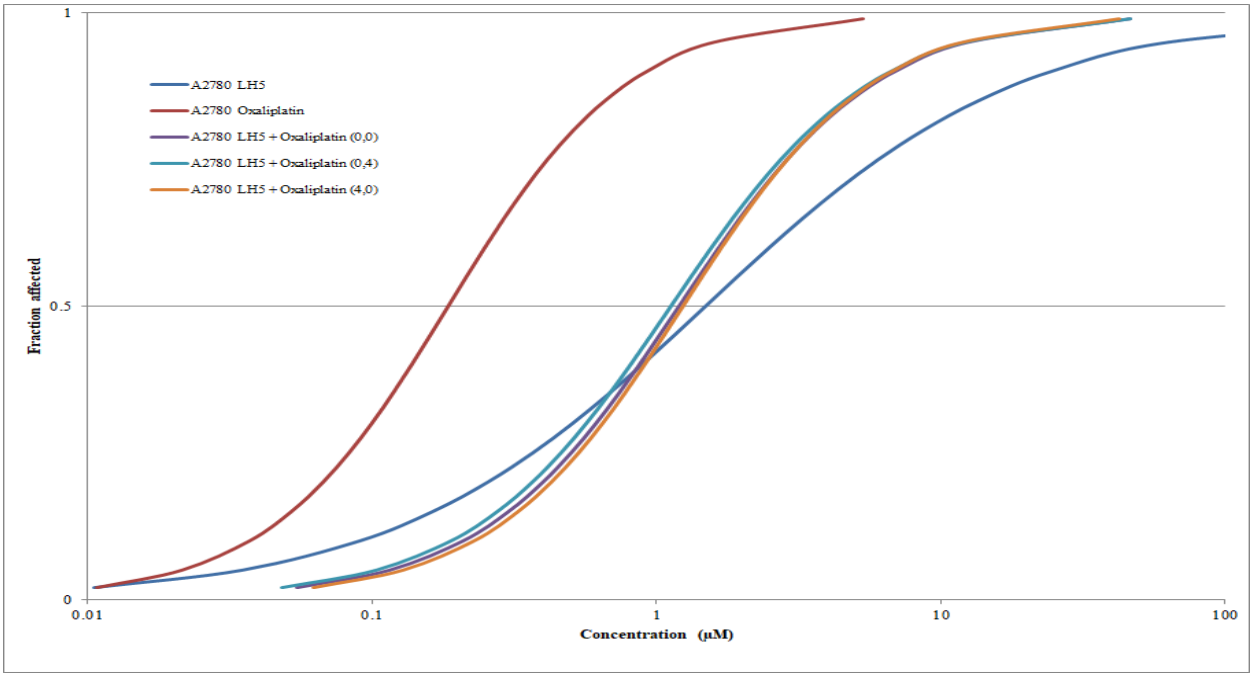

Figure 3.21: Activity versus concentration plots from combination of LH5 with Oxa against A2780 cell line

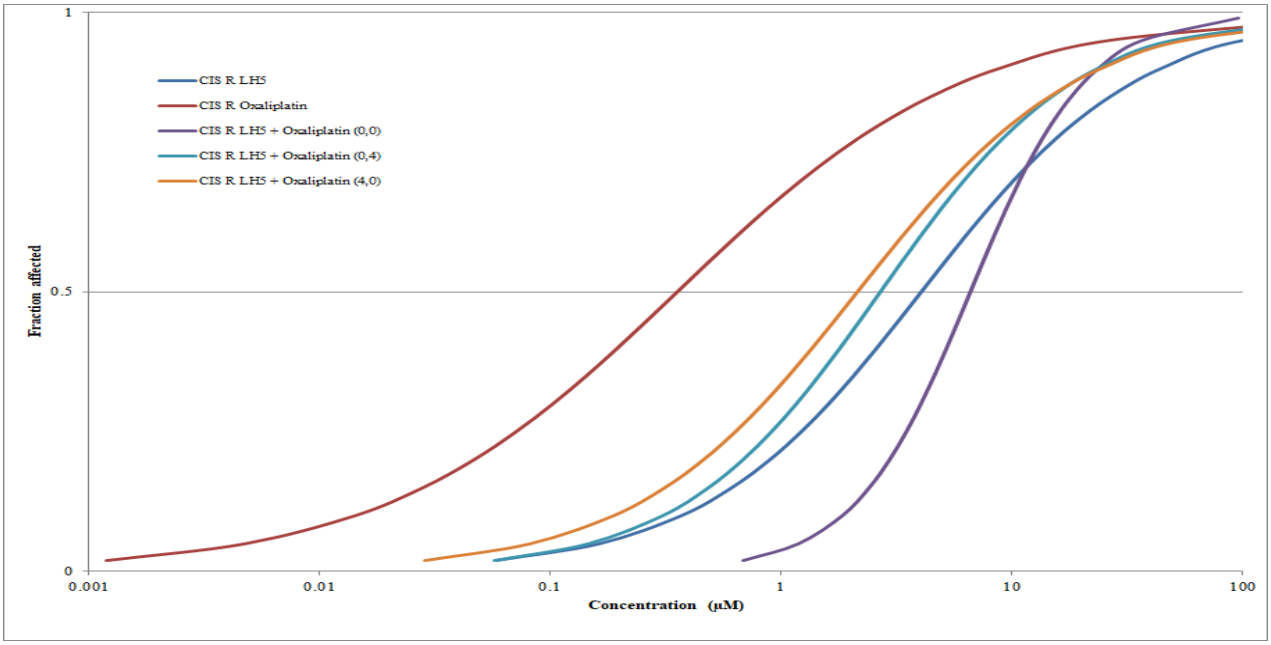

Figure 3.22: Activity versus concentration plots from combination of LH5 with Oxa against A2780^{cisR} cell line

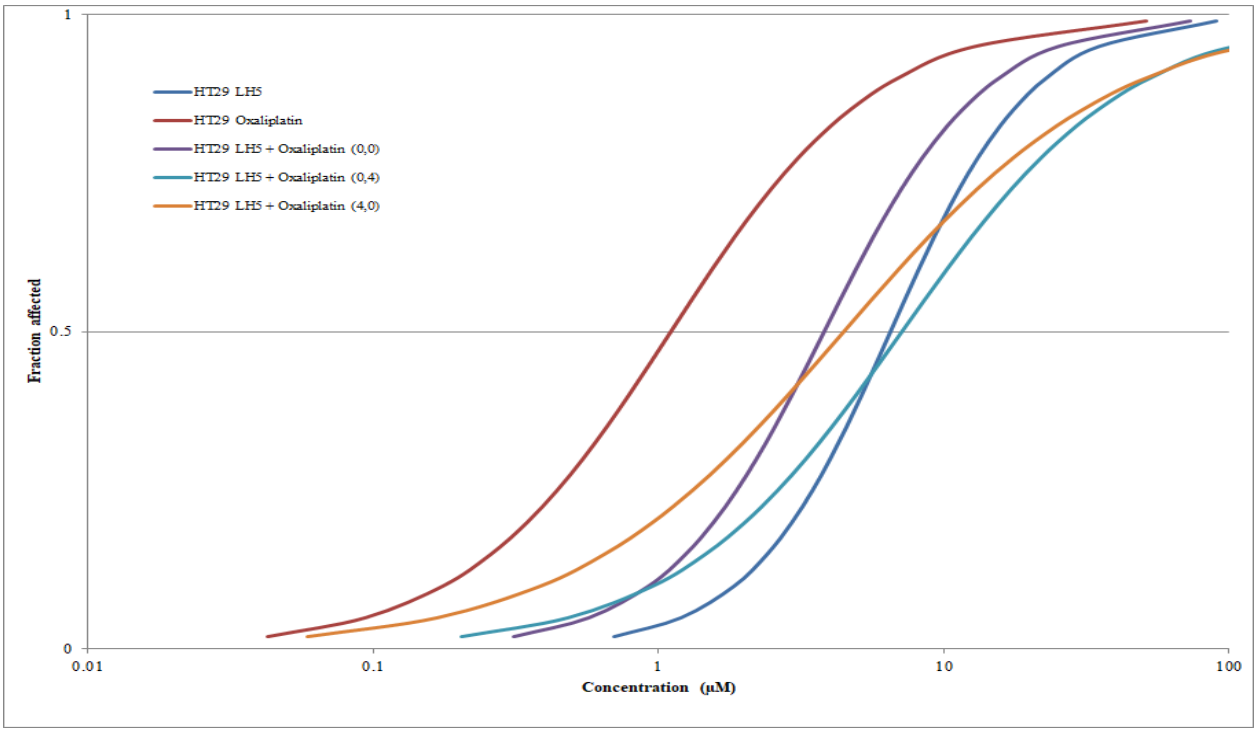

Figure 3.23: Activity versus concentration plots from combination of LH5 with Oxa against HT-29 cell line

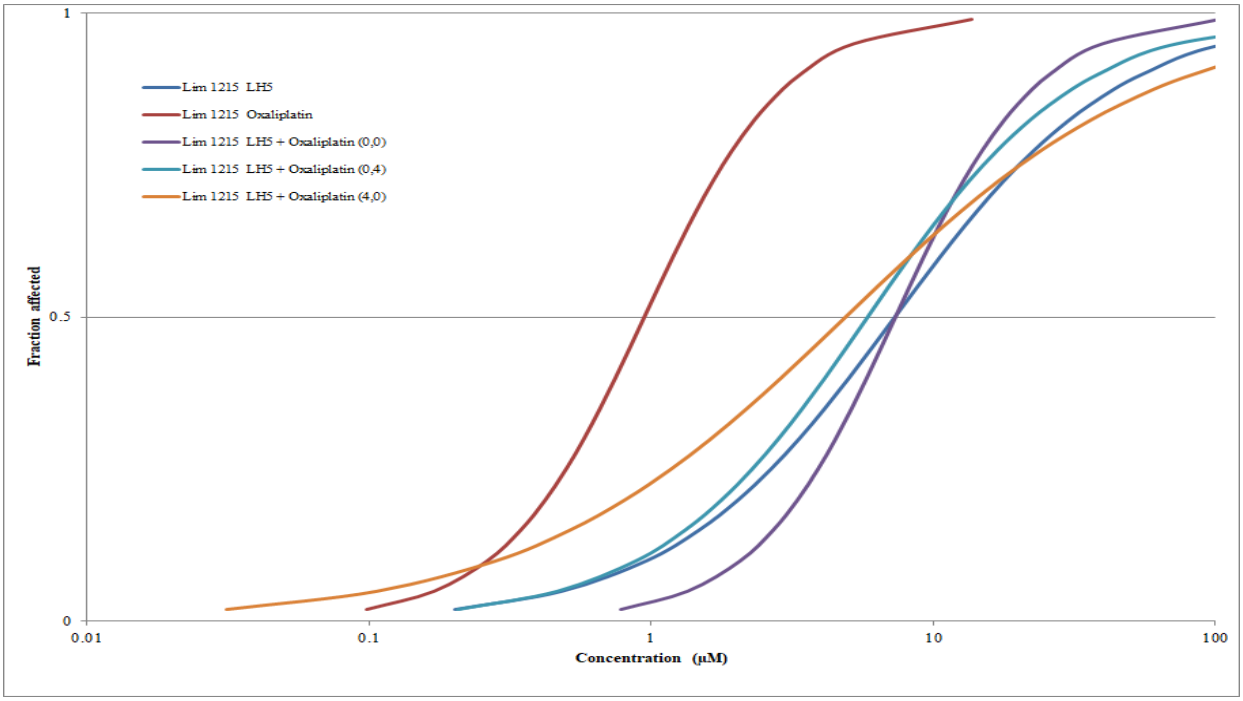

Figure 3.24: Activity versus concentration plots from combination of LH5 with Oxa against Lim-1215 cell line

From the dose response curve (Figure 3.21), it can be seen that 0/4 administration of LH5 with Oxa produced greatest cell kill against parent ovarian A2780 cell line whereas 4/0 addition of LH5 with Oxa was least effective. However, in resistant A2780^{cisR} ovarian cell line, it was 4/0 administration of LH5 with Oxa that produced the greatest cell kill while the bolus administration was least effective (Figure 3.22). In contrast, against both colorectal cancer cell lines it was the bolus administration of LH5 with Oxa that caused the greater cell kill at moderate and higher concentrations whereas 0/4 administration caused the least in HT-29 cell line especially at higher concentrations (Figure 3.23) and 4/0 administration caused the least in Lim-1215 cell line (Figure 3.24).

3.2.1.5 Combination of Gem with LH5

Figures 3.25 to 3.28 show the dose response curves obtained for the combination of Gem with LH5 against A2780 and A2780^{cisR} ovarian cancer cell lines, HT-29 and Lim-1215 colorectal cancer cell lines respectively at three sequences of administration (0/0, 0/4 and 4/0).

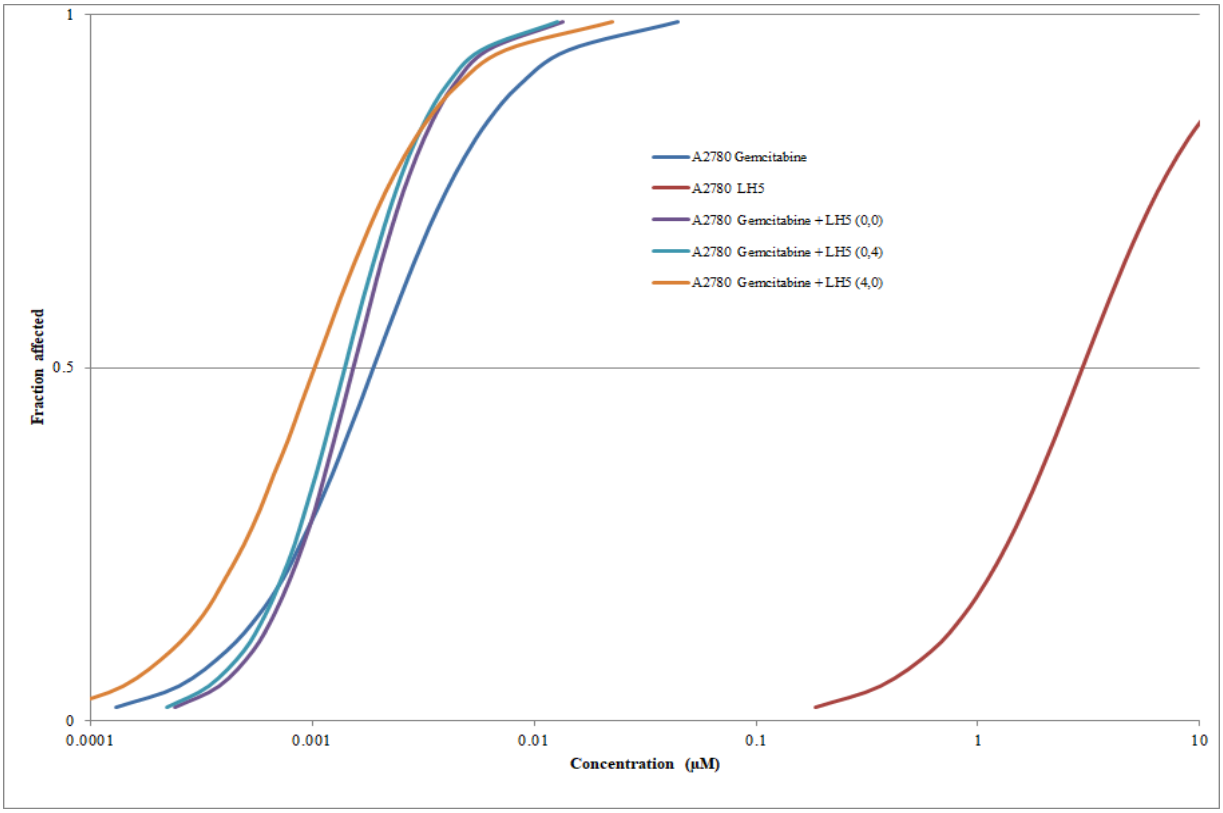

Figure 3.25: Activity versus concentration plots from combination of Gem with LH5 against A2780 cell line

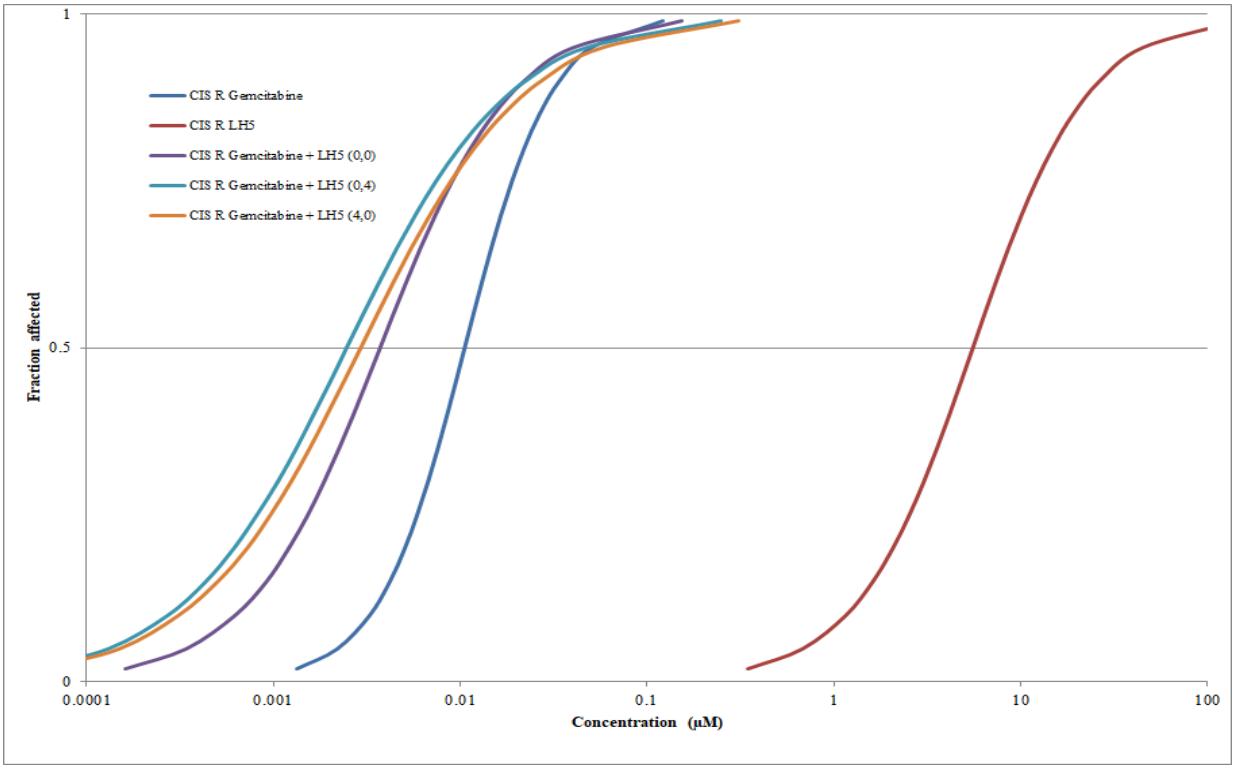

Figure 3.26: Activity versus concentration plots from combination of Gem with LH5 against A2780^{cisR} cell line

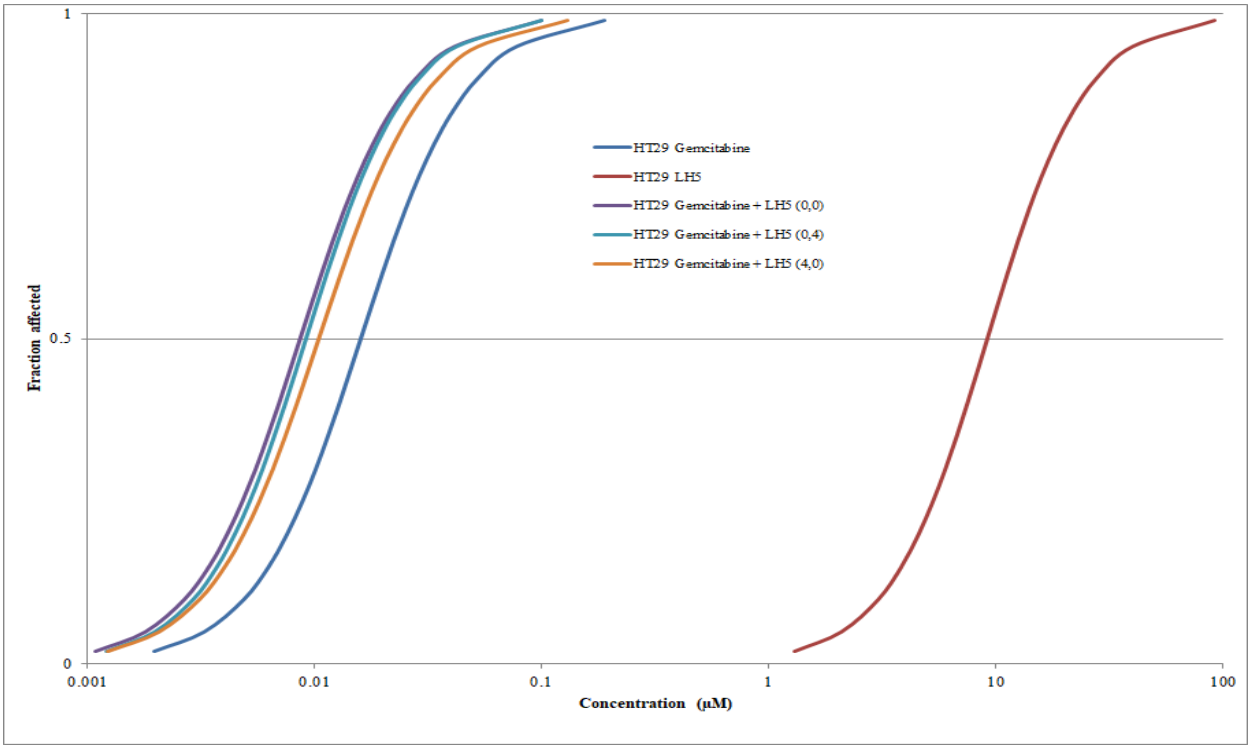

Figure 3.27: Activity versus concentration plots from combination of Gem with LH5 against HT-29 cell line

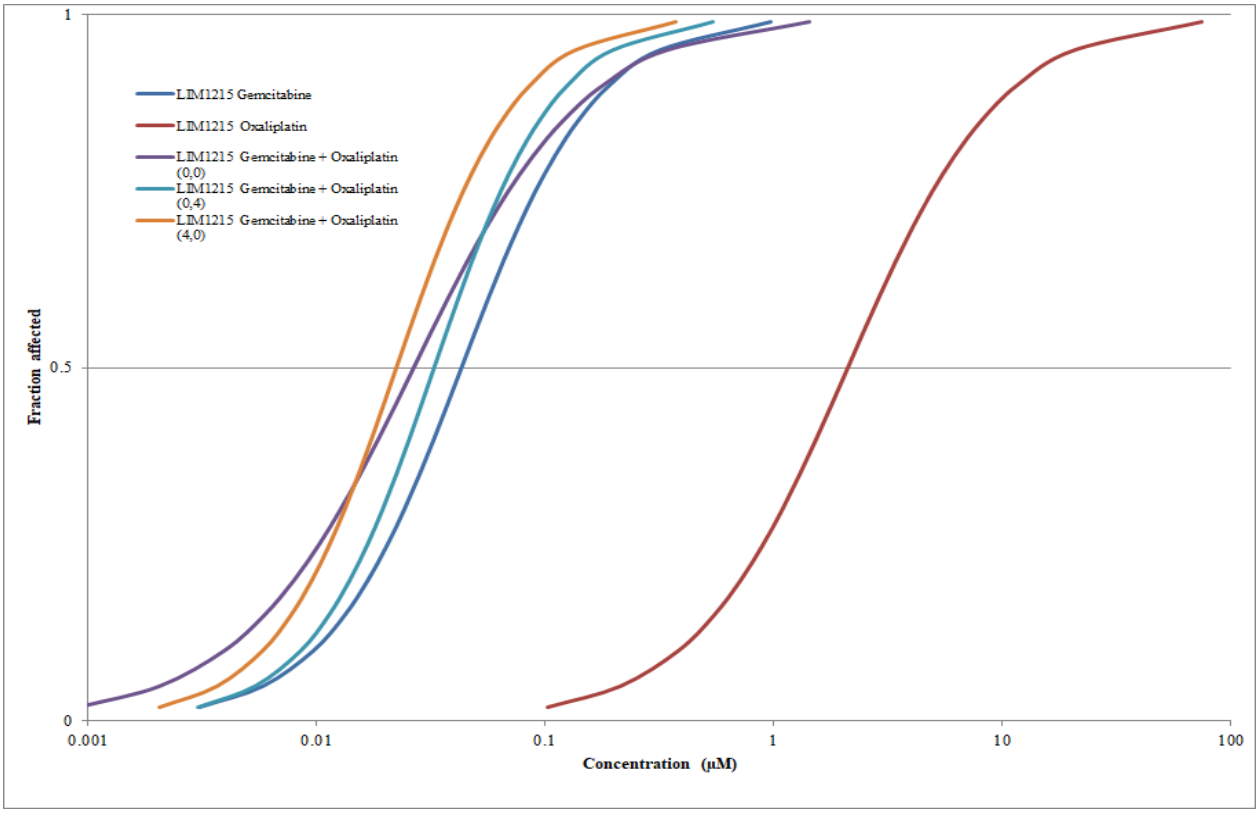

Figure 3.28: Activity versus concentration plots from combination of Gem with LH5 against Lim-1215 cell line

From the dose response curve (Figure 3.25), it can be seen that 4/0 administration of Gem with LH5 produced greatest cell kill against parent ovarian A2780 cell line whereas bolus administration of Gem with LH5 was least effective. However, in resistant A2780^{cisR} ovarian cell line, it was the 0/4 administration of Gem with LH5 that demonstrated greatest cell kill while 4/0 administration of the same was least effective (Figure 3.26). In contrast, against both colorectal cancer cell lines, it was the bolus administration of Gem with LH5 that produced the greatest cell kill while 4/0 administration caused the least cell kill (Figure 3.27 and Figure 3.28).

3.2.1.6 Combination of Gem with Cis

Figures 3.29 to 3.30 show dose response curves obtained from the combinations of Gem with Cis as applied to parent A2780 ovarian cancer cell line and resistant A2780^{cisR} ovarian cancer cell line respectively at three sequences of administration (0/0, 0/4 and 4/0).

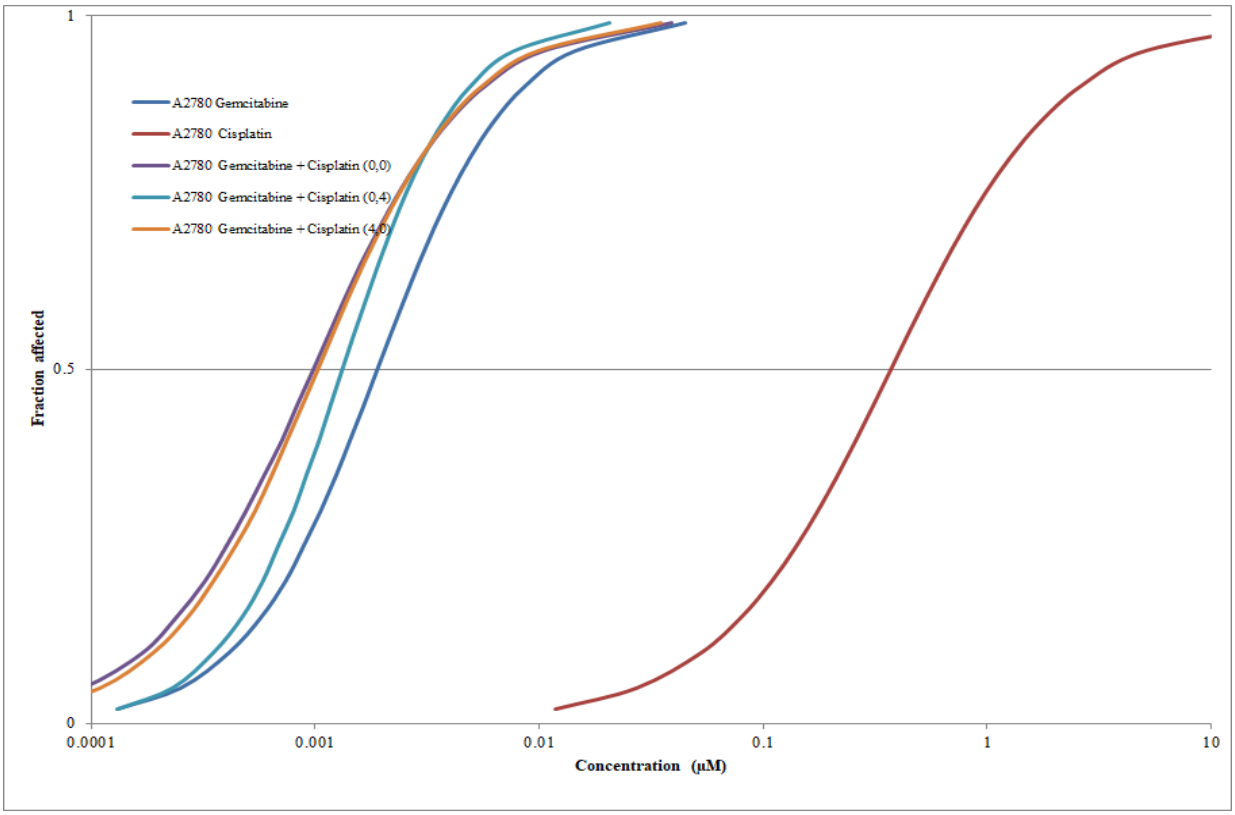

Figure 3.29: Activity versus concentration plots from combination of Gem with Cis against A2780 cell line

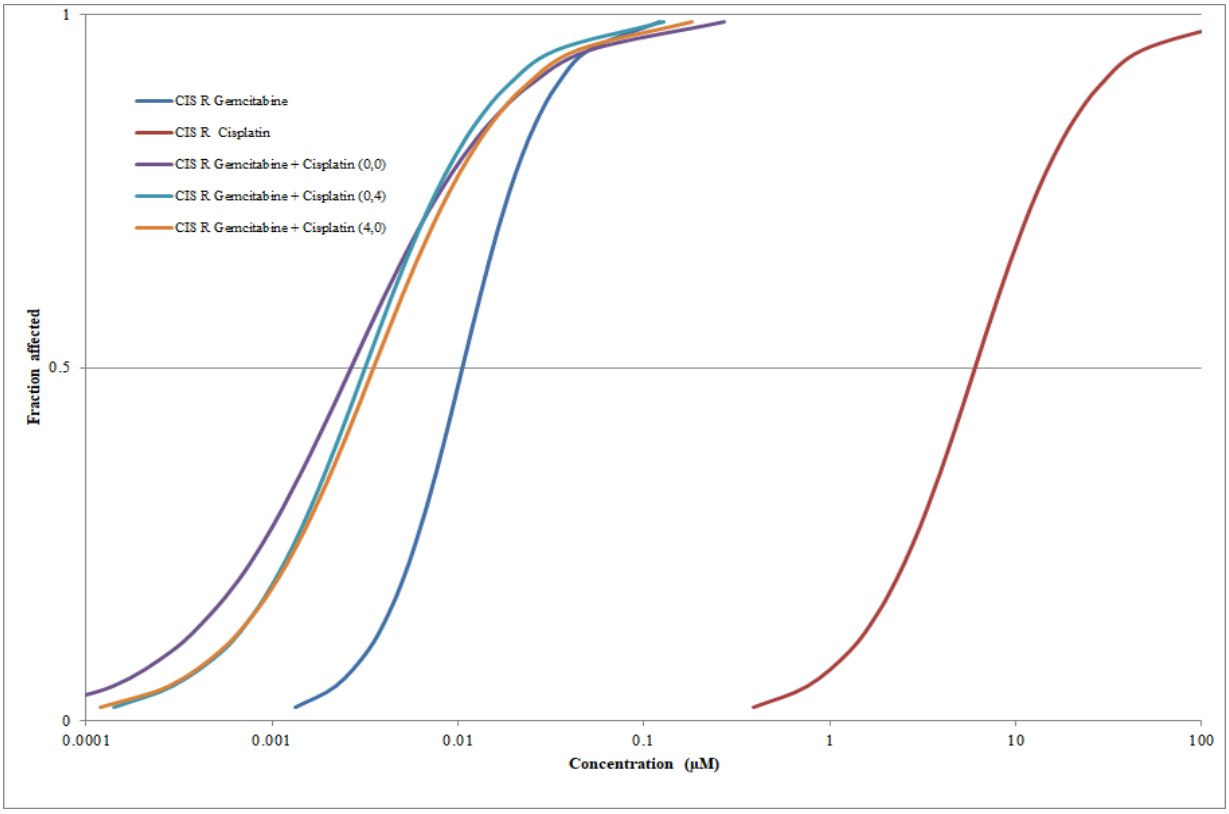

Figure 3.30: Activity versus concentration plots from combinations of Gem with Cis against A2780^{cisR} cell line

From the dose response curve (Figure 3.29), it can be said that bolus administration of Gem with Cis against parent ovarian A2780 cell line, produced greatest cell kill whereas 0/4 administration was least effective. However, in resistant A2780^{cisR} ovarian cell line 0/4 administration of Gem with Cis showed greatest cell kill and 4/0 administration of the same was least effective (Figure 3.30).

3.2.1.7 Combination of Gem with Oxa

Figures 3.31 to 3.32 show the dose response curves for the combinations of Gem with Oxa against HT-29 and Lim-1215 colorectal cancer cell lines at three sequences of administration (0/0, 0/4 and 4/0).

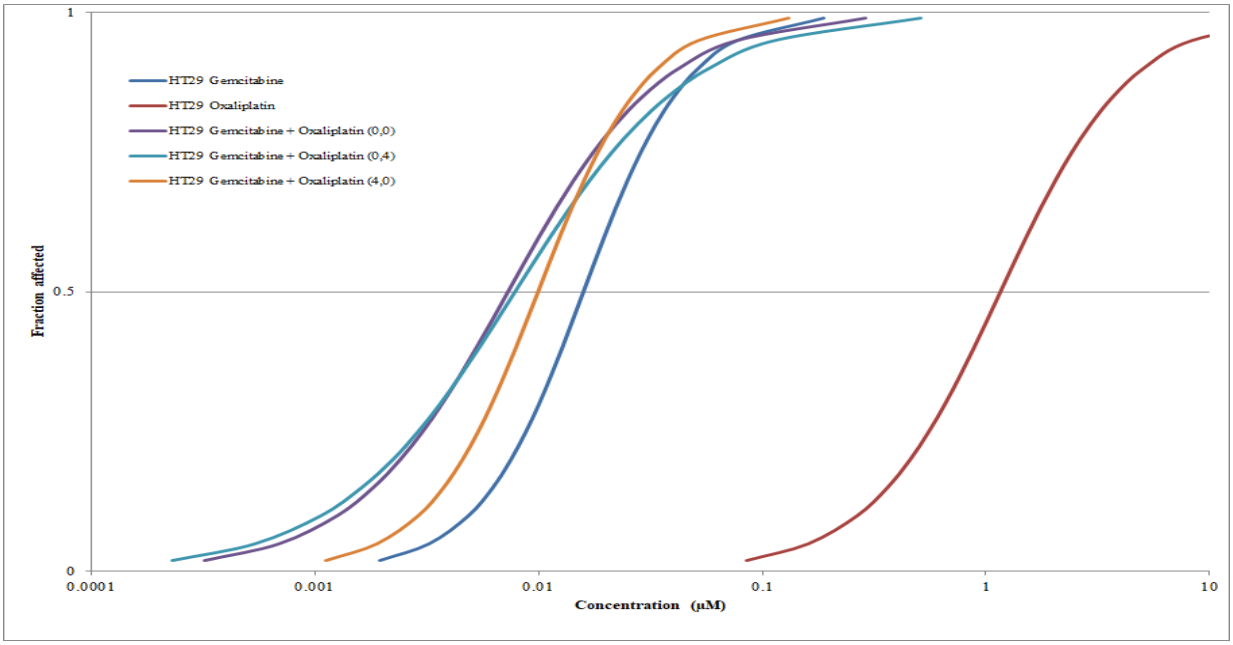

Figure 3.31: Activity versus concentration plots from combinations of Gem with Oxa against HT-29 cell line

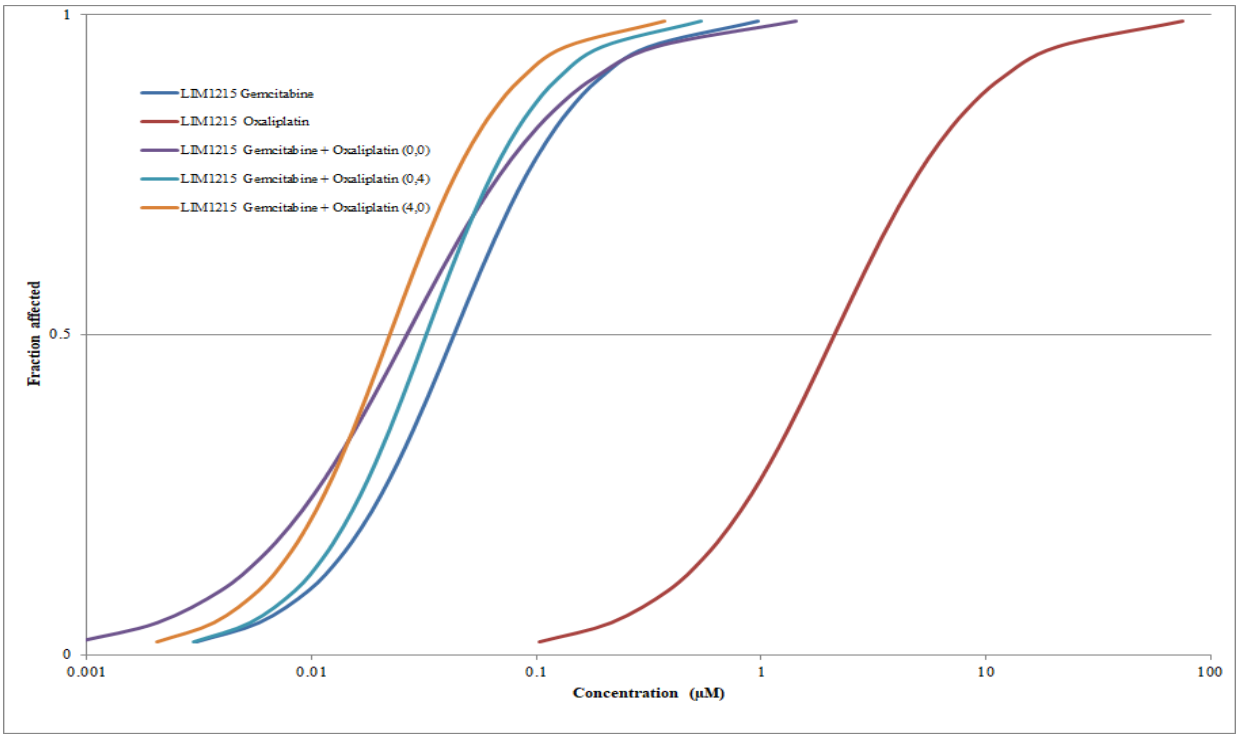

Figure 3.32: Activity versus concentration plots from combinations of Gem with Oxa against Lim-1215 cell line

From dose response curve (Figure 3.31), it can be seen that bolus administration of Gem with Oxa against HT-29 cell line produced the greatest cell kill whereas 0/4 administration of Gem with Cis was least effective. However, in Lim-1215 colorectal cancer cell line 4/0 administration of Gem with Oxa demonstrated the greatest cell kill and bolus administration was least effective (Figure 3.32).

3.2.1.8 Combination of Cuc with Cis

Figures 3.33 to 3.34 show the dose response curves obtained from the combinations of Cuc with Cis as applied to parent A2780 ovarian cancer cell line and resistant A2780^{cisR} ovarian cancer cell line respectively at three sequences of administration (0/0, 0/4 and 4/0).

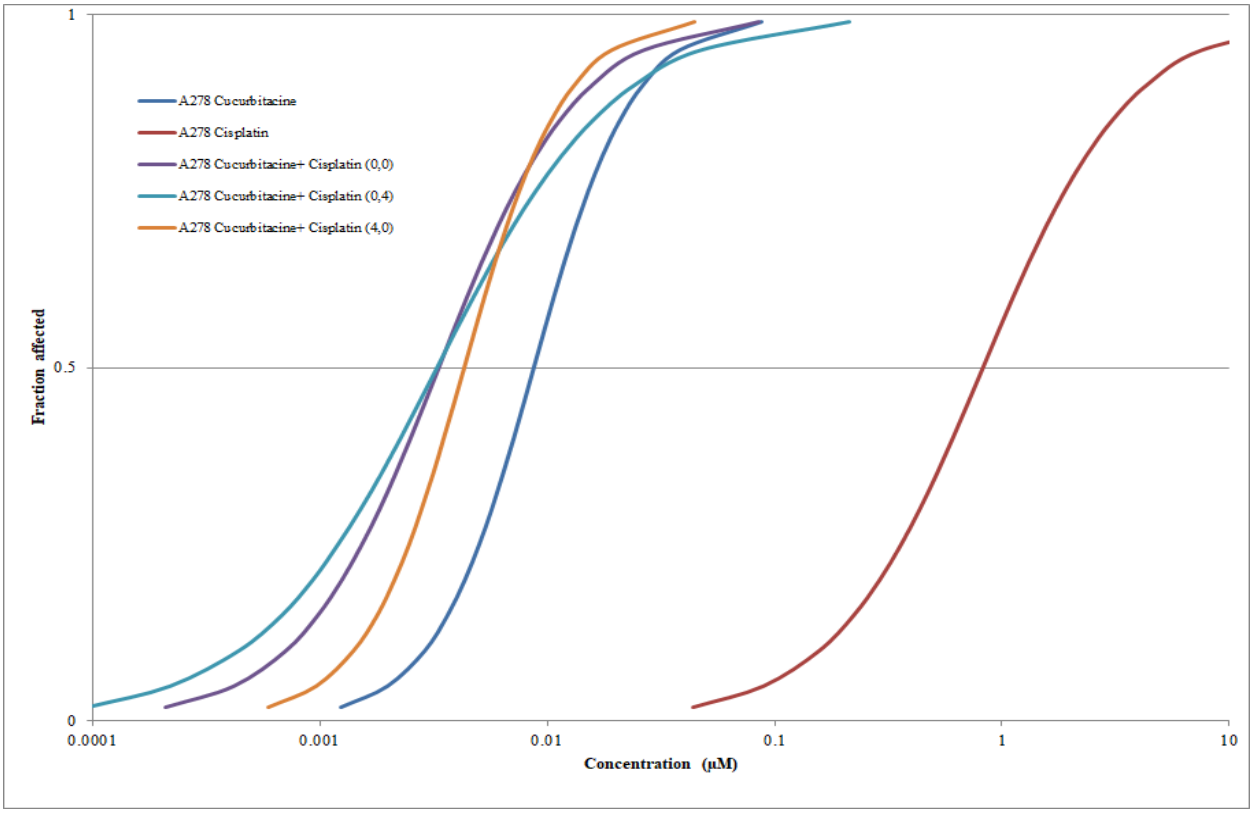

Figure 3.33: Activity versus concentration plots from combination of Cuc with Cis against A2780 cell line

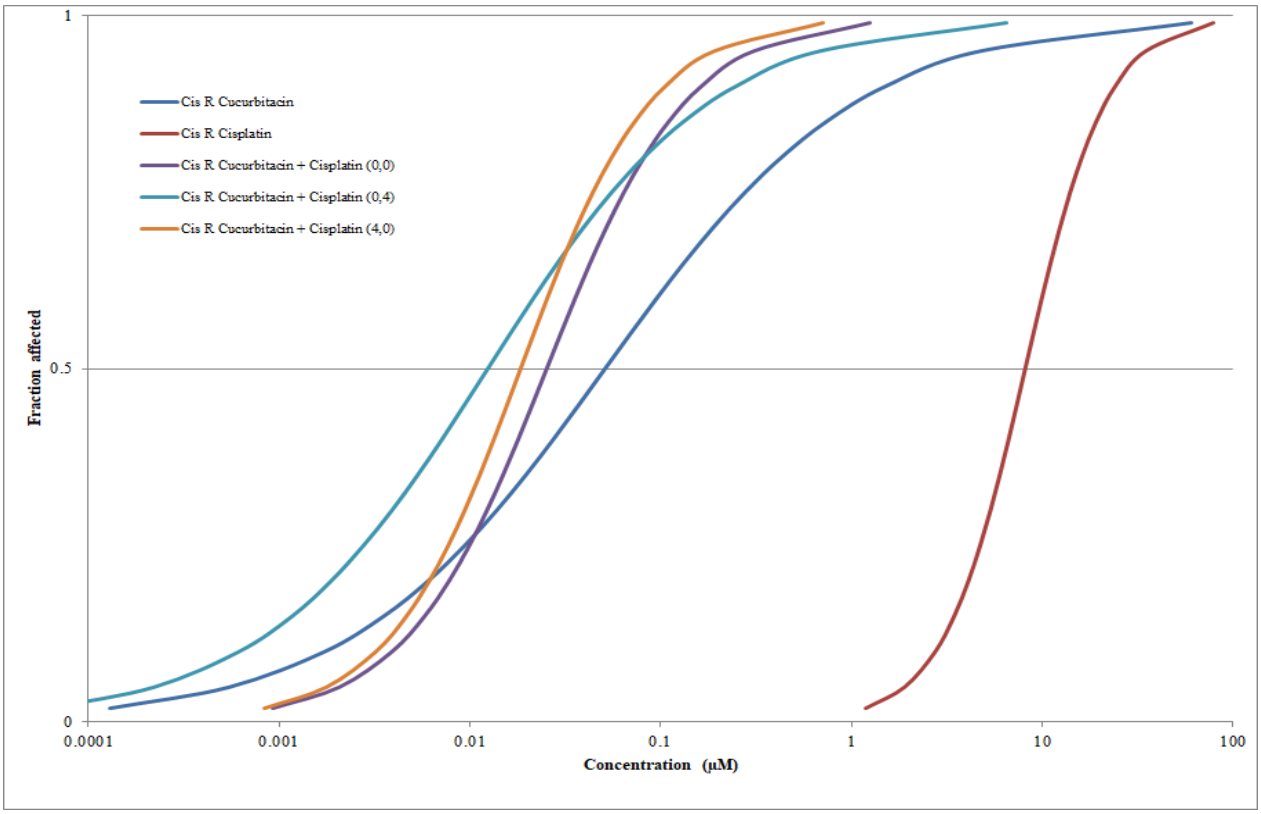

Figure 3.34: Activity versus concentration plots from combinations of Cuc with Cis against A2780^{cisR} cell line

From dose response curve (Figure 3.33), it can be seen that bolus administration of Cuc with Cis against parent ovarian A2780 cell line produced the greatest cell kill whereas 0/4 administration of Cuc with Cis was least effective. However, in resistant A2780^{cisR} ovarian cell line 4/0 administration of Cuc with Cis demonstrated the greatest cell kill and bolus administration of the same was least effective (Figure 3.34).

3.2.1.9 Combination of Cuc with LH5

Figures 3.35 to 3.36 show dose response curves for the combinations of Cuc with LH5 against A2780 and A2780^{cisR} ovarian cancer cell lines at three sequences of administration (0/0, 0/4 and 4/0).

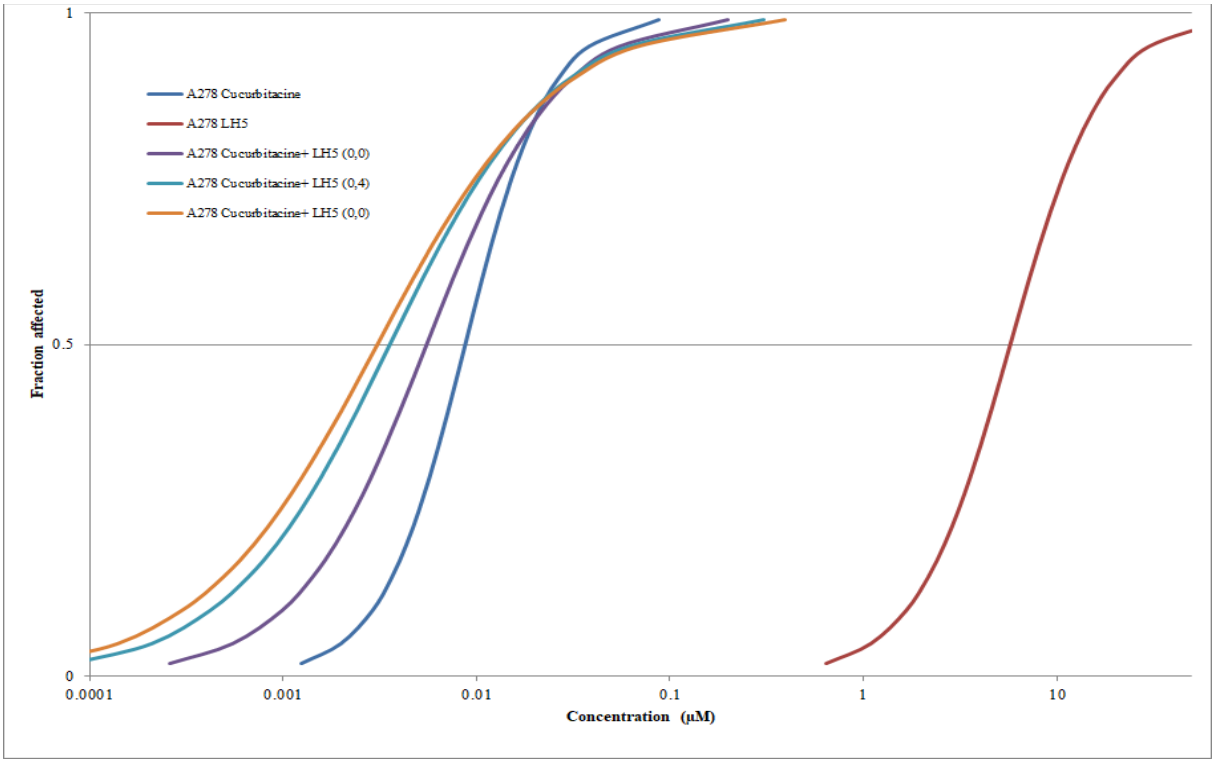

Figure 3.35: Activity versus concentration plots from combinations of Cuc with LH5 against A2780 cell line

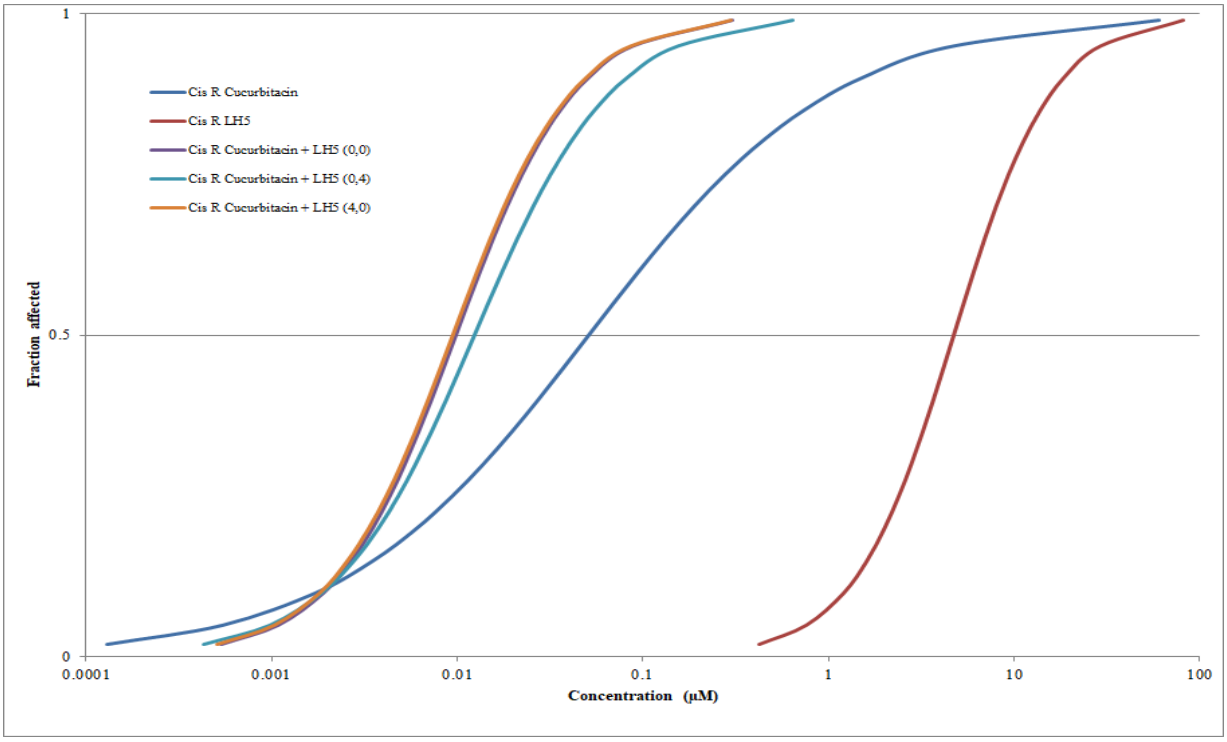

Figure 3.36: Activity versus concentration plots from combinations of Cuc with LH5 against A2780^{cisR} cell line

From dose response curve (Figure 3.35), it can be seen that 4/0 administration of Cuc with LH5 against parent ovarian A2780 cell line produced the greatest cell kill whereas bolus administration of Cuc with LH5 was least effective. However, in resistant A2780^{cisR} ovarian cell line 4/0 administration of Cuc with LH5 demonstrated the greatest cell kill and 0/4 administration of the same was least effective (Figure 3.36).

3.2.2 Combination Indices

Although dose response curves are visually attractive, they do not provide quantitative measure of combined drug action. On the contrary, combination indices (CI) provide quantitative measure of combined drug effects which are more accurate and precise. In the present study, CIs were calculated using Calcusyn software using Chou-Talalay method. Theoretically, CI can be defined as being the sum of concentration ratios of

the drugs used in combination and when working alone to provide a definite effect (e.g. ED_{50}, ED_{75}, ED_{90}). In this study, ED_{50} indicates the concentration of drug/drugs require to kill 50% of cells. Similarly, ED_{75} indicates 75% cell kill and ED_{90} indicates 90% cell kill.

3.2.2.1 Combination of Cis with LH5

Table 3.3 presents the CI values at different concentrations (ED_{50}, ED_{75} and ED_{90}) relating to binary combination of Cis with LH5 for the three sequences of administration: (0/0), (0/4) and (4/0) in human ovarian parent A2780 and resistant ovarian $A2780^{cisR}$ cancer cell lines, human colorectal HT-29 and Lim-1215 cell lines. Figure 3.37 gives the graphical representation of CI at ED_{50} obtained from combination of Cis with LH5 in the selected cell lines.

Table 3.3: CI values relating to binary combination of Cis and LH5 for different modes of administration in selected cell lines (D_m=medium effect dose, m=the exponent defining shape of the dose-effect curve, and r=the reliability coefficient)

	Drug	Sequence (h)	Molar Ratio	CI Values at					
Cell line				ED_{50}	ED_{75}	ED_{90}	D_m	M	R
A2780	Cis		(1:8.33)	N/A	N/A	N/A	0.382	0.914	0.967
	LH5			N/A	N/A	N/A	1.380	0.945	0.983
	Cis + LH5	0/0		2.37	1.54	1.00	0.2749	1.478	0.997
	Cis + LH5	0/4		1.77	1.18	0.79	0.204	1.422	0.980
	Cis + LH5	4/0		0.64	0.83	1.07	0.0749	0.763	0.991
A2780^{cisR}	Cis		(1:1.18)	N/A	N/A	N/A	4.632	0.995	0.992
	LH5			N/A	N/A	N/A	4.623	1.054	0.967
	Cis + LH5	0/0		1.14	1.10	1.07	2.417	1.059	0.991
	Cis + LH5	0/4		1.81	2.39	3.15	3.834	0.815	0.996
	Cis + LH5	4/0		1.37	1.13	0.94	2.899	1.244	0.999
HT-29	Cis		(1:5.28)	N/A	N/A	N/A	3.305	0.993	0.999
	LH5			N/A	N/A	N/A	4.440	1.322	0.999
	Cis + LH5	0/0		1.52	1.16	0.90	1.019	1.787	0.949
	Cis + LH5	0/4		1.05	1.09	1.14	0.7058	1.198	0.962
	Cis + LH5	4/0		1.44	1.10	0.85	0.967	1.787	0.932
Lim-1215	Cis		(1:3.80)	N/A	N/A	N/A	2.946	0.650	0.998
	LH5			N/A	N/A	N/A	6.417	0.833	0.948
	Cis + LH5	0/0		1.43	1.00	0.72	1.536	1.015	0.904
	Cis + LH5	0/4		0.98	0.65	0.45	1.053	1.062	0.991
	Cis + LH5	4/0		1.67	0.78	0.37	1.800	1.621	0.899

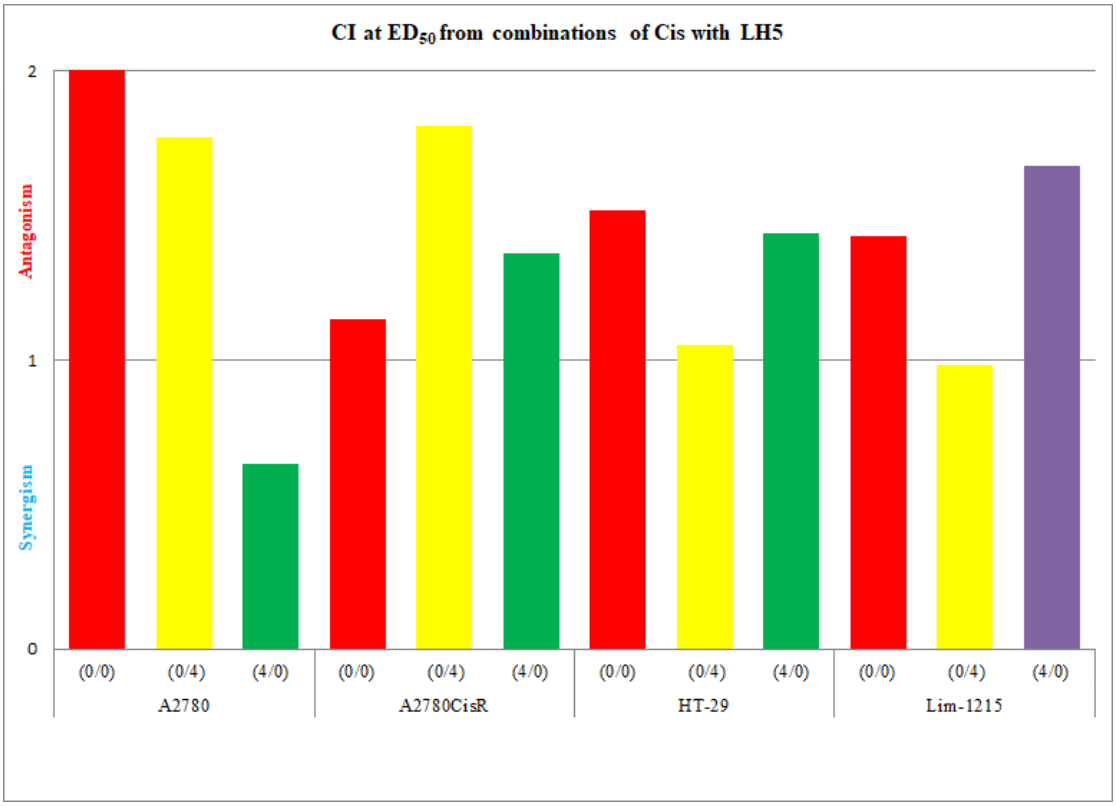

Figure 3.37: CI at ED_{50} for combinations of Cis with LH5 against tested cell lines

The results show that combination of Cis with LH5 generally produced antagonism against all tested cell lines except for the 4/0 sequence of administration against A2780 cell line (with greater synergistic cell kill shown at lower concentrations) and for 0/4 sequence of addition against Lim-1215 cell line (with greater synergism shown at higher concentrations).

3.2.2.2 Combination of Cis with Camp

Table 3.4 presents the CI values at different concentrations (ED_{50}, ED_{75} and ED_{90}) relating to binary combinations of Cis with Camp for the three sequences of administration: (0/0), (0/4) and (4/0) in parent A2780 human ovarian cancer cell line, resistant $A2780^{cisR}$ ovarian cancer cell line, HT-29 colorectal cancer cell line and Lim-1215 colorectal cancer cell line. Figure 3.38 gives the graphical representation of CI at ED_{50} obtained from combination of Cis with Camp in the selected cell lines.

Table 3.4: CI values relating to binary combination of Cis and Camp for different modes of administration in selected cell lines (Dm=medium effect dose, m=the exponent defining shape of the dose-effect curve, and r=the reliability coefficient)

	Drug	Sequence (h)	Molar Ratio	CI Values at					
Cell line				ED_{50}	ED_{75}	ED_{90}	D_m	M	R
A2780	Cis		(1:0.018)	N/A	N/A	N/A	0.382	0.914	0.967
	Camp			N/A	N/A	N/A	0.005	1.408	0.950
	Cis + Camp	0/0		1.68	1.34	1.12	0.276	1.533	0.999
	Cis + Camp	0/4		1.06	1.20	1.42	0.174	1.030	0.980
	Cis + Camp	4/0		1.17	1.30	1.49	0.193	1.056	0.996
$A2780^{cisR}$	Cis		(1:0.01)	N/A	N/A	N/A	4.632	0.995	0.992
	Camp			N/A	N/A	N/A	0.104	0.651	0.921
	Cis + Camp	0/0		0.87	0.72	0.63	2.770	1.028	0.996
	Cis + Camp	0/4		0.57	0.57	0.60	1.808	0.878	0.999
	Cis + Camp	4/0		0.71	0.56	0.47	2.269	1.081	0.961
HT-29	Cis		(1:0.01)	N/A	N/A	N/A	3.305	0.993	0.999
	Camp			N/A	N/A	N/A	0.017	1.254	0.999
	Cis + Camp	0/0		0.82	1.30	2.10	0.889	0.779	1
	Cis + Camp	0/4		0.87	0.93	1.01	0.946	1.083	0.977
	Cis + Camp	4/0		0.69	0.60	0.53	0.748	1.349	0.995
Lim-1215	Cis		(1:0.05)	N/A	N/A	N/A	2.946	0.650	0.998
	Camp			N/A	N/A	N/A	0.013	0.694	0.999
	Cis + Camp	0/0		1.07	1.19	1.33	1.420	0.632	0.998
	Cis + Camp	0/4		1.50	2.79	5.20	1.998	0.488	0.999
	Cis + Camp	4/0		0.76	0.85	0.94	1.019	0.635	0.995

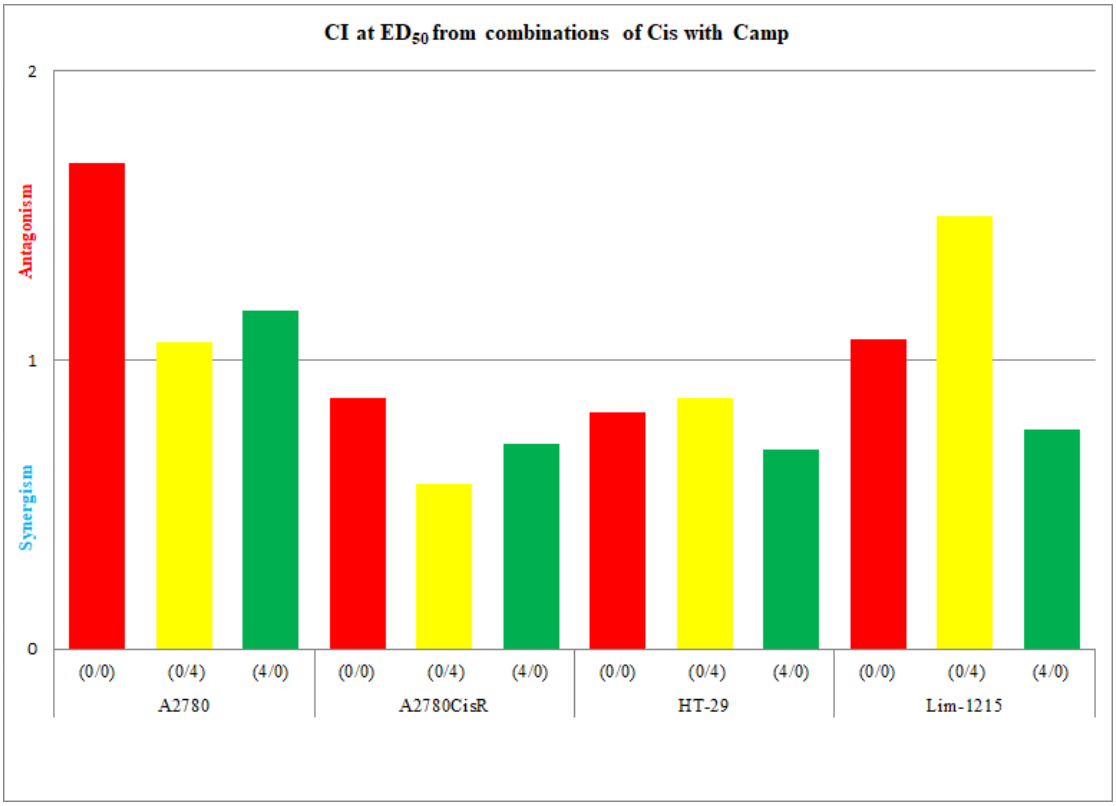

Figure 3.38: CI at ED_{50} for the combinations of Cis with Camp against tested cell lines

It can be seen from above results that, combination of Cis with Camp for all sequences of administration demonstrated synergism against $A2780^{cisR}$ and HT-29 cell lines. In other cell lines antagonism was predominant. However, 4/0 sequence of administration of Cis with Camp showed synergism against Lim-1215 colorectal tumour model. In general, greater synergism in cell kill was observed at lower concentrations than at higher concentrations as applied to combination of Cis with Camp against HT-29 cell line. However, the converse was true for $A2780^{cisR}$ cell line where synergism was in line with the added concentrations.

3.2.2.3 Combination of LH5 with Camp

Table 3.5 presents the CI values at different concentrations (ED_{50}, ED_{75} and ED_{90}) relating to binary combinations of LH5 with Camp for three modes of administration:

(0/0), (0/4) and (4/0) in parent A2780 human ovarian cancer cell line, resistant A2780^{cisR} ovarian cancer cell line, HT-29 colorectal cancer cell line and Lim-1215 colorectal cancer cell line. Figure 3.39 gives the graphical representation of CI at ED_{50} obtained from combination of LH5 with Camp in the selected cell lines.

Table 3.5: CI values relating to binary combination of LH5 and Camp for different modes of administration in selected cell lines (Dm=medium effect dose, m=the exponent defining shape of the dose-effect curve, and r=the reliability coefficient)

	Drug	**Sequence (h)**	**Molar Ratio**	**CI Values at**					
Cell line				ED_{50}	ED_{75}	ED_{90}	Dm	m	R
A2780	LH5		(1:0.002)	N/A	N/A	N/A	1.4852	0.786	0.918
	Camp			N/A	N/A	N/A	0.0056	1.494	0.987
	LH5 + Camp	0/0		1.55	1.04	0.78	1.463	1.561	0.982
	LH5 + Camp	0/4		1.12	0.86	0.74	1.053	1.308	0.951
	LH5 + Camp	4/0		1.27	0.94	0.78	1.191	1.367	0.964
A2780^{cisR}	LH5		(1:0.001)	N/A	N/A	N/A	4.034	0.917	0.871
	Camp			N/A	N/A	N/A	0.043	0.810	0.964
	LH5 + Camp	0/0		1.04	0.69	0.46	2.338	1.283	0.997
	LH5 + Camp	0/4		1.25	0.75	0.46	2.787	1.440	0.990
	LH5 + Camp	4/0		0.40	0.40	0.40	0.898	0.870	0.995
HT-29	LH5		(1:0.001)	N/A	N/A	N/A	6.524	1.746	0.998
	Camp			N/A	N/A	N/A	0.015	1.895	0.948
	LH5 + Camp	0/0		1.19	1.24	1.30	4.546	1.681	0.972
	LH5 + Camp	0/4		1.28	1.28	1.27	4.916	1.821	0.935
	LH5 + Camp	4/0		1.17	1.14	1.11	4.498	1.899	0.940
Lim-1215	LH5		(1:0.001)	N/A	N/A	N/A	7.296	1.083	1
	Camp			N/A	N/A	N/A	0.031	0.551	0.983
	LH5 + Camp	0/0		0.94	0.51	0.31	5.110	1.858	1
	LH5 + Camp	0/4		1.30	0.75	0.48	7.028	1.705	0.956
	LH5 + Camp	4/0		0.86	0.44	0.25	4.679	2.076	0.975

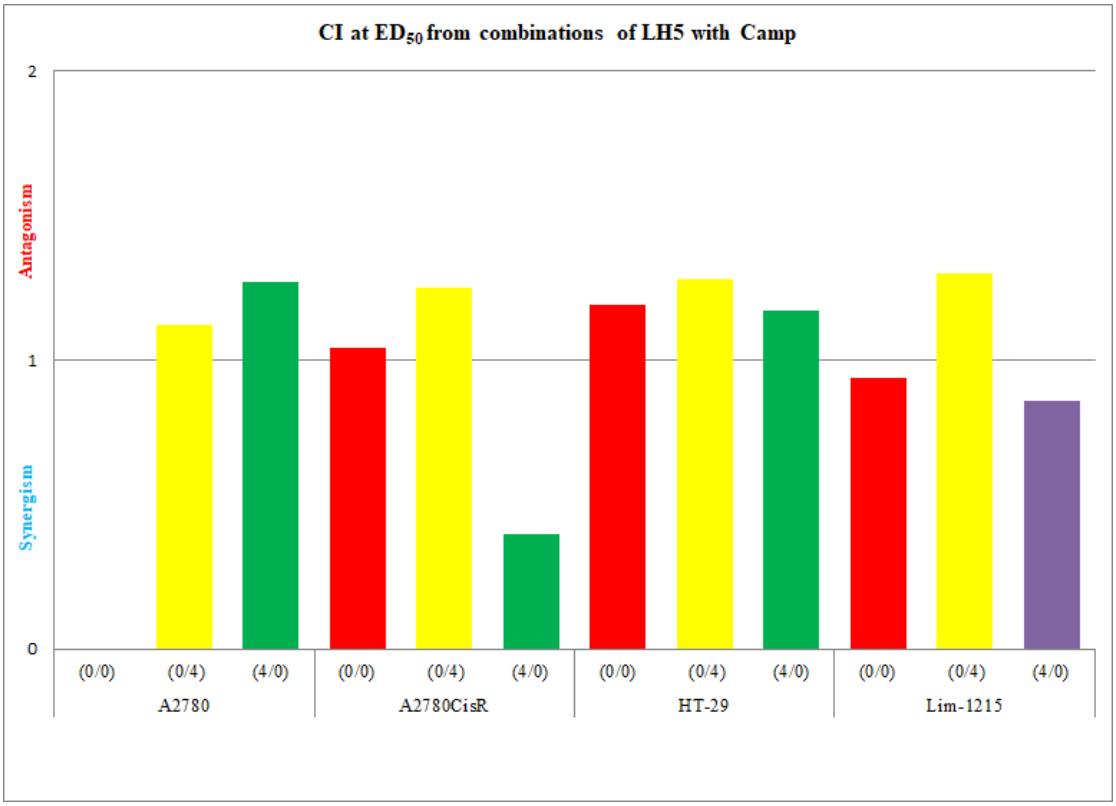

Figure 3.39: CI at ED_{50} for the combination of LH5 with Camp against tested cell lines

It is evident from above that, combination of LH5 with camp produced antagonism in general against the tested cell lines for all sequences of administration. However, 4/0 sequence of addition of LH5 with Camp applying to $A2780^{cisR}$ cell line demonstrated synergism at all added concentrations.

3.2.2.4 Combination of LH5 with Oxa

Table 3.6 presents the CI values at three different concentrations (ED_{50}, ED_{75} and ED_{90}) relating to sequenced binary combination of LH5 with Oxa for the three modes of administration: (0/0), (0/4) and (4/0) in parent A2780 human ovarian cancer cell line, resistant $A2780^{cisR}$ ovarian cancer cell line, HT-29 colorectal cancer cell line and Lim-1215 colorectal cancer cell line. Figure 3.40 gives the graphical representation of CI at ED_{50} obtained from combination of LH5 with Oxa in the selected cell lines.

Table 3.6: CI values relating to binary combination of LH5 and Oxa for different modes of administration in selected cell lines (D_m=medium effect dose, m=the exponent defining shape of the dose-effect curve, and r=the reliability coefficient)

	Drug	Sequence (h)	Molar Ratio	CI Values at					
Cell line				ED_{50}	ED_{75}	ED_{90}	Dm	M	R
A2780	LH5		(1:0.098)	N/A	N/A	N/A	1.485	0.786	0.918
	Oxa			N/A	N/A	N/A	0.184	1.367	0.953
	LH5 + Oxa	0/0		1.44	1.16	1.01	1.198	1.257	0.994
	LH5 + Oxa	0/4		1.35	1.10	0.98	1.124	1.233	0.990
	LH5 + Oxa	4/0		1.49	1.16	0.99	1.241	1.301	0.974
A2780^{cisR}	LH5		(1:0.104)	N/A	N/A	N/A	4.034	0.917	0.871
	Oxa			N/A	N/A	N/A	0.352	0.683	0.966
	LH5 + Oxa	0/0		3.61	1.69	0.82	6.633	1.718	0.999
	LH5 + Oxa	0/4		1.46	1.07	0.81	2.691	1.011	0.940
	LH5 + Oxa	4/0		1.16	0.96	0.83	2.126	0.902	0.988
HT-29	LH5		(1:0.134)	N/A	N/A	N/A	6.524	1.746	0.998
	Oxa			N/A	N/A	N/A	1.098	1.196	0.983
	LH5 + Oxa	0/0		1.05	1.00	0.98	3.808	1.552	0.990
	LH5 + Oxa	0/4		1.96	2.54	3.35	7.133	1.094	0.987
	LH5 + Oxa	4/0		1.22	1.97	3.23	4.443	0.898	0.964
Lim-1215	LH5		(1:0.071)	N/A	N/A	N/A	7.296	1.083	1
	Oxa			N/A	N/A	N/A	0.944	1.720	0.947
	LH5 + Oxa	0/0		1.55	1.23	1.01	7.333	1.736	0.979
	LH5 + Oxa	0/4		1.24	1.34	1.50	5.853	1.163	0.989
	LH5 + Oxa	4/0		1.03	1.81	3.29	4.883	0.770	0.999

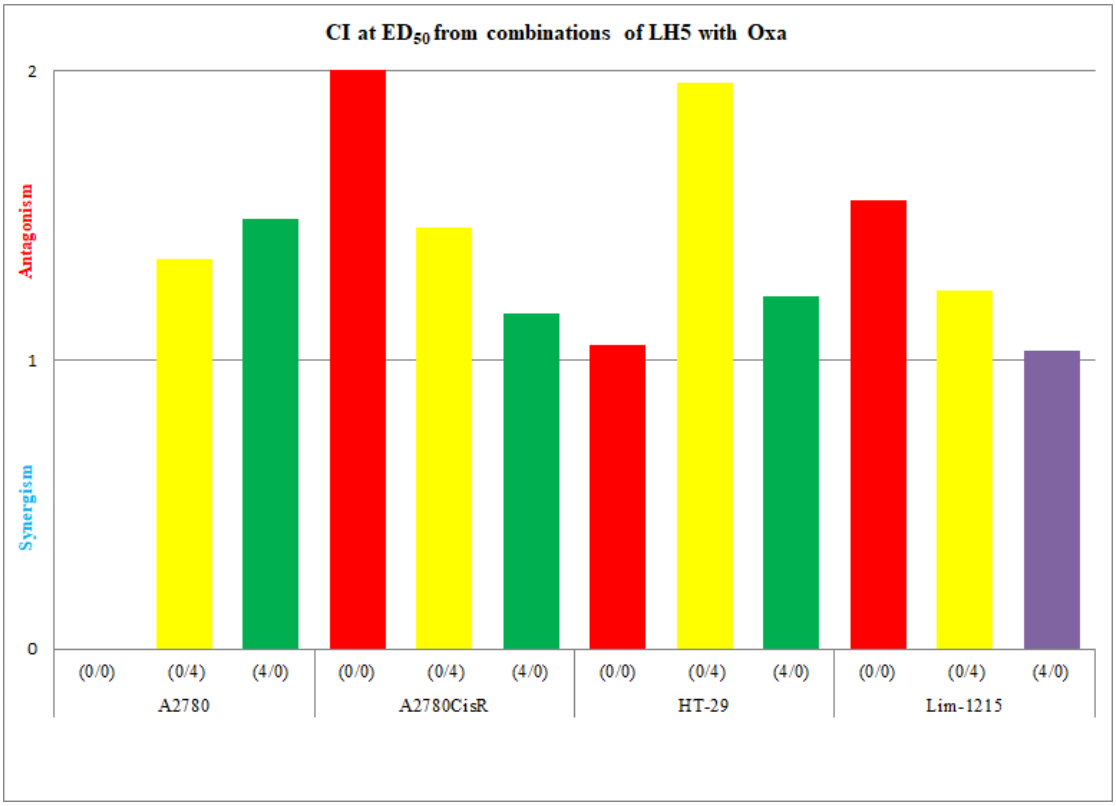

Figure 3.40: CI at ED_{50} from combination of LH5 with Oxa against tested cell lines

It can be observed from above results that combination of LH5 with Oxa did not produce synergism at any sequence of administration at ED_{50} level against the tested cell lines. However, against $A2780^{cisR}$ cell line mild enhancement in cell kill was observed at higher added concentrations (ED_{90} level) from combination of LH5 with Oxa at all sequences of administration.

3.2.2.5 Combination of Gem with LH5

Table 3.7 presents the CI values at three different concentrations (ED_{50}, ED_{75} and ED_{90}) relating to binary combination of Gem with LH5 for the three sequences of administration: (0/0), (0/4) and (4/0) in parent A2780 human ovarian cancer cell line, resistant $A2780^{cisR}$ ovarian cancer cell line, HT-29 colorectal cancer cell line and Lim-1215 colorectal cancer cell line. Figure 3.41 gives the graphical representation of CI at ED_{50} obtained from combination of Gem with LH5 in the selected cell lines.

Table 3.7: CI values relating to binary combination of Gem with LH5 for different modes of administration in selected cell lines (D_m=medium effect dose, m=the exponent defining shape of the dose-effect curve, and r=the reliability coefficient)

Cell line	Drug	Sequence (h)	Molar Ratio	CI Values at					
				ED_{50}	ED_{75}	ED_{90}	Dm	m	R
A2780	Gem		(1:1609.8)	N/A	N/A	N/A	0.001	1.452	0.996
	LH5			N/A	N/A	N/A	2.955	1.408	0.999
	Gem + LH5	0/0		1.64	1.28	1.00	0.001	2.110	0.982
	Gem + LH5	0/4		1.50	1.18	0.93	0.001	2.077	0.951
	Gem + LH5	4/0		1.10	1.06	1.03	0.001	1.486	0.988
A2780^{cisR}	Gem		(1:810.08)	N/A	N/A	N/A	0.008	1.110	0.933
	LH5			N/A	N/A	N/A	5.545	1.401	0.998
	Gem + LH5	0/0		0.89	1.07	1.31	0.003	1.232	0.957
	Gem + LH5	0/4		0.58	0.88	1.33	0.002	0.994	0.974
	Gem + LH5	4/0		0.70	1.05	1.61	0.002	0.986	0.943
HT-29	Gem		(1:581.66)	N/A	N/A	N/A	0.015	1.853	0.935
	LH5			N/A	N/A	N/A	9.199	1.992	0.977
	Gem + LH5	0/0		1.08	1.10	1.11	0.008	1.878	0.965
	Gem + LH5	0/4		1.15	1.15	1.15	0.009	1.920	0.989
	Gem + LH5	4/0		1.32	1.36	1.40	0.010	1.820	0.990
Lim-1215	Gem		(1:370.58)	N/A	N/A	N/A	0.043	1.481	0.893
	LH5			N/A	N/A	N/A	6.012	1.441	0.990
	Gem + LH5	0/0		1.15	0.97	0.82	0.013	1.863	0.928
	Gem + LH5	0/4		1.09	1.00	0.91	0.013	1.644	0.944
	Gem + LH5	4/0		1.21	1.05	0.90	0.014	1.807	0.921

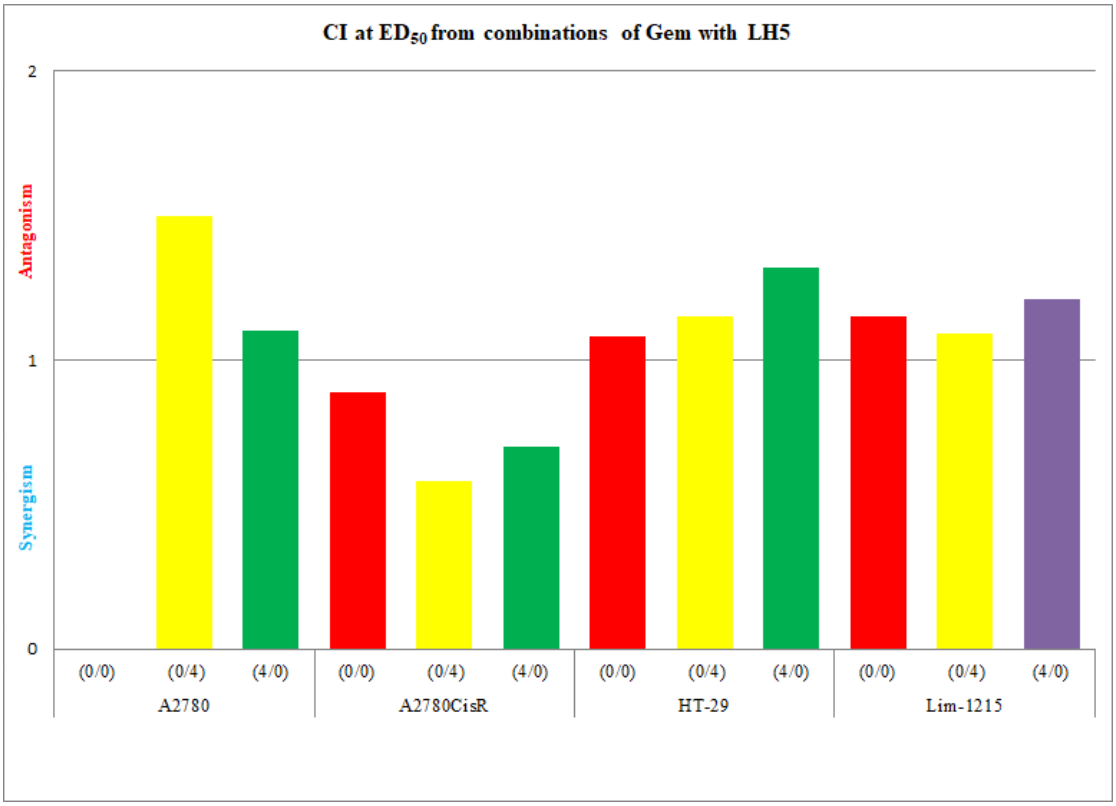

Figure 3.41: CI at ED_{50} from combination of Gem with LH5 against tested cell lines

It can be said from above results that combination of Gem with LH5 produced significant synergism at ED_{50} for all sequences of administration against $A2780^{cisR}$ cell line. Moreover, against Lim-1215 cell line mild synergism was observed at high concentration (ED_{90} level) for the combined administration of Gem with LH5 at all sequences of administration. Against HT-29 and A2780 cell lines the combined effect was predominantly antagonistic towards additiveness.

3.2.2.6 Combination of Gem with Cis

Table 3.8 presents the CI values at three different concentrations (ED_{50}, ED_{75} and ED_{90}) relating to binary combination of Gem with Cis for the three sequences of administration: (0/0), (0/4) and (4/0) in A2780 parent human ovarian cancer cell line and the resistant $A2780^{CcisR}$ ovarian cancer cell line. Figure 3.42 gives the graphical

representation of CI at ED_{50} obtained from combination of Gem with Cis in the selected cell lines.

Table 3.8: CI values relating to binary combination of Gem with Cis for different modes of administration in selected cell lines (D_m=medium effect dose, m=the exponent defining shape of the dose-effect curve, and r=the reliability coefficient)

	Drug	**Sequence (h)**	**Molar Ratio**	**CI Values at**					
Cell line				ED_{50}	ED_{75}	ED_{90}	Dm	m	R
A2780	Gem		(1:193.02)	N/A	N/A	N/A	0.001	1.452	0.996
	Cis			N/A	N/A	N/A	0.371	1.129	1
	Gem + Cis	0/0		1.02	1.05	1.08	0.000	1.24	0.994
	Gem + Cis	0/4		1.38	1.13	0.94	0.001	1.669	0.998
	Gem + Cis	4/0		1.07	1.06	1.06	0.001	1.301	0.995
$A2780^{cisR}$	Gem		(1:681.44)	N/A	N/A	N/A	0.010	1.878	0.883
	Cis			N/A	N/A	N/A	6.062	1.422	0.999
	Gem + Cis	0/0		0.54	0.83	1.28	0.002	0.994	0.989
	Gem + Cis	0/4		0.65	0.79	0.98	0.003	1.240	0.964
	Gem + Cis	4/0		0.72	0.94	1.23	0.003	1.164	0.965

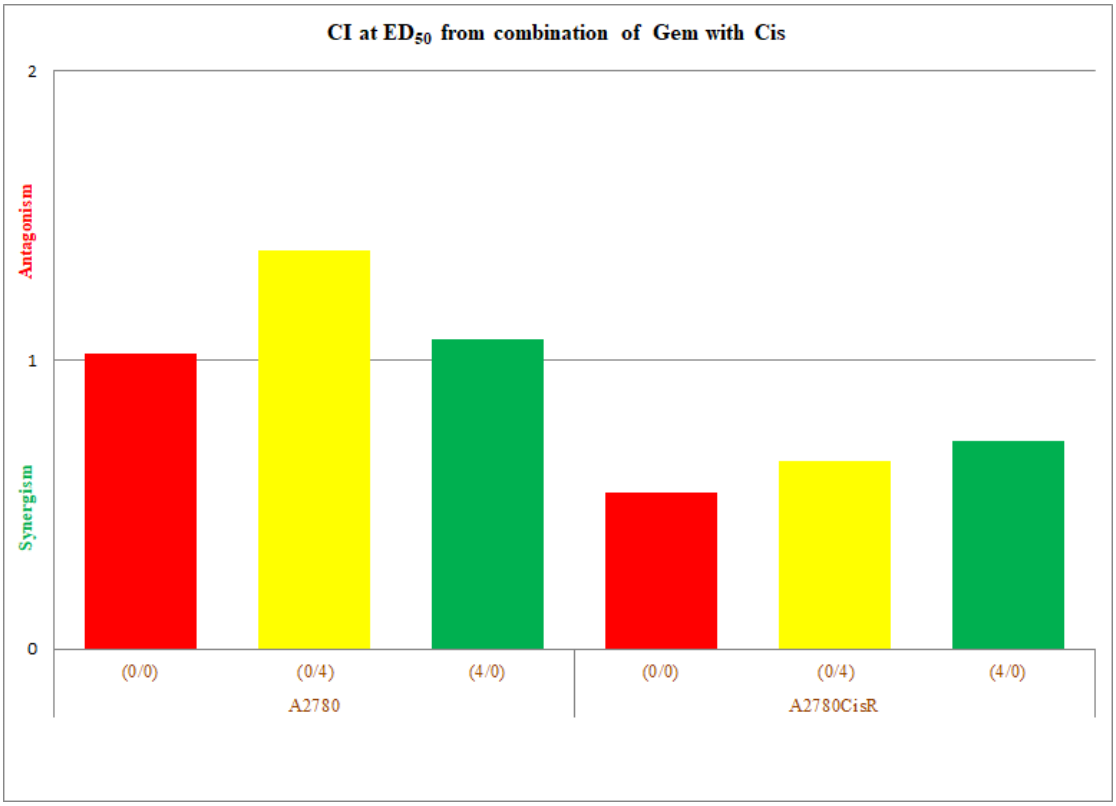

Figure 3.42: CI at ED_{50} for the combination of Gem with Cis against tested cell lines

It can be said from above results that combination of Gem with Cis produced significant synergism against $A2780^{cisR}$ cell line for all sequences of addition and all concentrations. But against A2780 cell line the combined effect was additive to antagonistic at all added concentrations and sequences of administration.

3.2.2.7 Combination of Gem with Oxa

Table 3.9 presents the CI values at three different concentrations (ED_{50}, ED_{75} and ED_{90}) relating to binary combinations of Gem with Oxa for the three sequences of administration: (0/0), (0/4) and (4/0) in HT-29 human colorectal cancer cell line and resistant Lim-1215 colorectal cancer cell line. Figure 3.43 gives the graphical representation of CI at ED_{50} obtained from combination of Gem with Oxa in the selected cell lines.

Table 3.9: CI values relating to binary combinations of Gem with Oxa for different modes of administration in selected cell lines (D_m=medium effect dose, m=the exponent defining shape of the dose-effect curve, and r=the reliability coefficient)

	Drug	Sequence (h)	Molar Ratio	CI Values at					
Cell line				ED_{50}	ED_{75}	ED_{90}	Dm	m	R
HT-29	Gem		(1:78.33)	N/A	N/A	N/A	0.015	1.853	0.935
	Oxa			N/A	N/A	N/A	1.152	1.491	0.953
	Gem + Oxa	0/0		0.95	1.18	1.47	0.007	1.248	0.982
	Gem + Oxa	0/4		1.02	1.43	2.01	0.007	1.100	0.992
	Gem + Oxa	4/0		1.30	1.24	1.18	0.01	1.785	0.970
Lim-1215	Gem		(1:26.47)	N/A	N/A	N/A	0.043	1.481	0.893
	Oxa			N/A	N/A	N/A	2.108	1.290	0.915
	Gem + Oxa	0/0		0.98	1.16	1.38	0.029	1.157	0.994
	Gem + Oxa	0/4		1.20	1.08	0.96	0.035	1.640	0.966
	Gem + Oxa	4/0		0.82	0.74	0.66	0.024	1.639	0.989

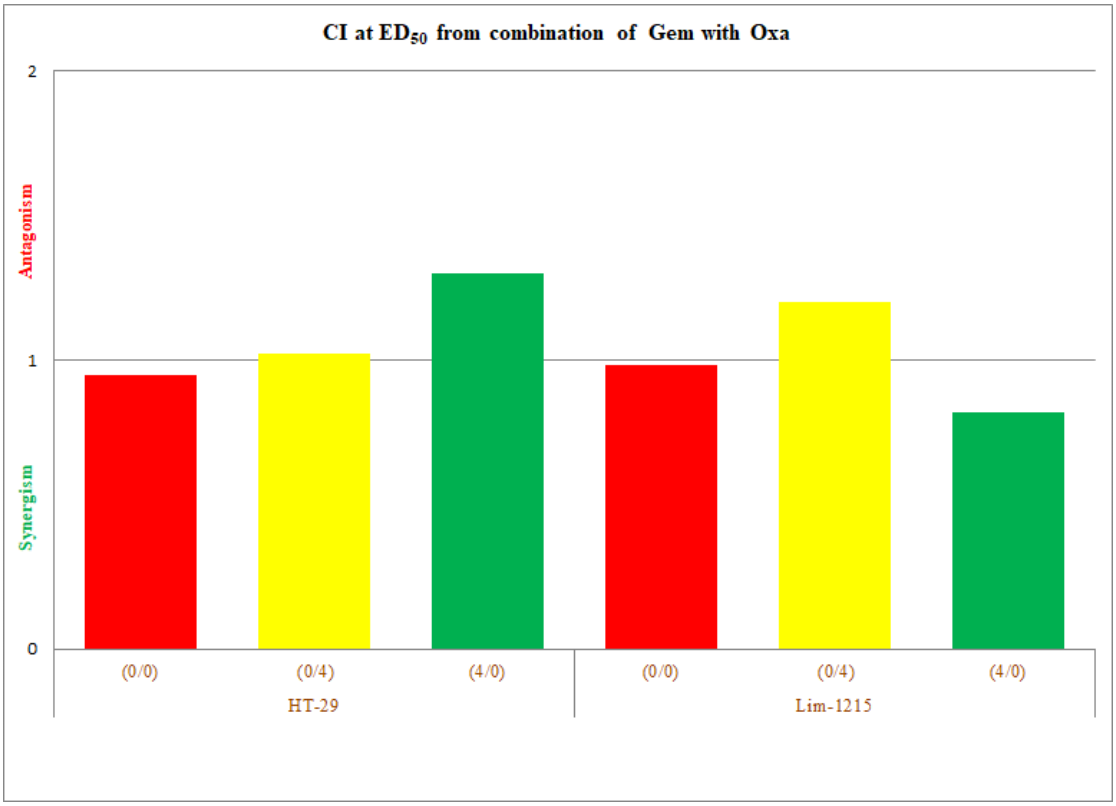

Figure 3.43: CI at ED_{50} for combination of Gem with Oxa against tested cell lines

It is evident from above results that, combination of Gem with Oxa produced additive to antagonistic effect against the tested cell lines irrespective sequence of addition and concentrations except for 4/0 sequence of administration against Lim-1215 cell line. Synergism was also found at all concentrations for the combination of Gem with Oxa for 4/0 sequence of addition against Lim-1215 cell line.

3.2.2.8 Combination of Cuc with Cis

Table 3.10 presents the CI values at three different concentrations (ED_{50}, ED_{75} and ED_{90}) relating to binary combinations of Cuc with Cis for the three modes of administration: (0/0), (0/4) and (4/0) in parent A2780 cell line and resistant $A2780^{cisR}$ cell line. Figure 3.44 gives the graphical representation of CI at ED_{50} obtained from combination of Cuc with Cis in the selected cell lines.

Table 3.10: CI values relating to binary combination of Cuc with Cis for different modes of administration in selected cell lines (D_m=medium effect dose, m=the exponent defining shape of the dose-effect curve, and r=the reliability coefficient)

Cell line	Drug	Sequence (h)	Molar Ratio	CI Values at					
				ED_{50}	ED_{75}	ED_{90}	Dm	m	R
A2780	Cuc		(1:81.36)	N/A	N/A	N/A	0.009	2.006	0.994
	Cis			N/A	N/A	N/A	0.823	1.328	0.997
	Cuc + Cis	0/0		0.72	0.79	0.90	0.003	1.418	0.999
	Cuc + Cis	0/4		0.70	0.98	1.38	0.003	1.099	0.999
	Cuc + Cis	4/0		0.92	0.82	0.75	0.004	1.966	0.989
$A2780^{cisR}$	Cuc		(1:305.47)	N/A	N/A	N/A	0.051	0.649	0.811
	Cis			N/A	N/A	N/A	8.168	2.018	0.977
	Cuc + Cis	0/0		1.43	1.61	2.14	0.025	1.179	0.999
	Cuc + Cis	0/4		0.70	1.39	3.26	0.012	0.733	0.911
	Cuc + Cis	4/0		1.04	1.11	1.39	0.018	1.256	0.998

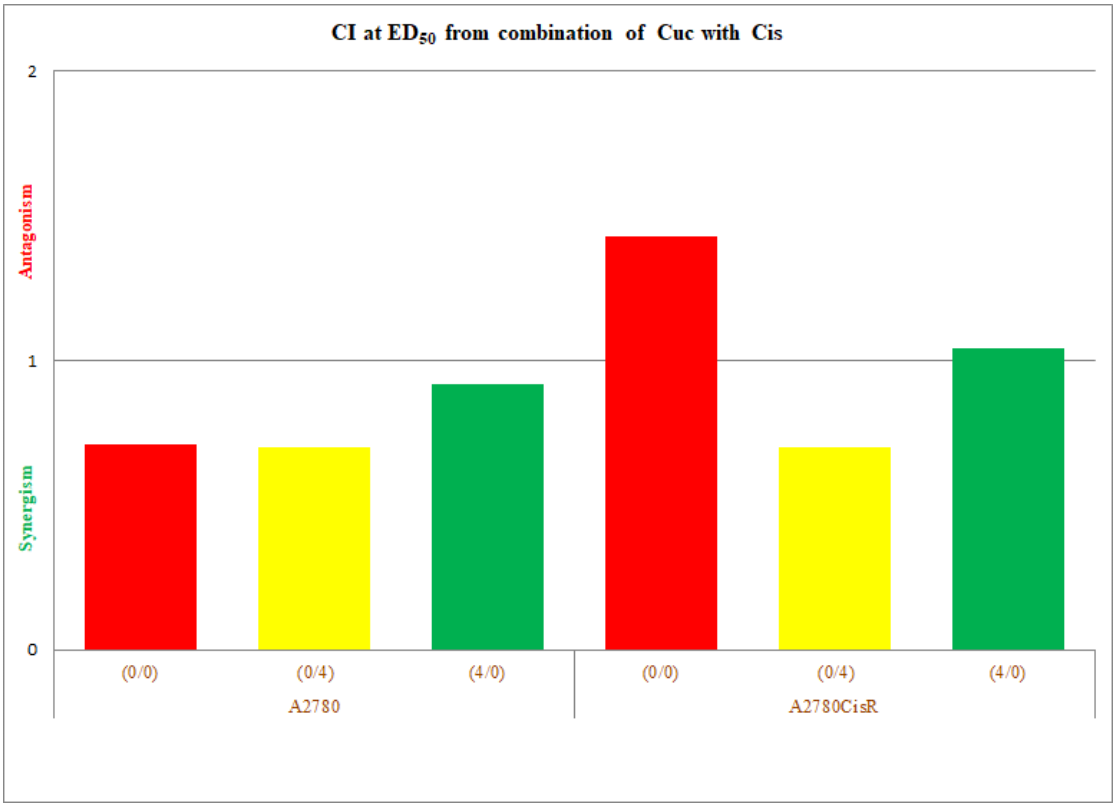

Figure 3.44: CI at ED_{50} from combination of Cuc with Cis against tested cell lines

It can be seen from above results that, combination of Cuc with Cis produced significant synergism against parent A2780 cell line for all sequences of addition and concentrations except for 0/4 sequence of administration at ED_{90} level. But against resistant $A2780^{cisR}$ cell line the combined effect was additive to antagonistic at all added concentrations and sequences of administration except for 0/4 sequence of administration at ED_{50} level.

3.2.2.9 Combination of Cuc with LH5

Table 3.11 presents the CI values at different concentrations (ED_{50}, ED_{75} and ED_{90}) relating to binary combinations of Cuc with LH5 for the three modes of administration: (0/0), (0/4) and (4/0) in parent A2780 cell line and resistant $A2780^{cisR}$ ovarian cancer tumour model. Figure 3.45 gives the graphical representation of CI at ED_{50} obtained from combination of Cuc with LH5 in the selected cell lines.

Table 3.11: CI values relating to binary combination of Cuc with LH5 for different modes of administration in selected cell lines (D_m=medium effect dose, m=the exponent defining shape of the dose-effect curve, and r=the reliability coefficient)

Cell line	Drug	Sequence (h)	Molar Ratio	CI Values at					
				ED_{50}	ED_{75}	ED_{90}	Dm	M	R
A2780	Cuc		(1:683.19)	N/A	N/A	N/A	0.009	2.006	0.994
	LH5			N/A	N/A	N/A	5.725	1.773	0.998
	Cuc + LH5	0/0		1.30	1.71	2.25	0.005	1.280	0.999
	Cuc + LH5	0/4		0.84	1.36	2.20	0.003	1.031	0.941
	Cuc + LH5	4/0		0.72	1.29	2.29	0.003	0.945	0.993
$A2780^{cisR}$	Cuc		(1:363.09)	N/A	N/A	N/A	0.051	0.649	0.811
	LH5			N/A	N/A	N/A	4.756	1.613	0.986
	Cuc + LH5	0/0		0.93	0.93	1.02	0.009	1.337	0.999
	Cuc + LH5	0/4		1.17	1.33	1.63	0.012	1.164	0.978
	Cuc + LH5	4/0		0.90	0.91	0.99	0.009	1.332	0.996

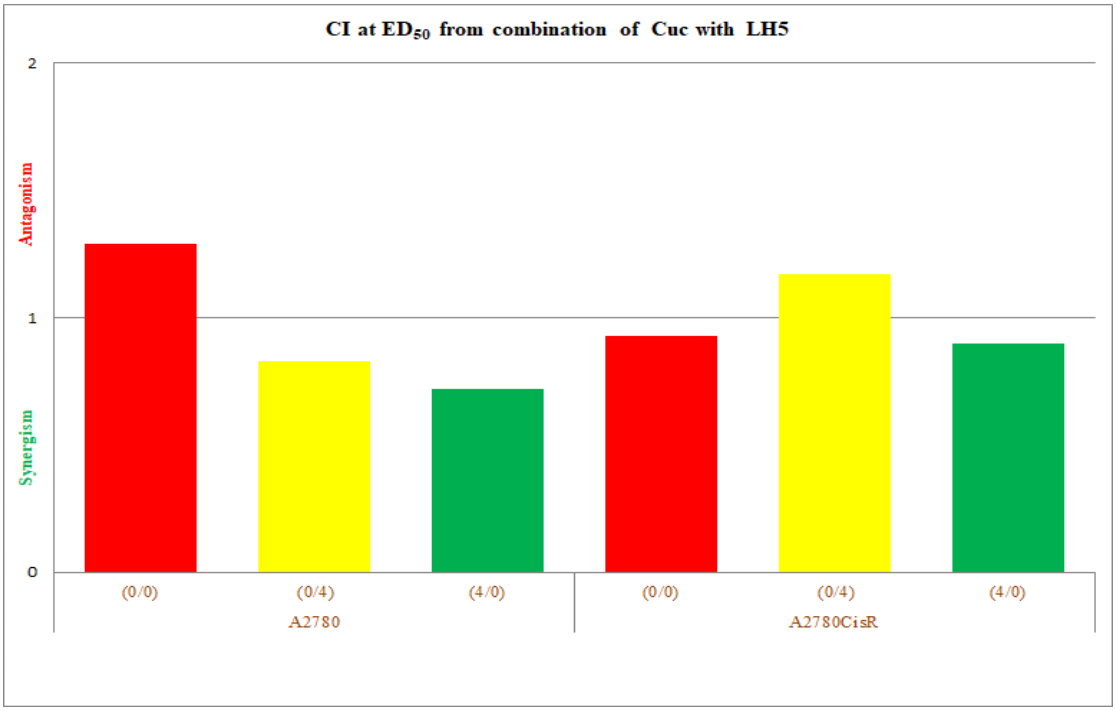

Figure 3.45: CI at ED_{50} for the combinations of Cuc with LH5 against tested cell lines

It is evident from above results that, combination of Cuc with LH5 produced synergism against A2780^{cisR} cell line for all sequences of addition and concentrations except for 0/4 sequence. In contrast, against A2780 cell line the combined effect was antagonistic for all added concentrations and sequences of administration except for ED_{50} level for 0/4 and 4/0 sequences of administration.

3.3 DNA damage study

As mentioned in the previous section, DNA damage study was conducted to seek relationship between combined drug action and DNA damage. This study was performed with the selected drugs alone or in combinations.

3.3.1 A2780 cell line

Table 3.12 gives mobility and net intensity of DNA band applying to A2780 cell line after selected drug treatments. A blank control is also included. Figures 3.46 to 3.48 give electrophoretograms, mobility and net intensity of DNA bands respectively.

Table 3.12: Mobility and intensity of DNA bands applying to A2780 cells after selected drug treatments

Band Serial	Band Name	DNA Mobility (mm)	Band Intensity
1	A2780-Blank	3.47	10404.79
2	Cisplatin	3.47	13058.43
3	LH5	3.72	3406.79
4	Cis+Camp-(0/0)	3.13	22383.12
5	Cis+Camp-(0/4)	3.04	53134.43
6	Cis+Camp-(4/0)	3.04	26911.8
7	Cis+LH5-(0/0)	3.21	11183.97
8	Cis+LH5-(0/4)	3.04	12427.84
9	Cis+LH5-(4/0)	2.87	13412.2

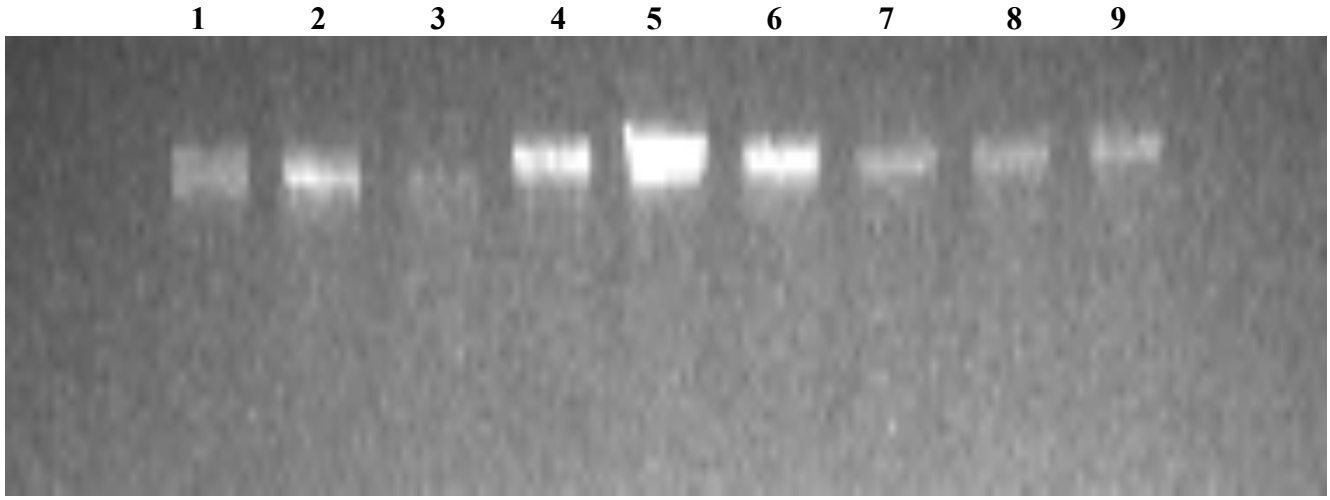

Figure 3.46: Electrophoretogram applying to cellular DNA obtained from drug treatment of A2780 cell line

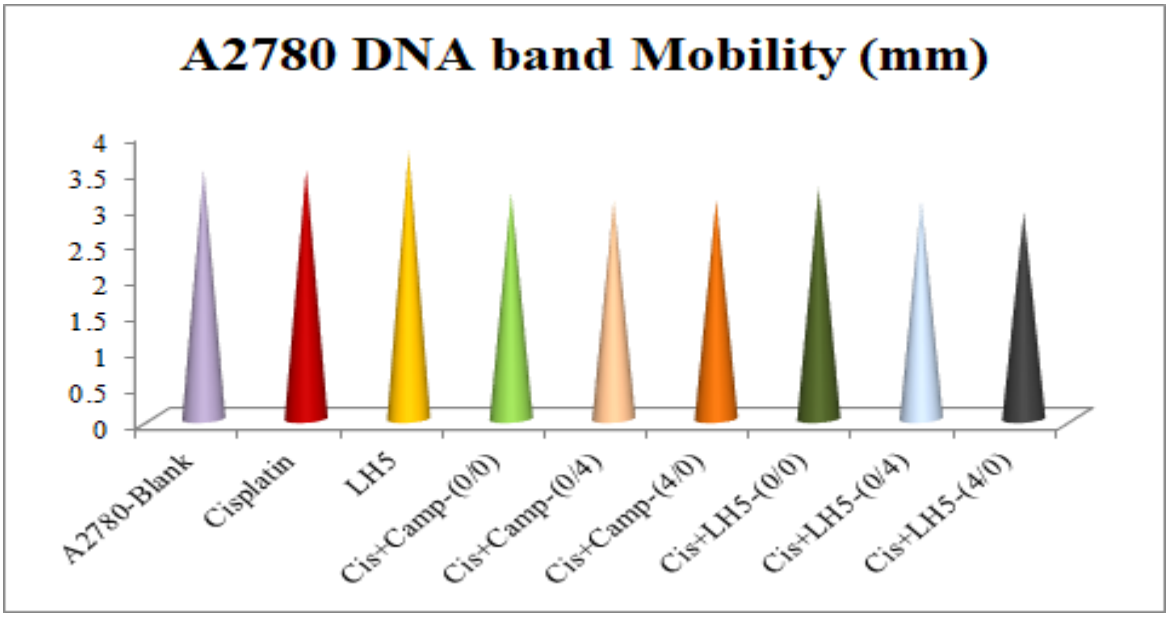

Figure 3.47: DNA band mobility applying to cellular DNA obtained from drug treatment of A2780 cell line

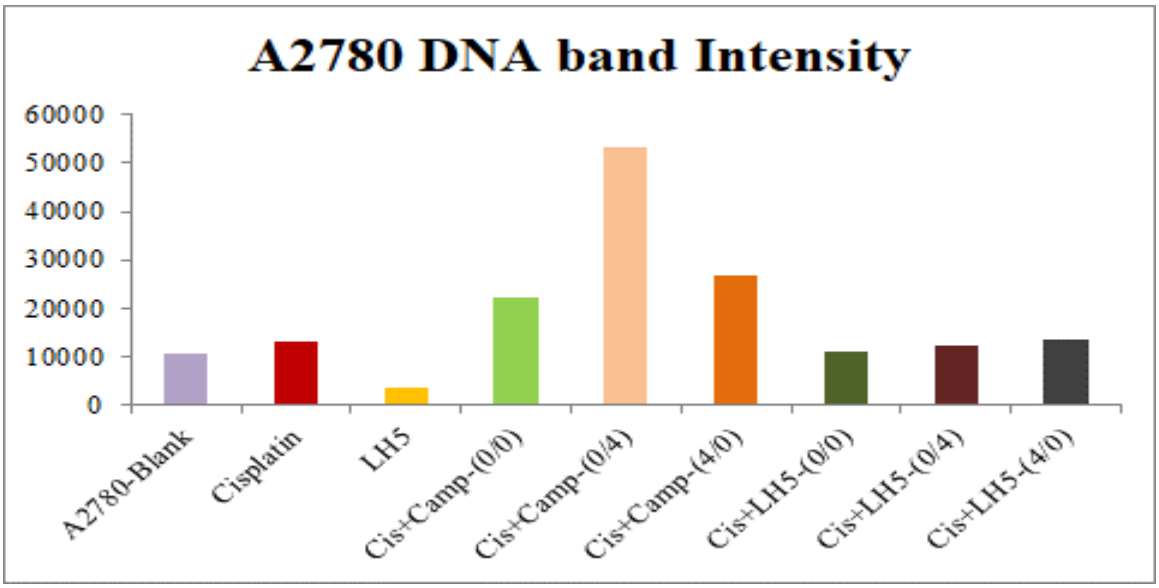

Figure 3.48: DNA fluorescence applying to cellular DNA obtained from drug treatment of A2780 cell line

It can be said from the above results that, LH5 alone caused the greatest DNA damage in A2780 cells. The least damage towards DNA was demonstrated for the combination of Cis with LH5 for 4/0 sequence of administration.

3.3.2 A2780^{cisR} cell line

Table 3.13 gives mobility and net intensity of DNA band applying to A2780^{cisR} cell line after selected drug treatments and blank control. Figure 3.49, figure 3.50 and figure 3.51 represents the electrophoretograms, mobility and net intensity of DNA bands respectively.

Table 3.13: Mobility and intensity of DNA bands applying A2780^{cisR} cells after selected drug treatments

Band Serial	Band Name	DNA Mobility (mm)	Band Intensity
1	A2780CisR-Blank	2.2	35991.54
2	Cisplatin	2.46	4194
3	LH5	2.54	6722
4	Cis+Camp-(0/0)	2.37	9958.62
5	Cis+Camp-(0/4)	2.37	11404.94
6	Cis+Camp-(4/0)	2.46	15486.5
7	Cis+LH5-(0/0)	2.29	15843
8	Cis+LH5-(0/4)	2.46	7280
9	Cis+LH5-(4/0)	1.95	20614.75

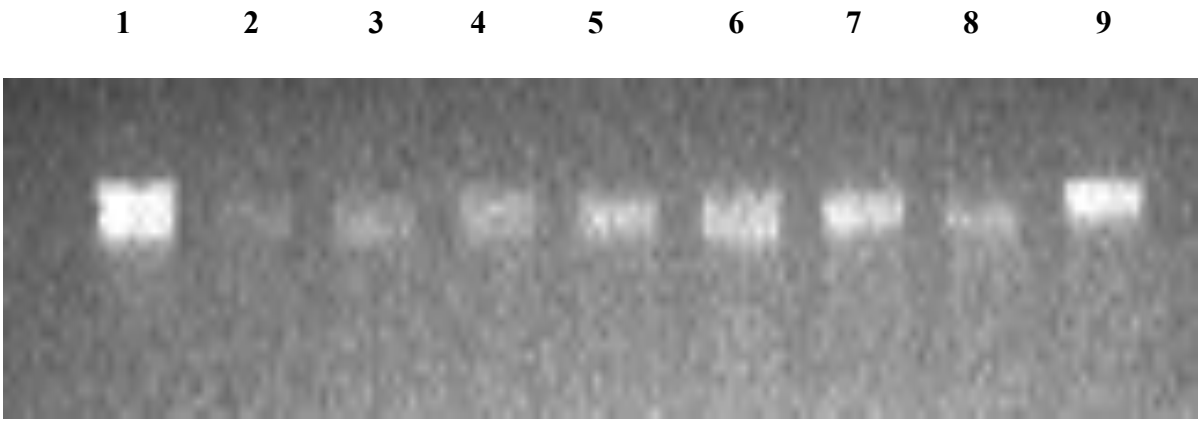

Figure 3.49: Electrophoretogram applying to cellular DNA obtained from drug treatment of A2780^{cisR} cell line

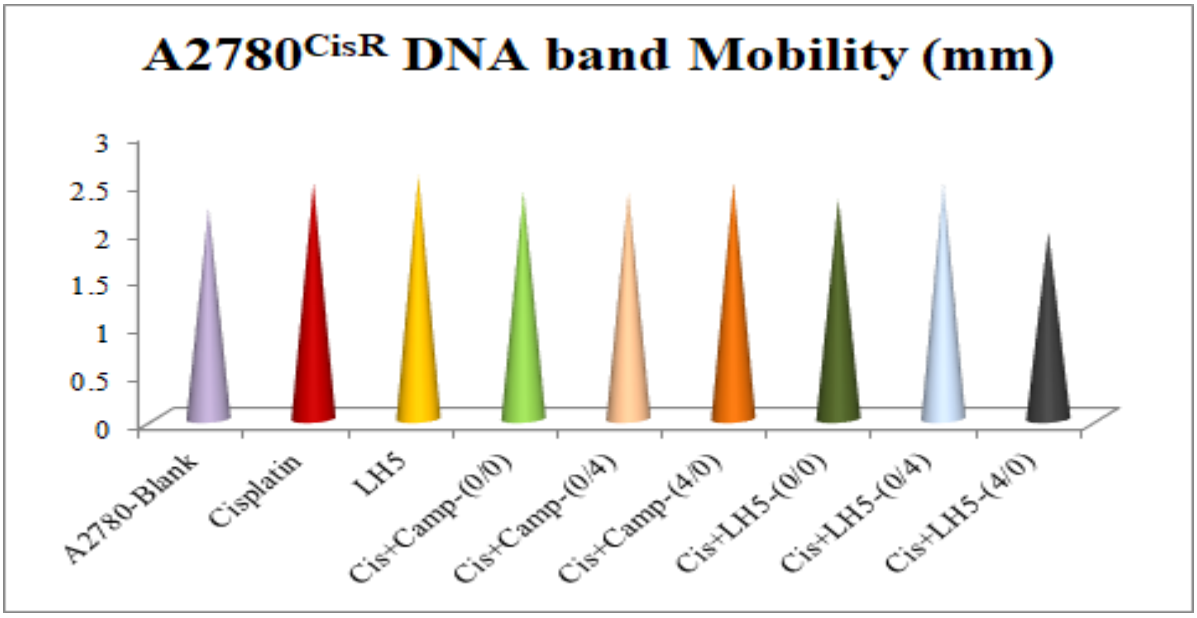

Figure 3.50: DNA band mobility obtained from the study in A2780^{cisR} cell line

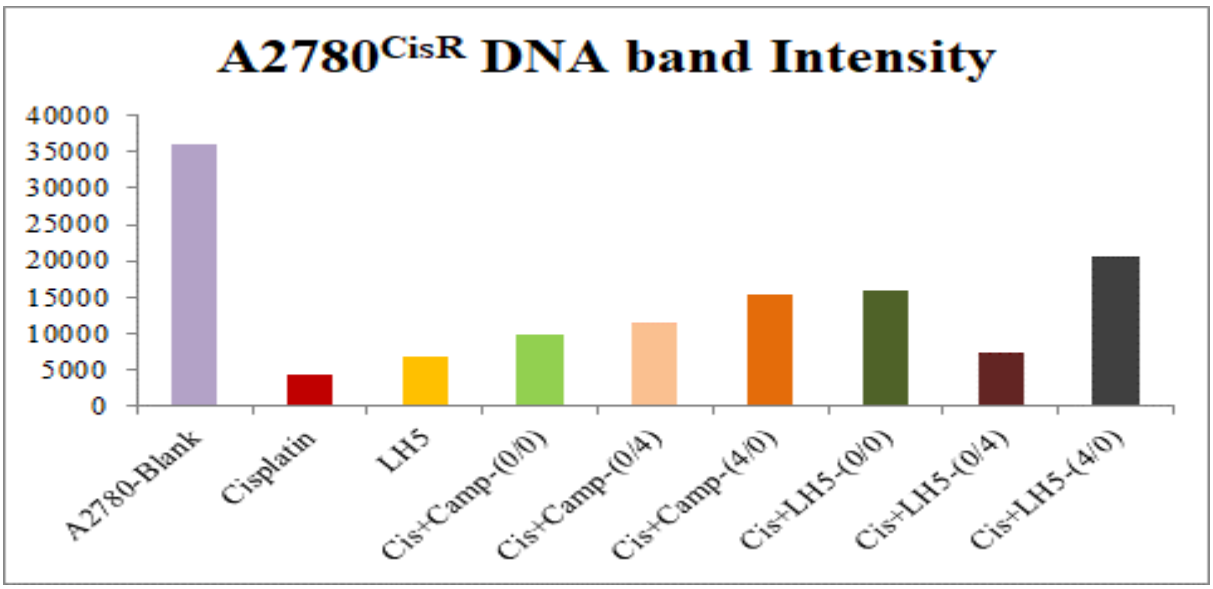

Figure 3.51: DNA fluorescence from the study in A2780^{cisR} cell line

It can be seen from the above results that, as in parent A2780 cell line, LH5 alone caused the greatest DNA damage in resistant A2780^{cisR} cells. Interestingly, the least DNA damage was also observed for the combination of Cis with LH5 using 4/0 sequence of administration as applied to parent A2780 cell line.

3.4 Cellular accumulation of Platinum and DNA binding study

3.4.1 Cellular accumulation of Platinum

Tables 3.14 to 3.17 give cellular accumulation of platinum expressed as nmol Pt per $5x10^6$ cells in A2780, $A2780^{cisR}$, HT-29 and Lim-1215 cancer cell lines respectively after selected drug treatments alone and in combinations.

Table 3.14: Accumulation of platinum in A2780 ovarian cancer cell line after drug treatments.

Selected sample	Combined effect at ED_{50}	Pt (nmol/$5x10^6$cell)	Standard deviation
Cis (alone)	Not applicable	0.36	0.01
LH5 (alone)	Not applicable	3.74	1.26
Oxa (alone)	Not applicable	0.01	0.00
Cis + Camp (0/0)	Antagonistic	3.12	0.24
Cis + Camp (0/4)	Additive	2.00	0.09
Cis + Camp (4/0)	Antagonistic	2.42	0.23
Cis + LH5 (0/0)	Antagonistic	3.16	0.46
Cis + LH5 (0/4)	Antagonistic	2.60	0.21
Cis + LH5 (4/0)	Synergistic	2.34	0.15
LH5 + Camp (0/0)	Antagonistic	1.90	0.38
LH5 + Camp (0/4)	Antagonistic	3.57	0.13
LH5 + Camp (4/0)	Antagonistic	3.29	0.46
LH5 + Oxa (0/0)	Antagonistic	2.05	0.09
LH5 + Oxa (4/0)	Antagonistic	2.86	0.30
Gem + Cis (0/4)	Additive	0.39	0.04

Table 3.15: Accumulation of platinum in A2780^{cisR} ovarian cancer cell line

Sample	Combined effect at ED_{50}	Pt (nmol/5x10^{6}cell)	Standard deviation
Cis (alone)	Not applicable	3.63	0.92
LH5 (alone)	Not applicable	11.48	0.19
Oxa (alone)	Not applicable	0.24	0.01
Cis + Camp (0/0)	Synergistic	2.55	0.22
Cis + Camp (0/4)	Synergistic	2.12	0.06
Cis + Camp (4/0)	Synergistic	1.61	0.17
Cis + LH5 (0/0)	Antagonistic	18.95	0.31
Cis + LH5 (0/4)	Antagonistic	15.04	0.46
Cis + LH5 (4/0)	Antagonistic	14.69	1.93
LH5 + Camp (0/0)	Additive	10.74	0.76
LH5 + Camp (0/4)	Antagonistic	15.18	0.69
LH5 + Camp (4/0)	Synergistic	11..73	0.15
LH5 + Oxa (0/0)	Antagonistic	10.32	0.48
LH5 + Oxa (4/0)	Antagonistic	19.60	1.57
Gem + Cis (0/4)	Synergistic	0.98	0.15

Table 3.16: Accumulation of platinum in HT-29 colorectal cancer cell line after drug treatments for selected drugs either alone or in combination

Sample	Combined effect at ED_{50}	Pt (nmol/5x10^6cell)	Standard deviation
Cis (alone)	Not applicable	1.59	0.27
LH5 (alone)	Not applicable	7.31	0.39
Oxa (alone)	Not applicable	0.12	0.00
Cis + Camp (0/4)	Synergistic	1.60	0.12
Cis + LH5 (0/0)	Antagonistic	10.69	1.38
LH5 + Oxa (0/0)	Additive	9.93	0.28

Table 3.17: Accumulation of platinum in Lim-1215 colorectal cancer cell line after drug treatments for selected drugs either alone or in combination

Sample	Combined effect at ED_{50}	Pt (nmol/5x10^6cell)	Standard deviation
Cis (alone)	Not applicable	1.49	0.19
LH5 (alone)	Not applicable	7.49	0.27
Oxa (alone)	Not applicable	0.06	0.01
Cis + Camp (0/4)	Antagonistic	1.60	0.12
Cis + LH5 (0/0)	Antagonistic	10.69	1.38
LH5 + Oxa (0/0)	Antagonistic	9.93	0.28
LH5 + Camp (0/0)	Synergistic	6.88	0.35
LH5 + Camp (0/4)	Antagonistic	7.30	0.87
LH5 + Camp (4/0)	Synergistic	8.78	0.25

It is observed from the study that no definite trend was followed by the combined drug treatments in regard to cellular accumulation of platinum in the tested cell lines. In some cases, synergistic treatment caused greater cellular accumulation of platinum than the platinum drug treated alone e.g. LH5 with Camp using 4/0 sequence of addition in colorectal Lim-1215 cell line. But in $A2780^{cisR}$ cell line reduced cellular accumulation

was evident from synergistic combined treatment of Cis with Camp at 0/0, 0/4 and 4/0 sequences of addition. Similar inconsistent results were also observed from antagonistic combined treatments as well.

3.4.2 DNA binding study

Tables 3.18 to 3.21 give the results of Pt–DNA binding levels, expressed as nmol Pt per mg of DNA in A2780, A2780^{cisR}, HT-29 and Lim-1215 cancer cell lines after treatments with selected drugs given alone and in combination.

Table 3.18: Platinum-DNA binding in A2780 ovarian cancer cell line after treatments with selected drugs

Selected sample	Combined effect at ED_{50}	Pt (nmol)/DNA(mg)	Standard deviation
Cis (alone)	Not applicable	0.27	0.02
LH5 (alone)	Not applicable	7.71	1.67
Oxa (alone)	Not applicable	0.13	0.01
Cis + Camp (0/0)	Antagonistic	0.61	0.04
Cis + Camp (0/4)	Additive	0.22	0.01
Cis + Camp (4/0)	Antagonistic	0.61	0.05
Cis + LH5 (0/0)	Antagonistic	8.71	0.13
Cis + LH5 (0/4)	Antagonistic	19.35	1.37
Cis + LH5 (4/0)	Synergistic	7.88	0.91
LH5 + Camp (0/0)	Antagonistic	2.78	0.21
LH5 + Camp (0/4)	Antagonistic	1.79	0.25
LH5 + Camp (4/0)	Antagonistic	2.67	0.03
LH5 + Oxa (0/0)	Antagonistic	3.15	0.22
LH5 + Oxa (4/0)	Antagonistic	9.13	0.25
Gem + Cis (0/4)	Additive	0.38	0.00

Table 3.19: Platinum-DNA binding in A2780^{cisR} ovarian cancer cell lines

Sample	Combined effect at ED_{50}	Pt (nmol)/DNA(mg)	Standard deviation
Cis (alone)	Not applicable	0.17	0.02
LH5 (alone)	Not applicable	3.66	0.44
Oxa (alone)	Not applicable	0.01	0.00
Cis + Camp (0/0)	Synergistic	0.22	0.01
Cis + Camp (0/4)	Synergistic	0.13	0.01
Cis + Camp (4/0)	Synergistic	0.22	0.03
Cis + LH5 (0/0)	Antagonistic	7.99	0.99
Cis + LH5 (0/4)	Antagonistic	6.28	0.24
Cis + LH5 (4/0)	Antagonistic	8.99	1.08
LH5 + Camp (0/0)	Additive	2.64	0.16
LH5 + Camp (0/4)	Antagonistic	3.14	0.34
LH5 + Camp (4/0)	Synergistic	2.94	0.38
LH5 + Oxa (0/0)	Antagonistic	1.36	0.26
LH5 + Oxa (4/0)	Antagonistic	9.59	2.18
Gem + Cis (0/4)	Synergistic	0.01	0.00

Table 3.20: Platinum-DNA binding in HT-29 colorectal cancer cell lines after treatments with selected drugs

Sample	Combined effect at ED_{50}	Pt (nmol)/DNA(mg)	Standard deviation
Cis (alone)	Not applicable	0.16	0.02
LH5 (alone)	Not applicable	1.62	0.17
Oxa (alone)	Not applicable	0.20	0.03
Cis + Camp (0/4)	Synergistic	0.18	0.02
Cis + LH5 (0/0)	Antagonistic	2.44	0.14
LH5 + Oxa (0/0)	Additive	1.03	0.01

Table 3.21: Platinum-DNA binding in Lim-1215 colorectal cancer cell lines

Sample	Combined effect at ED_{50}	Pt (nmol)/DNA(mg)	Standard deviation
Cis (alone)	Not applicable	0.62	0.11
LH5 (alone)	Not applicable	2.10	0.38
Oxa (alone)	Not applicable	0.47	0.03
Cis + Camp (0/4)	Antagonistic	0.25	0.01
Cis + LH5 (0/0)	Antagonistic	1.58	0.17
LH5 + Oxa (0/0)	Antagonistic	1.77	0.14
LH5 + Camp (0/0)	Synergistic	2.41	0.40
LH5 + Camp (0/4)	Antagonistic	2.07	0.45
LH5 + Camp (4/0)	Synergistic	2.42	0.09

From the above results it can be said that platinum-DNA binding levels in the tested cell lines were not directly related to the combined drug action associated with various drug combination. Likewise, cellular accumulation results applying to both synergistic

and antagonistic combinations did not follow any specific trend. In some instances, synergistic/antagonistic combinations demonstrated increased platinum-DNA binding than that from platinum drug alone. While in some instances, the converse is true. For example, antagonistic (0/0) combination of Cis and Camp produced higher P-DNA level than additive (0/4) combination of the two compounds in A2780 cell line.

3.5 Proteomics

The aim of the proteomic study was to provide mechanistic information in terms of changes in protein expression in the tested ovarian tumour cell lines (the parent cell line A2780 and the platinum refractory cell line A2780^{cisR}) in response to treatment with individual platinum drugs and their combinations with the phytochemical camptothecin. A2780 cell line was treated with Cis alone, Oxa alone, LH5 alone, Cis with Camp (0/0), Cis with LH5 (0/0), Cis with LH5 (4/0), LH5 with Camp (4/0) and LH5 with Oxa (0/0). Whereas A2780^{cisR} cell line was treated with Cis alone, Oxa alone, LH5 alone, LH5 with Camp (0/0), LH5 with Camp (0/4), LH5 with Camp (4/0), LH5 with Oxa (0/0) and LH5 with Oxa (4/0). The expression levels of proteins observed in platinum resistant cell line A2780^{cisR} were compared to those found in the parent A2780 cell line prior to and after drug treatments. Combination treatments displaying synergistic and antagonistic outcomes were chosen for further studies to identify the proteins involved in drug resistance.

3.5.1 Grouping of gels

Initially, gel images were divided into matched groups on the basis of hypothesis to be tested. In the present study, 18 matched groups were made having duplicate gel images. All of the matched groups were then brought together into two classes based on tested

cell lines which is shown in Figure 3.52. Then Melanie software was used to assign common matched ID numbers for individual protein spot in the corresponding gel images in each class. In the gels applying to A2780 untreated cell line, a total of 235 spots were found by the software. Whereas A2780^{cisR} reference gels gave 220 spots.

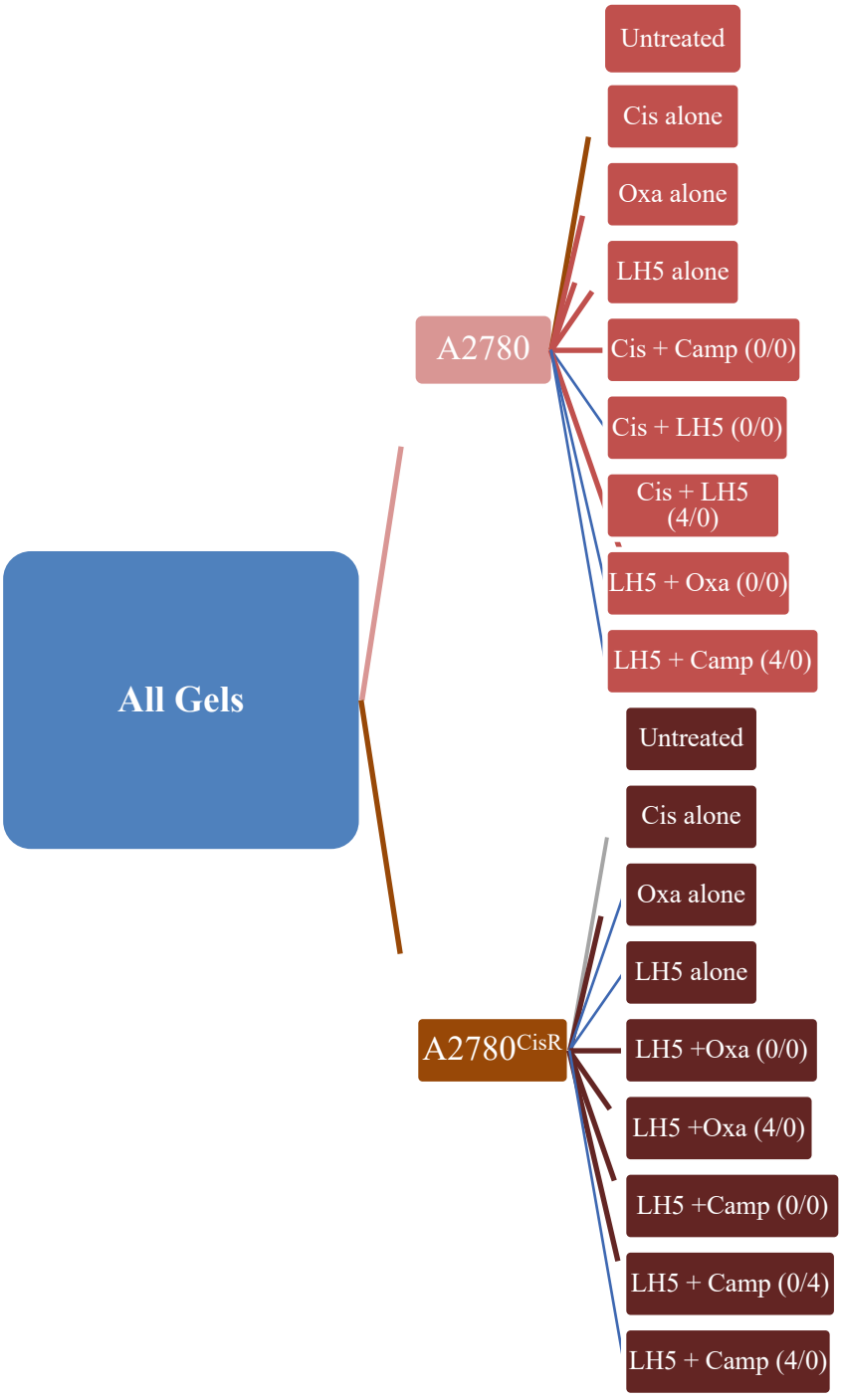

Figure 3.52: Grouping of gels for proteomics

The change in protein expression is considered to be significant if it has changed by a factor of 1.5 or higher. The number of proteins with significant changes in expression was found to vary from treatment to treatment. Finally, among the spots annotated in the A2780 and A2780^{cisR} gels, only 27 spots (9 from A2780 and 18 from A2780^{cisR}) were chosen for further proteomic analysis. Figure 3.53 (A2780 untreated) and Figure 3.54 (A2780^{cisR} untreated) represent the image of annotated reference gels used in the study. Figures 3.55 to 3.62 display the images of treatment gels for A2780 class. Figure 3.63 to Figure 3.70 display the images of treatment gels for A2780^{cisR} class.

Gel: A2780-Blank: spots identified								
3A	13	17	32	33 (landmark 2)	38A	41	43A	54

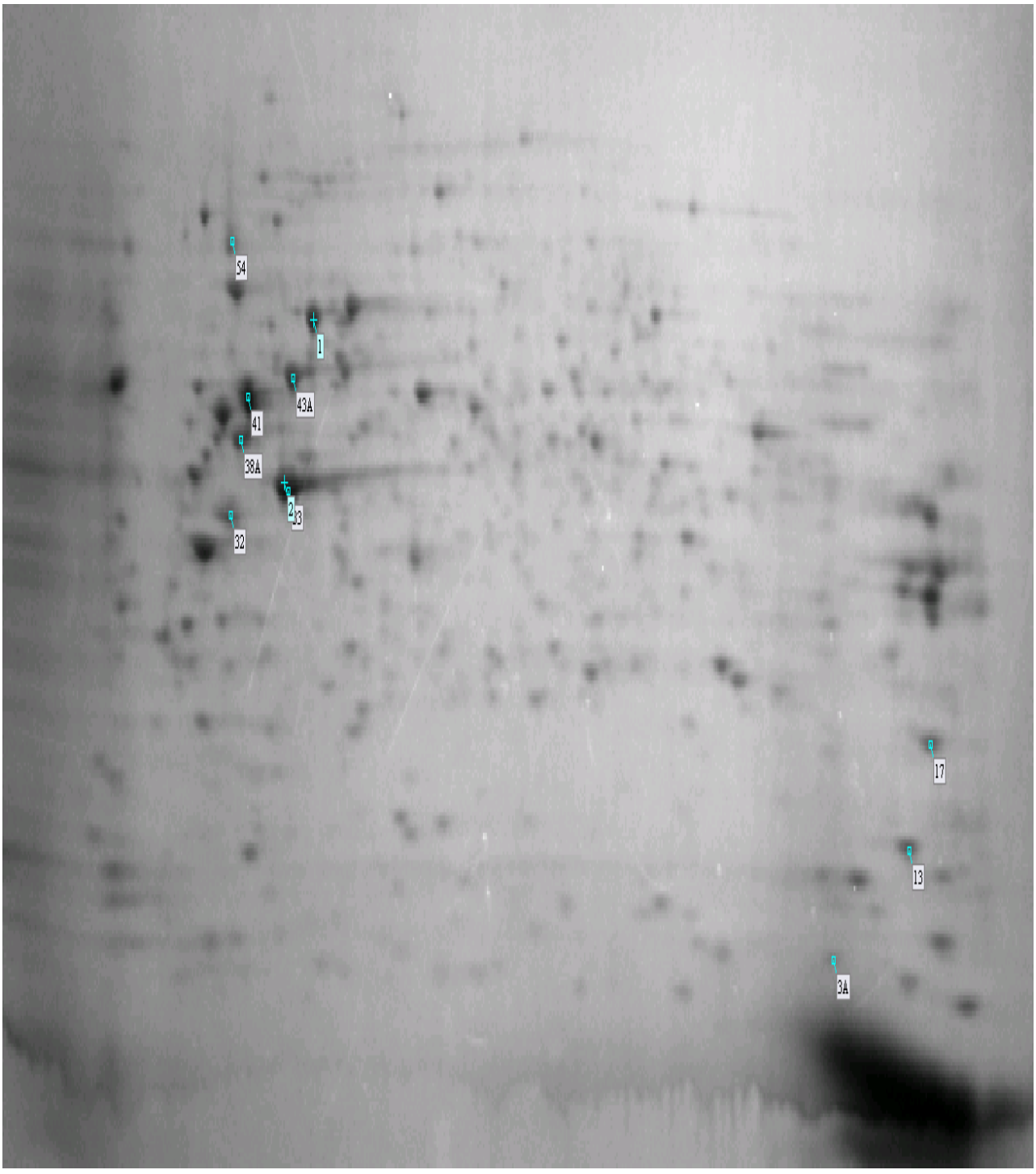

Figure 3.53: Two dimensional protein profile in annotated A2780 reference gel (Untreated)

Gel: CisR-Blank: Spots identified																	
6	8	12	16	21	33	37	42	45	48	50	60	76	99	100	111	120	179

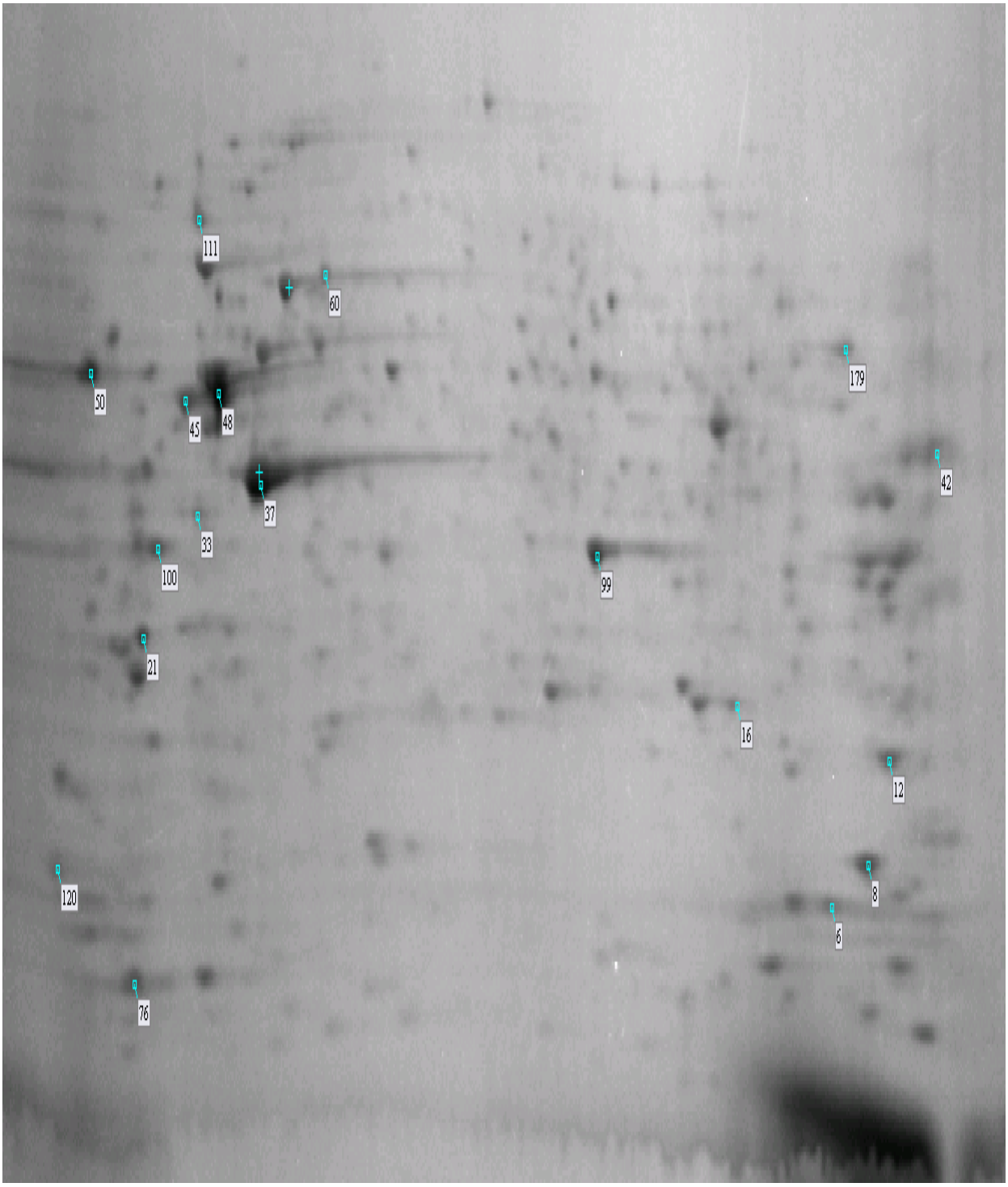

Figure 3.54: Two dimensional protein profile in annotated A2780^{cisR} reference gel (Untreated)

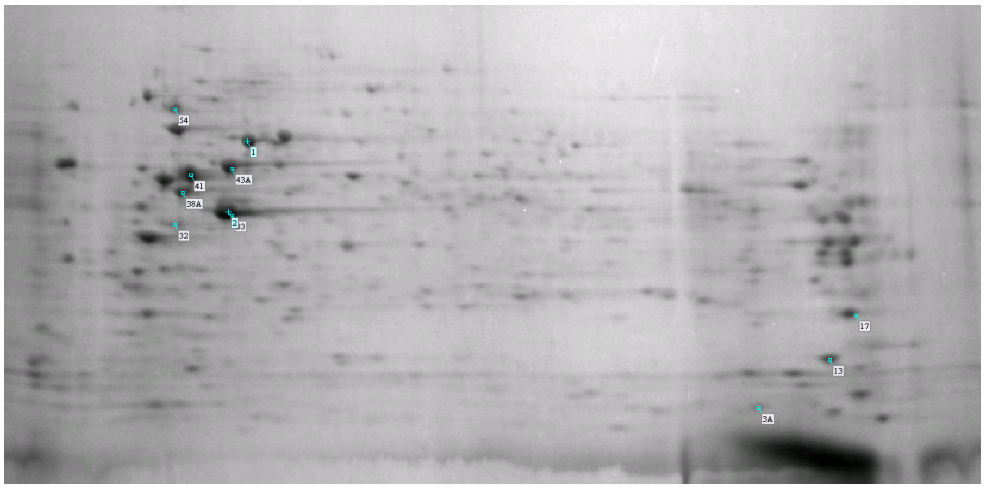

Figure 3.55: Cisplatin alone treated A2780 two dimensional protein gel image

Figure 3.56: Oxaliplatin alone treated A2780 two dimensional protein gel image

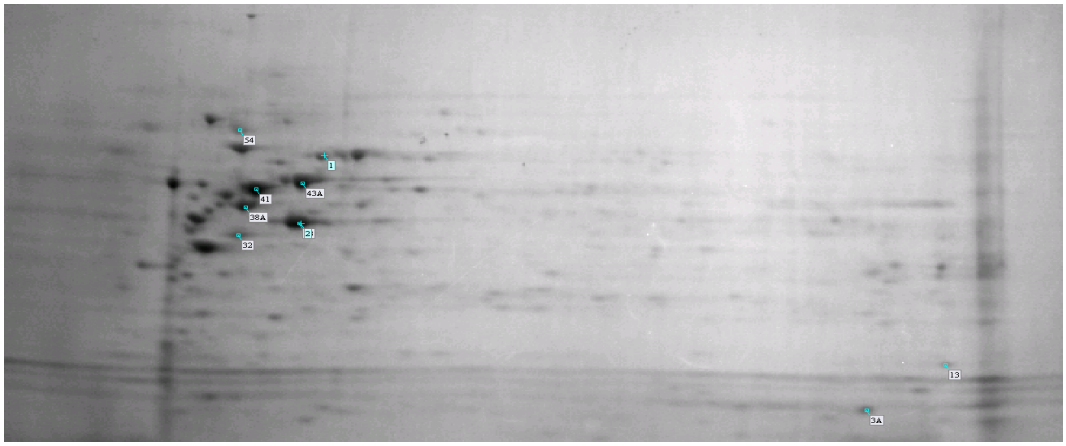

Figure 3.57: LH5 alone treated A2780 two dimensional protein gel image

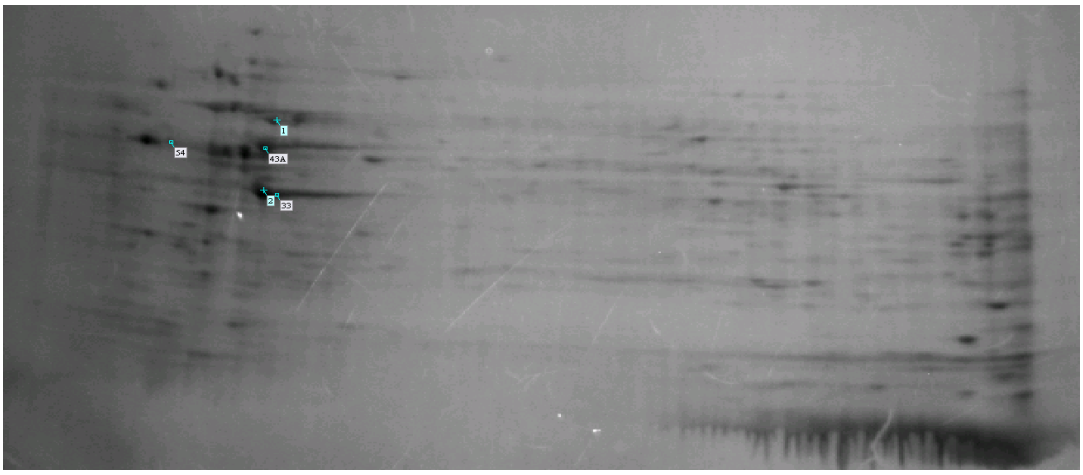

Figure 3.58: Cis + Camp (0/0) treated A2780 two dimensional protein gel image

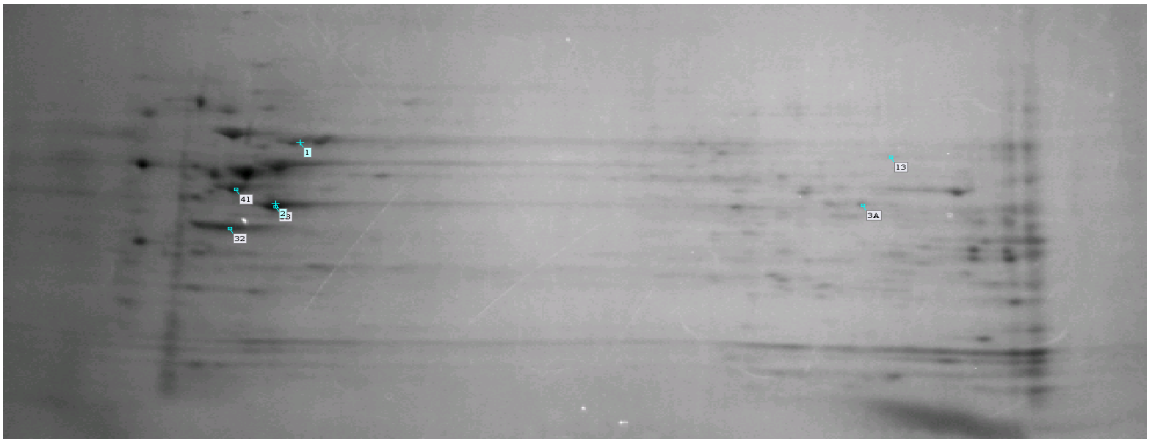

Figure 3.59: Cis + LH5 (0/0) treated A2780 two dimensional protein gel image

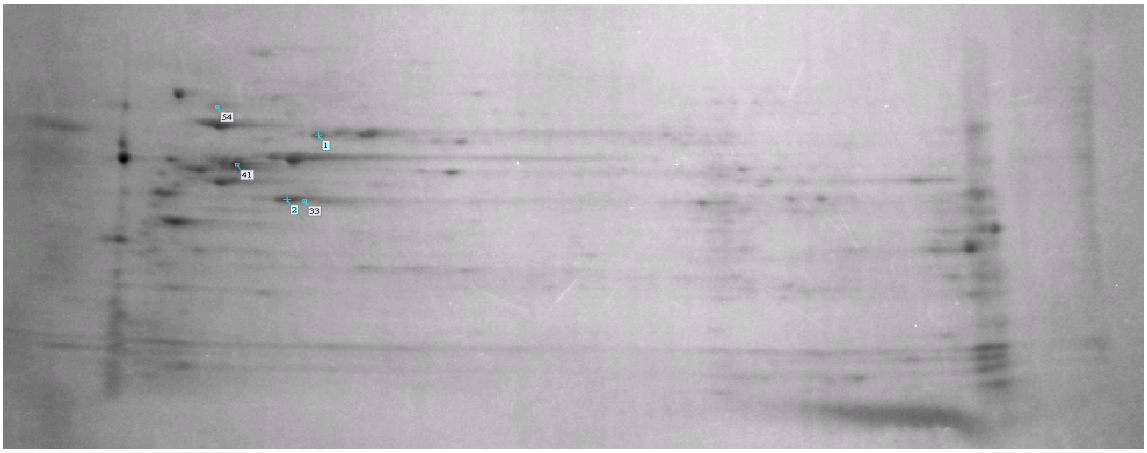

Figure 3.60: Cis + LH5 (4/0) treated A2780 two dimensional protein gel image

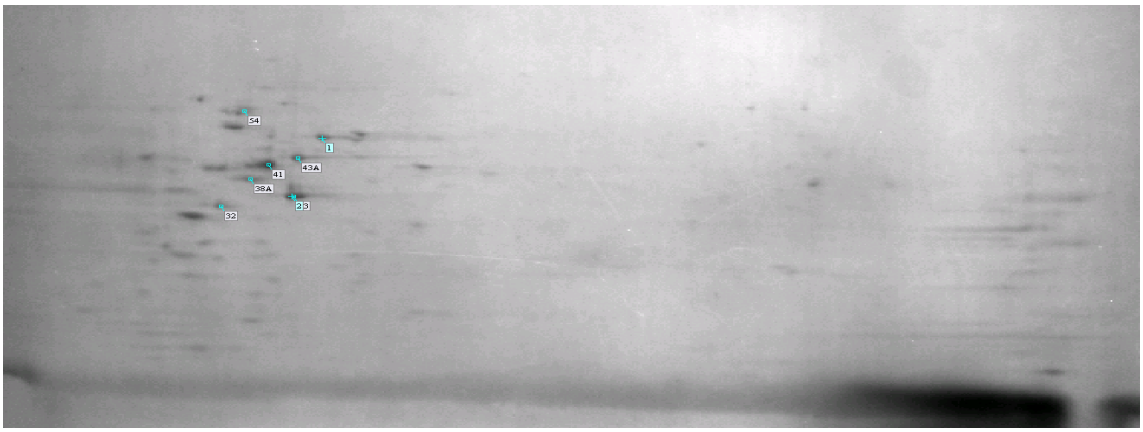

Figure 3.61: LH5 + Oxa (0/0) treated A2780 two dimensional protein gel image

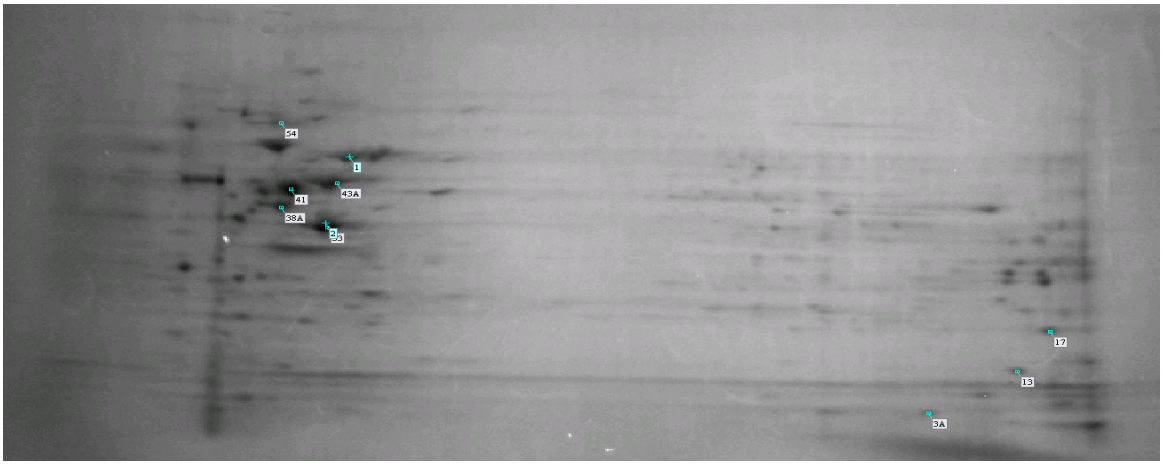

Figure 3.62: LH5 + Camp (4/0) treated A2780 two dimensional protein gel image

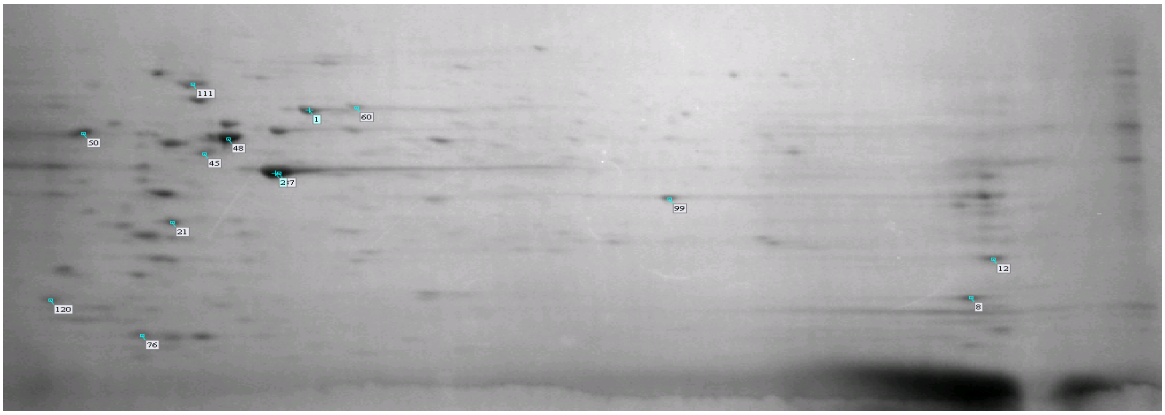

Figure 3.63: Cisplatin alone treated A2780^{cisR} two dimensional protein gel image

Figure 3.64: Oxaliplatin alone treated A2780^{cisR} two dimensional protein gel image

Figure 3.65: LH5 alone treated A2780^{cisR} two dimensional protein gel image

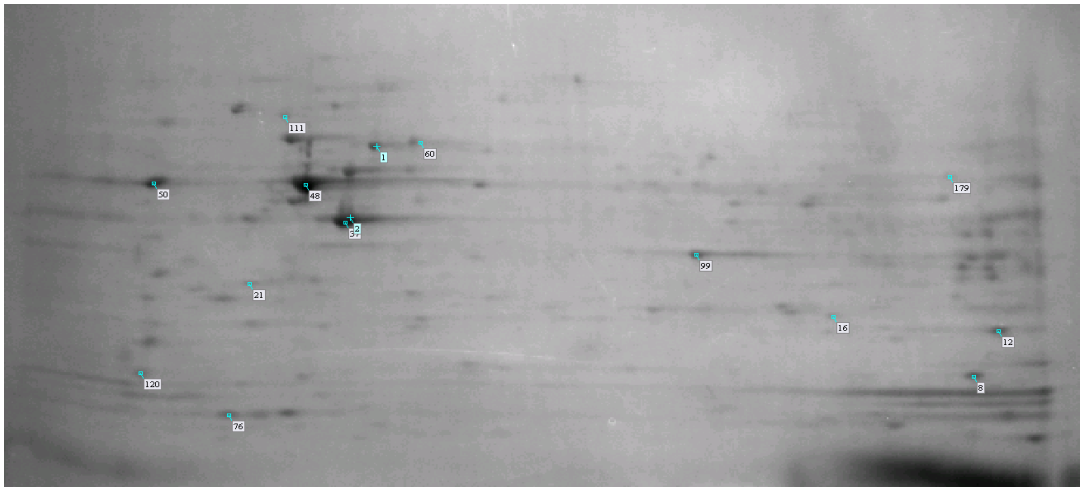

Figure 3.66: LH5 + Camp (0/0) treated A2780^{cisR} two dimensional protein gel image

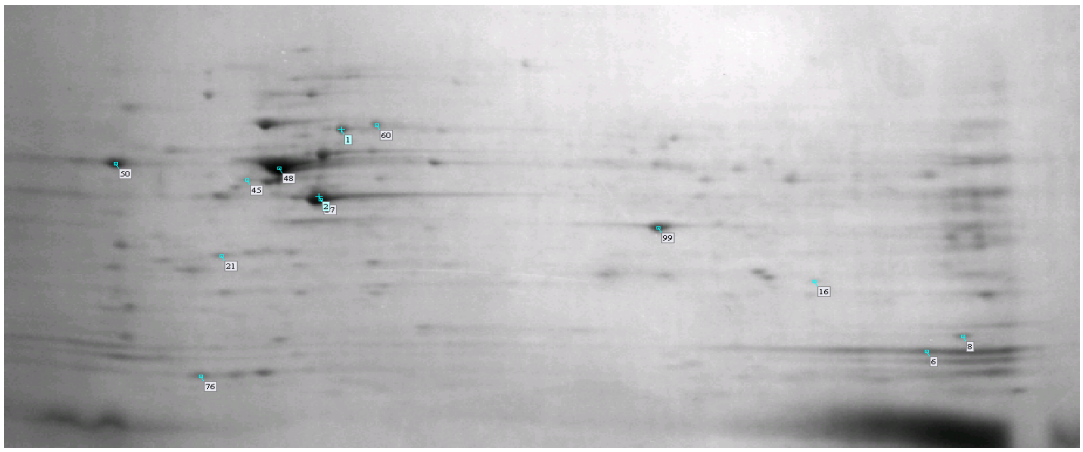

Figure 3.67: LH5 + Camp (0/4) treated A2780^{cisR} two dimensional protein gel image

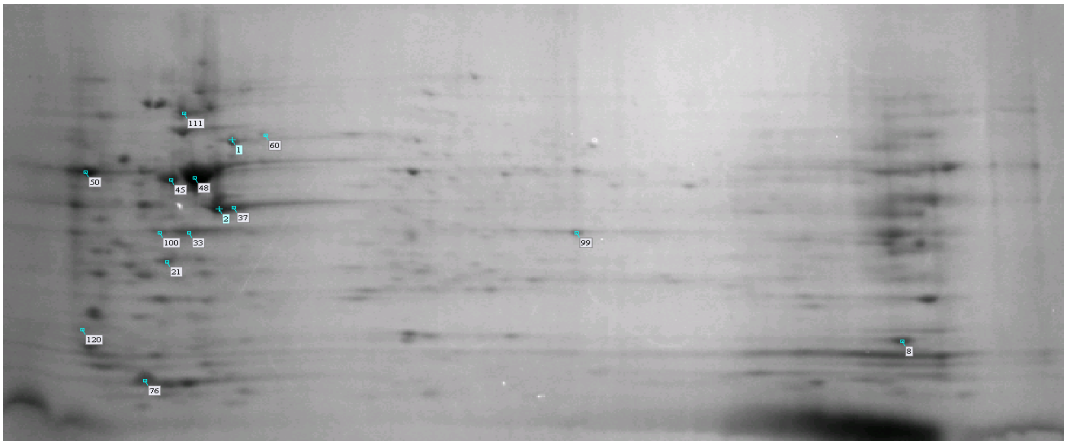

Figure 3.68: LH5 + Camp (4/0) treated A2780^{cisR} two dimensional protein gel image

Figure 3.69: LH5 + Oxa (0/0) treated A2780^{cisR} two dimensional protein gel image

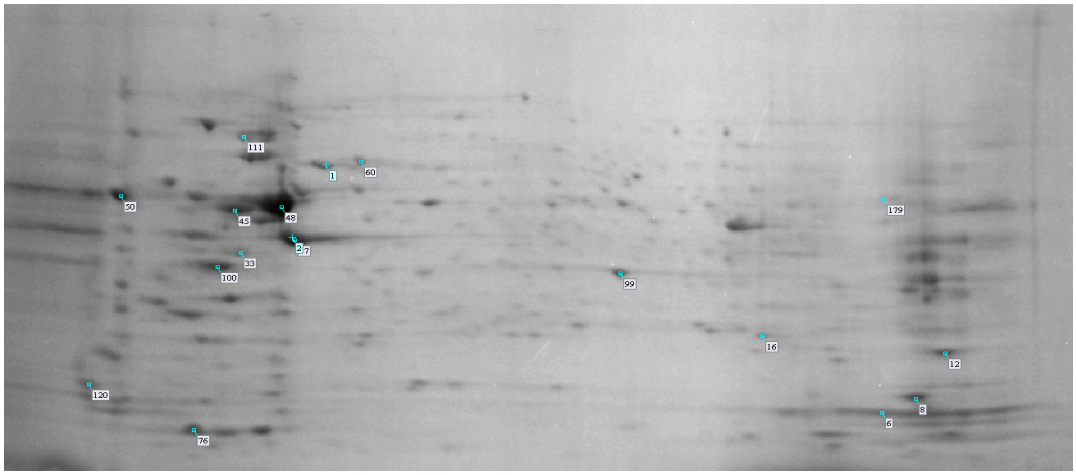

Figure 3.70: LH5 + Oxa (4/0) treated A2780^{cisR} two dimensional protein gel image

3.5.2 Protein expression

In the present study, 27 protein spots undergoing significant changes in expression as a result of treatment with single drugs (Cis, Oxa or LH5) or their combination with Camp were chosen for investigation using MALDI-MS technique. The corresponding masses of partial or fully fragmented peptides obtained from MS/MS scans were used to identify proteins based on Mascot score (with greater than or equal to 56 being considered as significant), iso-electric point (pI), protein mass (Mr), number of peptide matches and % of sequence coverage. The following table lists the selected protein

spots that showed significant changes in expression due to treatments with drugs administered alone or in combination in A2780 and A2780^{cisR} ovarian cancer cell lines.

Table 3.22 and Table 3.24 summarize the changes in expression of proteins after drug treatments compared to untreated A2780 cell line (used as reference) and A2780^{cisR} cell line (used as reference) respectively. In the table, UR=upregulated; DR=downregulated; NC=no change in expression; NF=not found (may be due to extreme downregulation). While Table 3.23 and Table 3.25 provide the summary of the information regarding the identified proteins.

Table 3.22: Altered expression of protein spots after treatment in A2780 cell line after selected treatments

	Changes in protein expression in A2780 cell line (Fold)							
	Single drug treatment			**Combined drug treatments**				
Match ID	**Cis**	**Oxa**	**LH5**	**Cis + Camp (0/0)**	**Cis + LH5 (0/0)**	**Cis + LH5 (4/0)**	**LH5 + Oxa (0/0)**	**LH5 + Camp (4/0)**
3A	DR(1.56)	NF	NF	NC	DR(3.7)	NF	NC	NF
13A	UR(1.5)	UR(2.48)	UR(3.05)	NC	DR(2.15)	NF	NC	NF
17A	UR(1.61)	UR(2.08)	DR(2.09)	UR(1.95)	DR(1.97)	NF	DR(2.12)	NF
32A	DR(4.25)	DR(8.41)	DR(1.98)	UR(2.57)	NF	NC	NF	DR(1.67)
33A	UR(1.71)	UR(1.97)	NC	UR(1.84)	NC	UR(1.73)	NC	DR(1.75)

38A	DR(5.19)	DR(1.5)	NF	UR(1.58)	DR(2.48)	DR(1.71)	NC	NC
41A	UR(1.82)	UR(1.67)	UR(1.96)	UR(4.07)	DR(2)	UR(1.58)	NC	NC
43A	DR(1.88)	NC	NC	UR(1.89)	UR(1.59)	NC	NC	NC
54A	DR(1.91)	NC	NC	DR(1.79)	NC	DR(4.7)	NC	NC

Table 3.23: Summary of the proteins identified in ovarian A2780 cell line

Spot	Accession Number	Name	% Coverage	Peptide Matches	Unique Peptide	Score
3A	Q9UII2	ATPase inhibitor, mitochondrial	11	21	3	342
13A	P23528	Cofilin-1	98	168	21	5654
17A	Q06830	Peroxiredoxin-1	81	238	19	6480
32A	P07910	Heterogeneous nuclear ribonucleoproteins C1/C2	39	152	18	5900
33A	P60709	Actin, cytoplasmic 1	81	375	1	13875
38A	P06576	ATP synthase subunit beta	54	274	23	10292
41A	P10809	60kDa heat shock protein	82	549	61	19056
43A	P08670	Vimentin	89	499	43	14404
54A	P08238	Heat shock protein HSP 90-beta	42	155	16	5262

Table 3.24: Altered expression of protein spots after treatment in A2780^{cisR} cell line after selected treatments

		Changes in protein expression in A2780^{cisR} cell line (Fold)						
	Single drug treatment			**Combined drug treatments**				
Match ID	**Cis**	**Oxa**	**LH5**	**LH5 + Camp (0/0)**	**LH5 + Camp (0/4)**	**LH5+Camp (4/0)**	**LH5 + Oxa (0/0)**	**LH5+Oxa (4/0)**
6	NF	UR(1.51)	NC	NF	UR(2.46)	NF	UR(1.59)	UR(1.62)
8	UR(1.66)	UR(2.03)	NC	DR(3.03)	DR(1.66)	DR(2.46)	DR(2.08)	NC
12	NC	UR(1.9)	NC	NC	DR(2.54)	DR(2.02)	DR(1.97)	NC
16	NC	NF	NC	DR(1.87)	UR(2.22)	NC	NC	UR(2.03)
21	NC	UR(2.12)	NC	DR(2.89)	DR(1.93)	DR(1.82)	DR(2.14)	NC
33	NF	UR(2.15)	UR(10.94)	NF	NC	UR(4.08)	UR(2)	NC
37	NC	DR(1.65)	NC	NC	NC	NC	NC	NC
42	DR(4.53)	NC	DR(1.83)	NF	DR(4.78)	NF	DR(1.55)	NF
45	NC	DR(4.09)	NC	NC	NC	NC	NC	UR(1.52)
48	NC	NC	UR(2.23)	NC	UR(1.55)	NC	NC	NC
50	NC	DR(2.52)	UR(3.03)	NC	NC	NC	NC	DR(1.65)
60	NC	NC	NC	NC	NC	NC	NC	NC
76	DR(3.39)	NC	NC	NC	NC	DR(1.85)	DR(5.35)	NC
99	NC	UR(1.51)	DR(1.94)	DR(2.03)	NC	DR(1.71)	NC	DR(1.61)
100	NC	NC	UR(3.95)	NF	UR(2.41)	DR(1.87)	NC	UR(3.51)
111	UR(2.15)	UR(2.01)	NC	UR(1.56)	DR(2.25)	UR(1.94)	NC	NC
120	NC	DR(1.68)	NF	DR(1.85)	NF	DR(8.2)	DR(5.55)	DR(3.69)
179	NF	NC	NF	DR(3.03)	DR(1.95)	NF	NC	NC

Table 3.25: Summary of the proteins identified in ovarian A2780^{cisR} cell line

Spot	Accession Number	Name	% Coverage	Peptide Matches	Unique Peptide	Score
6	P62937	Peptidyl-prolyl cis-trans isomerase A	82	160	16	4534
8	P23528	Cofilin-1	98	168	21	5654
12	Q06830	Peroxiredoxin-1	81	238	19	6480
16	P62826	GTP-binding nuclear protein Ran	53	141	15	4147
21	P67936	Tropomyosin alpha-4 chain	64	112	18	3528
33	P07910	Heterogeneous nuclear ribonucleoproteins C1/C2	39	152	18	5900
37	P60709	Actin, cytoplasmic 1	81	375	1	13875
42	P68104	Elogation factor 1-alpha	50	162	9	4684
45	P07437	Tubulin beta chain	55	218	3	7689
48	P08670	Vimentin	89	499	43	14404
50	P08670	Vimentin	69	122	38	3237
60	P38646	Stress-70 protein	47	48	26	1544
76	P62805	Histone H4	51	34	6	991
99	P04083	Annexin A1	69	291	24	10404
100	P06748	Nucleophosmin	44	98	14	2633
111	P08238	Heat shock protein HSP 90-beta	42	155	16	5262
120	P0DP23	Calmodulin-1	28	11	6	306
176	P14618	Pyruvate kinase	47	109	25	3866

Table 3.26: Changes in levels of protein expression in the platinum resistant A2780^{cisR} cell line expressed in folds following treatment with single drugs and their combinations as compared to untreated platinum sensitive A2780 cell line being used as reference: (UR=upregulation; DR=downregulation; NC= no change; PR=partially restored; OR=over restored; FR=fully restored; FUR= further upregulated; FDR=further downregulated; NF=not found, may be due to extreme downregulation)

Match ID	**A2780^{cisR} Untreated (Fold)**	**Changes in protein expression in A2780^{cisR} cell line**							
		Cis	**Oxa**	**LH5**	**LH5 + Camp (0/0)**	**LH5 + Camp (0/4)**	**LH5+Camp (4/0)**	**LH5 + Oxa (0/0)**	**LH5+Oxa (4/0)**
6	DR(1.52)	NF	FR	PR	NF	OR	NF	OR	OR
8	UR(1.5)	FUR	FUR	PR	OR	OR	OR	OR	FUR
12	UR(1.61)	FUR	FUR	FUR	FUR	OR	OR	OR	FUR
16	DR(2.03)	PR	NF	PR	FDR	OR	PR	FDR	FR
21	UR(1.4)	PR	FUR	FUR	OR	OR	OR	OR	PR
33	DR(4.25)	NF	PR	OR	NF	FDR	PR	PR	PR
37	UR(1.71)	FUR	PR	FUR	PR	PR	FUR	PR	PR
42	UR (2.85)	OR	PR	PR	NF	OR	NF	PR	NF
45	DR(1.31)	OR	FDR	OR	FDR	FDR	FDR	NC	OR
48	UR(1.82)	PR	FUR	FUR	FUR	FUR	PR	FUR	FUR
50	DR(1.32)	PR	FDR	OR	PR	PR	PR	FDR	FDR
60	DR(1.92)	PR	PR	NC	NC	FDR	PR	FDR	PR
76	UR (1.41)	OR	FUR	FR	PR	FR	OR	OR	PR
99	UR(4)	FUR	FUR	PR	PR	PR	PR	PR	PR
100	DR(5.16)	PR	FDR	PR	NF	PR	FDR	PR	PR
111	DR(1.91)	OR	OR	FDR	PR	FDR	FR	PR	FDR
120	UR(1.77)	FUR	PR	NF	OR	NF	OR	OR	OR
179	UR(1.9)	NF	PR	NF	OR	FR	NF	PR	PR

3.5.3 Mass spectral analysis of the protein

3.5.3.1 Mitochondrial ATPase inhibitor

Mitochondrial ATPase inhibitor (match ID 3A) was downregulated in A2780 cell line due to treatment with Cis alone and even more significantly with the combination treatment of Cis with LH5 using (0/0) sequence. It showed insignificant changes in expression in response to combined treatments: Cis+Camp (0/0) and LH5+Oxa (0/0). However, the protein was not detected after the treatments of Oxa alone, LH5 alone as well as combined treatments of Cis+LH5 (4/0) and LH5+Camp (4/0).

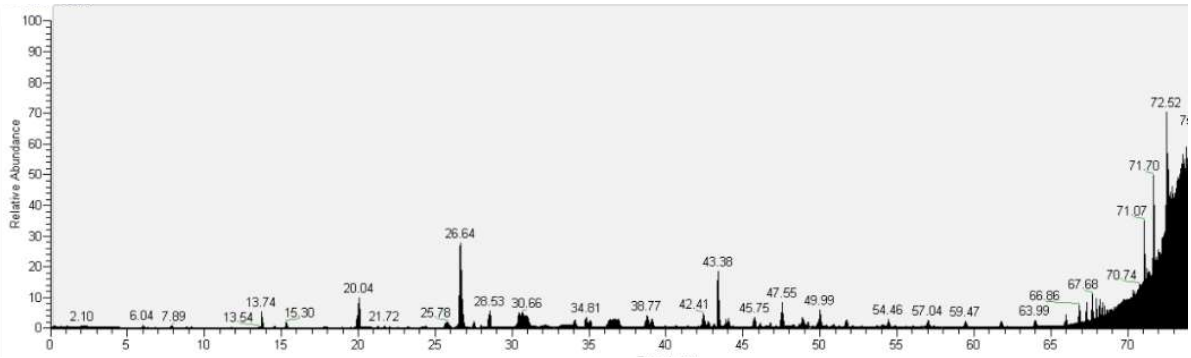

Figure 3.71: Mass spectrum for ATPase inhibitor, mitochondrial

3.5.3.2 Cofilin-1

Cofilin-1 was identified in both the cell lines: A2780 (match ID 13A) and A2780^{cisR} (match ID 8). The protein was significantly downregulated in expression A2780 cell line following treatment with combination of Cis with LH5 using (4/0) sequence. It was significantly upregulated due to single treatments with Cis, Oxa or LH5 as well as combined treatment with Cis+Camp (0/0) in the same cell line. However, Cofilin-1 was not detected after treatment with Cis+LH5 (4/0) sequence and with LH5 plus Camp (4/0) in A2780

tumour modele. No significant changes were observed following treatment with LH5+Oxa (0/0).

In case of A2780^{cisR} cell line, Cofilin-1 was upregulated following single treatments with Cis and Oxa but downregulated after combined treatments with LH5 plus Camp at all sequences of administration as well as LH5 with Oxa (0/0). When the expression of Cofilin-1 in resistant A2780^{cisR} cell line was compared with that in the parent A2780 cell line, it was found that the protein was upregulated by a factor of 1.5. After the treatments with Cis and Oxa alone and LH5+Oxa (4/0) the protein was further upregulated in A2780^{cisR} cell line. The expression of the protein was partially restored back following treatment with LH5 alone; over restored following the treatments with LH5+Camp (0/0), LH5+Camp (0/4), LH5+Camp (4/0) and LH5+Oxa (0/0).

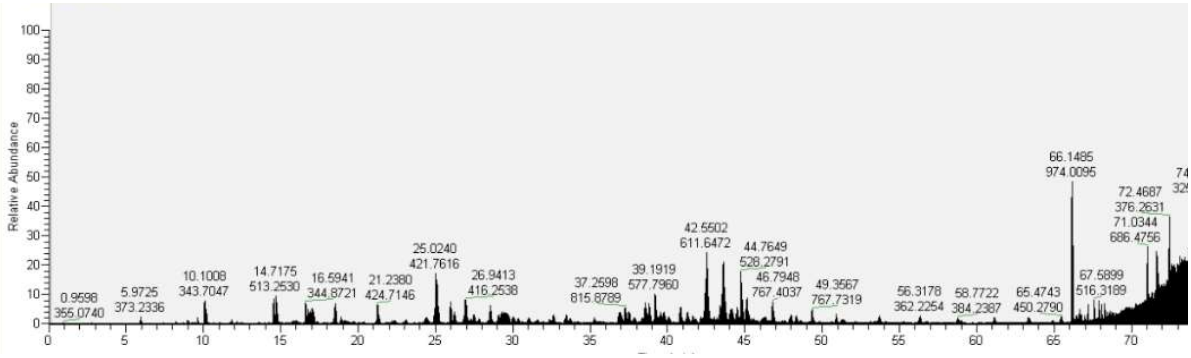

Figure 3.72: Mass spectrum for Cofilin-1

3.5.3.3 Peroxiredoxin-1

Peroxiredoxin-1 was identified in both A2780 (match ID 17A) and A2780^{cisR} cell line (match ID 12). The protein was upregulated following single treatments with Cis and Oxa; but downregulated as result of treatment with LH5 alone in A2780 cell line. It was not detected following combined treatments: Cis+LH5 (4/0) and LH5+Camp (4/0) in A2780 cell line. While combined treatments of Cis+LH5 (0/0) and LH5+Oxa (0/0) also caused downregulation of the protein in A2780 cell line.

In case of A2780^{cisR} cell line, Peroxiredoxin-1 was significantly downregulated following combined treatments with LH5 and Camp using 0/4 and 4/0 sequences of addition, and LH5 with Oxa using 0/0 sequence of addition.

When expression of Peroxiredoxin-1 in resistant A2780^{cisR} cell line was compared with that in parent A2780 cell line, it was found that the protein was upregulated in the resistant cell line by a factor of 1.6. After the treatments with Cis alone, Oxa alone, LH5 alone, LH5+camp (0/0) and LH5+Oxa (4/0) the protein was further upregulated in A2780^{cisR} cell line. But expression of the protein was over restored following the treatments of LH5+Camp (0/4), LH5+Camp (4/0) and LH5+Oxa (0/0).

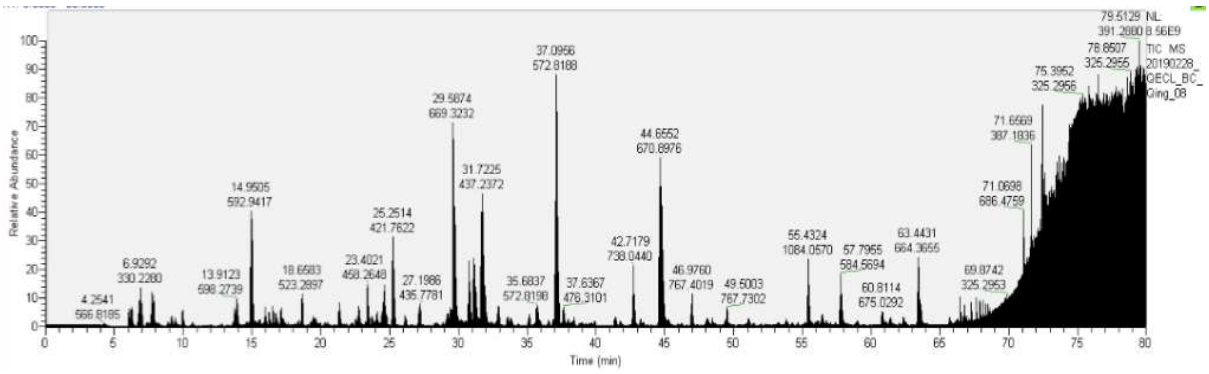

Figure 3.73: Mass spectrum for Peroxiredoxin-1

3.5.3.4 Heterogeneous nuclear ribonucleoproteins C1/C2

Heterogeneous nuclear ribonucleoprotein C1/C2 (HNR C1/C2) was identified in both A2780 (match ID 32A) and A2780^{cisR} cell line (match ID 33). The protein was significantly lowered in expression in A2780 cell line due to all single drug treatments (Cis, Oxa, and LH5). It was also downregulated following combined treatment : LH5+Camp (4/0) but upregulated following combined treatment: Cis+Camp (0/0) in A2780 cell line. The protein was not detectable following combined treatments: of LH5 + Oxa (0/0) and Cisplain+LH5 (0/0).

In case of A2780^{cisR} cell line, Heterogeneous nuclear ribonucleoprotein was significantly upregulated following single treatments with Oxa alone, LH5 alone as well as combined treatments: LH5 with Camp using 4/0 sequence of addition and LH5 with Oxa using 0/0 sequence of addition.

When expression of HNR C1/C2 in the resistant A2780^{cisR} cell line was compared with that in parent A2780 cell line, it was found that the protein was downregulated in the resistant cell line by a factor of 4.3 times. After the treatment with LH5+Camp (0/4) the protein was further downregulated in A2780^{cisR} cell line. The expression of the protein was partially restored back following the treatments of Oxa alone, LH5+Camp (4/0), LH5+Oxa (0/0) and LH5+Oxa (4/0); over restored following the treatment of LH5 alone. However, the protein was not detected after the treatments of Cis alone and LH5+Camp (0/0).

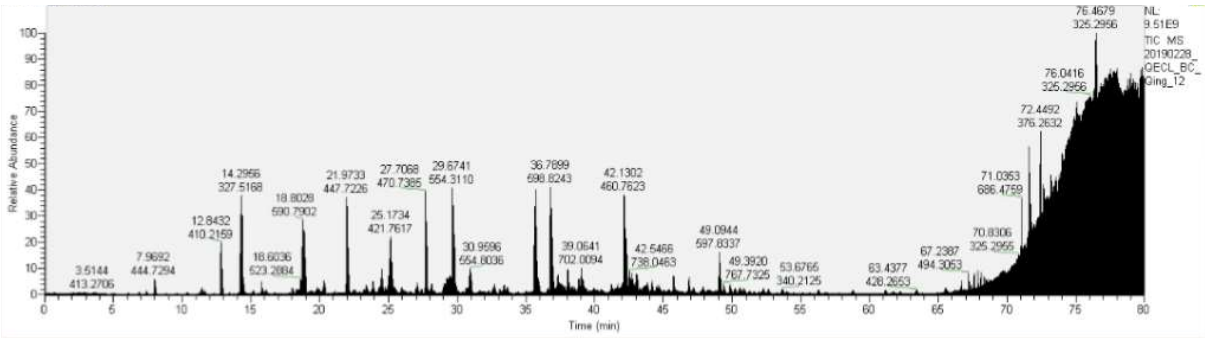

Figure 3.74: Mass spectrum for Heterogeneous nuclear ribonucleoprotein C1/C2

3.5.3.5 Actin, cytoplasmic 1

The protein was identified in both A2780 (match ID 33A) and A2780^{cisR} cell line (match ID 37). The protein was significantly upregulated in A2780 cell line due to all selected drug treatments irrespective of whether drugs were administered alone or in combination in A2780 cell line except for combined treatment of LH5 with Camp using 4/0 sequence of additin which demonstrated downregulation.

In case of A2780^{cisR} cell line, actin was significantly lowered in expression following single treatment with Oxa. Other treatments did not produce significant changes in the expression of the protein. When the expression of Actin in resistant A2780^{cisR} cell line was compared with that in parent A2780 cell line, it was found that the protein was upregulated in the resistant cell line by a factor of 1.7. After the treatment with Cis alone, LH5 alone and LH5+Camp (4/0) the protein was further upregulated in expression in A2780^{cisR} cell line. All other treatments resulted partial restoration of the protein.

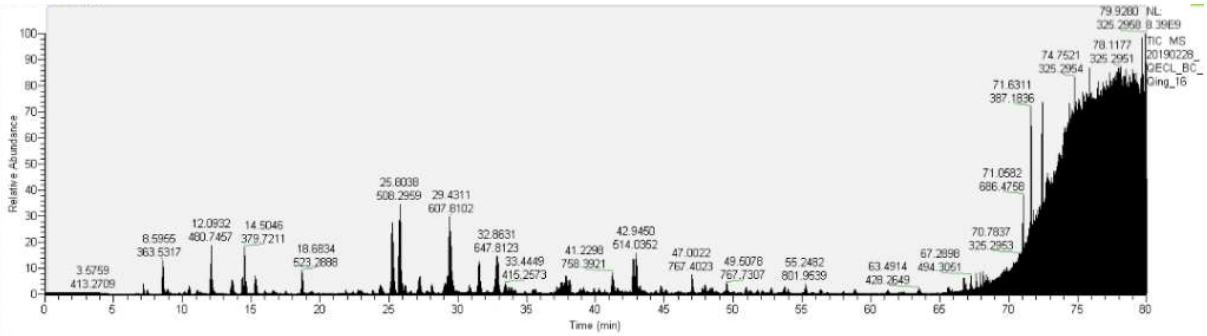

Figure 3.75: Mass spectrum for Actin, cytoplasmic 1

3.5.3.6 ATP synthase subunit beta

ATP synthase subunit beta (match ID 38A) displayed downregulation following single treatments with Cis and Oxa as well as combined treatments of Cis+LH5 (0/0) and Cis+LH5 (4/0) in A2780 parent ovarian cancer cell line. However, it was upregulated due to the combined treatment of Cis+Camp (0/0).

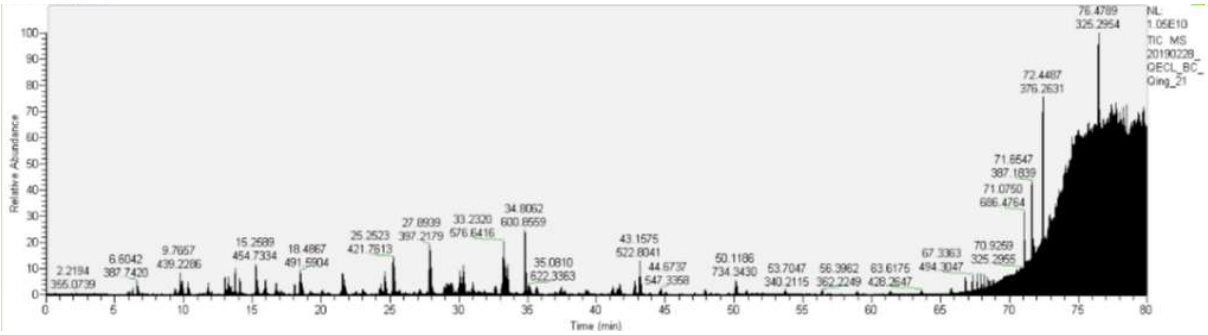

Figure 3.76: Mass spectrum for ATP synthase subunit beta

3.5.3.7 60kDa heat shock protein

60kDa heat shock protein (match ID 41A) was significantly upregulated in expression in A2780 cell line due to all selected single drug treatments in A2780 cell line. Among combination drug treatments, synergistic combination of Cis + LH5 (4/0) caused upregulation of the protein. Antagonistic combination treatment: Cis with LH5 using 0/0 sequence of addition demonstrated downregulation. But, two other antagonistic combinations did not show any significant change in expression of the protein.

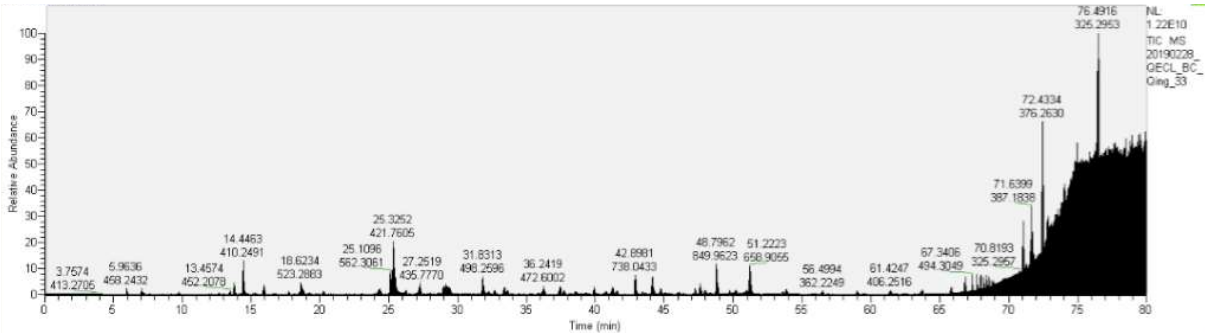

Figure 3.77: Mass spectrum for 60kDa heat shock protein

3.5.3.8 Vimentin

The protein was identified from in A2780 cell line (match ID 43A) and A2780^{cisR} cell line (match ID 48 and 50). The protein was significantly downregulated in expression in A2780 cell line due to treatment with Cis alone but upregulated after combined treatments:

Cis+LH5 (0/0) and Cis+Camp (0/0). Other treatments did not cause significant change in the expression of vimentin in A2780 tumour model.

In case of resistant A2780^{cisR} cell line, the protein was significantly upregulated following single treatment with LH5 alone as well as combined treatments with LH5 with Camp using 4/0 sequence of administration. However, vimentin was downregulated following treatments with Oxa alone and combined treatment of LH5 with Oxa using 4/0 sequence of addition. When the expression of vimentin in resistant A2780^{cisR} cell line was compared with that in parent A2780 cell line, it was found that the protein was upregulated by a factor of 1.8. After the treatments with Oxa alone, LH5 alone, LH5+Camp (0/0), LH5+Camp (0/4), LH5+Oxa (0/0) and LH5+Oxa (4/0) the protein was further upregulated in A2780^{cisR} cell line. The expression of the protein was partially restored following the treatments of Cis alone and LH5+Camp (4/0).

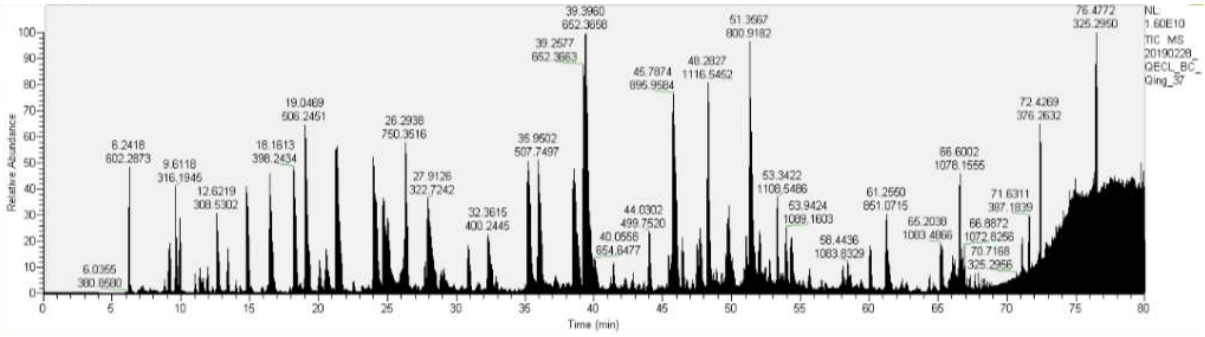

Figure 3.78: Mass spectrum for Vimentin

3.5.3.9 Heat shock protein HSP 90-beta

The protein was identified in both A2780 (match ID 54A) and A2780^{cisR} cell line (match ID 111). The protein was significantly downregulated in expression in A2780 cell line due to treatment with Cis alone, combination treatments: Cis+LH5 (4/0) and Cis+Camp (0/0).

Other treatments did not cause significant change in expression of the protein in A2780 cell line.

In the case of A2780^{cisR} cell line, the protein was significantly upregulated following single treatments of Cis alone, Oxa alone as well as combined treatments of LH5 with Camp using 0/0 sequence of addition and 4/0 sequence of addition. However, HSP 90-beta was downregulated following treatments of LH5 with Camp using 0/4 sequence of addition. When the expression of HSP 90-beta in resistant A2780^{cisR} cell line was compared with that in parent A2780 cell line, it was found that the protein was downregulated by 1.91 times. After the treatments with LH5 alone, LH5+camp (0/4) and LH5+Oxa (4/0) the protein was further downregulated in A2780^{cisR} cell line. The expression of the protein was over restored following the treatments of Cis alone and Oxa alone; partially restored following treatments of LH5+Camp (0/0) and LH5+Oxa (0/0).

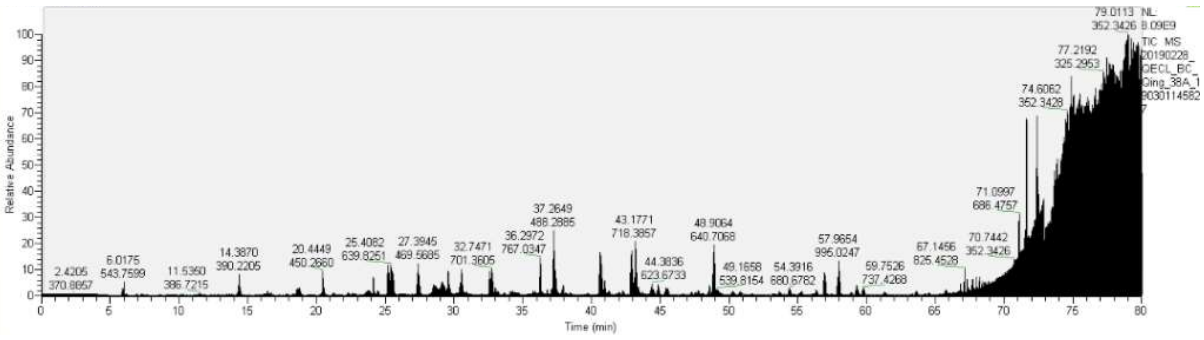

Figure 3.79: Mass spectrum for Heat shock protein HSP 90-beta

3.5.3.10 Peptidyl-prolyl cis-trans isomerase A

Peptidyl-prolyl cis-trans isomerase A protein (match ID 6) has been identified only in A2780^{cisR} cell line which was significantly upregulated following treatments with Oxa alone, LH5+Oxa (0/0), LH5+Oxa (0/4) and LH5+Camp (0/4). However, the protein was not detected after the treatments with Cis alone, LH5+Camp (0/0) and LH5+Camp (4/0).

When the expression of Peptidyl-prolyl cis-trans isomerase A in resistant A2780^{cisR} cell line was compared with that in parent A2780 cell line, it was found that the protein was downregulated by a factor of 1.5. The expression of the protein was over restored following the treatments of LH5+Camp (0/4), LH5+Oxa (0/0) and LH5+Oxa (4/0). The protein was disappeared after the treatments with LH5+Camp (0/0) and LH5+Camp (4/0). The protein was fully restored following treatment with Oxa alone.

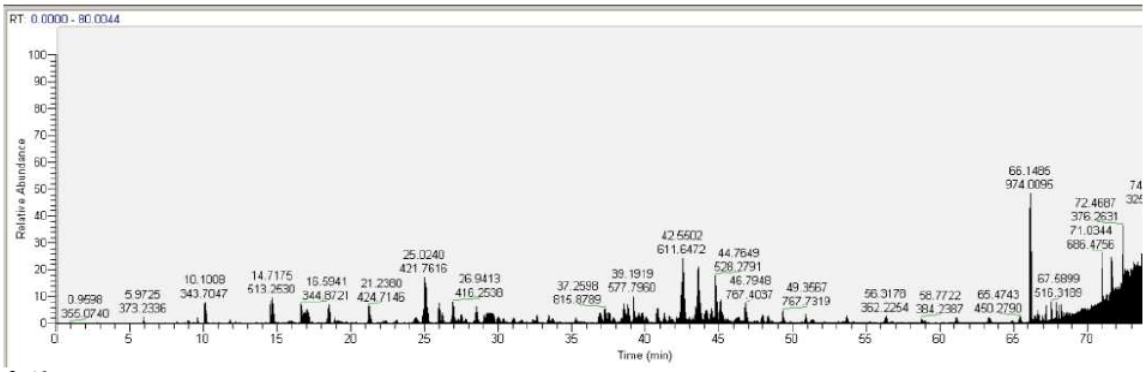

Figure 3.80: Mass spectrum for Peptidyl-prolyl cis-trans isomerase A

3.5.3.11 GTP-binding nuclear protein Ran

GTP-binding nuclear protein Ran (match ID 16) has been identified in A2780^{cisR} cell line which was significantly upregulated following treatments with LH5+Camp (0/4) and LH5+Oxa (0/4). However, the protein was significantly downregulated after the combined treatment of LH5+Camp (0/0).

When the expression of GTP-binding nuclear protein Ran in resistant A2780^{cisR} cell line was compared with that in parent A2780 cell line, it was found that the protein was downregulated by 2.03 times. The expression of the protein was further down regulated following the treatments with LH5+Camp (0/0) and LH5+Oxa (0/0). The protein was partially restored following the treatments with Cis alone, LH5 alone and LH5+Camp (4/0). The protein was over restored following the treatment of LH5+Camp (0/4); fully restored following the treatment with LH5+Oxa (4/0). However, the protein was disappeared after the treatment with Oxa alone.

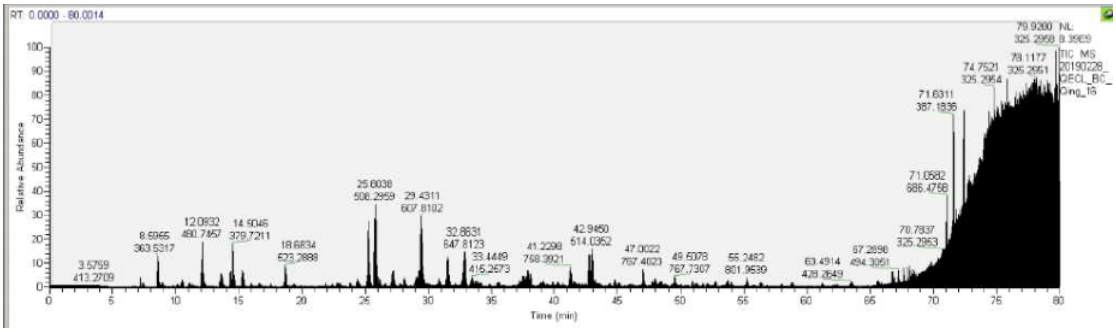

Figure 3.81: Mass spectrum for GTP-binding nuclear protein Ran

3.5.3.12 Tropomyosin alpha-4 chain

Tropomyosin alpha-4 chain (match ID 21) has been identified in A2780^{cisR} cell line which was significantly downregulated following all selected combined treatments LH5+Oxa (0/4). However, the protein was significantly upregulated after single drug treatment of Oxa.

When the expression of Tropomyosin alpha-4 chain in resistant A2780^{cisR} cell line was compared with that in parent A2780 cell line, it was found that the protein was upregulated by a factor of 1.4. The expression of the protein was further upregulated following the treatments with Oxa alone and LH5 alone. The protein was over restored following the treatments with LH5+Camp (0/0), LH5+Camp (0/4), LH5+Camp (4/0) and LH5+Oxa (0/0). The protein was partially restored following the treatments with Cis alone and LH5+Oxa (4/0).

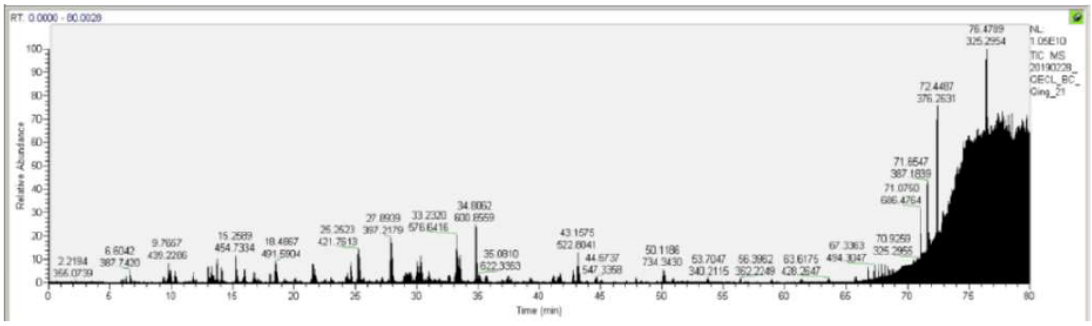

Figure 3.82: Mass spectrum for Tropomyosin alpha-4 chain

3.5.3.13 Elongation factor 1-alpha

Elongation factor 1-alpha (match ID 42) was detected in A2780^{cisR} cell line which was significantly downregulated following treatments with Cis alone, LH5 alone, LH5+Camp (0/4) and LH5+Oxa (0/0). The protein was not detectable after the combined treatments of LH5+Camp (0/0), LH5+Camp (4/0) and LH5+Oxa (0/4).

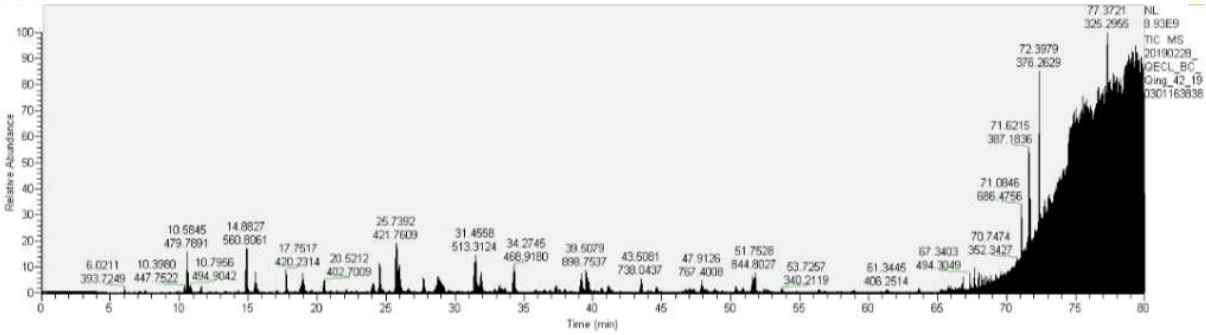

Figure 3.83: Mass spectrum for Elogation factor 1-alpha

3.5.3.14 Tubulin beta chain

Tubulin beta chain (match ID 45) has been identified in A2780^{cisR} cell line which was significantly downregulated following single treatment of Oxa alone but upregulated after the combined treatment of LH5+Oxa (4/0). Other single and combined drug treatments did not cause significant changes in the expression of the protein in A2780^{cisR} cell line.

When the expression of tubulin beta chain in resistant A2780^{CcsR} cell line was compared with that in parent A2780 cell line, it was found that the protein was downregulated by a factor of 1.3. The expression of the protein was further down regulated following the treatments with Oxa alone, LH5+Camp (0/0), LH5+Camp (0/4) and LH5+Camp (4/0). The protein was over restored following the treatments with Cis alone, LH5 alone and LH5+Oxa (4/0).

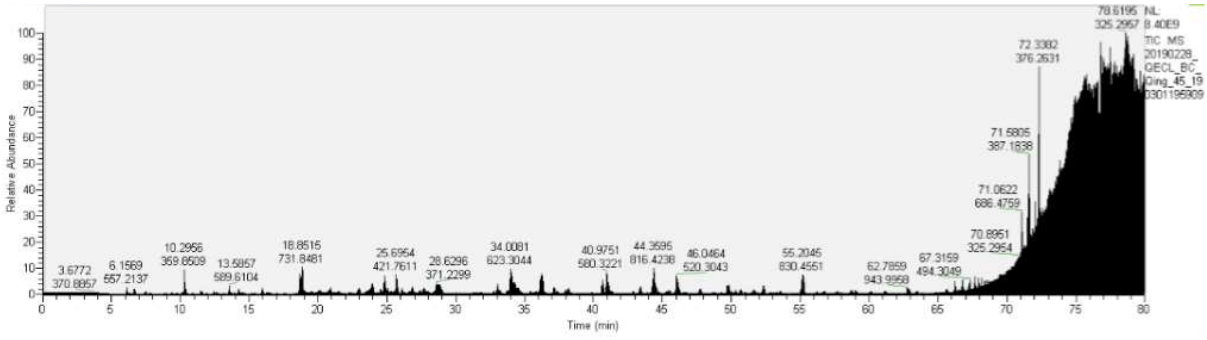

Figure 3.84: Mass spectrum for Tubilin beta chain

3.5.3.15 Stress-70 protein

Stress-70 protein (match ID 60) has been identified in A2780^{cisR} cell line which did not show any significant change in expression following the selected treatments administered alone or in combinations.

When the expression of the protein in resistant A2780^{cisR} cell line was compared with that in parent A2780 cell line, it was found that the protein was downregulated by a factor of 1.9. The expression of the protein was further downregulated following treatments with LH5+Camp (0/0) and LH5+Oxa (0/0). The protein was partially restored back following the treatments with Cis alone, Oxa alone, LH5+Camp (0/4) and LH5+Oxa (4/0).

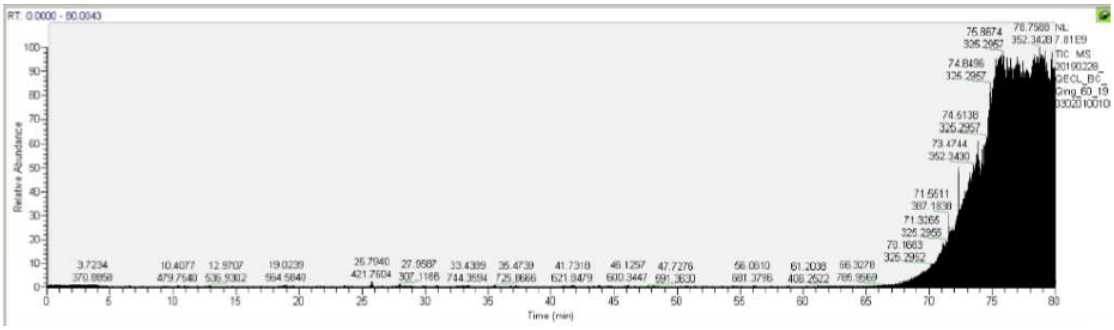

Figure 3.85: Mass spectrum for Stress-70 protein

3.5.3.16 Histone H4

Histone H4 (match ID 76) has been identified in A2780^{cisR} cell line which was significantly downregulated following single treatment of Cis alone as well as combined treatments of LH5+Camp (4/0) and LH5+Oxa (0/0). Other single and combined drug treatments did not cause significant changes in the expression of the protein in A2780^{cisR} cell line.

The protein was downregulated following all the treatments except Oxa alone in A2780^{cisR} cell line.

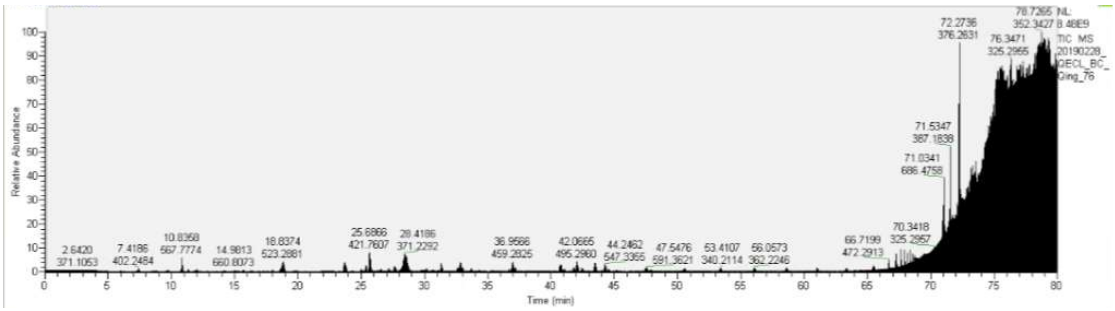

Figure 3.86: Mass spectrum for Histone H4

3.5.3.17 Annexin A1

Annexin A1 (match ID 99) has been identified in A2780^{cisR} cell line which was significantly downregulated following single treatment with LH5 alone as well as combined treatments with LH5+Camp (0/0), LH5+Camp (4/0) and LH5+Oxa (4/0). However, Oxa alone treatment caused upregulation of Annexin A1. Other single and combined drug treatments did not cause significant changes in the expression of the protein in A2780^{cisR} cell line.

When the expression of Annexin-A1 in resistant A2780^{cisR} cell line was compared with that in parent A2780 cell line, it was found that the protein was upregulated by a factor of 4.0. After the treatments with Cis alone and Oxa alone the protein was further upregulated in expression in A2780^{cisR} cell line. All other treatments caused partial upregulation of the protein.

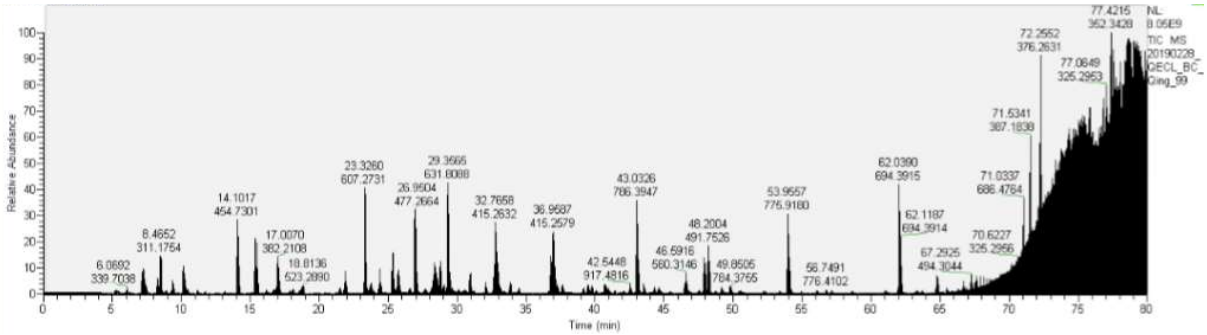

Figure 3.87: Mass spectrum for Annexin A1

3.5.3.18 Nucleophosmin

Nucleophosmin (match ID 100) has been identified in A2780^{cisR} cell line which was significantly upregulated following single treatment of LH5 alone as well as combined treatments of LH5+Camp (0/4) and LH5+Oxa (4/0). However, LH5+Camp (4/0) treatment caused downregulation of nucleophosmin. Other single and combined drug treatments did not cause significant changes in the expression of the protein in A2780^{cisR} cell line.

When the expression of nucleophosmin in resistant A2780^{cisR} cell line was compared with that in parent A2780 cell line, it was found that the protein was downregulated by a factor of 5.2. The expression of the protein was further downregulated following the treatments with Oxa alone and LH5+Camp (4/0). All other treatments caused partial upregulation of the protein except LH5+Camp (0/0) which caused disappearance of the protein in A2780^{cisR} cell line.

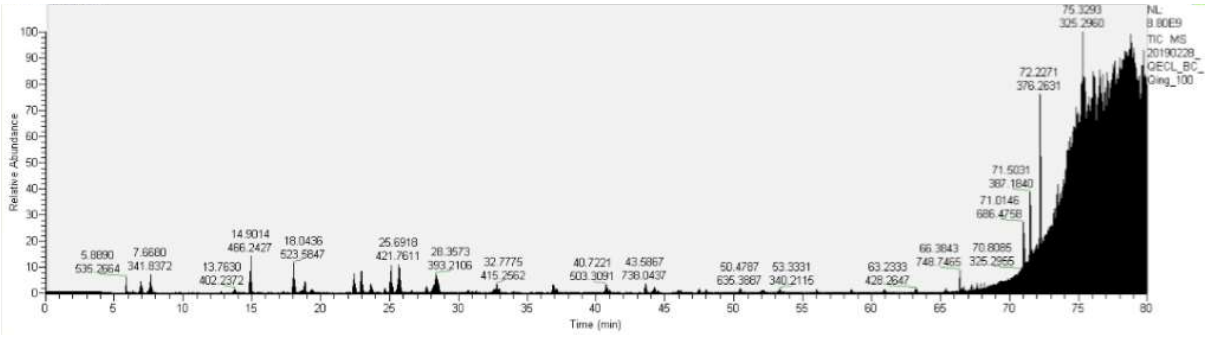

Figure 3.88: Mass spectrum for Nucleophosmin

3.5.3.19 Calmodulin-1

Calmodulin-1 (match ID 120) has been identified in A2780^{cisR} cell line which was significantly upregulated following single treatment of Oxa alone as well as all selected combined treatments except LH5+Camp (0/4). Other single and combined drug treatments caused disappearance of the protein or no significant changes in the expression of the protein in A2780^{cisR} cell line.

When the expression of Calmodulin-1 in resistant A2780^{cisR} cell line was compared with that in parent A2780 cell line, it was found that the protein was upregulated by a factor of 1.8. After the treatment with Cis alone the protein was further upregulated in A2780^{cisR} cell line. The expression of the protein was over restored following the treatments of LH5+Camp (0/0), LH5+Camp (4/0), LH5+Oxa (0/0) and LH5+Oxa (4/0). Oxa alone treatment caused partial restoration of the protein. LH5 alone and LH5+Camp (0/4) caused disappearance of the protein in A2780^{cisR} cell line.

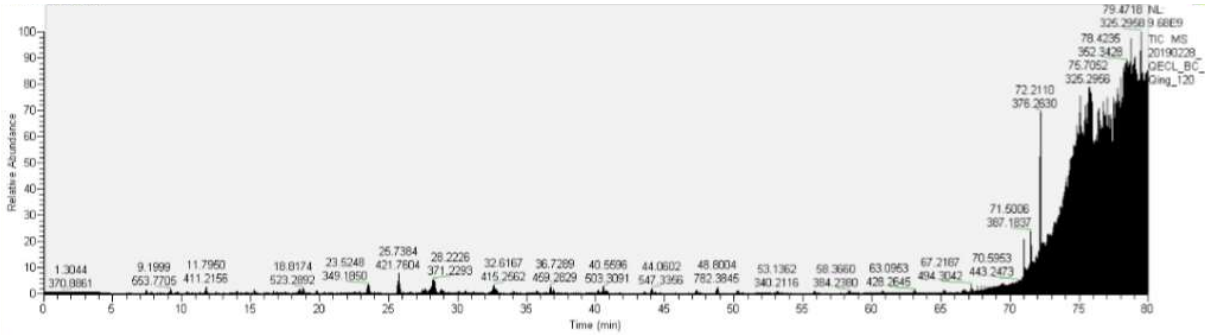

Figure 3.89: Mass spectrum for Calmodulin-1

3.5.3.20 Pyruvate kinase

Pyruvate kinase (match ID 179) has been identified in A2780^{cisR} cell line which was significantly downregulated following combined treatments of LH5+Camp (0/0) and LH5+Camp (0/4). Other single and combined drug treatments caused disappearance of the protein or no significant changes in the expression of the protein in A2780^{cisR} cell line.

When the expression of Pyruvate kinase in resistant A2780^{cisR} cell line was compared with that in parent A2780 cell line, it was found that the protein was upregulated by a factor of 1.9. The expression of the protein was partially restored following the treatments with Oxa alone, LH5+Oxa (0/0) and LH5+Oxa (4/0). Cis alone, LH5 alone and LH5+Camp (0/4) caused disappearance of the protein in A2780^{cisR} cell line. LH5+Camp (0/0) treatment over restored the protein, however LH5+Camp (4/0) treatment fully restored the protein.

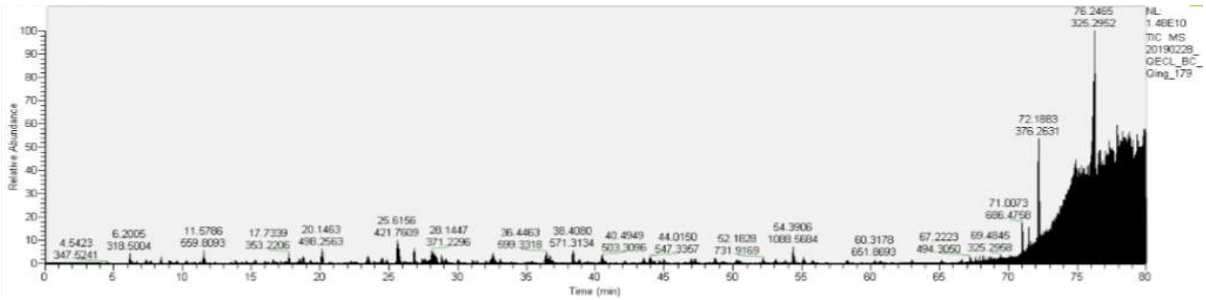

Figure 3.90: Mass spectrum for Pyruvate kinase

3.6 Bioinformatics

After search was made through The Cancer Genome Atlas, a total of 577 cases of ovarian cancer with 87 features have been observed. Among all practical cases, 535 of them had RNA-seq gene expression data for over 19000 genes. In the present study, genes that correspond to the 20 key proteins identified in the proteomic studies have been employed. Using the data, ovarian cancer-specific survival has been investigated as a single outcome variable. Among the investigated data, 48 ovarian cancer patients did not contain any clinical data which were omitted from the analysis. Patient ID in the both clinical and RNAseq datasets have been matched with 529 patients being identified as having data available for both. It has been found from the study that, tumour, normal, and control samples spans are from 01 to 09, from 10 to 19 and from 20 to 29 respectively

Six clinical factors (family history, age at initial diagnosis, age at onset of menopause, histological grade and stages of tumour, tumour size and received anticancer therapy) along with RNA-seq data sets have been matched and 529 patients have been identified with data available for both. Among the observed clinical factors, all were classified as a categorical data except age of the patient. The age distribution of investigated ovarian cancer patients is shown in Figure 3.91. Descriptive summary statistics of other selected clinical factors is presented in Table 3.27.

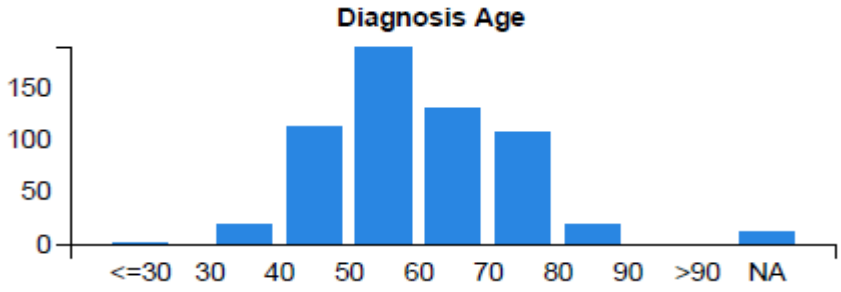

Figure 3.91: Age distribution at time of diagnosis

Table 3.27: Descriptive statistics of clinical predictors

Characteristics	Category	Frequency	Percentage
Race	Alaska native or American Indian	3	0.51
	Asian	20	3.46
	Black or African-American	34	5.89
	Hawaii native or other Pacific Islands	1	0.17
	Others	27	4.67
	White	492	85.26
Tumour Site	Bilateral	396	72.52
	Left	80	14.65
	Right	70	12.82
Stages of Cancer	Stage IA	2	0.34
	Stage IB	3	0.52
	Stage IC	11	1.91
	Stage IIA	4	0.69
	Stage IIB	5	0.87
	Stage IIC	21	3.66
	Stage IIIA	8	1.39
	Stage IIIB	24	4.18
	Stage IIIC	407	71.02
	Stage IV	88	15.35
Anatomic Site	Omentum	3	0.51
	Ovary	572	99.13
	Peritonium Ovary	2	0.34
Histological Grades	G1	6	1.04
	G2	69	12.02
	G3	486	84.66
	G4	1	0.17
	GB	2	0.34
	GX	10	1.74

3.6.1 Survival pattern of the identified proteins

Survival function has been used to estimate the survival of the patients for dysregulated and normal groups which was applied to each of the 20 genes corresponding to the identified proteins. This was done by applying product limit estimator. The significance in the role of the transcriptoms is represented by their p-values in differential survival consequence to compare their expression level into two categories (dysregulated and normal).

The relative likelihood of death risk in ovarian cancer as applied to each gene has been estimated by Cox PH regression model. Table 4 presents the estimated Coefficients (β), with respect to the hazard ratios (HR), and p-values obtained from the experiment. It is found that p-values for genes ACTB, HST1H4F, HNRNPC, HSP90AB1 and PKM are

statistically significantly associated with their expression in the survival analyses. In Figure 3.92, it can be seen that patients with dysregulated expression of ACTB, HST1H4F, HNRNPC, HSP90AB1 and PKM genes had lower survival rates, in comparison with the control group.

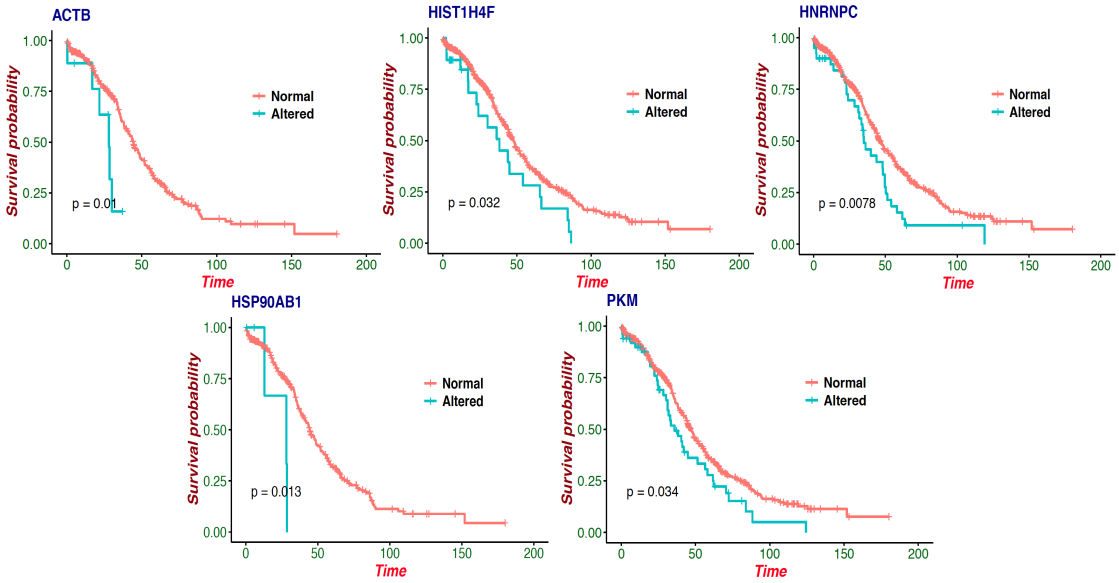

Figure 3.92: Survival pattern for dysregulated and normal groups for statistically significant genes

Table 3.28: Summary statistics of the Cox proportional Hazard Model for RNA-Seq data.

ACTB	1.3385	3.8132	0.0017
ANXA1	1.8436	6.3192	0.0671
ATP5B	-0.625	0.5353	0.3801
ATP5F1B	-0.141	0.8685	0.8432
ATP5IF1	0.1478	1.1593	0.5845
ATPIF1	0.2603	1.2974	0.3109
CALM1	-0.797	0.4505	0.1151
CFL1	-0.277	0.7581	0.3205
EEF1A1	0.2255	1.2529	0.2393
HIST1H4A	-0.494	0.6101	0.0631
HIST1H4B	-0.236	0.7898	0.3444
HIST1H4C	0.4793	1.615	0.157
HIST1H4D	-0.487	0.6145	0.404
HIST1H4E	-0.487	0.6144	0.0657
HIST1H4F	0.5029	1.6535	0.0339
HIST4H4	0.2607	1.2979	0.1568
HNRNPC	0.4908	1.6336	0.0085
HSP90AB1	1.3547	3.8757	0.0218
HSPA9	0.5413	1.7183	0.0717
HSPD1	-0.538	0.5841	0.1336
NPM1	0.3966	1.4867	0.2236
PKM	0.369	1.4463	0.0347
PPIA	-0.536	0.585	0.1404
PRDX1	-0.228	0.7963	0.1876
RAN	-0.369	0.6917	0.376
TPM4	0.2896	1.3359	0.1306
TUBB	-0.346	0.7077	0.1352
VIM	0.5609	1.7522	0.3353

3.6.2 Pathways and functional analyses of the identified significant proteins

Several significant pathways have demonstrated association with the identified regulated genes. Genes related to the signaling pathways and corresponding p-values are given in Table 3.29. Biological process pathways (obtained from ontology enrichment analysis) that are associated with identified genes that are believed to be significant are given in Table 3.30.

Table 3.29: Top significant pathways linked with selected 20 significant genes with adjusted p values

Alcoholism	5.57E-07	HIST1H4A;HIST1H4B;HIST4H4;CALM1;HIST1H4C;HIST1H4D;HIST1H4E;HIST1H4F
Systemic lupus erythematosus	9.55E-07	HIST1H4A;HIST1H4B;HIST4H4;HIST1H4C;HIST1H4D;HIST1H4E;HIST1H4F
Viral carcinogenesis	1.28E-06	HIST1H4A;PKM;HIST1H4B;HIST4H4;HIST1H4C;HIST1H4D;HIST1H4E;HIST1H4F
Fluid shear stress and atherosclerosis	0.017694762	HSP90AB1;CALM1;ACTB
Legionellosis	0.019984314	EEF1A1;HSPD1
Pathogenic Escherichia coli infection	0.019984314	TUBB;ACTB
Tuberculosis	0.033974067	HSPA9;CALM1;HSPD1
Gastric acid secretion	0.035506545	CALM1;ACTB
Pertussis	0.036374573	CFL1;CALM1
RNA degradation	0.039027401	HSPA9;HSPD1
Hypertrophic cardiomyopathy (HCM)	0.044545616	TPM4;ACTB

Table 3.30: Top 60 Gene Ontology pathways related to the top 20 significant genes in ovarian cancer and their corresponding p-values.

Ribosomal small subunit export from nucleus	GO:0000056	2.29E-04	NPM1;RAN
Chromatin silencing at rDNA	GO:0000183	4.26E-02	HIST1H4A
Enhancer sequence-specific DNA binding	GO:0001158	2.73E-02	HNRNPC;ACTB
Retina homeostasis	GO:0001895	1.04E-02	PRDX1;ACTB
Neutrophil mediated immunity	GO:0002446	4.39E-02	EEF1A1;HSP90AB1;PKM;TUBB;PPIA
Mitochondrial proton-transporting ATP synthase complex	GO:0005753	3.38E-03	ATP5B;ATPIF1
Actin filament	GO:0005884	2.07E-02	ANXA1;TPM4
Focal adhesion	GO:0005925	8.25E-05	HSPA9;NPM1;ANXA1;TPM4;CFL1;VIM;PPIA;ACTB
RNA-dependent DNA biosynthetic process	GO:0006278	3.08E-03	HSP90AB1;PPIA
Nucleosome assembly	GO:0006334	2.43E-02	NPM1;HIST1H4A
DNA replication-independent nucleosome assembly	GO:0006336	1.09E-02	NPM1;HIST1H4A

Chromatin remodeling	GO:0006338	1.12E-02	NPM1;HNRNPC;ACTB
Regulation of translation	GO:0006417	1.03E-02	NPM1;HIST1H4A;VIM;RAN
Muscle contraction	GO:0006936	1.74E-02	TPM4;VIM;CALM1
Response to unfolded protein	GO:0006986	6.99E-04	HSPA9;HSP90AB1;HSPD1
Protein alkylation	GO:0008213	6.23E-03	EEF1A1;CALM1
Actin cytoskeleton	GO:0015629	6.25E-03	EEF1A1;ANXA1;TPM4;HNRNPC;ACTB
ATPase activity	GO:0016887	4.70E-02	HSPA9;ATP5B;HSPD1
Nucleoside-triphosphatase activity	GO:0017111	2.64E-02	EEF1A1;HSPA9;ATP5B;RAN;HSPD1
Viral life cycle	GO:0019058	8.99E-03	HSP90AB1;PPIA;RAN
Kinase binding	GO:0019900	2.51E-02	EEF1A1;NPM1;HSP90AB1;CALM1;ACTB
Substantia nigra development	GO:0021762	1.31E-02	CALM1;ACTB
Muscle filament sliding	GO:0030049	1.04E-02	TPM4;VIM
Myeloid cell differentiation	GO:0030099	1.37E-02	HSPA9;ATPIF1
Erythrocyte differentiation	GO:0030218	8.89E-03	HSPA9;ATPIF1
Chromatin remodeling at centromere	GO:0031055	7.51E-03	NPM1;HIST1H4A

Positive regulation of cellular biosynthetic process	GO:0031328	2.55E-02	NPM1;HSP90AB1;VIM
Chromatin assembly	GO:0031497	2.81E-02	NPM1;HIST1H4A
Purine ribonucleoside binding	GO:0032550	2.55E-02	EEF1A1;TUBB;RAN
Guanyl ribonucleotide binding	GO:0032561	3.03E-02	EEF1A1;TUBB;RAN
CENP-A containing nucleosome assembly	GO:0034080	6.65E-03	NPM1;HIST1H4A
Positive regulation of cellular amide metabolic process	GO:0034250	2.50E-02	NPM1;VIM
Centromere complex assembly	GO:0034508	9.38E-03	NPM1;HIST1H4A
DNA replication-dependent nucleosome organization	GO:0034723	3.88E-02	HIST1H4A
Nucleosome organization	GO:0034728	3.99E-02	NPM1;HIST1H4A
Secretory granule lumen	GO:0034774	8.51E-03	EEF1A1;HSP90AB1;PKM;TUBB;PPIA
Positive regulation of protein dephosphorylation	GO:0035307	7.07E-03	HSP90AB1;CALM1
Interleukin-12-mediated signaling pathway	GO:0035722	8.49E-04	HSPA9;CFL1;PPIA
Ribonucleoprotein granule	GO:0035770	4.08E-02	TUBB;ACTB

Regulation of gene expression, epigenetic	GO:0040029	3.55E-02	HIST1H4A;ACTB
ATP-dependent chromatin remodeling	GO:0043044	6.65E-03	HNRNPC;ACTB
Negative regulation of apoptotic process	GO:0043066	4.32E-02	HSPA9;NPM1;ANXA1;CFL1; HSPD1
Negative regulation of programmed cell death	GO:0043069	2.29E-02	HSPA9;NPM1;ANXA1;CFL1; HSPD1
Histone exchange	GO:0043486	9.38E-03	NPM1;HIST1H4A
Positive regulation of blood vessel endothelial cell migration	GO:0043536	1.42E-02	ATP5B;ANXA1
Regulation of phosphoprotein phosphatase activity	GO:0043666	8.89E-03	HSP90AB1;CALM1
Regulation of myeloid cell differentiation	GO:0045637	2.81E-02	HSPA9;HIST1H4A
Negative regulation of myeloid cell differentiation	GO:0045638	3.38E-03	HSPA9;HIST1H4A
Positive regulation of translation	GO:0045727	3.90E-02	NPM1;VIM
Positive regulation of gene expression, epigenetic	GO:0045815	1.55E-02	HIST1H4A;ACTB
Positive regulation of T cell activation	GO:0050870	3.05E-02	ANXA1;HSPD1
Chaperone-mediated protein complex assembly	GO:0051131	2.01E-03	HSP90AB1;HSPD1

Regulation of posttranscriptional gene silencing	GO:0060147	2.07E-02	HIST1H4A;RAN
Cytoplasmic vesicle lumen	GO:0060205	1.75E-03	EEF1A1;HSP90AB1;PKM;PPIA
Regulation of gene silencing by RNA	GO:0060966	2.07E-02	HIST1H4A;RAN
Cellular response to interleukin-12	GO:0071349	8.49E-04	HSPA9;CFL1;PPIA
Nucleic acid metabolic process	GO:0090304	4.08E-02	HNRNPC;RAN
Polymeric cytoskeletal fiber	GO:0099513	1.16E-02	ANXA1;TPM4;TUBB;VIM
Regulation of cell cycle G2/M phase transition	GO:1902749	4.45E-02	NPM1;TUBB
Ficolin-1-rich granule lumen	GO:1904813	1.47E-03	EEF1A1;HSP90AB1;PKM;PPIA

Figure 3.93 shows the protein-protein interaction network created using STRING software. Target proteins are found to be directly associated with the gold standard ovarian cancer signatures and exist within same cluster. All of the identified biomarkers are found to be linked to each other through the protein-protein interaction network as presented in Figure 3.93.

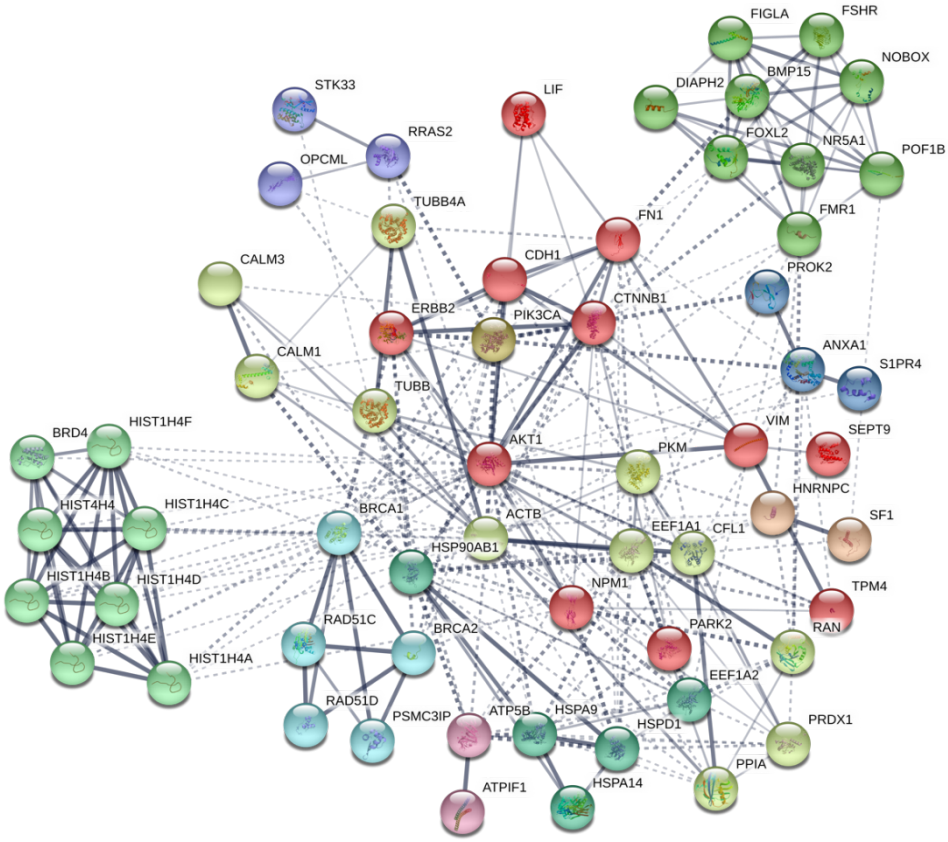

Figure 3.93: Protein-protein interaction network of the identified proteins

4 Discussion

Preamble:

The present study aims to investigate the combined drug actions from binary combinations of selected chemotherapeutic drugs and designed complexes (cisplatin, oxaliplatin, LH5, gemcitabine, camptothecin and cucurbitacin B). Several other studies (damage to DNA, accumulation of platinum within the cell, Pt binding to DNA and proteomic) were also conducted to get a mechanistic insight into specific combined drug actions. In this section, the results obtained from the present study have been discussed, considering the existing knowledge and literature.

4.1 Cytotoxicity of drugs alone

Before starting the experiments on combined drug actions, the antitumour activity of individual compounds was determined. As the drugs were combined on the basis of their IC_{50} values in a combination study, the knowledge of the cytotoxic profile of each compound in the experimental setup was a prerequisite in this combination study. The study was conducted in ovarian tumour models, using two different cancer cell lines (A2780 and A2780^{cisR}), and colorectal cancer models ((HT-29, Lim-1215 and Lim-2405). As drugs used in the present study (cisplatin, oxaliplatin, gemcitabine and camptothecin) are used primarily to treat ovarian and colorectal cancers in clinic, only those cancer models were chosen for investigation. The parent A2780 and its cisplatin-resistant counterpart A2780^{cisR} ovarian cell lines were used to compare activity in both. Among the selected compounds, gemcitabine demonstrated the greatest antitumour activity in the cell lines (see Table 3.1 and Table 3.2), while the monofunctional platinum compound, LH5, presented minimal antitumour activity.

Among the five cell lines, cisplatin showed highest activity (the lowest IC_{50} value) in A2780 ovarian cancer cell line and lowest activity in the $A2780^{cisR}$ cell line. In other cell lines, the activity order for cisplatin was HT-29>Lim-1215>Lim-2405. The IC_{50} values observed for cisplatin in the ovarian cancer models of the present study were slightly lower than the previously reported values for the drug in the same cell lines. Also the RF values (the quotient of IC_{50} in the refractory cell line over that in the responsive cell line) for cisplatin obtained from the present study were higher than the earlier reports (Nessa, Beale et al. 2012; Huq, Yu et al. 2014; Alamro 2015; Arzuman, Beale et al. 2015). The observed IC_{50} values for cisplatin in the tested colorectal cell lines were slightly lower than the previous reported values in the same cell lines, which is similar to the ovarian cancer cell lines (Almoyad 2018; Bali 2018). The differences in the observed IC_{50} values in the present study, compared with the previous studies, could be due to a change in the characteristics of the cancer cells. Variations of response to different chemotherapeutics is common, due to batch variations, time and experimental set up (He, Zhu et al. 2016).

Camptothecin is the second highest sensitive compound among the selected chemotherapeutic drugs in the present study. Among the tested cell lines, camptothecin showed the greatest activity in the ovarian cancer cell A2780 and least in the cell line $A2780^{cisR}$ (see Table 3.1 and Table 3.2). In other cell lines, order of activity for camptothecin is Lim-2405>Lim-1215>HT-29. The IC_{50} values obtained for camptothecin in the present study can also be expressed in nanomolar (nM) levels, which is similar to the values observed in earlier studies of breast cancer cell lines. For example, camptothecin provided IC_{50} values at 7 nM in the MDA-157 breast cancer cell line, 150 nM in the G1-101A breast cancer cell line (Jones, Clements et al. 1997) and 61.1 nM in the C6 glioma cell line (Pavillard, Kherfellah et al. 2001). The greater

antitumour activity of camptothecin may be attributed to its unique mode of action and the reversible inhibition of DNA Topoisomerase I. DNA Topoisomerase is a highly expressed enzyme occurring in multiple types of tumours that serves many functions, including: chromosomal recombination, repair of DNA and transcription, and assembly of chromatin (Li, Zu et al. 2006). As mentioned in the introduction section (1.9.2.5), camptothecin exerts its cytotoxic action via stabilisation of the so-called cleavable topoisomerase I-DNA complex. Subsequently, collision with DNA replication fork occurs, which ultimately leads to double stranded DNA breaks, followed by cell death. Due to this unique mechanism of action, camptothecin demonstrates antitumour action as a single agent in a wide range of tumour types (Thomas, Rahier et al. 2004). Moreover, camptothecin may also intervene with the DNA repair mechanism, which, in turn, potentiates its anticancer activity.

LH5 is a new monofunctional platinum compound synthesised and characterised by Laila Arzuman in the host laboratory, that demonstrated significant anticancer activity in the ovarian cancer models (Arzuman, Beale et al. 2016). However, in the present study, LH5 displayed least antitumour activity in the cell lines, when compared to other clinically used drugs. This is the first report of the antitumour action of LH5 in colorectal cancer cell lines, with IC_{50} values ranging from 5.25 to 7.93 μM. When the activity of LH5 is compared to the ovarian and colorectal cancer models, it can be seen that antitumour activity is greater in the colorectal cancer models than in the ovarian cancer models. As a single agent, LH5 demonstrated moderate anticancer activity when compared to the clinical standard cisplatin and other synthesised monofunctional platinum compounds. Among the synthesised monofunctional platinum complexes existing in the literature, the order of anticancer activity (on the basis of IC_{50} values in cancer cell lines) can be seen as:

phenanthriplatin>LH3>LH6>LH3>LH5>LH4>LH2>LH1>cDPCP>pyriplatin (Lovejoy, Todd et al. 2008; Lovejoy, Serova et al. 2011; Park, Wilson et al. 2012; Arzuman, Beale et al. 2014; Arzuman, Beale et al. 2014; Arzuman, Beale et al. 2015; Arzuman, Beale et al. 2015; Arzuman, Beale et al. 2016). Monofunctional platinum compounds are rule-breaker platinums that have been reported to have the ability to overcome drug resistance. Different binding patterns (monodentate at N7 position of guanine residues, with no significant distortion of the DNA double helix) of the monofunctional platinums has been implicated as a result of their ability to overcome resistance (Park, Wilson et al. 2012). Moreover, rule-breaker platinums block transcription, almost to the same extent as cisplatin, but the repair of rule-breaker platinum adducts by the mammalian excinuclease is noticeably reduced, compared to that of cisplatin or oxaliplatin damage.

Oxaliplatin displayed the greatest antitumour activity in the Lim-2405 colorectal cancer cell line, whereas least activity was shown in colorectal cancer cell line HT-29. In other tested cell lines, the order of activity of oxaliplatin is the A2780>A2780^{cisR}>Lim-1215 cell line. The IC_{50} values for oxaliplatin obtained from the present study are similar to the values obtained from earlier reports in the host laboratory (Almoyad 2018; Bali 2018). The underlying mechanisms for the anticancer activity of oxaliplatin have been highlighted in the introduction section (1.9.2.2).

Gemcitabine demonstrated the highest antitumour activity among the selected compounds, with IC_{50} values at nM concentrations in all tested cell lines. The most sensitive cell line to gemcitabine was the A2780 ovarian cancer cell line, whereas the least sensitive was the Lim-1215 colorectal cancer cell line. In other tested cell lines, the order of the activity of oxaliplatin was the A2780^{cisR}>HT-29>Lim-2405 cell line. In a study carried out earlier, Moorsel reported IC_{50} values of 2.2 nM and 625 nM in the

A2780 and A2780^{cisR} cell lines after 72 hours exposure to gemcitabine through MTT assay (Van Moorsel, Veerman et al. 1998). Veronique et al. reported an IC_{50} value of 0.6 nM for gemcitabine in the A2780 cell line under the same experimental conditions (Van Haperen, Veerman et al. 1994), whereas IC_{50} values obtained in the present study under the same experimental conditions were 0.02 nM and 9 nM in A2780 and A2780^{cisR} cell lines, respectively.

As stated in the introduction section (1.9.2.5), gemcitabine is a potent inhibitor of DNA synthesis. After entry into the cells, with the help of nucleoside transporters, gemcitabine becomes self-potentiated through conversion into gemcitabine triphosphate in the presence of the deoxycytidine kinase enzyme or the thymidine kinase 2 enzyme. Gemcitabine triphosphate then competes with deoxycytidine triphosphate, acting as a weak inhibitor of DNA polymerase. Moreover, gemcitabine triphosphate is incorporated into the DNA and, subsequently, terminates DNA polymerisation and single-strand breakage (Mini, Nobili et al. 2006). Gemcitabine triphosphate is also incorporated into RNA, which leads to the inhibition of RNA synthesis. Ultimately, cell death occurs through apoptosis, which is induced by the activation of several caspases (e.g., caspase 8 and caspase 3).

In the present study, cucurbitacin B was tested for its antitumour activity only in the ovarian cancer models. As evidenced in Table 3.1, cucurbitacin B acts as a promising antitumour agent for ovarian cancer (when administered alone), having IC_{50} values at nanomolar levels (6 nM in the A2780 tumour model and 20 nM in the A2780^{cisR} cell line). The present study may be the first report on the strong anticancer potential of cucurbitacin B in ovarian cancer. However, the compound has already been found to show antitumour activity in many other types of cancer. The IC_{50} values of cucurbitacin B obtained from previously reported *in vitro* studies are presented in Table 4.1.

Table 4.1: Antitumour activity of cucurbitacin B in various cancer cell lines obtained from earlier studies

Cell line	Type of cancer	IC_{50} value (nM)	Reference
MDA-MB-231	Breast	30	(Wakimoto, Yin et al. 2008)
ZR-75-1	Breast	32	(Wakimoto, Yin et al. 2008)
MCF-7	Breast	36	(Wakimoto, Yin et al. 2008)
T47D	Breast	118	(Wakimoto, Yin et al. 2008)
BT474	Breast	136	(Wakimoto, Yin et al. 2008)
MDA-MB-453	Breast	418	(Wakimoto, Yin et al. 2008)
MiaPaCa-2, PL45, SU86.8, AsPC-1 and Panc-1	Pancreatic	100	(Thoennissen, Iwanski et al. 2009)
PC-3 and LNCaP	Prostate	300	(Gao, Islam et al. 2014)
U87, T98G, U118, U343 and U37	Glioblastoma	100	(Yin, Wakimoto et al. 2008)

When the IC_{50} values of Table 4.1 are compared with the values obtained from the present study, it can be seen that cucurbitacin B is more potent in ovarian cancer than in other types of cancer. The anticancer mechanism of cucurbitacin B was attributed to the disruption of microtubules and F-actin (Wakimoto, Yin et al. 2008); the inhibition of the stat-3 signalling pathway (Chan, Li et al. 2010); the blockage of G2/M and the S cell cycle phase (Chan, Meng et al. 2010; Yasuda, Yogosawa et al. 2010); the induction of apoptosis (inhibition of bcl-2, cyclinA, cyclinB1, cyclinD1, cmyc, cdc25C and β-catenin, PARP cleavage and caspase 3/7 activation) (Lee, Iwanski et al. 2010; Dakeng, Duangmano et al. 2012; Kausar, Munagala et al. 2013); and the inhibition of JAK2 and stat-5 (Zheng, Liu et al. 2014).

4.2 Activity of drugs in combination

4.2.1 Combination of Cis with LH5

In the ovarian tumour models, the combination of Cis with LH5 demonstrated synergy only with the 4/0 sequence at ED_{50} and ED_{75} in the A2780 human ovarian cancer cell line. No significant potentiation in the combined drug action was found from the combination of Cis with LH5 in the resistant $A2780^{cisR}$ ovarian cancer cell line. In contrast, in the Lim-1215 colorectal cancer model, the combination of Cis with LH5 produced an increased cell kill, applying to the 0/4 and 4/0 sequences of addition irrespective of drug concentration, except for the ED_{50} level with the 4/0 addition. Greater synergy in cell kill was observed at higher added concentrations (ED_{75} and ED_{90}), compared to lower added concentrations (ED_{50}) in the Lim-1215 cell line. In the HT-29 cell line, the combined activity of Cis with LH5 mostly antagonistic, except at the ED_{90} level, with bolus and 4/0 sequences of administration, where synergy was found. From the above discussion, it can be said that no specific sequence of administration of Cis with LH5 produced synergy in all tested cell lines. Similarly, no specific level of added drug concentrations of Cis with LH5 demonstrated synergy in all tested cell lines. Likewise, the combination of Cis with LH5 did not show synergy in any of the tested cell lines and for the three sequences of administration or drug concentrations.

This is the first study where cisplatin has been combined with the monofunctional platinum compound, LH5, in any cancer model. Similar to the findings of the present study, a previous study also reported a sequence-dependent synergistic effect from the combination of cisplatin with monofunctional platinums (LH1 and LH2) at the ED_{50} level. No definite sequence of administration produced synergy in the parent (A2780)

or resistant ($A2780^{cisR}$ and $A2780^{ZD0473R}$) ovarian cancer cell lines at the ED_{50} level (Arzuman, Beale et al. 2015). However, another study showed that cisplatin, in combination with another monofunctional platinum compound, LH6, demonstrated strong synergy in three ovarian cancer cell lines (A2780, $A2780^{cisR}$ and $A2780^{ZD0473R}$) for all the three sequences of drug addition at the ED_{50} level (Arzuman, Beale et al. 2015).

The monofunctional platinum compound, LH1, possesses three 3-hydroxy pyridine ligands in its structure, whereas LH2 possesses three imidazole ligands in its structure, and LH6 possesses three imidazo (1,2-α) pyridine ligands in its structure. In contrast, LH5, used in the present study, contains three quinolone ligands in its structure. The mechanism of cytotoxicity for all monofunctional compounds could be the same, as discussed in the introduction section. But cisplatin, in combination with different monofunctional platinums, exhibited different combined effects. So, it can be hypothesised that synergy is also dependent on the individual nature of the combined drugs and not with the definite class of the drugs.

4.2.2 Combination of Cis with Camp

The results obtained from the study applying to ovarian tumour models suggest that the combination of Cis with Camp could be beneficial in overcoming drug resistance. In the resistant $A2780^{cisR}$ cell line, Cis, in combination with Camp, demonstrated synergy at all sequences of drug administrations and concentrations. Among the three sequences of administration, the 4/0 sequence produced the strongest synergy in the $A2780^{cisR}$ cell line. The higher, added concentrations (ED_{75} and ED_{90}) exhibited greater synergy than the lower concentration (ED_{50}), from the combination of Cis with Camp in $A2780^{cisR}$ cell line. However, in the parent ovarian A2780 cell line, the same combination of Cis

with Camp did not produce synergy at any sequence of administration or added concentration.

In the colorectal cancer models, a combination of Cis with Camp demonstrated greater synergy in the HT-29 cell line than in the Lim-1215 tumour model. In the HT-29 cell line, a combination of Cis with Camp showed synergy at the ED_{50} level for all sequences of drug addition, and the most synergistic effect was observed with the 4/0 sequence of administration. Among the added drug concentrations, the higher added concentrations demonstrated greater synergistic action than the lower added concentrations in the HT-29 cell line. In contrast, a combination of Cis with Camp showed greater cell kill only in the 4/0 sequence of administration for all added drug concentrations in the Lim-1215 cell line, and more in the ED_{50} level.

In the literature, not much information can be found regarding the combined drug actions for cisplatin and camptothecin. However, several preclinical studies (both *in vitro* and *in vivo*) have been conducted to investigate the drug action association of the combination of cisplatin with clinically approved camptothecin derivatives (irinotecan and topotecan). Cisplatin, in combination with irinotecan, demonstrated synergistic cell kill in lung cancer (Fukuda, Nishio et al. 1996), oesophageal cancer (Takiyama, Terashima et al. 1997), leukaemia, bladder cancer and ovarian cancer (Keane, El-Galley et al. 1998). However, some studies reported additive effects from combination of cisplatin with irinotecan in ovarian cancer, gastric colon and oesophageal cancers (Katz, Vick et al. 1990; Ma, Maliepaard et al. 1998). Also, a synergistic effect was produced by the combination of topotecan with cisplatin in teratocarcinoma, glioma, ovarian cancer and lung cancer (Kaufmann, Peereboom et al. 1996; Waud, Rubinstein et al. 1996; Romanelli, Perego et al. 1998). The underlying mechanism for the observed synergy from the combination of cisplatin with topoisomerase I inhibitors has been

associated with interference of topoisomerase I inhibitor in repairing cisplatin-induced DNA interstrand crosslinks (De Jonge, Sparreboom et al. 1998).

4.2.3 Combination of LH5 with Camp

LH5, in combination with Camp, displayed synergy in both the parent and cisplatin-resistant A2780 ovarian cancer cell lines at all sequences of drug addition at the ED_{75} and ED_{90} levels. However, at the ED_{50} level, only a 4/0 sequence of administration of LH5 with Camp demonstrated synergy in the $A2780^{cisR}$ ovarian cancer cell line. The bolus administration of LH5 with Camp produced an additive effect, whereas a 0/4 addition produced an antagonistic effect in the ovarian $A2780^{cisR}$ cancer cell line. In contrast, in the parent A2780 cell line, a combination of LH5 with Camp showed antagonism at all sequences of addition at the ED_{50} level.

In the colorectal cancer cell lines, LH5 in combination with Camp, demonstrated synergy only in the Lim-1215 cell line, whereas the effect was antagonistic in the HT-29 cell line. A synergistic effect in the Lim-1215 cell line was observed for all sequences of drug addition and concentrations, except at ED_{50} level, with a 0/4 sequence of addition. The synergistic effect was found to heighten with the increase in concentrations for the three sequences of addition in the Lim-1215 cell line. The highest synergy was shown in the 4/0 sequence with the addition of LH5 with Camp.

This is the first study to describe the combined drug action between a monofunctional platinum and a topoisomerase I inhibitor. However, in an earlier study, LH5, in combination with capsaicin, and LH5, in combination with curcumin, demonstrated a strong synergy in three ovarian tumour models (A2780, $A2780^{cisR}$ and $A2780^{ZD0473R}$). The authors reported that all sequences of administration produced a synergistic effect, with the most synergy observed with the bolus addition. Similar to the findings of the

present study, higher added concentrations (ED_{90} and ED_{75}) displayed more synergy than lower added concentrations (ED_{50}) (Arzuman, Beale et al. 2016). A cellular accumulation of platinum (Table 3.15 and Table 3.17) and a platinum-DNA binding study (Table 3.19 and Table 3.21) revealed that observed synergy from the combination of LH5 with Camp in the $A2780^{cisR}$ and Lim-1215 cell lines could be due to the increased accumulation of platinum in the cell and increased platinum–DNA binding. However, the exact mechanisms behind the synergy observed in the present study from the combination of LH5 with Camp at the ED_{90} level with a 4/0 sequence of addition, remains open to question.

4.2.4 Combination of LH5 with Oxa

LH5, in combination with oxaliplatin, predominantly displayed antagonism in the tested cell lines in the present study for all sequences of drug combination and added concentrations. However, additive effects were observed in the A2780 cell line at the ED_{90} for all the three sequences of administration. Moreover, mild synergy was also evidenced at the ED_{90} level in the $A2780^{cisR}$ cell line for all the three sequences of addition. This is the first ever report of the combined drug action of a monofunctional platinum and oxaliplatin. The antagonism observed from the combination of LH5 with oxaliplatin may be due to the decreased cellular accumulation of platinum (Table 3.14), as well as to decreased platinum-DNA binding (Table 3.21), as evidenced in mechanistic studies. This conclusion is also supported by the greater cellular accumulation of platinum (Table 3.16) from the additive combination of LH5 with oxaliplatin in the HT-29 cell line. As there is no previous information regarding the combination of monofunctional platinums with oxaliplatin, the obtained results could not be discussed in much detail.

4.2.5 Combination of Gem with LH5

In general, the combination of gemcitabine with LH5 demonstrated additive to antagonistic effects at all the three sequences of addition and concentrations in the tested cell lines. However, synergy was found at the ED_{50} level for all sequences of administration in $A2780^{cisR}$ cell line and at the ED_{90} level for all sequences in the Lim-1215 cell line. This is the first ever study to investigate the combined drug action from gemcitabine with any monofunctional platinum. However, a mechanistic study was not conducted to reveal the mechanism for combined drug actions.

4.2.6 Combination of Gem with Cis

The combination of gemcitabine with cisplatin displayed additive effect for bolus and the 4/0 sequence of drug administration in the ovarian A2780 cancer cell line at all added concentrations. However, 0/4 sequence of drug addition showed antagonism at the ED_{50} and ED_{75} and synergy at the ED_{90} in the A2780 cell line. In contrast, in the $A2780^{cisR}$ cell line, gemcitabine, in combination with cisplatin, exhibited synergy at all the three sequences of administration and at all concentrations, except for at the ED_{90} at bolus and for the 4/0 sequence of administration. Greater synergy was observed at lower concentrations (ED_{50} and ED_{75}) than at higher concentrations (ED_{90} level). Bolus administration of gemcitabine with cisplatin produced the highest synergy at the ED_{50} level in the $A2780^{cisR}$ cell line.

Synergy from the combination of gemcitabine with cisplatin was also found in an earlier study (Bergman, van Haperen et al. 1996). The authors reported that long-term exposure of gemcitabine with cisplatin produced synergistic effects in ovarian cancer models (parent A2780 cell line, cisplatin-resistant $A2780^{cisR}$ cell line and gemcitabine-resistant A2780 cell line), human head and neck squamous cell carcinoma models

(UMSCC-22B cell line) and the murine colon carcinoma cell line, C26-10. Sequenced administration (4/0 and 0/4) displayed more synergy when compared to the simultaneous administration of gemcitabine with cisplatin. Synergy from the combination of gemcitabine with cisplatin was neither associated with the increased accumulation of the drug nor with increased DNA damage (Bergman, van Haperen et al. 1996), implying that the increased cell kill was not associated with DNA damage or drug DNA binding.

It has also been confirmed from the present study that observed synergy from the combination of gemcitabine with cisplatin has neither been associated with increased platinum uptake (Table 3.15) nor increased platinum DNA binding (Table 3.19). The synergistic interaction between gemcitabine and cisplatin is possibly due to the result of the incorporation of gemcitabine into DNA and/or due to cisplatin DNA adduct formation, which may be affected by each other. Further studies are required to reveal the real facts underlying the synergistic outcome from the combination of gemcitabine with cisplatin.

4.2.7 Combination of Gem with Oxa

In the present study, combined drug actions between gemcitabine and oxaliplatin have been investigated only in colorectal cancer cell lines (HT-29 and Lim-1215). Combination of gemcitabine and oxaliplatin demonstrated antagonism, predominantly in the HT-29 cell line, irrespective of the sequence of drug addition and concentrations. However, bolus administration and the 0/4 sequence of administration at the ED_{50} level displayed mild synergistic and additive effects, respectively.

In the Lim-1215 cell line, the combination of gemcitabine with oxaliplatin mainly showed synergy at different sequences of administration and concentrations. However, additiveness and mild antagonism have also been observed in a few instances; e.g., 0/4 sequence of administration at ED_{50} (antagonistic) and ED_{75} (additive), and bolus administration at ED_{75} and ED_{90} (antagonistic). The most synergistic effect was observed with the 4/0 sequence of administration of gemcitabine with oxaliplatin, where synergy existed at all added concentrations. The trend of synergy observed at the 4/0 sequence of administration from the combination of gemcitabine with oxaliplatin in the Lim-1215 cell line was $ED_{90}>ED_{75}>ED_{50}$. No study has been conducted to obtain the mechanistic insight of observed synergy.

Synergy from a combination of gemcitabine with oxaliplatin has also been reported in colorectal cancer models (HCT 116 and CoLo 320 DM cell lines) in a previous study. The 0/2 sequence of addition of gemcitabine with oxaliplatin displayed greater synergy than the 2/0 sequence of administration of gemcitabine with oxaliplatin in the HCT 116 cell line (Faivre, Raymond et al. 1999). In contrast, the authors reported that the 0/2 sequence of addition of gemcitabine with oxaliplatin was synergistic, but the 2/0 sequence of addition of gemcitabine was additive in the CoLo 320 DM cell line. The same study also revealed that the combination of gemcitabine with oxaliplatin was better than the combination of gemcitabine with cisplatin, from the point of synergistic outcomes in the tested colorectal cell lines. Moreover, the study of the leukemic cell line (CEM) also revealed that the combination of gemcitabine with oxaliplatin was synergistic. Several clinical studies also demonstrated the effectiveness of the combination therapy of gemcitabine with oxaliplatin in pancreatic, lung and biliary cancer (Louvet, André et al. 2002; Verderame, Russo et al. 2006; Takahashi, Morizane et al. 2018). As studies do exist in the literature regarding the combined drug actions of

gemcitabine with oxaliplatin in preclinical animal models and clinical studies, in future, attempts can be taken to evaluate the synergistic action of this selected combination.

4.2.8 Combination of Cuc with Cis

The combination of cucurbitacin B with cisplatin produced synergistic outcome in the parent A2780 ovarian cancer cell line for all the three sequences of addition and concentrations, except in the ED_{90} level at a 0/4 sequence of administration, where mild antagonism was found. In the case of the bolus administration of cucurbitacin B with cisplatin, observed synergy in A2780 cell line was found to increase with increase in drug concentration. However, the converse was true in the 4/0 sequence of administration of cucurbitacin B with cisplatin in the A2780 cell line, where the highest synergy was found at the ED_{50} level and the lowest at the ED_{90} level. In the $A2780^{cisR}$ cell line, the combined drug action obtained from the combination of cucurbitacin B and cisplatin was antagonistic. However, synergy was found at the ED_{50} level for the 0/4 sequence of administration of cucurbitacin B with cisplatin in the $A2780^{cisR}$ cell line.

This is the first substantive study where the combined effect of cucurbitacin B with cisplatin has been investigated in ovarian tumour models. However, previous studies demonstrated the synergistic activity resulting in the combination of cucurbitacin B with cisplatin in laryngeal carcinoma and cutaneous carcinoma (Chen, Leiter et al. 2010; Liu, Peng et al. 2010). Moreover, synergy was also observed from the combination of cucurbitacin B with docetaxel and methotrexate in laryngeal carcinoma and osteosarcoma, respectively (Liu, Zhang et al. 2008; Lee, Thoennissen et al. 2011). However, the mechanism behind the synergy from the combination of cucurbitacin B with different chemotherapeutic drugs, remains open to question.

4.2.9 Combination between Cuc and LH5

The combination of cucurbitacin B and LH5 has demonstrated an antagonistic outcome in the A2780 parent ovarian cancer cell line for all the three sequences of addition and concentrations, except for at the ED_{50} level at the 0/4 and 4/0 sequences of administration. However, the synergistic outcome was predominant for the combination of cucurbitacin B with LH5 in its resistant counterpart, the $A2780^{cisR}$ cell line. Both the bolus and 4/0 sequences of drug administration as applied to cucurbitacin B and LH5 exhibited synergy at the ED_{50} and ED_{75} levels in the $A2780^{cisR}$ cell line, whereas the effect was additive at the ED_{90} level with bolus and 4/0 sequences of drug addition as applied to cucurbitacin B and LH5 in the same cell line. The combined effect was antagonistic in the 0/4 sequence of addition of cucurbitacin B with LH5 at all concentrations in $A2780^{cisR}$ cell line. This is the first study to report the combined drug action between cucurbitacin B and monofunctional platinums in any cancer model. No mechanistic study has been done to reveal mechanistic information regarding combined drug actions.

4.3 DNA damage study

The changes in intensity or mobility of DNA bands from drug-treated cells, compared to those from untreated cells, indicate changes in DNA, such as DNA damage. In the present study, two platinum drugs (cisplatin and LH5) and six combinations (Cis with LH5 and Cis with Camp, each at three different sequences) were investigated for interaction with ovarian A2780 and $A2780^{cisR}$ cancer cell lines. When study was conducted with DNA obtained from A2780 cells, the results proved that LH5 caused the highest damage to DNA (having the greatest decrease in the intensity of the DNA band, compared to the untreated band). The findings corroborated the earlier report,

where LH5 was found to cause greater DNA damage than cisplatin (Arzuman, Beale et al. 2016). Among the six combinations investigated, only Cis with LH5 at the 4/0 sequence of drug addition was synergistic in action at ED_{50} in the A2780 parent human ovarian cancer cell line, while Cis with Camp at the 0/4 sequence was additive in action, and other selected combinations were antagonistic in action at the ED_{50} level in the A2780 parent ovarian cancer cell line. The study shows that cells treated with platinum drugs only (Cis or LH5) caused greater DNA damage than any of the investigated combinations. However, no correlation could be established between the combined drug action with DNA damage from the study with the DNA obtained from A2780 cells.

Among the selected combinations, three (Cis with Camp at 0/0; Cis with Camp at 0/4 and Cis with Camp at 4/0) were synergistic at the ED_{50} level and the other three (Cis with LH5 at 0/0; Cis with LH5 at 0/4 and Cis with LH5 at 4/0) were antagonistic at the ED_{50} in the $A2780^{cisR}$ cell line. It was observed that synergistic combinations caused higher DNA damage (a higher increase in mobility and a greater decrease in intensity of DNA bands) compared to all antagonistic combinations, except for Cis with LH5 at 0/4, which displayed the greatest DNA damage, although it was antagonistic in action in the $A2780^{cisR}$ cell line. Moreover, the results showed that Cis alone and LH5 alone caused greater damage to DNA than all the selected combinations investigated in the present study. Thus, it could not be concluded that the synergy from the combinations of Cis with Camp in the $A2780^{cisR}$ cell line was due to greater DNA damage.

Rather, it can be concluded that cytotoxicity of the drugs is not a direct result of DNA damage when both binding nature and extent of binding with DNA are believed to have a greater impact on recognition of the downstream proteins that are believed to be

involved in the signalling mechanisms associated with cell survival or apoptotic cell death.

4.4 Study on cellular accumulation

The entry of drugs into cells is the prerequisite for exerting their pharmacological effect. The access of platinum inside the cell is the key determinant for the anticancer activity of platinum drugs. Moreover, the increased efflux of platinum is one of the primary mechanisms for resistance to platinum drugs. It has been assumed that observed synergy from the combination study could be due to increased cellular accumulation of platinum and antagonism is from the opposite.

The present study was conducted with three platinum drugs alone (Cis, LH5 and Oxa) and their selected combinations in the A2780, A2780^{cisR}, HT-29 and Lim-1215 cell lines to find the association between combined drug action and cellular accumulation of platinum. Twelve combinations were selected for the A2780 and A2780^{cisR} cell lines; three combinations were selected for the HT-29 cell line; and six combinations were selected for the Lim-1215 cell line. However, the study could not find any definite correlation between the combined drug action and cellular accumulation of platinum in any of the studied cell lines. In some instances, synergistic combinations demonstrated a greater cellular accumulation of platinum compared to that from platinum drug administered alone; e.g., the synergistic combination of LH5 with Camp at the 4/0 sequence of administration displayed a greater accumulation of platinum than LH5 administered alone in the Lim-1215 cell line. In contrast, the synergistic combination of Gem and Cis at the 0/4 sequence of administration displayed a lower accumulation of platinum than Cis administered alone in the A2780^{cisR} cell line. Likewise, the antagonistic combination of Cis with Camp for 4/0 sequence of addition showed a

greater accumulation of platinum than Cis administered alone in the A2780 cell line. To the contrary, the antagonistic bolus administration of LH5 with Camp demonstrated a lower accumulation of platinum, compared to LH5 administered alone in the A2780 cell line. When the study was conducted with additive combinations, similar phenomena were observed. The additive bolus combination of LH5 with Oxa displayed a greater accumulation of platinum than Oxa/LH5 administered alone. The amount was even greater than that found in LH5 alone and Oxa alone. However, additive combinations of Cis with Camp at the 0/4 sequence of addition showed a lower platinum accumulation than Cis administered alone in the A2780 cell line. Thus, it can be seen that combined drug actions obtained from the selected platinum drug combinations in the tested cell lines were not solely dependent on total platinum contents inside the cell.

4.5 Platinum-DNA binding study

Platinum drugs generally exert their antitumour activity through their interactions with DNA. Thus, it is rational to assume that combined drug actions obtained from the selected combinations, involving a platinum drug as a component, may be associated with the extent of Pt-DNA binding. Similar to the cellular accumulation study, three platinum drugs (Cis, LH5 and Oxa) and their selected combinations were investigated in four cell lines (A2780, A2780^{cisR}, HT-29 and Lim-1215).

The synergistic combination in A2780 cell line showed increased platinum–DNA binding compared to that of the platinum drug alone, giving support to the idea that cell kill is linked to platinum–DNA binding. In contrast, antagonistic and additive combinations in the A2780 cell line did not follow any definite trend. Antagonistic combinations of Cis with Camp at 0/0 and 4/0 sequences; Cis with LH5 at 0/0 and 0/4

sequences and LH5 with Oxa at a 4/0 sequence of administration, exhibited a greater level of platinum–DNA binding compared to that from platinum drug administered alone in the A2780 cell line. In contrast, other antagonistic combinations (LH5 with Camp at 0/0, 0/4 and 4/0; LH5 with Oxa at 0/0) displayed lower platinum-DNA binding than the platinum drug administered alone in the A2780 cell line.

In the A2780^{cisR} cell line, two synergistic combinations (Cis with Camp at 0/0 and 4/0) demonstrated a higher platinum-DNA binding than the platinum drug administered alone in the A2780^{cisR} cell line, showing a direct relationship between increased cell kill and extent of platinum–DNA binding. However, synergistic combinations of Cis with Camp for 0/4 sequence of administration and LH5 with Camp for 4/0 sequence of administration showed a lower platinum–DNA binding than from platinum drugs administered alone in the A2780^{cisR} cell line, indicating that the sequence of administration is a key determinant of the combined drug action. In particular, the results indicate that the administration of Cis four hours after the administration of Camp fails to enhance platinum action towards the cell kill. This decreased level of platinum–DNA binding is not unexpected because there is less time available for platinum–DNA binding.

Four antagonistic combinations showed higher platinum-DNA binding and two antagonistic combinations produced lower platinum–DNA binding than that from platinum drugs administered alone in the A2780^{cisR} cell line. A similar variation of response in the extent of platinum–DNA binding from different combinations also followed in the colorectal cancer models. It can thus be concluded from the present study that synergy from combinations of different drugs is disproportionately related to platinum-DNA binding.

The absence of a direct relationship between cytotoxicity and platinum-DNA binding is not uncommon. For example, oxaliplatin showed a lesser extent of platinum-DNA binding than cisplatin in several previous studies and in the present study (Faivre, Chan et al. 2003). But oxaliplatin is more cytotoxic than cisplatin, or at least equipotent in different cancers. In this study, it was found that LH5 demonstrated a greater extent of platinum-DNA binding, but it had a lower cytotoxicity than oxaliplatin and cisplatin in the tested cell lines. The present study suggests the idea that it is the nature of platinum-DNA binding and not the extent of platinum-DNA binding that is more likely to be the key determinant in the antitumour activity of platinum drugs.

4.6 Proteomic

Proteomics have produced abundant datasets for potential diagnostic, predictive and therapeutic implications in cancer. The two basic technologies behind these studies in cancer cells are two-dimensional polyacrylamide gel electrophoresis (2D-PAGE) and mass spectrometry (MS). In the present study, the matrix-assisted laser desorption ionisation (MALDI)-MS technique was used to identify proteins believed to be linked to combined drug actions. Nine proteins were found from the study in the A2780 parent ovarian cancer cell line, which demonstrated a significant change in expression and was regarded to be linked with observed synergy/antagonism or additiveness. In contrast, 18 proteins were identified from the $A2780^{cisR}$ cell line and are considered to be important in regard to their observed combined drug actions.

On the basis of the molecular functions of the identified proteins from the A2780 cell line, they can be grouped into the following classes:

- Metastasis-related cytoskeletal proteins: Cofilin 1, actin cytoplasmic 1 and vimentin

- Enzymes: ATPase mitochondrial inhibitor, peroxiredoxin-1 and ATP synthase subunit beta
- Heat shock proteins: 60kDa and HSP 90-beta
- Protein synthesis-related proteins: Heterogeneous nuclear ribonucleoproteins C1/C2

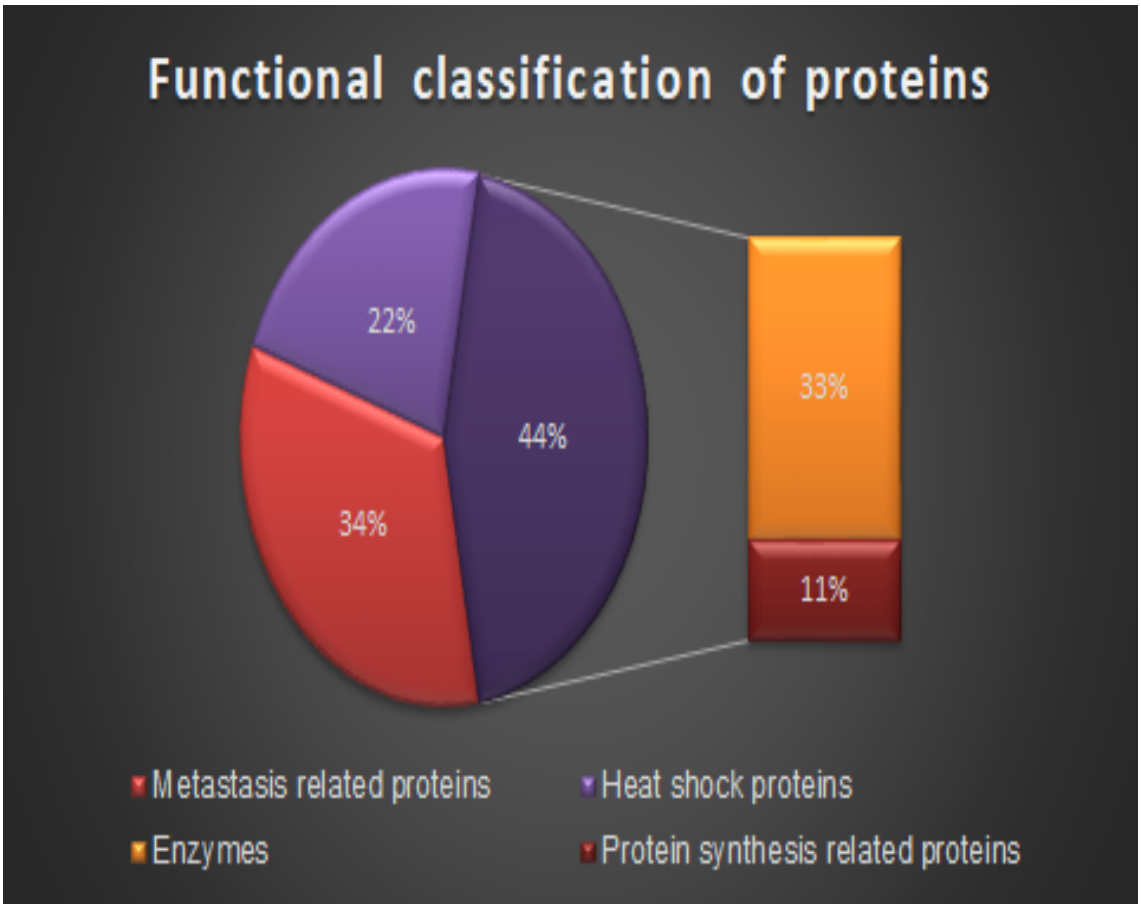

Figure 4.1: Functional classification of the proteins identified from the A2780 cells

The proteins identified from the A2780^{cisR} cell line have also been classified on the basis of their molecular functions, as follows:

- Metastasis-related cytoskeletal proteins: Cofilin 1, Tropomyosin alpha-4 chain, actin cytoplasmic 1, tubulin beta chain and vimentin

- Enzymes: peroxiredoxin-1, pyruvate kinase and peptidyl-prolyl Cis-trans isomerase A
- Heat shock proteins: stress-70 protein, nucleophosmin and heat shock protein HSP 90-beta
- Protein synthesis-related proteins: GTP-binding nuclear protein Ran, elongation factor 1-alpha, histone H4 and heterogeneous nuclear ribonucleoproteins C1/C2
- Calcium-binding proteins: annexin A1 and calmodulin-1

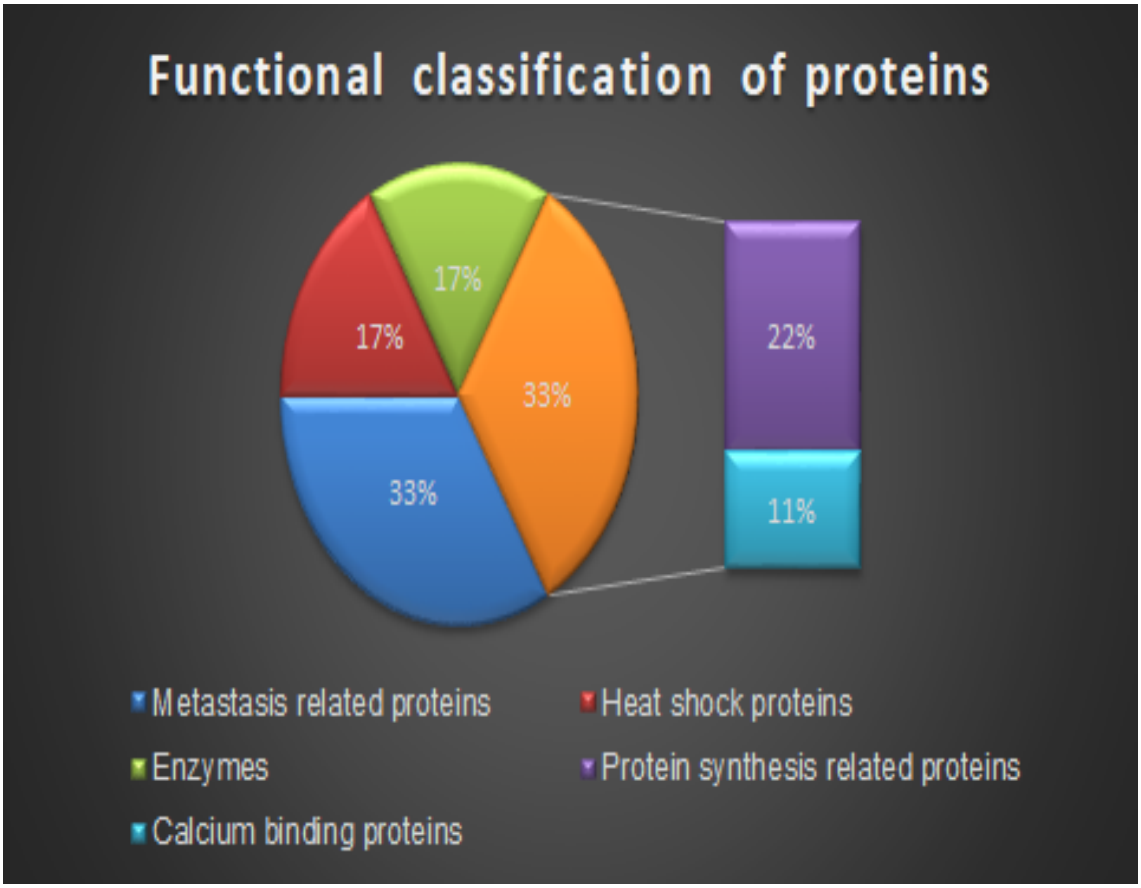

Figure 4.2: Functional classification of the proteins identified from A2780^{cisR} cells

It is evident from Figures 4.1 and 4.2 that most of the identified proteins belong to the metastasis-related cytoskeleton group, followed by enzymes and then heat shock proteins (molecular chaperones). Few other proteins fall into the protein synthesis-related class and calcium-binding class.

4.6.1 Cofilin 1

Cofilin 1 is a small protein of 18 kDa that can bind both monomeric actin (G-actin) and filamentous actin (F-actin). It is the most abundant protein, accounting for more than 90% of all expressed cofilins (Cofilin 1, Cofilin 2 and destrin). Cofiln 1 plays a significant role in the polymerisation and depolymerisation of actin filaments through severing the filaments. Assembly or disassembly of actin filaments is dependent upon the concentration of active Cofin 1 (a lower concentration discourages depolymerisation, whereas a higher concentration encourages polymerisation) (Shishkin, Eremina et al. 2016). Remodelling of the actin cytoskeleton is considered to be important in the invasion and metastasis of cancer cells. In addition, Cofilin1 has been linked with cytochrome-c mediated apoptosis. Upregulation of Cofilin 1 has been evidenced in pancreatic cancer, glioblastoma, colorectal cancer, lung cancer, breast cancer, oral cancer and ovarian cancer (Alam, Yu et al. 2020). However, downregulation of Cofilin 1 is also evidenced in lymphoma, hepatic, cervical and colon cancers (Alam 2018).

In the present study, Cofilin 1 was identified in both the A2780 (spot 13A) and $A2780^{cisR}$ cell lines (spot 8). The protein has demonstrated upregulation following treatments with Cis alone, Oxa alone and LH5 alone in the A2780 cell line. The highest upregulation was caused by LH5 alone (3.05 times), followed by Oxa alone (2.48 times). Antagonistic combined treatments of LH5 with Camp at the 0/0 sequence caused a downregulation of the protein in the A2780 cell line. However, two other antagonistic treatments did not change the expression of the protein significantly in the same cell line. Interestingly, the protein disappeared following both synergistic (Cis with LH5 at 4/0) and antagonistic (LH5 with Camp at 4/0) treatments in the A2780 cell line.

In the study of the A2780^{cisR} cell line, Cofilin 1 was upregulated after treatment with Cis alone and Oxa alone. However, the protein did not exhibit a significant change in expression after treatment with LH5 alone. In contrast, all combined treatments caused a downregulation of Cofilin 1 in the A2780^{cisR} cell line, except for LH5 with Oxa at the 4/0 sequence, which did not cause any significant change in expression of the protein. When the expression of Cofilin 1 in the untreated A2780^{cisR} cell line was compared to that found in the untreated-parent A2780 cell line, the protein was upregulated by one and a half. Further upregulation of the protein in the resistant cell line was observed following treatments with Cis alone and Oxa alone. But treatments with LH5 alone caused only partial restoration of the protein in the resistant cell line. All combined treatments, except LH5 with Oxa at the 4/0 sequence over-restored Cofilin 1 in the A2780^{cisR} cell line. It is not clearly understood why all types of combined treatments (additive LH5 with Camp at 0/0, synergistic LH5 with Camp at 4/0 and antagonistic LH5 with Oxa at 0/0) caused a downregulation of Cofilin 1 in the A2780^{cisR} cell line. The controversial behaviour of Cofilin 1 was also demonstrated in earlier studies in the host laboratory and elsewhere (Tsai, Lin et al. 2015; Bali 2018). The authors proposed that the elevated expression of Cofilin 1 may cause cell cycle arrest, but does not encourage apoptosis.

4.6.2 Tropomycin alpha-4 chain

Tropomyosin is a key structural element of a cytoskeletal microfilament, which possesses four isoforms in mammals: Tropomyosin 1, Tropomyosin 2, Tropomyosin 3 and Tropomyosin 4. The Tropomyosin alpha-4 chain is found to be predominantly involved in the contraction of smooth and skeletal muscle cells, promotion of neurite branching and the maintenance of cytoskeletal stability in non-muscular cells. The

aberrant expression of the Tropomycin alpha-4 chain was associated with several cancer types; e.g., lung, breast, esophageal, ovarian, cervical and prostate (Yang, Zheng et al. 2018). In some cancers (breast, esophageal and ovarian), the upregulation of the Tropomyosin alpha-4 chain was detected, compared to the levels found in normal cells (Jazii, Najafi et al. 2006; Sahab, Man et al. 2010; Tang, Beer et al. 2013). However, the converse is true for other types of cancers (cervical and lung), where a reduced level of the protein was observed (Kopantzev, Monastyrskaya et al. 2008; Lomnytska, Becker et al. 2011).

In the present study, Tropomyosin alpha-4 chain was detected in only the $A2780^{cisR}$ cell line, as spot number 21. The protein was upregulated following treatment with Oxa alone, but did not show any significant change in expression following treatments with Cis alone and LH5 alone. All types of selected combined treatments caused a downregulation of the Tropomyosin alpha-4 chain, except for the antagonistic combined treatment of LH5 and Oxa at a 4/0 combination, where no meaningful change in expression of the protein was observed. Additive combination treatment of LH5 with Camp at a 0/0 sequence of administration demonstrated highest downregulation of the protein, followed by antagonistic combined treatment of LH5 with Oxa at 0/0 administration. The synergistic combined treatment of LH5 with Camp at 4/0 also caused a downregulation of the Tropomyosin alpha-4 chain, but to a lesser extent than in the antagonistic and additive treatments. The Tropomyosin alpha-4 chain exhibited upregulation by 1.4 times in untreated $A2780^{cisR}$ cell line, compared to the level found in untreated A2780 cell line. Further upregulation of the protein was evidenced following the treatments with Oxa alone and LH5 alone, while treatments with Cis alone caused partial restoration of the Tropomyosin alpha-4 chain in the $A2780^{cisR}$ cell line. Strangely, all types of combined drug treatments (additive, synergistic and

antagonistic) demonstrated over-restoration of the protein in the A2780^{cisR} line. On balance, the Tropomyosin alpha-4 chain is considered to be an anti-apoptotic in action protein in the A2780^{cisR} line.

4.6.3 Actin, cytoplasmic 1

The actin family of proteins is abundant in all eukaryotic cells and serves many vital functions, including: cell motility, control of cell shape, adhesion of cells, signal transduction, wound healing, immune response, embryonic development, gene transcription and muscle contraction. Among the six isoforms of actin, beta and gamma, cytoplasmic actins are found in almost all cell types and are indispensable to the survival of cells. Actin, cytoplasmic 1 is also known as beta actin, which has previously been considered to be a reference gene, but now such usage has been challenged. Beta actin plays an important role in nvasiveness and metastasis of cancer cells and an altered expression of the protein has been evidenced in many types of cancer, including: liver, skin, kidney, colon, gastric, pancreatic, breast and ovarian (Guo, Liu et al. 2013).

In the present study, beta actin was identified in both the A2780 (spot 33A) and A2780^{cisR} cell lines (spot 37). The protein was upregulated following treatment with Cis and Oxa alone, but remained unchanged following treatment of LH5 alone in the A2780 cell line. Treatment with an antagonistic combination of Cis with Camp using 0/0 sequence caused the upregulation of beta actin, although treatment with another antagonistic combination of LH5 with Camp at 4/0 caused its downregulation. However, treatment with two other antagonistic combinations did not cause significant change in expression of the protein. Treatment with a synergistic combination of Cis with LH5 at 4/0 caused the upregulation of beta actin in the A2780 cell line.

Beta actin did not display significant changes in expression following all single and combined drug treatments, except with Oxa alone in the A2780^{cisR} cell line. When the expression of beta actin was compared in the untreated-parent and untreated-resistant cell lines, beta actin demonstrated an upregulation by a factor of 1.7 in the A2780^{cisR} cell line. The protein was further heightened in expression in the A2780^{cisR} cell line after treatment with Cis alone, LH5 alone and the synergistic combination of LH5 with Camp using 4/0 sequence. All other single and combined treatments caused a partial restoration of the protein in the resistant cell line. The variation in the expression of actin, cytoplasmic 1, following various drug treatments, made it problematic to find a clear relationship between the nature of the protein and its action on the cancer cells.

4.6.4 Tubulin beta chain

Microtubules are polymers of alpha- and beta-tubulin heterodimers. After the polymerisation process, a hollow cylindrical microtubule is formed, having one end containing alpha tubulin and the other end, beta tubulin. Microtubules demonstrate GTP-dependent dynamic instability by growing or shortening their length through the addition or deletion of alpha- or beta-tubulin subunits (Edelman and Shvartsbeyn 2012). Among the nine isoforms of beta tubulin, the tubulin beta chain is one of the isoforms that is responsible for mitosis and intracellular transport (Nogales, Wolf et al. 1998). Dysregulated expression of the tubulin beta chain is evident in various solid cancers and recognised to be a potential cause for resistance to chemotherapy. The elevated expression of beta tubulin was observed in colorectal cancer, breast carcinoma and oesophageal carcinoma (Alam, Yu et al. 2020).

In the present study, the tubulin beta chain was detected in the A2780^{cisR} cell line as spot number 45, which was downregulated by 4.09 times following treatment with Oxa

alone. However, the protein did not show significant changes in expression following treatments with Cis alone and LH5 alone. Moreover, none of the selected combined treatments showed significant changes in expression of the tubulin beta chain, except for in the antagonistic combined treatment of LH5 with Oxa at 4/0, which demonstrated an upregulation.

The tubulin beta chain has displayed more downregulation in the untreated A2780^{cisR} cell line than in the level of expression found in the untreated A2780 cell line. Following treatments with Cis alone and LH5 alone, the protein exhibited over-restoration in the A2780^{cisR} cell line. However, treatment with Oxa alone caused further downregulation of the protein in the same cell line. Interestingly, all types of combinations (additive, synergistic and antagonistic) caused further downregulation of the protein in the A2780^{cisR} cell line, which did not allow for ascertainment of the nature of the protein in the present study. Similar to our findings, the variation of response of the Tubulin beta chain, following different combined treatments, was evident in a previous study in the host laboratory (Bali 2018).

4.6.5 Vimentin

Vimentin is a type III intermediate filament that is predominantly observed in mesenchymal cells. The primary function of vimentin is to provide mechanical and structural support to the cells, as well as to maintain the integrity of a cell. Moreover, the protein plays an important role in the adhesion and migration of cells, cellular survival and signalling mechanisms, wound healing, as well as lipid metabolism (Alam 2018). Vimentin also serves a purpose in the metastasis of cancer cells by playing a key role in the epithelial-to-mesenchymal transition (EMT) process. The expression of vimentin is believed to be the established biomarker that distinguishes between

metastatic and non-metastatic breast cancers. Earlier studies reported the upregulation of vimentin in various cancers, including: prostate carcinoma, ovarian carcinoma, lung carcinoma and gastric carcinoma (Alam 2018).

In the present study, vimentin was identified in both the parent A2780 ovarian cancer cell line as well as in the A2780^{cisR} cell line as spot numbers 43A and 48, respectively. In the parent A2780 cell line, the protein was found to be downregulated by 1.88 times following treatment with Cis alone and no significant change in expression was observed after treatments with Oxa alone and LH5 alone. Two antagonistic treatments (Cis with Camp at 0/0 and Cis with LH5 at 0/0) caused an upregulation of vimentin and no significant change of the protein was observed with the synergistic treatment of Cis with LH5 at 4/0. In the A2780^{cisR} cell line, vimentin showed an upregulation of 2.33 times after treatment with LH5 alone and no significant change in expression was observed after treatments with Cis alone and Oxa alone. Among the combined treatments, only the antagonistic combination of LH5 with Camp at 0/4 caused an upregulation of vimentin. No other combinations [LH5 with Camp (0/0), LH5 with Camp (4/0), LH5 with Oxa (0/0) and LH5 with Oxa (4/0)] showed a significant change in the expression of vimentin. When the expression of vimentin was compared in the untreated-parent and untreated-resistant cell lines, the protein demonstrated an upregulation by 1.82 times in the A2780^{cisR} cell line. On balance, vimentin is seen to be an apoptotic protein in ovarian cancer cell lines.

4.6.6 Peptidyl-prolyl Cis-trans isomerase A

Cyclophilins are ubiquitous proteins that show peptidyl-prolyl isomerase activity and catalyse the isomerisations of peptide bonds. Through isomerisation reactions, the transformation of peptide bonds convert into a Cis form at proline residues and thus

expedite protein folding (Nigro, Pompilio et al. 2013). Among the several types of cyclophilins discovered, only seven types (cyclophilin A, cyclophilin B, cyclophilin C, cyclophilin D, cyclophilin E, cyclophilin 40 and cyclophilin NK) are found in humans. The alternative name for cyclophilin A is Peptidyl-prolyl Cis-trans isomerase A (PPIA), which is an 18 kDa low-molecular weight protein composed of 165 amino acids. PPIA serves many important functions in cells, including: trafficking, folding and assembly of proteins and the intonation of immune system and cellular signalling. Moreover, PPIA is also involved in cellular proliferation, migration and differentiation. The elevated expression of PPIA has been reported in cancers of various organs; e.g., lung, liver, pancreas, colon, endometrium, oesophagus, and skin (Alam, Yu et al. 2020).

In the present study, PPIA was identified in the A2780^{cisR} cell line as spot number 6, which was upregulated following treatment with Oxa alone and disappeared following treatment with Cis alone. Treatment with LH5 alone did not cause any significant change in the expression of PPIA in the A2780^{cisR} cell line. All antagonistic combined treatments caused an upregulation of the protein in the A2780^{cisR} cell line. The synergistic combined treatment of LH5 with Camp at 4/0 caused the disappearance of PPIA in the A2780^{cisR} cell line, which could have occurred due to extreme downregulation. The expression of the protein was also absent following the additive combined treatment of LH5 with Camp at 0/0 in the A2780^{cisR} cell line. When the expression of PPIA was compared in the untreated-parent and untreated-resistant cell lines, the protein demonstrated a downregulation of 1.52 times in the A2780^{cisR} cell line. The protein was fully restored following treatment with Oxa alone and partially restored following treatment with LH5 alone in the A2780^{cisR} cell line. Following antagonistic combined treatments, the PPIA level was over-restored in the A2780^{cisR} cell line. However, the spot disappeared after synergistic and additive treatments. From

the above discussion, it can be concluded that PPIA may be an anti-apoptotic protein in ovarian cancer. This finding is supported by earlier reports from the host laboratory and elsewhere (Mikuriya, Kuramitsu et al. 2007; Alam 2018).

4.6.7 Pyruvate kinase

An emerging hallmark of cancer is 'altered energy metabolism', which is characterised by an elevated glucose uptake and preferred glycolysis in oxygen presence, called aerobic glycolysis (also known as the Warburg effect). Numerous proteins, including pyruvate kinase, play significant roles in the growth and metabolic reprogramming of tumour cells. Pyruvate kinase regulates the process of glycolysis by catalysis, in the production of pyruvate and ATP from phosphoenolpyruvate and ADP. Four isozymes of pyruvate kinase have been discovered and these are: PKL, PKR, PKM1 and PKM2. Among the four isoforms, PKM2 has been found to commonly express in cancer cells and is also found to confer cancer cells of the glycolytic phenotype. Moreover, the protein is responsible for channelling the glycolytic intermediates to synthesise nucleic acids, amino acids and lipids that tumour cells need. Upregulation of PKM2 has been found in various neoplasias; e.g., lung cancer, breast carcinoma, prostate carcinoma, cervical cancer, renal cancer and colon cancer (Keller, Tan et al. 2012; Shang, He et al. 2017).

In the present study, pyruvate kinase was identified in A2780^{cisR} cell line as spot number 179. The protein disappeared following treatment with Cis alone and LH5 alone, possibly due to the extreme downregulation of the protein following the treatment. Treatment with Oxa alone also caused a downregulation of pyruvate kinase, but the change was less than 1.5 times. Following combined treatments, the synergistic

combinations of LH5 with Camp using 4/0 sequence of administration resulted in disappearance of the protein, due to extreme downregulation in the 2780^{cisR} cell line. The additive combined treatment of LH5 and Camp at the 0/0 sequence of administration also produced a downregulation of pyruvate kinase by 3.03 times. Two antagonistic treatments did not cause any significant change in its expression. It can be said from the above discussion that pyruvate kinase inhibitors could be designed to be new anticancer drugs.

This assumption was also reinforced by the expression of the protein in untreated-parent A2780 cell line was compared with that in untreated $A2780^{cisR}$ cell line. Pyruvate kinase was upregulated in untreated resistant cell line by 1.9 times that of the parent cell line. Over-restoration of the protein was observed following additive treatment and the protein disappeared following synergistic treatment in the $A2780^{cisR}$ cell line. Thus, it can be concluded that the overexpression of pyruvate kinase may result in a resistance to ovarian cancer that could be overcome by downregulating the protein. This inference is also supported by a previous study (Shang, He et al. 2017).

4.6.8 Peroxiredoxin 1

Peroxiredoxins are a family of non-seleno proteins that are primarily responsible for maintaining the redox homeostasis of cells in association with other enzymes. Peroxyredoxins use redox-active cysteines that transform into cellular thiols to reduce peroxides. According to the presence of cysteine residues, peroxyredoxins are classified into three sub-families: typical 2-cys-peroxiredoxins, atypical 2-cys-peroxiredoxins and 1-cys-peroxiredoxins. Typical 2-cys-peroxiredoxins were further grouped into four categories: peroxiredoxin 1, peroxiredoxin 2, peroxiredoxin 3 and peroxiredoxin 4 (Liu, Zhou et al. 2013). Peroxiredoxin 1 were originally identified as a scavenger of H_2O_2,

but it is now claimed to regulate the multiple functions of immunomodulation, regulation of the transcription and redox regulation. Overexpression of peroxiredoxin 1 was observed in pancreatic, oral, ovarian, oesophageal, thyroid and lung cancers (Kang, Rhee et al. 2005). However, the antitumour effect of peroxiredoxin 1 in breast cancer has also been well-established from several studies (Park, Jo et al. 2016).

In the present study, peroxiredoxin 1 was identified in both the parent A2780 cell line and the A2780^{cisR} cell line as spot numbers 17A and 12, respectively. In A2780 cell line, the protein was upregulated following treatment with Cis alone and Oxa alone, but treatment with LH5 alone caused its downregulation. The protein disappeared following treatment with synergistic combination of Cis with LH5 using 4/0 sequence of administration. However, different antagonistic combined treatments produced inconsistent results on the expression of peroxiredoxin 1 in the A2780 cell line. A similar inconsistency in the expression of peroxiredoxin was also evidenced from the study in the A2780^{cisR} cell line following treatments with different combinations (additive, synergistic and antagonistic). Thus, the role of peroxiredoxin 1 in ovarian cancer remained undetermined in the present study.

4.6.9 ATPase inhibitor mitochondrial

The ATPase inhibitor mitochondrial protein is also known as a natural inhibitor protein (IF1) which is basic in nature, has high thermal stability and is highly conserved. The protein consists of 106 amino acid residues in humans and is the principal regulator for ATP hydrolytic activity. Under ischaemic conditions, IF1 binds at the interface of the αE-βE subunits of ATP synthase, followed by sequential hydrolysis of two ATP. Consequently, IF1 becomes lured within two subunits, leading to enzyme inhibition. In addition to the established role of IF1, the inhibitor protein demonstrates key roles in

the normoxia, inhibition of cell apoptosis and the determination of cellular fate, in response to the reactive oxygen species. IF1 is also known to favour tumorigenesis by metabolic reprogramming via suppression of ATP synthesis and subsequent induction of the Warburg effect (Sgarbi, Barbato et al. 2018). Overexpression of IF1 in cancer cells, as compared to that found in untransformed cells, has been reported in colon cancer, breast cancer, ovarian cancer, lung cancer and hepatic cancer (Yin, Lu et al. 2015).

In the present study, the ATPase inhibitor mitochondrial protein was identified as spot number 3A in A2780 cell line. The protein was downregulated 1.56 times following treatment with Cis alone. The protein disappeared following treatment with Oxa alone and LH5 alone believed to be due to extreme downregulation. The protein also became extinct following treatment with synergistic combination of Cis with LH5 using 4/0 sequence of administration again assumed due to extreme downregulation. The protein remained unchanged following antagonistic treatments of Cis with Camp at 0/0 and LH5 with Oxa at 0/0 administration in the A2780 cell line. Thus, it can be said that the downregulation of the ATPase inhibitor mitochondrial protein can provide benefits in ovarian cancer. Designing analogues of the ATPase inhibitor mitochondrial protein could be an excellent strategy in overcoming cancer.

4.6.10 ATP synthase subunit beta

The ATP synthase enzyme is an essential element of the oxidative phosphorylation process, which is accountable for the production of ATP by using the electrochemical energy produced by the proton gradient across the inner mitochondrial membrane. Structurally, the ATP synthase enzyme can be divided into two major parts: F1 (causing oxidative phosphorylation) and Fo (responsible for oligomycin sensitivity). The three-

dimensional structure of ATP synthase mimics assembly of two motors having a shared common rotor shaft that is stabilized by a peripheral stator stalk. The F1 part of the ATP synthase enzyme is found to consist of different subunits: 3α, 3β, γ, δ and ε. The central stalk is composed of the γ, δ and ε subunits and the alternate arrangement of 3α and 3β forms a hexameric ring with a central cavity (Jonckheere, Smeitink et al. 2012). As cancer cells rearrange their energy metabolism by enhancing aerobic glycolysis (as a key pathway for the establishment of metabolic energy), the altered expression of ATP synthase (considered to be the core hub of oxidative phosphorylation) has been observed in many cells, compared with its expression in normal tissues (Esparza-Moltó and Cuezva 2018).

In the present study, ATP synthase subunit beta has been identified as spot number 38A in A2780 cell line. The protein was downregulated by 5.19 times and 1.5 times following treatments with Cis alone and Oxa alone in A2780 cell line. The protein disappeared completely following treatment with LH5 alone. Treatment with the synergistic combination of Cis with LH5 using 4/0 sequence also caused a downregulation of the ATP synthase subunit beta. In contrast, the antagonistic combination treatments caused either upregulation or no significant change in the expression of the protein in A2780 cell line. This study may be the first report to describe the association of the altered expression of ATP synthase subunit beta in ovarian cancer. The present study suggests that ATP synthase subunit beta could be anti-apoptotic in action. It is thought that further studies would be required to determine the exact nature of ATP synthase subunit beta.

4.6.11 Stress 70 protein, mitochondrial

There are two types of stress 70 proteins: mitochondrial (mortalin) and cytoplasmic. Mortalin plays an important role in the import and refolding of proteins present in the mitochondria, and in the protection of cells from glucose deprivation and serum deprivation. Moreover, the protein protects the cells from accumulation of reactive oxygen species and blocks apoptosis induction via p53 (Jubran, Kocsis et al. 2017). A positive correlation between mortalin expression and the clinical stage, perineural invasion, metastasis towards the lymph node and lower overall survival, has been detected in many patients. The elevated expression of mortalin has been found in many cancers including: pancreatic cancer (Cui, Li et al. 2017), cholangiosarcoma (Kang, Cai et al. 2017), ovarian cancer (Hu, Yang et al. 2016) and hepatocellular carcinoma (Cheng, Zhang et al. 2019).

In the present study, the protein was identified as spot number 60 in the $A2780^{cisR}$ cell line. However, no significant change in expression of mortalin was observed after drug treatment alone (Cis, Oxa and LH5). Interestingly, none of the combined treatments (either additive/synergistic or antagonistic) caused significant change in expression of mortalin. However, the protein was downregulated by 1.92 times more in untreated $A2780^{cisR}$ cell line than in untreated A2780 cell line. It could be interpreted from the study that the mechanism of selected combinations (additive LH5 with Camp at 0/0; synergistic LH5 with Camp 4/0; antagonistic LH5 with Camp 0/4; antagonistic LH5 with Oxa 0/0 and antagonistic LH5 with Camp 0/4) might not be related to the expression of mortalin. Moreover, mortalin may not be associated with cisplatin resistance in the A2780 cell line.

4.6.12 Nucleophosmin

Nucleophosmin is one of the four members of the nucleophosmin/nucleoplasmin family. It is mostly located in the nucleoli, but it can undergo nucleocytoplasmic shuttling. The N-terminal chain of the folded nucleophosmin molecule is arranged into eight antiparallel beta-strands. Five nucleophosmin molecules are connected in a complex, with an uneven charge distribution and negative-charge buildup on one side of the pentamer. In contrast, the C-terminal chain encompasses residues that are basic in nature, thus causing accumulation of a positive charge at this area that is responsible for binding to nucleic acids, ATP and ribonuclease activity (Brodská, Šašinková et al. 2019). Nucleophosmin is involved in many cellular activities, such as duplication of centrosome, maturation and biogenesis of rRNA, DNA repair and chaperone activity. The elevated expression of nucleophosmin has been evidenced in many solid tumours; e.g., prostate, liver, thyroid, glioma, colon, gastric and pancreatic cancers (De Cola, Franceschini et al. 2018).

In the present study, the protein was identified as spot number 100 in $A2780^{cisR}$ cell line. Nucleophosmin was upregulated by 3.95 times after treatment with LH5 alone in $A2780^{cisR}$ cell line but remained unchanged following treatment with Cis alone and Oxa alone. The additive treatment of LH5 with Camp at 0/0 and the synergistic treatment of LH5 with Camp at 4/0 caused a downregulation of nucleophosmin, while antagonistic treatments caused an upregulation of nucleophosmin. It can be inferred from the present study that the downregulation of nucleophosmin provided benefits in ovarian cancer. Attempts can be made to design inhibitors of nucleophosmin as new anticancer drugs. Earlier studies also claimed that nucleophosmin demonstrated an anti-apoptotic nature in colorectal cancer (Zhao, Liu et al. 2007; Bali 2018).

4.6.13 60 kDa heat shock protein

Heat shock proteins are the oldest defense system in all living entities with elevated expression under stressed conditions; e.g., infections, increased temperatures, radiation, heavy metals, ethanol and oxidants. Heat shock proteins have been divided into different families, depending on their molecular weight, including: 27KDa proteins (HSP27), 70KDa proteins (HSP70), 60 KDa proteins (HSP60) and 90KDa proteins (HSP90). Among these, HSP60 is mostly present in the mitochondrial matrix and the outer mitochondrial membrane of all mammalian cells. In combination with HSP70, it acts as a chaperone and provides support in the correct folding of newly synthesised proteins (Kimura, Enns et al. 1993; TEKKEŞİN, Mutlu et al. 2011). Moreover, HSP60 may induce apoptosis via the caspase-dependent pathway inside the mitochondria, where an association between the HSP60/HSP10 complex and pro-caspase-3 takes place and, consequently, HSP60 is released into the cytoplasm. Upregulation of HSP60 has been observed in various tumours such as breast carcinoma, bowel cancer, bronchial tumour, ovarian carcinoma, prostate and cervical cancers (Hwang, Lee et al. 2009).

In the present study, HSP60 was identified in A2780 cell line as spot number 41A. All single drug treatments caused an upregulation of the protein, where the highest upregulation was produced following the treatment with LH5 alone. Among the combined treatments, the synergistic combination of Cis with LH5 at 4/0 caused an upregulation of the protein of 1.58 times. However, the antagonistic combination of Cis with Camp at 0/0 also caused an upregulation of HSP60 of 4.07 times. In contrast, the antagonistic combination of Cis with LH5 at 0/0 caused a downregulation of the protein of 2 times. But two other selected antagonistic treatments (LH5 with Oxa at 0/0 and LH5 with Camp at 4/0) did not change the expression of HSP60 significantly. Due to the variations in response, in regard to the expression of HSP60 following different

drug treatments in combination, the exact role of the protein remained unclear. At least it can be assumed that combined drug actions of the selected combinations might not be associated with the expression of HSP60.

4.6.14 HSP 90 beta

Heat shock protein 90 (HSP90) is a molecular chaperone that is believed to facilitate stabilisation and activation of about 350 different client proteins; e.g., HER2, EGFR, BRAF, AKT, HIF-1α, STAT-3, etc. HSP90 is an ATP-dependent molecule that possesses intrinsic ATPase activity, which serves in protein folding, protein trafficking and client protein maturation. Several client proteins controlled by HSP90 are known to be oncogenic and contribute to important tumorigenic properties, including: angiogenesis, metastasis, resistance and cell death. Overexpression of HSP90 has been evidenced in many cancers; e.g., ovarian, colorectal, gastric, breast, lung and endometrial cancers (Wu, Liu et al. 2017). Recent studies have proved that HSP90 inhibitors can be developed as promising anticancer agents. Inhibition of HSP90 affects the complex network of key signalling molecules and pathways. For example, HSP90 suppression can inhibit the HIF-1α and STAT-3 expressions in tissue samples taken from rectal cancer patients (Shaib, Nagaraju et al. 2019). Moreover, the pharmacologic inhibition of HSP90 disrupts the ATP-driven chaperone cycle leading to the ubiquitin-mediated proteasomal degradation of client proteins (Samant, Clarke et al. 2014).

In the present study, HSP90 was identified in both parent A2780 and resistant A2780^{cisR} cell lines as spot number 54A and 111, respectively. It can be seen from the study that the protein is downregulated following treatment with Cis alone by 1.91 times in A2780 cell line. Synergistic combined treatment of Cis with LH5 caused a downregulation of HSP90 by 4.7 times in the A2780 cell line. Oxa alone, LH5 alone and antagonistic

combined treatments did not produce a significant change in the expression of HSP90. As the synergistic combination caused a greater downregulation of HSP90 than with single drug treatment and antagonistic combinations did not cause a significant change in expression of the protein, it can be concluded that the inhibition of HSP90 is an excellent strategy to treat ovarian cancer. However, cisplatin resistance in A2780^{cisR} cell line might not be associated with changes in expression of HSP90 because the protein was downregulated in the untreated A2780^{cisR} cell line and, after different combined treatments, an inconsistent outcome was evidenced.

4.6.15 Heterogeneous nuclear ribonucleoproteins C1/C2

Heterogeneous nuclear ribonucleoproteins (hnRNPs) represent a group of RNA-binding proteins with core responsibility being binding with new mRNA via RNA recognition motifs and regulation of the stability of mRNA. On the basis of structure and function, hnRNPs have been classified into several major subtypes: hnRNPs A/B family (hnRNP A1, hnRNP A2/B1, A18 hnRNP), hnRNP C1/C2, hnRNP K and hnRNP P2. Among the above-mentioned subtypes, HnRNP C1/C2 has been demonstrated to serve a key role in mRNA transcript packaging, splicing, mRNA stability and nuclear retention. HnRNP C1/C2 is usually found in the nucleoplasm although not in the nucleoli (Haley, Paunesku et al. 2009; Hope and Murray 2011). From several studies, it has been established that hnRNP C1/C2 coordinates the DNA damage response and radiation-induced apoptosis pathways. Moreover, an elevated expression of hnRNP C1/C2 has been observed in 30 lung cancer cell lines from an immunohistochemistry study (Pino, Pıo et al. 2003). Specifically, hnRNP C1 expression was greater than hnRNP C2 in the tested lung cancer cell lines.

In the present study, hnRNP C1/C2 was identified in both the A2780 and A2780^{cisR} cell line as spot number 32A and 33 respectively. The protein was downregulated following all single drug treatments in A2780 cell line. Treatment with Cis alone caused a downregulation of the protein by 4.25 times; treatment with Oxa alone caused a downregulation of 8.41 times and treatment with LH5 alone caused a downregulation of 1.98 times in the A2780^{cisR} cell line. In contrast, the variation in expression of hnRNP C1/C2 from different combined treatments in the A2780 cell line makes it difficult to determine the role of the protein in ovarian cancer.

The HnRNP C1/C2 protein has been downregulated by 4.25 times in untreated A2780^{cisR} cell line than that found in the untreated A2780 cell line. The protein was upregulated following treatment with Oxa alone (by 2.15 times) and LH5 (by 10.94 times) alone in A2780^{cisR} cell line; however, it was not detectable following treatment with Cis. Moreover, the synergistic combined treatment of LH5 with Camp at 4/0 also caused an upregulation of the protein by 4.08 times in the A2780^{cisR} cell line. It can be assumed that the downregulation of HnRNP C1/C2 could be associated with resistance in the A2780^{cisR} cell line; however, confirmation of this is required from further studies.

4.6.16 GTP-binding nuclear protein Ran

Ran is a G protein that belongs to the Ras superfamily of guanosine triphosphatases (GTPases). Ran cycles between sites and has an active GTP-binding state and an inactive guanosine diphosphate (GDP)-binding state that acts in various cellular processes, such as for the regulation of DNA replication, in the nucleocytoplasmic transportation of molecules through the nuclear pore complex and has control of cell divisions (mainly microtubule nucleation and spindle assembly) (Fan, Lu et al. 2013).

Increased Ran expression levels have also been found in soft tissue sarcoma, renal cancer, colon cancer, ovarian carcinoma and pancreatic cancer (Deng, Lu et al. 2013). Ran has been reported to be a promising anticancer drug target because silencing Ran expression induces more apoptosis in cancer cells than normal cells (Yuen, Chan et al. 2012).

In the present study, Ran was identified in A2780^{cisR} cell line as spot number 16. The protein disappeared following treatment with Oxa alone and did not show any significant change in expression following treatment with Cis alone and LH5 alone. The synergistic combined treatment of LH5 with Camp using 4/0 sequence of administration also did not change the expression of Ran significantly. Following different antagonistic combined treatments, Ran demonstrated a variation in expression (upregulation, downregulation and no change) in the A2780^{cisR} cell line. The results of the present study indicate that combined drug actions of the selected combinations might not be related to the expression of Ran.

4.6.17 Elongation factor 1-alpha

Eukaryotic elongation factor 1 alpha (eEF1A) is found to play vital role in the process of protein synthesis. The two isoforms of eEf1A are eEF1A1 and eEF1A2, which share a >90% sequence identity and have the same function in mRNA translation and markedly different expression patterns in mammals (Yang, Lu et al. 2015). Although eEF1A1 is found in nearly all tissues, except in skeletal muscle, eEF1A2 is expressed only in a few organs: muscle tissues, brain, heart and aorta. EEF1A proteins bind and hydrolyse GTP and catalyse the association of tRNAs to ribosome during protein elongation. Also, EEF1A proteins, from different sources, bind to F-actin and

depolymerise α-tubulin microtubules. The characteristics are in line with the idea that proteins play key roles in the regulation of cytoskeletal organisation. The eEF1A ability to modulate cell growth and apoptosis links it to cancer. The altered expression of eEF1A has been associated with the development and invasion of cancer into the prostate, lungs, liver, ovaries, stomach, breasts and pancreas (Yang, Lu et al. 2015).

In the present study, the elongation factor 1 alpha protein has been identified as spot number 42 in A2780^{cisR} cell line. The protein was downregulated by 4.53 times following treatment with Cis alone and by 1.83 times following treatment with LH5 alone. However, treatment with Oxa alone did not change the expression of the protein significantly. Following additive and synergistic combined treatments, the protein disappeared, which could be due to extreme downregulation. However, antagonistic combined treatments also caused a downregulation of eEFA1, but to a lesser extent, when compared to synergistic and additive treatments. The protein was upregulated by 2.85 times in untreated A2780^{cisR} cell line, compared to the level observed in the untreated parent A2780 cell line. The protein was over-restored following treatment with Cis alone and partially restored following treatment with Oxa alone and LH5 alone. Additive and synergistic combined treatments caused disappearance of the protein in A2780^{cisR} cell line. Therefore, it can be assumed from the present study that elongation factor 1 alpha may be responsible for cisplatin resistance in A2780^{cisR} cell line. The downregulation of elongation factor 1 alpha is beneficial in treating ovarian cancer as well as in overcoming cisplatin resistance.

4.6.18 Histone H4

Histone H4 is a core protein of nucleosome that forms chromatin in combination with H2A, H2B and H3. Histone H4 can undergo acetylation and methylation during the

regulation of gene transcription and also phosphorylation at the S1 cell cycle phase during mitosis (Chou, Wang et al. 2014). Cancer cells had loss of histone H4 monoacetylated and trimethylated forms, in comparison with normal cells. Moreover, the elevated expression of histone deacetylases was observed in various types of cancer (West and Johnstone 2014). Currently, inhibitors of histone deacetylases are being designed to be anticancer agents and entered into clinical trials (Dung, Dung et al. 2017) . In addition, methylation at K5 of histone H4 has been reported to be involved in cancer.

In the present study, histone H4 has been identified as spot number 76 in $A2780^{cisR}$ cell line. Expression of the protein was found to decrease after treatment with Cis alone by 3.39 times and no significant change was observed following treatments with Oxa alone and LH5 alone. The synergistic combined treatment of LH5 with Camp at 4/0 also a caused downregulation of the protein. Additive and most antagonistic treatments did not produce any significant change in expression of histone H4. Compared to expression of histone H4 in untreated-parent A2780 cell line, the protein exhibited upregulation by 1.41 times in untreated $A2780^{cisR}$ cell line. Following treatment with Cis alone, the protein was over-restored in $A2780^{cisR}$ cell line. Synergistic combined treatment of LH5 with Camp at 4/0 also over-restored the protein. Therefore, it can be proposed that histone H4 could act as an anti-apoptotic protein in ovarian cancer. Upregulation of histone H4 may be associated with cisplatin resistance in $A2780^{cisR}$ cell line. The downregulation of histone H4 could be a new strategy of cancer treatment.

4.6.19 Calmodulin-1

Calmodulin is considered to be the primary supervisor of Ca^{2+}-dependent signalling in all eukaryotic cells. The protein is highly conserved during evolution and ubiquitously

distributed in all cells. Initially, the protein was discovered to be a cyclic nucleotide phosphodiesterase. It can interact with a wide range of target proteins and modulate their activity in several ways. Calmodulin-1 is considered to serve various functions, including: cytoskeletal architecture and function, cell proliferation, cell motility, apoptosis, autophagy, maintenance of homeostasis, folding of proteins, regulation of osmosis, muscle contraction and gene expression (Berchtold and Villalobo 2014). Moreover, Ca^{2+}-calmodulin pathways are strongly linked to the proliferation and survival of different types of tumour cells (Stanislaus, Bakhtiar et al. 2012). Several antagonists of calmodulin have been designed to be anticancer agents and have demonstrated significant potential. Among 20 members of the calmodulin family, calmodulin-1 is the most prominent. However, no report has been found in the literature regarding the involvement of the calmodulin 1 protein, specifically in cancer.

In the present study, calmodulin-1 has been identified as spot number 120 in $A2780^{cisR}$ cell line. The protein underwent decrease in expression after treatment with Oxa alone and did not show a significant change in expression following treatment with Cis alone. Treatment with LH5 alone caused disappearance of the protein in $A2780^{cisR}$ cell line, possibly due to extreme downregulation. The synergistic combined treatment of LH5 with Camp at 4/0 caused the highest downregulation (8.51 times) of the calmodulin-1 protein. The protein was upregulated by 1.77 times in untreated $A2780^{cisR}$ cell line, compared to the expression observed in the parent A2780 cell line. It has been proposed that calmodulin-1 acts as an anti-apoptotic protein in ovarian cancer. The elevated expression of calmodulin-1 could have a role in developing cisplatin resistance in ovarian cancer. Designing antagonists of calmodulin-1 may be a strategy used in treating ovarian cancer, as well as for combatting resistance.

4.6.20 Annexin A1

Annexin A1 is the predominant member of the Annexin superfamily, that was initially identified to be a glucocorticoid-regulated anti-inflammatory protein that plays a vital role in adaptive and innate immune responses. The protein, Annexin A1, can exist either as a secreted extracellular protein (cleaved) or intracellular protein (full-length). Annexin A1 is a 37 kDa protein, composed of 346 amino acids. The N-terminal region of the protein is known as the regulatory part, which is responsible for phosphorylation and proteolysis (Alam 2018). In addition to its role in inflammation, Annexin A1 has also been found to play a role in tumorigenesis; i.e., cellular proliferation and differentiation, apoptosis, cellular migration and invasion. Initially, Annexin A1 was considered to be a diagnostic or prognostic biomarker in cancer, due to its differential expression between normal and cancerous tissue samples. But controversial expressions of Annexin A1 in different types of cancers raise the question: whether it is a blessing or a curse in cancer (Foo, Yap et al. 2019).

In the present study, Annexin A1 has been identified as spot number 99 in $A2780^{cisR}$ cell line. The protein was upregulated following treatment with Oxa alone and downregulated following treatment with LH5 alone in $A2780^{cisR}$ cell line. In contrast, no significant change in expression of Annexin A1 was found following treatment with Cis alone. Similarly, a variation in the response of Annexin A1 expression was also demonstrated following different combined drug treatments. Thus, it was not possible to ascertain the role of Annexin A1 in ovarian cancer from the present study.

Putting it all together in context

In the present study, nine proteins were identified from the A2780 parent ovarian cancer cell line that displayed a significant change in expression following selected treatments

[Cis alone, Oxa alone, LH5 alone, Cis and Camp in combination (0/0), Cis and LH5 in combination (0/0), Cis and LH5 in combination (4/0), LH5 and Oxa in combination (0/0) and LH5 and Camp in combination (4/0)] In contrast, 18 proteins were identified from A2780^{cisR} cell line that showed significant changes in expression following different treatments [Cis alone, Oxa alone, LH5 alone, LH5 and Camp in combination (0/0), LH5 and Camp in combination (0/4), LH5 and Camp in combination (4/0), LH5 with Oxa in combination (0/0) and LH5 and Oxa in combination (4/0)]. However, the total number of identified proteins was reduced to 20 after the elimination of exactly matched proteins from both cell lines. The significantly expressed identified proteins have been classified into different groups: metastasis-related cytoskeletal proteins (Cofilin 1, Tropomyosin alpha-4 chain, actin cytoplasmic 1, tubulin beta chain and vimentin); enzymes (ATPase mitochondrial inhibitor, peroxiredoxin-1, ATP synthase subunit beta, pyruvate kinase and peptidyl-prolyl Cis-trans isomerase A); heat shock proteins (60kDa heat shock protein, stress-70 protein, nucleophosmin and heat shock protein HSP 90-beta); protein synthesis-related proteins (GTP-binding nuclear protein Ran, elongation factor 1-alpha, histone H4 and heterogeneous nuclear ribonucleoproteins C1/C2); and calcium-binding proteins (annexin A1 and calmodulin-1). Among the above-mentioned proteins, six proteins have been suggested to be anti-apoptotic in ovarian cancer: peptidyl-prolyl Cis-trans isomerase A, pyruvate kinase, nucleophosmin, elongation factor -1 alpha, histone H4, ATP synthase subunit beta and calmodulin-1. Moreover, two proteins (ATPase inhibitor mitochondrial protein and vimentin) have been identified to be apoptotic proteins.

4.7 Bioinformatics

A Cox PH ratio analysis was performed using data on the RNASeq expression to estimate the survival curve. This was done using the product limit procedure. In addition, a log rank test for each of the studied genes was applied to discover any differences of statistical significance between the groups of altered and unaltered genes. From the univariate analysis, the identified five significant genes were ACTB, HIST1H4F, HNRNPC, HSP90AB1 and PKM. Among the mentioned five significant genes, altered expression of HIST1H4F has also been found to cause less survival of ovarian cancer patients compared to non-altered group in an earlier study conducted in the host laboratory (Arzuman, Moni et al. 2019). Similarly, downregulation of HNRNPC has been correlated with prolonged median disease-free survival in ovarian serous cystadenocarcinoma patients (Kleemann, Schneider et al. 2018). In an earlier study, silencing of PKM2 demonstrated improved efficacy of the clinically used anticancer ant against multidrug resistant ovarian cancer (Talekar, Ouyang et al. 2015). Moreover, overexpression of PKM2 demonstrated significant association with ovarian cancer ($p < 0.001$) and poor progression-free survival rates ($p = 0.01$) as compared with unaltered group patients (Chao, Huang et al. 2017). In a very recent network modeling analysis, it has been reported that downregulation of HSP90AB1 is responsible for worst survival outcome in ovarian cancer (Shahjaman, Jui et al. 2020). However, the use of ACTB as a reference gene in studies involving ovarian cancer has become questionable from the present study.

Eleven pathways have found to be associated with the identified genes from the ontology enrichment analysis through the Enrichr software tool. Among the associated pathways, most of the identified genes were linked with alcoholism, systemic lupus erythematosus and viral carcinogenesis. Although the present study demonstrates the

correlation between the identified genes and alcoholism, earlier analyses revealed no significant association between ovarian cancer and alcoholism (Kelemen, Bandera et al. 2013; Latino-Martel, Cottet et al. 2016). Likewise, earlier studies did not show any association between systemic lupus erythematosus and ovarian cancer (Tessier-Cloutier, Clarke et al. 2014; Mao, Shen et al. 2016). However, viral carcinogenesis has been correlated positively with the increased incidence of ovarian cancer (Ingerslev, Hogdall et al. 2017).

5 Conclusion

Cancer is considered to be the most dreadful disease of the current age and chemotherapy plays a significant role in combatting cancer. However, drug resistance and dose-limited toxicity are the main obstacles in the use of chemotherapeutic agents. Cancer relapse and the side effects of chemotherapy could be reduced by applying synergistic or additive combinations of chemotherapeutic agents. With that aim in mind, multiple tumour active compounds (cisplatin, oxaliplatin, LH5, gemcitabine, camptothecin and cucurbitacin B) have been combined in a binary mode using three different sequences (bolus, 0/4 h and 4/0 h) in the ovarian and colorectal cancer models in the present study. Several mechanistic studies have been attempted to identify the underlying mechanisms of combined drug actions.

From the antitumour activity study of individual drugs in the A2780 ovarian cancer cell line, the activity order was gemcitabine>cucrurbitacine-B>camptothecine>cisplatin>oxaliplatin>LH5. In the case of cisplatin resistance in the $A2780^{cisR}$ cell line, the activity order was gemcitabine>cucrurbitacin-B>camptothecin>oxaliplatin>cisplatin>LH5. In contrast, the activity order was camptothecin>gemcitabine>cisplatin>oxaliplatin>LH5 in the HT-29 and Lim-1215 colorectal cancer cell lines. A similar trend was observed in the Lim-2405 colorectal cancer cell line, being camptothecin>gemcitabine>oxaliplatin>cisplatin>LH5. Nine sets of drug combinations (Cis with LH5, Cis with Camp, LH5 with Camp, LH5 with Oxa, Gem with LH5, Gem with Cis, Gem with Oxa, Cuc with Cis and Cuc with LH5) were investigated for their combined drug actions in the ovarian and/or colorectal cancer models. Among the tested drug combinations, Cis, in combination with Camp, and Gem, in combination with Cis, at all added concentrations (ED_{50}, ED_{75} and ED_{90})

and all sequences of additions (bolus, 0/4 h and 4/0 h), proved to be beneficial in overcoming cisplatin resistance in the A2780^{cisR} ovarian cell line. Moreover, Gem, in combination with LH5, at all sequences of addition at the ED_{50} level, demonstrated an advantageous effect in overcoming cisplatin resistance in the ovarian cancer model. The 4/0 h addition of LH5 with Camp was also found to be helpful in overcoming cisplatin resistance in the ovarian cancer model. The combination of Cuc and Cis produced significant synergy in the A2780 ovarian cancer cell line. In the colorectal cancer models (HT-29 and/or Lim-1215 cell line), the combination of Cis with Camp; LH5 with Camp and Gem with Oxa, demonstrated dose- and sequence-dependent synergy.

The DNA interaction study revealed that LH5 caused the greatest damage to DNA among all the tested individual drugs. However, no correlation was observed between the selected combined drug actions and DNA damage. Moreover, the cellular accumulation of the platinum study also could not find any definite correlation between combined drug actions and the cellular accumulation of platinum in any of the studied cell lines. The Platinum-DNA binding study in the A2780 cell line revealed that synergistic combinations demonstrated an increased platinum-DNA binding than with the platinum drug alone. However, the antagonistic and additive combinations studied in the A2780 cell line did not follow any definite trend. In contrast, synergy from combinations of different drugs in the A2780^{cisR}, HT-29 and Lim-1215 cell lines demonstrated a disproportionate relationship with platinum-DNA binding.

The proteomic study identified 20 proteins from the A2780 and A2780^{cisR} cell lines that displayed significant changes in expression following drug treatments, either alone or in combination. The identified proteins have been classified into several categories; e.g., metastasis-related cytoskeletal proteins (cofilin 1, actin cytoplasmic 1, tropomyosin alpha-4 chain, tubulin beta chain and vimentin); enzymes (peroxiredoxin-

1, pyruvate kinase, peptidyl-prolyl cis-trans isomerase A, ATPase mitochondrial inhibitor and ATP synthase subunit beta); heat shock proteins (60kDa heat shock protein, stress-70 protein, nucleophosmin and HSP 90-beta heat shock protein); protein synthesis-related proteins (GTP-binding nuclear protein Ran, elongation factor 1-alpha, histone H4 and heterogeneous nuclear ribonucleoproteins C1/C2); and calcium binding proteins (annexin A1 and calmodulin-1). Among the above-mentioned proteins, peptidyl-prolyl cis-trans isomerase A, pyruvate kinase, nucleophosmin, elongation factor-1 alpha, histone H4, ATP synthase subunit beta and calmodulin-1, have been identified as being anti-apoptotic proteins in ovarian cancer in the present study. In contrast, the ATPase mitochondrial inhibitor protein has been identified as being an apoptotic protein.

A bio-informatics study was performed using The Cancer Genome Atlas data for ovarian cancer patients, considering genes corresponding to the 20 proteins discovered in the proteomic study. It has been found from the study that cancer patients with altered expressions of the ACTB, HST1H4F, HNRNPC, HSP90AB1 and PKM genes, had lower survival rates, in comparison with the control group. Eleven pathways have been identified in genes with corresponding proteins. The protein-protein interaction network created by the STRING software also revealed that target proteins have a direct link to the gold benchmark ovarian cancer biomarkers.

Future directions: As research is a continuous and enduring journey, the *in vitro* synergistic effect obtained from the combinations of different sets (i.e., Gem with LH5, LH5 with Camp and Cuc with Cis) could be investigated further, for activity and safety, using a suitable animal model. A Western blot analysis could be employed further to confirm the nature of the proteins (apoptotic or anti-apoptotic) discovered in the present study. The five genes identified as significantly associated with the survival of ovarian

cancer patients, from the bio-informatics part of the present study, could be used as applicants for further therapeutic drug discovery.

6 References

Abdullah, A., F. Huq, et al. (2003). "Studies on platinum (II) complexes of the forms: cis-PtL (NH." Journal of Inorganic Biochemistry **96**: 85.

Adami, H.-O., M. Lambe, et al. (1994). "Parity, age at first childbirth, and risk of ovarian cancer." The Lancet **344**(8932): 1250-1254.

Alam, M. (2018). "Studies on novel palladiums alone and in combination with phytochemicals in tumour models."

Alam, M. N., J. Q. Yu, et al. (2020). "Cisplatin in combination with emetine and patulin showed dose and sequence dependent synergism against ovarian cancer." Synergy **10**: 100060.

Alam, M. N., J. Q. Yu, et al. (2020). "Dose and Sequence Dependent Synergism from the Combination of Oxaliplatin with Emetine and Patulin Against Colorectal Cancer." Anti-Cancer Agents in Medicinal Chemistry (Formerly Current Medicinal Chemistry-Anti-Cancer Agents) **20**(2): 264-273.

Alamro, A. A. S. (2015). "Studies on combination between tumour active compounds in ovarian tumour models."

Alcindor, T. and N. Beauger (2011). "Oxaliplatin: a review in the era of molecularly targeted therapy." Current oncology **18**(1): 18.

Almoyad, M. (2018). "Synergism from combination of targeted therapy and phytochemicals in colorectal cancer."

Anwar, M. (2018). "Natural compounds in combination with platinum drugs administered to ovarian cancer models towards synergistic outcomes."

Arnold, M., M. S. Sierra, et al. (2017). "Global patterns and trends in colorectal cancer incidence and mortality." Gut **66**(4): 683-691.

Arzuman, L., P. Beale, et al. (2014). "Synergism from combinations of tris (benzimidazole) monochloroplatinum (II) chloride with capsaicin, quercetin, curcumin and cisplatin in human ovarian cancer cell lines." Anticancer research **34**(10): 5453-5464.

Arzuman, L., P. Beale, et al. (2015). "Combination of genistein and cisplatin with two designed monofunctional platinum agents in human ovarian tumour Models." Anticancer research **35**(11): 6027-6039.

Arzuman, L., P. Beale, et al. (2015). "Monofunctional Platinum-containing Pyridine-based Ligand Acts Synergistically in Combination with the Phytochemicals Curcumin and Quercetin in Human Ovarian Tumour Models." Anticancer research **35**(5): 2783-2794.

Arzuman, L., P. Beale, et al. (2016). "Synthesis of tris (quinoline) monochloroplatinum (II) chloride and its activity alone and in combination with capsaicin and curcumin in human ovarian Cancer cell lines." Anticancer research **36**(6): 2809-2818.

Arzuman, L., P. Beale, et al. (2014). "Synthesis of a monofunctional platinum compound and its activity alone and in combination with phytochemicals in ovarian tumor models." Anticancer research **34**(12): 7077-7090.

Arzuman, L., M. A. Moni, et al. (2019). "Protein Expression Patterns in ovarian cancer cells Associated with Monofunctional Platinums Treatment." bioRxiv: 628958.

Bahcall, O. G. (2013). "iCOGS collection provides a collaborative model." Nature genetics **45**(4): 343.
Bali, H. (2018). "Synergism from combination of platinum drugs and selected phytochemicals in colorectal cancer."
Berchtold, M. W. and A. Villalobo (2014). "The many faces of calmodulin in cell proliferation, programmed cell death, autophagy, and cancer." Biochimica et Biophysica Acta (BBA)-Molecular Cell Research **1843**(2): 398-435.
Bergman, A. and G. Peters (2006). "Gemcitabine. Mechanism of action and resistance." Cancer drug discovery and development: deoxynucleoside analogs in cancer therapy. Totawa, NJ: Humana Press Inc **225**.
Bergman, A. M., V. R. van Haperen, et al. (1996). "Synergistic interaction between cisplatin and gemcitabine in vitro." Clinical Cancer Research **2**(3): 521-530.
Binenbaum, Y., S. Na'ara, et al. (2015). "Gemcitabine resistance in pancreatic ductal adenocarcinoma." Drug Resistance Updates **23**: 55-68.
Bray, F., J. Ferlay, et al. (2018). "Global cancer statistics 2018: GLOBOCAN estimates of incidence and mortality worldwide for 36 cancers in 185 countries." CA: a cancer journal for clinicians **68**(6): 394-424.
Brodská, B., M. Šašinková, et al. (2019). "Nucleophosmin in leukemia: Consequences of anchor loss." The international journal of biochemistry & cell biology.
Burt, R. W. (2000). "Colon cancer screening." Gastroenterology **119**(3): 837-853.
Burtt, J. J., P. A. Thompson, et al. (2016). "Non-targeted effects and radiation-induced carcinogenesis: a review." Journal of Radiological Protection **36**(1): R23.
Carrick, S., S. Parker, et al. (2009). "Single agent versus combination chemotherapy for metastatic breast cancer." Cochrane Database of Systematic Reviews(2).
Casagrande, J., M. Pike, et al. (1979). "" Incessant ovulation" and ovarian cancer." The Lancet **314**(8135): 170-173.
Chan, K. T., K. Li, et al. (2010). "Cucurbitacin B inhibits STAT3 and the Raf/MEK/ERK pathway in leukemia cell line K562." Cancer letters **289**(1): 46-52.
Chan, K. T., F. Y. Meng, et al. (2010). "Cucurbitacin B induces apoptosis and S phase cell cycle arrest in BEL-7402 human hepatocellular carcinoma cells and is effective via oral administration." Cancer letters **294**(1): 118-124.
Chao, T.-K., T.-S. Huang, et al. (2017). "Pyruvate kinase M2 is a poor prognostic marker of and a therapeutic target in ovarian cancer." PLoS One **12**(7): e0182166.
Chen, W., A. Leiter, et al. (2010). "Cucurbitacin B inhibits growth, arrests the cell cycle, and potentiates antiproliferative efficacy of cisplatin in cutaneous squamous cell carcinoma cell lines." International journal of oncology **37**(3): 737-743.
Cheng, W., B. Zhang, et al. (2019). "Elevated Mortalin correlates with poor outcome in hepatocellular carcinoma." Annals of diagnostic pathology **42**: 59-63.
Chou, R.-H., Y.-N. Wang, et al. (2014). "EGFR modulates DNA synthesis and repair through Tyr phosphorylation of histone H4." Developmental cell **30**(2): 224-237.
Chou, T.-C. (2010). "Drug combination studies and their synergy quantification using the Chou-Talalay method." Cancer research **70**(2): 440-446.
Chou, T.-C. (2018). The combination index (CI< 1) as the definition of synergism and of synergy claims, Elsevier.

Chou, T.-C. and P. Talalay (1984). "Quantitative analysis of dose-effect relationships: the combined effects of multiple drugs or enzyme inhibitors." Advances in enzyme regulation **22**: 27-55.
Corthay, A. (2014). "Does the immune system naturally protect against cancer?" Frontiers in immunology **5**: 197.
Croce, C. M. (2008). "Oncogenes and cancer." New England journal of medicine **358**(5): 502-511.
Cui, X., Z. Li, et al. (2017). "Mortalin expression in pancreatic cancer and its clinical and prognostic significance." Human pathology **64**: 171-178.
Dakeng, S., S. Duangmano, et al. (2012). "Inhibition of Wnt signaling by cucurbitacin B in breast cancer cells: Reduction of Wnt-associated proteins and reduced translocation of galectin-3-mediated β-catenin to the nucleus." Journal of cellular biochemistry **113**(1): 49-60.
Dasari, S. and P. B. Tchounwou (2014). "Cisplatin in cancer therapy: molecular mechanisms of action." European journal of pharmacology **740**: 364-378.
De Cola, A., M. Franceschini, et al. (2018). "N6L pseudopeptide interferes with nucleophosmin protein-protein interactions and sensitizes leukemic cells to chemotherapy." Cancer letters **412**: 272-282.
De Jonge, M., A. Sparreboom, et al. (1998). "The development of combination therapy involving camptothecins: a review of preclinical and early clinical studies." Cancer treatment reviews **24**(3): 205-220.
De Rosa, M., U. Pace, et al. (2015). "Genetics, diagnosis and management of colorectal cancer." Oncology reports **34**(3): 1087-1096.
Deng, L., Y. Lu, et al. (2013). "Ran GTPase protein promotes human pancreatic cancer proliferation by deregulating the expression of Survivin and cell cycle proteins." Biochemical and biophysical research communications **440**(2): 322-329.
Dung, D. T. M., P. T. P. Dung, et al. (2017). "Exploration of novel 5′(7′)-substituted-2′-oxospiro[1,3]dioxolane-2,3′-indoline-based N-hydroxypropenamides as histone deacetylase inhibitors and antitumor agents." Arabian Journal of Chemistry **10**(4): 465-472.
Edelman, M. J. and M. Shvartsbeyn (2012). "Epothilones in development for non–small-cell lung cancer: novel anti-tubulin agents with the potential to overcome taxane resistance." Clinical lung cancer **13**(3): 171-180.
Esparza-Moltó, P. B. and J. M. Cuezva (2018). "The role of mitochondrial H+-ATP synthase in cancer." Frontiers in oncology **8**: 53.
Faivre, S., D. Chan, et al. (2003). "DNA strand breaks and apoptosis induced by oxaliplatin in cancer cells." Biochemical pharmacology **66**(2): 225-237.
Faivre, S., E. Raymond, et al. (1999). "Supraadditive effect of 2′, 2′-difluorodeoxycytidine (gemcitabine) in combination with oxaliplatin in human cancer cell lines." Cancer chemotherapy and pharmacology **44**(2): 117-123.
Fan, H., Y. Lu, et al. (2013). "High Ran level is correlated with poor prognosis in patients with colorectal cancer." International journal of clinical oncology **18**(5): 856-863.
Foo, S. L., G. Yap, et al. (2019). "Annexin-A1–A Blessing or a Curse in Cancer?" Trends in molecular medicine.
Fukuda, M., K. Nishio, et al. (1996). "Synergism between cisplatin and topoisomerase I inhibitors, NB-506 and SN-38, in human small cell lung cancer cells." Cancer research **56**(4): 789-793.

Galluzzi, L., L. Senovilla, et al. (2012). "Molecular mechanisms of cisplatin resistance." Oncogene **31**(15): 1869.
Gao, Y., M. S. Islam, et al. (2014). "Inactivation of ATP citrate lyase by Cucurbitacin B: A bioactive compound from cucumber, inhibits prostate cancer growth." Cancer letters **349**(1): 15-25.
Garner, R. C. (1998). "The role of DNA adducts in chemical carcinogenesis." Mutation Research/Fundamental and Molecular Mechanisms of Mutagenesis **402**(1-2): 67-75.
Guerrieri, M., R. Gesuita, et al. (2014). "Treatment of rectal cancer by transanal endoscopic microsurgery: experience with 425 patients." World journal of gastroenterology: WJG **20**(28): 9556.
Guinney, J., R. Dienstmann, et al. (2015). "The consensus molecular subtypes of colorectal cancer." Nature medicine **21**(11): 1350.
Guo, C., S. Liu, et al. (2013). "ACTB in cancer." Clinica Chimica Acta **417**: 39-44.
Haggar, F. A. and R. P. Boushey (2009). "Colorectal cancer epidemiology: incidence, mortality, survival, and risk factors." Clinics in colon and rectal surgery **22**(04): 191-197.
Haley, B., T. Paunesku, et al. (2009). "Response of heterogeneous ribonuclear proteins (hnRNP) to ionising radiation and their involvement in DNA damage repair." International journal of radiation biology **85**(8): 643-655.
Hanahan, D. and R. A. Weinberg (2011). "Hallmarks of cancer: the next generation." cell **144**(5): 646-674.
He, Y., Q. Zhu, et al. (2016). "The changing 50% inhibitory concentration (IC50) of cisplatin: a pilot study on the artifacts of the MTT assay and the precise measurement of density-dependent chemoresistance in ovarian cancer." Oncotarget **7**(43): 70803.
Hope, N. R. and G. I. Murray (2011). "The expression profile of RNA-binding proteins in primary and metastatic colorectal cancer: relationship of heterogeneous nuclear ribonucleoproteins with prognosis." Human pathology **42**(3): 393-402.
Hu, Y., L. Yang, et al. (2016). "Oncogenic role of mortalin contributes to ovarian tumorigenesis by activating the MAPK–ERK pathway." Journal of cellular and molecular medicine **20**(11): 2111-2121.
Huq, F., J. Q. Yu, et al. (2014). "Combinations of platinums and selected phytochemicals as a means of overcoming resistance in ovarian cancer." Anticancer research **34**(1): 541-545.
Hwang, Y. J., S. P. Lee, et al. (2009). "Expression of heat shock protein 60 kDa is upregulated in cervical cancer." Yonsei medical journal **50**(3): 399-406.
Ingerslev, K., E. Hogdall, et al. (2017). "The potential role of infectious agents and pelvic inflammatory disease in ovarian carcinogenesis." Infectious agents and cancer **12**(1): 25.
Jasperson, K. W., T. M. Tuohy, et al. (2010). "Hereditary and familial colon cancer." Gastroenterology **138**(6): 2044-2058.
Jazii, F. R., Z. Najafi, et al. (2006). "Identification of squamous cell carcinoma associated proteins by proteomics and loss of beta tropomyosin expression in esophageal cancer." World journal of gastroenterology: WJG **12**(44): 7104.
Johnson, C. M., C. Wei, et al. (2013). "Meta-analyses of colorectal cancer risk factors." Cancer causes & control **24**(6): 1207-1222.

Jonckheere, A. I., J. A. Smeitink, et al. (2012). "Mitochondrial ATP synthase: architecture, function and pathology." Journal of inherited metabolic disease **35**(2): 211-225.
Jones, C. B., M. K. Clements, et al. (1997). "Sensitivity to camptothecin of human breast carcinoma and normal endothelial cells." Cancer chemotherapy and pharmacology **40**(6): 475-483.
Jubran, R., J. Kocsis, et al. (2017). "Circulating mitochondrial stress 70 protein/mortalin and cytosolic Hsp70 in blood: risk indicators in colorectal cancer." International journal of cancer **141**(11): 2329-2335.
Kang, Q., J.-B. Cai, et al. (2017). "Mortalin promotes cell proliferation and epithelial mesenchymal transition of intrahepatic cholangiocarcinoma cells in vitro." Journal of clinical pathology **70**(8): 677-683.
Kang, S. W., S. G. Rhee, et al. (2005). "2-Cys peroxiredoxin function in intracellular signal transduction: therapeutic implications." Trends in molecular medicine **11**(12): 571-578.
Katz, E. J., J. S. Vick, et al. (1990). "Effect of topoisomerase modulators on cisplatin cytotoxicity in human ovarian carcinoma cells." European Journal of Cancer and Clinical Oncology **26**(6): 724-727.
Kaufmann, S. H., D. Peereboom, et al. (1996). "Cytotoxic effects of topotecan combined with various anticancer agents in human cancer cell lines." JNCI: Journal of the National Cancer Institute **88**(11): 734-741.
Kausar, H., R. Munagala, et al. (2013). "Cucurbitacin B potently suppresses non-small-cell lung cancer growth: identification of intracellular thiols as critical targets." Cancer Letters **332**(1): 35-45.
Keane, T., R. El-Galley, et al. (1998). "Camptothecin analogues/cisplatin: an effective treatment of advanced bladder cancer in a preclinical in vivo model system." The Journal of urology **160**(1): 252-256.
Kelemen, L. E., E. V. Bandera, et al. (2013). "Recent alcohol consumption and risk of incident ovarian carcinoma: a pooled analysis of 5,342 cases and 10,358 controls from the Ovarian Cancer Association Consortium." BMC cancer **13**(1): 28.
Keller, K. E., I. S. Tan, et al. (2012). "SAICAR stimulates pyruvate kinase isoform M2 and promotes cancer cell survival in glucose-limited conditions." Science **338**(6110): 1069-1072.
Kgatle, M. M., C. W. Spearman, et al. (2017). "DNA oncogenic virus-induced oxidative stress, genomic damage, and aberrant epigenetic alterations." Oxidative medicine and cellular longevity **2017**.
Kimura, E., R. E. Enns, et al. (1993). "Correlation of the survival of ovarian cancer patients with mRNA expression of the 60-kD heat-shock protein HSP-60." Journal of clinical oncology **11**(5): 891-898.
Kiraz, Y., A. Adan, et al. (2016). "Major apoptotic mechanisms and genes involved in apoptosis." Tumor Biology **37**(7): 8471-8486.
Kleemann, M., H. Schneider, et al. (2018). "MiR-744-5p inducing cell death by directly targeting HNRNPC and NFIX in ovarian cancer cells." Scientific reports **8**(1): 1-15.
Kopantzev, E. P., G. S. Monastyrskaya, et al. (2008). "Differences in gene expression levels between early and later stages of human lung development are opposite to those between normal lung tissue and non-small lung cell carcinoma." Lung Cancer **62**(1): 23-34.

Koul, S., J. M. McKiernan, et al. (2004). "Role of promoter hypermethylation in Cisplatin treatment response of male germ cell tumors." Molecular cancer **3**(1): 16.
Kumar, V., A. K. Abbas, et al. (2014). Robbins and Cotran pathologic basis of disease, professional edition e-book, Elsevier health sciences.
La Vecchia, C. (2001). "Epidemiology of ovarian cancer: a summary review." European Journal of Cancer Prevention **10**(2): 125-129.
Latino-Martel, P., V. Cottet, et al. (2016). "Alcoholic beverages, obesity, physical activity and other nutritional factors, and cancer risk: a review of the evidence." Critical reviews in oncology/hematology **99**: 308-323.
Lazzari, C., N. Karachaliou, et al. (2018). "Combination of immunotherapy with chemotherapy and radiotherapy in lung cancer: is this the beginning of the end for cancer?" Therapeutic advances in medical oncology **10**: 1758835918762094.
Lee, D. H., G. B. Iwanski, et al. (2010). "Cucurbitacin: ancient compound shedding new light on cancer treatment." The Scientific World Journal **10**: 413-418.
Lee, D. H., N. H. Thoennissen, et al. (2011). "Synergistic effect of low-dose cucurbitacin B and low-dose methotrexate for treatment of human osteosarcoma." Cancer letters **306**(2): 161-170.
Li, Q.-Y., Y.-G. Zu, et al. (2006). "Review camptothecin: current perspectives." Current medicinal chemistry **13**(17): 2021-2039.
Lister, T., M. Cullen, et al. (1978). "Comparison of combined and single-agent chemotherapy in non-Hodgkin's lymphoma of favourable histological type." Br Med J **1**(6112): 533-537.
Liu, C.-X., H.-C. Zhou, et al. (2013). "Targeting peroxiredoxins against leukemia." Experimental cell research **319**(2): 170-176.
Liu, J., H. Meng, et al. (2019). "Identification of potential biomarkers in association with progression and prognosis in Epithelial Ovarian Cancer by integrated bioinformatics analysis." Frontiers in genetics **10**: 1031.
Liu, T., H. Peng, et al. (2010). "Cucurbitacin B, a small molecule inhibitor of the Stat3 signaling pathway, enhances the chemosensitivity of laryngeal squamous cell carcinoma cells to cisplatin." European journal of pharmacology **641**(1): 15-22.
Liu, T., M. Zhang, et al. (2008). "Combined antitumor activity of cucurbitacin B and docetaxel in laryngeal cancer." European journal of pharmacology **587**(1-3): 78-84.
Liu, Y. Q., W. Q. Li, et al. (2015). "Perspectives on biologically active camptothecin derivatives." Medicinal research reviews **35**(4): 753-789.
Lomnytska, M., S. Becker, et al. (2011). "Differential expression of ANXA6, HSP27, PRDX2, NCF2, and TPM4 during uterine cervix carcinogenesis: diagnostic and prognostic value." British journal of cancer **104**(1): 110.
Louvet, C., T. André, et al. (2002). "Gemcitabine combined with oxaliplatin in advanced pancreatic adenocarcinoma: final results of a GERCOR multicenter phase II study." Journal of Clinical Oncology **20**(6): 1512-1518.
Lovejoy, K. S., M. Serova, et al. (2011). "Spectrum of cellular responses to pyriplatin, a monofunctional cationic antineoplastic platinum (II) compound, in human cancer cells." Molecular cancer therapeutics **10**(9): 1709-1719.
Lovejoy, K. S., R. C. Todd, et al. (2008). "cis-Diammine (pyridine) chloroplatinum (II), a monofunctional platinum (II) antitumor agent: Uptake, structure,

function, and prospects." Proceedings of the National Academy of Sciences **105**(26): 8902-8907.
Lu, D., T. Lu, et al. (2015). "Cancer bioinformatics, its impacts on cancer therapy." Metabolomics **5**(2): e133.
Lynam-Lennon, N., S. G. Maher, et al. (2009). "The roles of microRNA in cancer and apoptosis." Biological Reviews **84**(1): 55-71.
Ma, J., M. Maliepaard, et al. (1998). "Synergistic cytotoxicity of cisplatin and topotecan or SN-38 in a panel of eight solid-tumor cell lines in vitro." Cancer chemotherapy and pharmacology **41**(4): 307-316.
Mao, S., H. Shen, et al. (2016). "Systemic lupus erythematosus and malignancies risk." Journal of cancer research and clinical oncology **142**(1): 253-262.
Marshall, C. J. (1991). "Tumor suppressor genes." Cell **64**(2): 313-326.
Masters, J., R. Thomas, et al. (1996). "Sensitivity of testis tumour cells to chemotherapeutic drugs: role of detoxifying pathways." European Journal of Cancer **32**(7): 1248-1253.
Mikuriya, K., Y. Kuramitsu, et al. (2007). "Expression of glycolytic enzymes is increased in pancreatic cancerous tissues as evidenced by proteomic profiling by two-dimensional electrophoresis and liquid chromatography-mass spectrometry/mass spectrometry." International journal of oncology **30**(4): 849-855.
Miller, R. W., J. L Young Jr, et al. (1995). "Childhood cancer." Cancer **75**(S1): 395-405.
Mini, E., S. Nobili, et al. (2006). "Cellular pharmacology of gemcitabine." Annals of oncology **17**(suppl_5): v7-v12.
Nessa, M. U., P. Beale, et al. (2012). "Combinations of resveratrol, cisplatin and oxaliplatin applied to human ovarian cancer cells." Anticancer research **32**(1): 53-59.
Nogales, E., S. G. Wolf, et al. (1998). "Structure of the αβ tubulin dimer by electron crystallography." Nature **391**: 199.
O'Connell, J. B., M. A. Maggard, et al. (2004). "Colon cancer survival rates with the new American Joint Committee on Cancer sixth edition staging." Journal of the National Cancer Institute **96**(19): 1420-1425.
Olsen, C. M., C. M. Nagle, et al. (2013). "Obesity and risk of ovarian cancer subtypes: evidence from the Ovarian Cancer Association Consortium." Endocrine-related cancer **20**(2): 251-262.
Panczyk, M. (2014). "Pharmacogenetics research on chemotherapy resistance in colorectal cancer over the last 20 years." World Journal of Gastroenterology: WJG **20**(29): 9775.
Park, G. Y., J. J. Wilson, et al. (2012). "Phenanthriplatin, a monofunctional DNA-binding platinum anticancer drug candidate with unusual potency and cellular activity profile." Proceedings of the National Academy of Sciences **109**(30): 11987-11992.
Park, M. H., M. Jo, et al. (2016). "Roles of peroxiredoxins in cancer, neurodegenerative diseases and inflammatory diseases." Pharmacology & Therapeutics **163**: 1-23.
Pavillard, V., D. Kherfellah, et al. (2001). "Effects of the combination of camptothecin and doxorubicin or etoposide on rat glioma cells and camptothecin-resistant variants." British journal of cancer **85**(7): 1077.

Pino, I., R. Pıo, et al. (2003). "Altered patterns of expression of members of the heterogeneous nuclear ribonucleoprotein (hnRNP) family in lung cancer." Lung cancer **41**(2): 131-143.
Plummer, M., S. Franceschi, et al. (2015). "Global burden of gastric cancer attributable to Helicobacter pylori." International journal of cancer **136**(2): 487-490.
Prat, J. and F. C. o. G. Oncology (2014). "Staging classification for cancer of the ovary, fallopian tube, and peritoneum." International Journal of Gynecology & Obstetrics **124**(1): 1-5.
Reid, B. M., J. B. Permuth, et al. (2017). "Epidemiology of ovarian cancer: a review." Cancer biology & medicine **14**(1): 9.
Riman, T., S. Nilsson, et al. (2004). "Review of epidemiological evidence for reproductive and hormonal factors in relation to the risk of epithelial ovarian malignancies." Acta obstetricia et gynecologica Scandinavica **83**(9): 783-795.
Romanelli, S., P. Perego, et al. (1998). "In vitro and in vivo interaction between cisplatin and topotecan in ovarian carcinoma systems." Cancer chemotherapy and pharmacology **41**(5): 385-390.
Rosen, S. A., J. F. Buell, et al. (2000). "Initial presentation with stage IV colorectal cancer: how aggressive should we be?" Archives of Surgery **135**(5): 530-534.
Safaei, R. and S. B. Howell (2005). "Copper transporters regulate the cellular pharmacology and sensitivity to Pt drugs." Critical reviews in oncology/hematology **53**(1): 13-23.
Sahab, Z. J., Y.-G. Man, et al. (2010). "Alteration in protein expression in estrogen receptor alpha-negative human breast cancer tissues indicates a malignant and metastatic phenotype." Clinical & experimental metastasis **27**(7): 493-503.
Samant, R. S., P. A. Clarke, et al. (2014). "E3 ubiquitin ligase Cullin-5 modulates multiple molecular and cellular responses to heat shock protein 90 inhibition in human cancer cells." Proceedings of the National Academy of Sciences **111**(18): 6834-6839.
Sgarbi, G., S. Barbato, et al. (2018). "The role of the ATPase inhibitor factor 1 (IF1) in cancer cells adaptation to hypoxia and anoxia." Biochimica et Biophysica Acta (BBA)-Bioenergetics **1859**(2): 99-109.
Sgourakis, G., S. Lanitis, et al. (2011). "Transanal endoscopic microsurgery for T1 and T2 rectal cancers: a meta-analysis and meta-regression analysis of outcomes." The American surgeon **77**(6): 761-772.
Shahjaman, M., F. T. Z. Jui, et al. (2020). "Improved identification of core biomarkers and drug repositioning for ovarian cancer: an integrated bioinformatics approach." Network Modeling Analysis in Health Informatics and Bioinformatics **9**(1): 1-14.
Shaib, W. L., G. P. Nagaraju, et al. (2019). "Interaction of heat shock protein 90 with hypoxia inducible factor and signal transducer and activator of transcription in colon cancer." Process Biochemistry **86**: 151-158.
Shang, Y., J. He, et al. (2017). "CHIP/Stub1 regulates the Warburg effect by promoting degradation of PKM2 in ovarian carcinoma." Oncogene **36**(29): 4191.
Shen, J., S. Yu, et al. (2019). "Identification of key biomarkers associated with development and prognosis in patients with ovarian carcinoma: Evidence from bioinformatic analysis." Journal of ovarian research **12**(1): 1-13.

Shishkin, S., L. Eremina, et al. (2016). "Cofilin-1 and other ADF/cofilin superfamily members in human malignant cells." International journal of molecular sciences **18**(1): 10.
Shu, X., X. Xiong, et al. (2016). "Base-resolution analysis of cisplatin–DNA adducts at the genome scale." Angewandte Chemie International Edition **55**(46): 14246-14249.
Siani, L. and C. Pulica (2014). "Stage I-IIIC right colonic cancer treated with complete mesocolic excision and central vascular ligation: quality of surgical specimen and long term oncologic outcome according to the plane of surgery." Minerva chirurgica **69**(4): 199-208.
Singh, R., Z. Fazal, et al. (2019). "Mechanisms of cisplatin sensitivity and resistance in testicular germ cell tumors." Cancer drug resistance (Alhambra, Calif.) **2**(3): 580.
Søndenaa, K., P. Quirke, et al. (2014). "The rationale behind complete mesocolic excision (CME) and a central vascular ligation for colon cancer in open and laparoscopic surgery." International journal of colorectal disease **29**(4): 419-428.
Sriram, D., P. Yogeeswari, et al. (2005). "Camptothecin and its analogues: a review on their chemotherapeutic potential." Natural product research **19**(4): 393-412.
Stanislaus, A., A. Bakhtiar, et al. (2012). "Knockdown of PLC-gamma-2 and calmodulin 1 genes sensitizes human cervical adenocarcinoma cells to doxorubicin and paclitaxel." Cancer cell international **12**(1): 30.
Takahashi, H., C. Morizane, et al. (2018). "731P Phase II clinical trial of gemcitabine plus oxaliplatin combination therapy (GEMOX) in patients with advanced pancreatic adenocarcinoma with a family history of pancreatic/breast/ovarian/prostate cancer or personal history of breast/ovarian/prostate cancer (FABRIC study)." Annals of Oncology **29**(suppl_8): mdy282. 114.
Takiyama, I., M. Terashima, et al. (1997). Remarkable synergistic interaction between camptothecin analogs and cisplatin against human esophageal cancer cell lines. Proc Am Assoc Cancer Res.
Talekar, M., Q. Ouyang, et al. (2015). "Cosilencing of PKM-2 and MDR-1 sensitizes multidrug-resistant ovarian cancer cells to paclitaxel in a murine model of ovarian cancer." Molecular cancer therapeutics **14**(7): 1521-1531.
Tang, H.-Y., L. A. Beer, et al. (2013). "Protein isoform-specific validation defines multiple chloride intracellular channel and tropomyosin isoforms as serological biomarkers of ovarian cancer." Journal of proteomics **89**: 165-178.
TEKKEŞİN, M. S., S. Mutlu, et al. (2011). "Expression of heat shock proteins 27, 60 and 70 in oral carcinogenesis: An immunohistochemical study." Turkish Journal of Oncology **26**(3).
Tessier-Cloutier, B., A. E. Clarke, et al. (2014). "Systemic lupus erythematosus and malignancies: a review article." Rheumatic Disease Clinics **40**(3): 497-506.
Thoennissen, N. H., G. B. Iwanski, et al. (2009). "Cucurbitacin B induces apoptosis by inhibition of the JAK/STAT pathway and potentiates antiproliferative effects of gemcitabine on pancreatic cancer cells." Cancer research **69**(14): 5876-5884.
Thomas, C. J., N. J. Rahier, et al. (2004). "Camptothecin: current perspectives." Bioorganic & medicinal chemistry **12**(7): 1585-1604.
Tsai, C.-H., L.-T. Lin, et al. (2015). "Over-expression of cofilin-1 suppressed growth and invasion of cancer cells is associated with up-regulation of let-7

microRNA." Biochimica et Biophysica Acta (BBA)-Molecular Basis of Disease **1852**(5): 851-861.
Van Driel, W. J., S. N. Koole, et al. (2018). "Hyperthermic intraperitoneal chemotherapy in ovarian cancer." New England Journal of Medicine **378**(3): 230-240.
Van Haperen, V. W. R., G. Veerman, et al. (1994). "Development and molecular characterization of a 2′, 2′-difluorodeoxycytidine-resistant variant of the human ovarian carcinoma cell line A2780." Cancer research **54**(15): 4138-4143.
Van Moorsel, C., G. Veerman, et al. (1998). Mechanisms of synergism between gemcitabine and cisplatin. Purine and pyrimidine metabolism in man IX, Springer**:** 581-585.
Verderame, F., A. Russo, et al. (2006). "Gemcitabine and oxaliplatin combination chemotherapy in advanced biliary tract cancers." Annals of Oncology **17**(suppl_7): vii68-vii72.
Wakimoto, N., D. Yin, et al. (2008). "Cucurbitacin B has a potent antiproliferative effect on breast cancer cells in vitro and in vivo." Cancer science **99**(9): 1793-1797.
Waud, W., L. Rubinstein, et al. (1996). In vivo combination chemotherapy evaluations of topotecan with cisplatin and temozolomide. Proc. Am. Assoc. Cancer Res.
Wermann, H., H. Stoop, et al. (2010). "Global DNA methylation in fetal human germ cells and germ cell tumours: association with differentiation and cisplatin resistance." The Journal of pathology **221**(4): 433-442.
West, A. C. and R. W. Johnstone (2014). "New and emerging HDAC inhibitors for cancer treatment." The Journal of clinical investigation **124**(1): 30.
Wu, J., T. Liu, et al. (2017). "Heat shock proteins and cancer." Trends in pharmacological sciences **38**(3): 226-256.
Yang, R., G. Zheng, et al. (2018). "The clinical significance and biological function of tropomyosin 4 in colon cancer." Biomedicine & Pharmacotherapy **101**: 1-7.
Yang, S., M. Lu, et al. (2015). "Overexpression of eukaryotic elongation factor 1 alpha-2 is associated with poorer prognosis in patients with gastric cancer." Journal of cancer research and clinical oncology **141**(7): 1265-1275.
Yardley, D. A. (2013). "Drug resistance and the role of combination chemotherapy in improving patient outcomes." International journal of breast cancer **2013**.
Yasuda, S., S. Yogosawa, et al. (2010). "Cucurbitacin B induces G2 arrest and apoptosis via a reactive oxygen species-dependent mechanism in human colon adenocarcinoma SW480 cells." Molecular nutrition & food research **54**(4): 559-565.
Yin, D., N. Wakimoto, et al. (2008). "Cucurbitacin B markedly inhibits growth and rapidly affects the cytoskeleton in glioblastoma multiforme." International Journal of Cancer **123**(6): 1364-1375.
Yin, T., L. Lu, et al. (2015). "ATPase inhibitory factor 1 is a prognostic marker and contributes to proliferation and invasion of human gastric cancer cells." Biomedicine & Pharmacotherapy **70**: 90-96.
Yuen, H.-F., K.-K. Chan, et al. (2012). "Ran is a potential therapeutic target for cancer cells with molecular changes associated with activation of the PI3K/Akt/mTORC1 and Ras/MEK/ERK pathways." Clinical Cancer Research **18**(2): 380-391.

Yunos, N. M., P. Beale, et al. (2010). "Studies on combinations of platinum with paclitaxel and colchicine in ovarian cancer cell lines." Anticancer research **30**(10): 4025-4037.
Zhang, Q. C., D. Petrey, et al. (2012). "PrePPI: a structure-informed database of protein–protein interactions." Nucleic acids research **41**(D1): D828-D833.
Zhao, L., L. Liu, et al. (2007). "Differential proteomic analysis of human colorectal carcinoma cell lines metastasis-associated proteins." Journal of cancer research and clinical oncology **133**(10): 771-782.
Zheng, Q., Y. Liu, et al. (2014). "Cucurbitacin B inhibits growth and induces apoptosis through the JAK2/STAT3 and MAPK pathways in SH-SY5Y human neuroblastoma cells." Molecular medicine reports **10**(1): 89-94.

7 Appendices

7.1 APPENDIX-I

Exponentially gowing cells in culture media seeded into cell culture dish and allowed to attach overnight

⇩

Platinum drugs/phytochemicals at their IC_{50} values added to selected cell lines to culture plates.

⇩

Cells collected 24 h after the addition of the first drug and transferred into 10 mL centrifugal tubes

⇩

Tubes spun at 3500 rpm for 2 min at 4°C to obtain the pellet

⇩

Pellet washed with PBS; cells resuspended with PBS for cell counting.

⇩

Suspensions transferred into centrifugal tubes; tubes spun at 14000 rpm for 2 min at 4°C to provide pellet; pellet stored at -20°C

7.2 APPENDIX-II

The pellets were resuspended in 300 µl of ACL solution buffer, 20 µl of protenase K was added, mixed well and incubated at 55° C for 10 minutes

⇓

10 µl of RNase A (20mg/ml) was mixed by vortexing, incubated for 5 min at room temperature and vortexed again for 20 seconds

⇓

The Eppendorf tubes were centrifuged for 5 minutes at 12,000 rpm for 5 minutes

⇓

200 µl of supernatant was pipetted into new Eppendorf tubes and 200 µl of AB solution was added to tube. The content of each tube was mixed by occasionally inverting and left for 2 minutes

⇓

All the solution was loaded to EZ-10 spin columns and centrifuged at 2000 X g (4000 rpm) for 2 minutes. The flow through were discarded

⇓

500 µl of wash solution was added and spun at 10000 rpm for 1 minute, process was repeated again

⇓

The flow through were discarded and spun at 10000 rpm for an additional 1 minute

⇓

The columns were placed into Eppendorf tubes and 200 µl of elution buffer was added into the center part of the membrane in the every column

⇓

After incubation at 50° C for 2 minutes, the tubes were spun at 10000 rpm for 2 minutes to elute the DNA from the column

⇓

DNA quantity is measured by UV absorption spectrophotometer (Varian Cary 1E UV-Visible with Varian Cary Temperature Controller) at A260 (1.0 OD unit was considered of 50 µg)

⇓

Purified genomic DNA was stored at -20° C for further assay

7.3 APPENDIX-III

Cell lysis Buffer constituents & cell lysis method

Chemicals	Amount
8 M Urea	24.04 g
2 M Thiourea	7.61 g
4 % CHAPS	2.00 g
65 mM DTT	501 µL
mQ water up to	50 mL
Protease inhibitor (1 tablet/ 10 mL)	5 tablets

- Urea was dissolved in 10 mL of mQ water by heating it in a 45°C water bath to avoid carbamylation artifact in Isoelectric focusing (IEF)
- Other chemicals were then added and the volume was made up to 50 mL with mQ water and aliquoted into 10 mL tubes.
- 500 µL of lysis buffer was added to the cell pellets and mixed well. The cells were aspirated repeatedly using a 25-gauge needle to assure that the cells lysed.
- Then, the cells were centrifuged at 13000 rpm for 30 min at 4°C. The supernatant was transferred and aliquoted into new 1.5 mL centrifuge tubes and stored at -80°C until assayed.

Determination of protein concentration

- The lyophilized Bovine serum albumin (BSA) was reconstituted by adding 20 mL of mQ water and mixed well until dissolved. The dye reagent was prepared by diluting 1 part Dye Reagent Concentrate with 4 parts mQ, then filtered through a 0.22 µm membrane filter.
- Then four dilutions of the protein standard were prepared as following

	BSA (µg/mL)	BSA (µL)	mQ water (µL)
1	1400	50	0
2	350	12.5	37.5
3	87.5	12.5	37.5
4	21.88	12.5	37.5

- Using a 96 well plate, 10 µL of protein was pipetted into the corresponding wells then 200 µL of diluted dye reagent was added to all the wells. The plate was then mixed using a microplate mixer and incubated at room temperature for 5 min.
- The absorbance was measured at 595 nm using microplate reader BIO-RAD Model 3550. The following standard curve was used to determine the protein concentration of the samples.

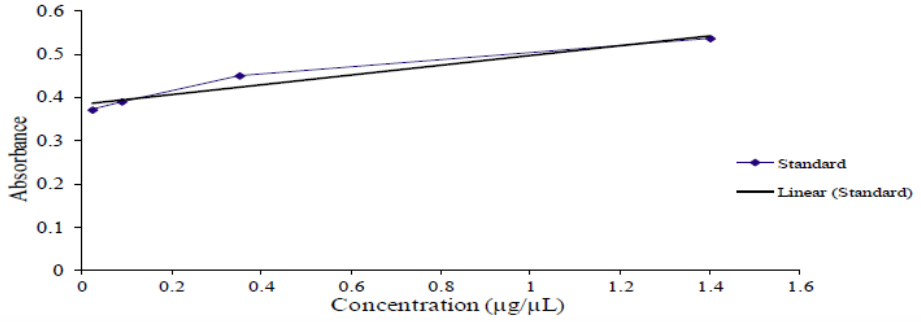

Isoelectric Focusing (IEF)

- 200µg of protein sample was mixed with the rehydration solution (prepared by following table) to a final volume of 180 µL.

Chemicals	Amount
8 M Urea	24 g
2 M Thiourea	7.6 g
60 mM DTT	0.5 g
4 % CHAPS	2 g
0.2 % Carrier ampholyte	250 µL
DeStreak	600 µL
0.0002 % Bromophenol Blue	100 µL
mQ water	to 50 mL

- The rehydration solution/protein sample was pipetted to each slot of the IPG strip rehydration tray. Then, the IPG strip was positioned in slots with the gel facing down. The rehydration tray was left on the orbital shaker overnight.
- After rehydration, dry wicks were placed within the indentation of the channels of the focusing tray and rehydrated with 5-8 µL of mQ water. The wicks were used to collect salts and other contaminants that produce high conductivity which alters the gradient and causes discontinuities in the gel.
- The IPG strip was transferred to the electrophoresis unit for first dimension-IEF with the gel side down.
- Presence of any trapped air bubbles beneath the strips was checked carefully and was removed (if any). Lid onto the tray was placed where positive "+" to the left when the inclined portion of the tray is on the right.

- Then, 2-3 mL of mineral oil was layered on the strip until the strip was completely covered to avoid evaporation of sample and carbon dioxide absorption during focusing.
- Then the focusing tray was placed into the PROTEAN IEF cell and the cover was closed. PROTEAN IEF cell was then programmed and started to initiate the electrophoresis run.
- After completion of electrophoresis run, strips were hold vertically with the forceps to let the mineral oil drain from the strip for ~5 seconds.
- A picture of the strips was then taken using ChemiDocTMMP Imaging system (BIO-RAD, Australia)

Preparation for second dimension gel electrophoresis

Prior to running the second dimension, the IPG strips were equilibrated with the anionic detergent sodium dodecyl sulfate (SDS) solution that denatured these proteins and forms negatively charged protein/SDS complex. Equilibration serves to saturate the IPG strip with the SDS buffer system required for the second-dimension separation. The amount of SDS linked into the protein is directly proportional to its weight, thus proteins that are totally coupled to SDS will migrate in polyacrylamide gel (SDS-PAGE) only due to their weight (which is the bases of the second dimension). The saturation of the IPG strip with SDS buffer was also required to maintain its pH condition in a range appropriate for electrophoresis. The equilibration buffer (EB) was prepared by mixing the required chemicals as stated below until the solution is clear.

Chemicals	**Amount**
SDS	3 g
6 M Urea	36 g
50% Glycerol	24 mL
1.5 M Tris HCl, pH 8.8	40 mL
Bromophenol blue	200 µl
mQ water	to 100 mL

The preparation of 50% Glycerol involved dissolving 50 mL of glycerol in 50 mL of water. Tris HCl (1.5 M) was prepared by adding the water to Tris. Concentrated hydrochloric acid was slowly added to the Tris solution until the pH 8.8 was reached.

The Tris solution was made up to 100 mL. The amounts of the chemicals used were listed as below:

Chemicals	Amount
Tris	18.18 g
Double distilled water	to 80 mL
4 M HCl	7.5 mL
mQ water	to 100 mL

- For the first equilibration step, 50 mL of the EB was mixed with 0.5 g Dithiothreitol (DTT) to produce EB-DTT solution. DTT ensures that disulfide bridges are broken and preserves the fully reduced state of denatured and unalkylated proteins. Each of the strips was positioned in the slot of a new set of rehydration tray. To each slot in the tray, 4 mL of EB-DTT solution was pipetted onto the gel and it was equilibrated for 15 min on a rocker.
- For the second equilibration step, 50 mL of EB was mixed with 0.5 g iodoacetamide (IAA) to produce EB-IAA solution. The IPG strip was transferred to a new slot of the tray, in which 4 mL of EB-IAA solution was pipetted onto the gel. The strip was equilibrated for 15 min on a rocker. This step helped to reduce point streaking and other artifacts in the second-dimension separation.

Running the gels for 2-D electrophoresis

The second dimension electrophoresis was performed using Criterion™ TGX™ pre-cast gels in a Criterion Dodeca™ Cell separation unit (BIO-RAD, Australia). The unit was composed of a chamber which was filled with Stock solutions of x10 time's concentrated Tris/Glycine/SDS electrophoresis running buffer (ERB) (25 mM Tris,

192 mM Glycine, 0.1% SDS, pH 8.3). The ERB was prepared by mixing all the chemicals listed below:

Chemicals	Amount
Tris base	30.25 g
Glycine	144.1 g
SDS	10 g
mQ water	to 1 L

- The individual gel cassette was removed from the packaging, washed with mQ water and laid on the bench.
- The IPG strip was washed with the electrophoresis buffer and positioned on top of the gel cassette.
- The IPG strip was inserted into the gel cassette until it touched the gel making sure no air bubbles were trapped.
- To seal the gel cassettes, agarose solution was used (BIO-RAD, Australia). Agarose sealing solution was melted using microwave oven at 800W for 1 minute.
- Finally, the gel cassette was inserted into the electrophoresis separating unit. The unit was covered and connected to the power pack. The electrophoresis was run at constant 200 V for 100 min.
- At the conclusion of the SDS-PAGE, the gel cassette was placed into a tray with mQ water, the cassette was opened and the IPG strip was removed.

Gel staining

For visualization of the proteins after separation using 2D-gel Coomasie blue staining was used. The stain was chosen due to its compatibility with protein sequencing by mass spectrometry and for its quality in protein quantitation. Hence, Coomassie blue staining was used for isolating the proteins.

- The gel was stained with 50 mL of Bio-Safe Coomassie Stain (BIO-RAD, Australia) for 60 min, in which the gel was placed on an orbital shaker for the staining period.
- The stain was then discarded, and the gel was washed with mQ for 15-30 min. The water was replaced with fresh water and the gel was left for further washing overnight.
- A picture of the gel was then taken using ChemiDoc™ MP Imaging system (BIO-RAD, Australia).

Gel preservation

In order to prolong the life of the gel, solutions of Sodium Azide (0.005%) was prepared. Sodium Azide (0.005 g) was added to 100 mL of mQ water. Then, to the gel, 100 mL of Sodium Azide solution was added and stored at room temperature for future analysis.

Protein identification

The protein spots were cut and placed in a 96-well plate. The protein gel spots were destained using 120 µL of freshly prepared (50% acetonitrile/50 mM NH_4HCO_3) solution and heated at 37°C for 30 min with mild shaking. The solution was then discarded. The gels were treated with 25 µL acetonitrile (ACN) and left to dry for 15 min. The solution was discarded then the spots were left to dry with the lid left open in the oven at 37°C for 15 min followed by cooling at 4°C. The spots were digested with 10 µL trypsin for 10 min on ice. The trypsin supernatants were placed in 96-well plate at 4°C followed by 10 µL addition of 25 mM NH_4HCO_3 for overnight digestion at 37°C. Trypsin was added to digest the proteins into smaller peptides (before proline and arginine in the amino acid sequence).

The resulting peptides were extracted with 0.1% TFA then extracted and concentrated by C18 zip-tips (Millipore, µ-C18, P10 size) on Xcise (Proteome Systems). A 1 µL aliquot was manually spotted onto a MALDI AnchorChip plate with 1 µL of matrix (CHCA, 1mg/mL in 90% v/v ACN, 0.1% TFA) and left to dry in air.

Data acquisition

Matrix Assisted Laser Desorption Ionisation mass spectrometry (MALDI-MS) was performed with 4800 plus MALDI TOF/TOF Analyser (AB Sciex). A neodymium-doped yttrium aluminum garnet (Nd:YAG) laser (355 nm) was used to irradiate the sample. Spectra were acquired in reflectron MS scan mode in the mass range of 700 to 4000 Da. The instrument was then switched to MS/MS (TOF-TOF) mode where the eight strongest peptides from the MS scan were isolated and fragmented by collision induced dissociation (CID), then re-accelerated to measure their masses and intensities. A near point calibration was applied and would give a typical mass accuracy of 50 ppm or less.

Data processing

The data on peptides masses were exported in a format suitable for submission to the database search program, Mascot (Matrix Science Ltd, London, UK). The peaklists were searched against *Homo sapiens* entries in the SwissProt database. High scores in the database search would indicate a likely match (confirmed and qualified by operator inspection). The protein identification for this study was undertaken at Australian Proteome Analysis Facility (APAF) the infrastructure provided by the Australian Government through the National Collaborative Research Infrastructure Strategy (NCRIS).